

Planning of Unbalanced Radial Distribution Systems with Reactive and Distributed Energy Sources Using Evolutionary Computing Techniques

*Dissertation submitted to the
National Institute of Technology Rourkela
in partial fulfillment of the requirements
of the degree of*

Doctor of Philosophy

in

Electrical Engineering

by

Padarbinda Samal

(Roll Number: 513EE1005)

under the supervision of

***Prof. Sanjeeb Mohanty
and***

Prof. Sanjib Ganguly (Co-Supervisor)



October, 2017

Department of Electrical Engineering
National Institute of Technology Rourkela



Electrical Engineering
National Institute of Technology Rourkela

October 23, 2017

Supervisor's Certificate

This is to certify that the work presented in this dissertation entitled "*Planning of Unbalanced Radial Distribution systems with Reactive and Distributed Energy Sources Using Evolutionary Computing Techniques*", Roll Number 513EE1005, is a record of original research carried out by him under my *supervision* and guidance in partial fulfillment of the requirements of the degree of *Doctor of Philosophy in Electrical Engineering*. Neither this dissertation nor any part of it has been submitted for any degree or diploma to any institute or university in India or abroad.

Prof. Sanjib Ganguly

Co-Supervisor

Assistant Professor

Department of Electronics and Electrical
Engineering

Indian Institute of Technology

Guwahati, Assam, and India, Pin Code: 781039

Prof. Sanjeeb Mohanty

Principal Supervisor

Assistant Professor

Department of Electrical Engineering

National Institute of Technology

Rourkela, Odisha, and India

Pin Code: 769008



Electrical Engineering
National Institute of Technology Rourkela

October 23, 2017

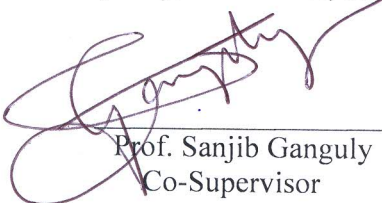
Certificate of Examination

Roll Number: 513EE1005

Name: Padarbinda Samal

Title of Dissertation: Planning of Unbalanced Radial Distribution systems with Reactive and Distributed Energy Sources Using Evolutionary Computing Techniques

We the below signed, after checking the dissertation mentioned above and the official record book (s) of the student, hereby state our approval of the dissertation submitted in partial fulfillment of the requirements of the degree of Doctor of Philosophy in Electrical Engineering at National Institute of Technology Rourkela. We are satisfied with the volume, quality, correctness, and originality of the work.


Prof. Sanjib Ganguly
Co-Supervisor

Prof. Sanjeeb Mohanty
Principal Supervisor

Prof. S. Maity
Member (DSC)

Prof. M. Patnaik
Member (DSC)

Prof. A. K. Sahoo
Member (DSC)

Prof. S. Das
Member (DSC)

External Examiner

A.K. Panda
Chairman (DSC)

J. K. Satpathy
Head of the department

Dedicated
To
My Parents

...Padarbinda Samal

Declaration of Originality

I, Padarbinda Samal, Roll Number 513EE1005 hereby declare that this dissertation entitled "*Planning of Unbalanced Radial Distribution Systems with Reactive and Distributed Energy Sources Using Evolutionary Computing Techniques*" represents my original work carried out as a doctoral student of NIT Rourkela and, to the best of my knowledge, it contains no material previously published or written by another person, nor any material presented for the award of any other degree or diploma of NIT Rourkela or any other institution. Any contribution made to this research by others, with whom I have worked at NIT Rourkela or elsewhere, is explicitly acknowledged in the dissertation. Works of other authors cited in this dissertation have been duly acknowledged under the section "Bibliography". I have also submitted my original research records to the scrutiny committee for evaluation of my dissertation.

I am fully aware that in case of any non-compliance detected in future, the Senate of NIT Rourkela may withdraw the degree awarded to me on the basis of the present dissertation.

October, 2017
NIT Rourkela

Padarbinda Samal

Acknowledgement

It has been a pleasure for me to work on this dissertation. I hope the reader will find it not only interesting and useful, but also comfortable to read.

The research reported here has been carried out in the **Dept. of Electrical Engineering, National Institute of Technology Rourkela**. I am greatly indebted to many persons for helping me complete this dissertation.

First and foremost, I would like to express my sense of gratitude and indebtedness to my supervisors **Prof. Sanjeeb Mohanty**, Asst. Professor, Department of Electrical Engineering, NIT Rourkela and **Prof. Sanjib Ganguly** (Co-Supervisor) Department of Electronics and Electrical Engineering, IIT Guwahati, for their inspiring guidance, encouragement, and untiring effort throughout the course of this work. Their timely help and painstaking efforts made it possible to present the work contained in this thesis. I consider myself fortunate to have worked under their guidance. Also, I am indebted to them for providing all official and laboratory facilities.

I am grateful to Director, **Prof. A. Biswas** and **Prof. Jitendra Kumar Satpathy**, Head of Electrical Engineering Department, National Institute of Technology, Rourkela, for their kind support and concern regarding my academic requirements.

I am grateful to my Doctoral Scrutiny Committee members, **Prof. A. K. Panda**, **Prof. M. Pattnaik**, **Prof. S. Maity** and **Prof. M. N. Islam**, for their valuable suggestions and comments during this research period. I express my thankfulness to the faculty and staff members of the Electrical Engineering Department for their continuous encouragement and suggestions.

I express my heartfelt thanks to the **International Journal Reviewers** for giving their valuable comments on the published papers in different International Journals, which helps to carry the research work in a right direction. I also thank the **International Conference Organizers** for intensely reviewing the published papers.

I would also like to thank my friends, **Mr. Damodar Panigrahy**, **Mr. Joseph Sanam**, **Mr. Rajendra K Khadanga**, **Mr. Amit Kumar**, **Mr. Srihari Nayak**, **Mr. Noby George**, **Mrs. S. Swain**, **Mrs. J. Mishra**, and **Mrs. A. Chatterjee** for extending their technical and personal support.

I express my deep sense of gratitude and reverence to my beloved Mother **Smt. Tarulata Mohapatra**, father **Sri. Rudra Charan Samal**, my wife **Smt. S. Parida**, my sisters **Smt. S. N. Swain**, and **S. Routray**, my brother-in-laws **Sri. P. K. Swain** and **Sri. P. Routray** who supported and encouraged me all the time, no matter what difficulties I encountered. I would like to express my love and affection on my nephews **A. I. Swain**,

A. Swain, and S. Routray. I would like to express my greatest admiration to **all my family members** for their positive encouragement that they showered on me throughout this research work. Without my family's sacrifice and support, this research work would not have been possible. It is a great pleasure for me to acknowledge and express my appreciation to all **my well wishers** for their understanding, relentless supports, and encouragement during my research work. Last but not the least, I wish to express my sincere thanks to all those who helped me directly or indirectly at various stages of this work.

This section would remain incomplete without remembering my Grandmother **K. Samal** and Grandfather **N. Samal**, who left their souls. I would like to express my love and respect for their everlasting affection and support.

Above all, I would like to thank **The Almighty God** for the wisdom and perseverance that he has been bestowed upon me during this research work, and indeed, throughout my life.

October, 2017
NIT Rourkela

Padarbinda Samal
Roll Number: 513EE1005

Abstract

The distribution system plays a key role in power system as it provides energy to the consumers safely, reliably, and economically. However, due to high R/X ratio, and low operating voltages, most of the losses occur in the distribution system. Moreover, distribution systems are generally unbalanced due to unequal single phase loads at the three phases of the system, and also additional unbalancing is introduced due to non equilateral conductor spacing. This, causes the voltage, the current, and the power unbalance in the system. Further, the total neutral current of the system increases causing unwanted tripping of the relay. Hence, the service quality and the reliability of the distribution system reduces. Therefore, a suitable phase balancing strategy is required to mitigate the phase unbalancing in the unbalanced distribution systems. Also, apart from reducing the phase unbalancing in the unbalanced distribution systems, a suitable strategy is required to minimize the system power loss. In this regard, it is necessary for the distribution engineers to plan the unbalanced distribution systems in order to reduce the losses, voltage unbalances, and neutral current of the system for safe and reliable operation. Most of the approaches for the planning of the unbalanced distribution systems are based upon metaheuristic algorithms. Moreover, the recent research has focused only on either phase balancing or simultaneous phase balancing and conductor sizing optimization in unbalanced distribution systems using metaheuristic algorithms. However no work has been carried out to study the impact of the simultaneous optimization of the phase balancing, the conductor sizing, the capacitor location and sizing, the DG location and sizing, DSTATCOM location, and rating on system power loss, voltage unbalance, etc. utilizing these algorithms. As the metaheuristic algorithms are random in nature, the convergence is not guaranteed in a single simulation run. Hence, it is necessary to perform a statistical comparison among them in order to understand their relative merits and demerits for multiple simulation runs.

In this thesis, the impact of the simultaneous optimization of the phase balancing and the conductor sizing on the planning problems/objective functions of the unbalanced distribution system such as; the power loss, the voltage unbalance, the total neutral current, and the complex power unbalance studied using various metaheuristic algorithms

such as the DE, the CSA, the PSO, and the GA. In the first step, these objective functions are optimized separately; then they are aggregated with weights into a multi-objective optimization problem. Further, a performance comparison in terms of the mean value of the objective functions and standard deviation (SD) carried out.

The reactive power compensating devices, such as the Capacitor, and the DSTATCOM has been integrated into the planning problem for the power loss minimization, the voltage profile improvement, and the voltage unbalance mitigation of the unbalanced distribution systems. Moreover, a three phase unbalanced modelling of the DSTATCOM has been developed. In this thesis, the effect of the simultaneous optimization of the phase balancing, the conductor sizing, the capacitor sizing, and the simultaneous optimization of the phase balancing, the conductor sizing, and the DSTATCOM sizing on the planning problem investigated. Both, single and multi-objective optimization approach are used in order to solve this problem. Also, statistical performance among the metaheuristic algorithms such as; the DE, the CSA, the PSO, and the GA in terms of the mean value of the objective function and SD carried out.

Further, the renewable sources such as the DG and a combined DG and DSTATCOM has been incorporated into the unbalanced system in order to study their impact on various planning problems.

Keywords: Unbalanced Distribution System; Phase Balancing; Conductor Sizing; Capacitor; Distribution Static Compensator; Distributed Generation; Evolutionary Computing Algorithms.

Contents

Supervisor’s Certificate	ii
Certificate of Examination	iii
Dedication	iv
Declaration of Originality	v
Acknowledgment	vi
Abstract	viii
List of Figures	xiv
List of Tables	xvii
List of Abbreviations	xx
List of Notations	xxi
1 Introduction and Literature Survey	1
1.1 Introduction	1
1.2 An Overview of Unbalanced Distribution Networks Planning.....	2
1.3 Unbalanced Distribution Networks planning problem.....	6
1.4 Approaches for the Unbalanced Distribution Networks Planning	7
1.5 Review of Literature	8
1.6 Motivation	13
1.7 Research Objectives and Scope	14
1.8 Dissertation Outline	15
2 Planning of Unbalanced Radial Distribution Systems Using Evolutionary Computing Algorithms in the Absence of DG, Capacitor, and DSTATCOM	17
2.1 Introduction	17
2.2 Problem Formulation	18
2.3 Proposed Approach.....	22
2.3.1 Differential Evolution (DE) Algorithm: An Overview	22

2.3.1.1	Mutation.....	22
2.3.1.2	Crossover	23
2.3.1.3	Selection	23
2.3.1.4	Encoding Strategy.....	23
2.3.1.5	Flow Chart of the Proposed Approach using DE	24
2.3.2	Overview of cuckoo search algorithm.....	24
2.3.2.1	Flow chart of the implementation of the cuckoo search algorithm	25
2.3.3	Overview of particle swarm optimization algorithm.....	26
2.3.3.1	Flow chart of the implementation of PSO algorithm ...	27
2.3.4	Overview of genetic algorithm	28
2.3.4.1	Flow chart of the implementation of GA algorithm	28
2.4	Three Phase Forward-Backward Sweep Load Flow Algorithm.....	29
2.5	Simulation Results and Discussion.....	35
2.5.1	Results of Single Objective Optimization	39
2.5.2	Results of Multi-Objective Optimization	39
2.6	Summary.....	44

3 Planning of Unbalanced Radial Distribution Systems with Capacitor

	Using Evolutionary computing Algorithms	45
3.1	Introduction	46
3.2	Problem Formulation	46
3.3	Implementation of DE and CSA for the planning problem	46
3.3.1	Three phase forward-backward sweep load flow algorithm incorporating capacitor	47
3.3.1.1	Incorporation of Capacitor model in the distribution load flow	47
3.3.2	Proposed Planning Approach Using DE and CSA.....	48
3.3.2.1	Decision variable representation	48
3.3.3	Flow chart of the planning approach using DE and CSA.....	49
3.4	Simulation Results and Discussion	51
3.4.1	Results of Single Objective Optimization	53
3.4.2	Results of Multi-Objective Optimization	54

3.5	Summary	60
4	Planning of Unbalanced Radial Distribution Systems with DSTATCOM Using Evolutionary Computing Algorithms	61
4.1	Introduction	61
4.2	A three-phase unbalanced modelling of DSTATCOM.....	62
4.3	Problem Formulation	65
4.4	Implementation of DE for the planning problem.....	65
4.4.1	Three phase forward-backward sweep load flow algorithm incorporating DSTATCOM.....	65
4.4.2	Proposed Planning Approach Using DE and CSA.....	68
4.4.2.1	Decision variable representation	68
4.5	Simulation Results and Discussion	70
4.5.1	Results of Single Objective Optimization	72
4.5.2	Results of Multi-Objective Optimization	73
4.6	Summary	81
5	Planning of Unbalanced Radial Distribution Systems with DG Using Evolutionary Computing Algorithms	82
5.1	Introduction	82
5.2	Problem Formulation	83
5.3	Implementation of DE and CSA for the planning problem	83
5.3.1	Three phase forward-backward sweep load flow algorithm incorporating DG.....	83
5.3.1.1	Incorporation of DG model in distribution load flow.....	84
5.3.2	Proposed Planning Approach Using DE and CSA.....	85
5.3.2.1	Encoding Strategy.....	85
5.3.2.2	Flow Chart of the Proposed Approach using DE and CSA	86
5.4	Simulation Results and Discussion	88
5.4.1	Results of Single Objective Optimization	88
5.4.2	Results of Multi-Objective Optimization	90
5.5	Summary	96

6	Planning of Unbalanced Radial Distribution Systems with DG and DSTATCOM Using Evolutionary Computing Algorithms	97
6.1	Introduction	97
6.2	Problem Formulation	98
6.3	Implementation of DE and CSA for the planning problem	98
6.3.1	Three phase forward-backward sweep load flow algorithm incorporating DG and DSTATCOM	99
6.3.1.1	Incorporation of DG and DSTATCOM model in the distribution load flow	99
6.3.2	Proposed Planning Approach Using DE and CSA	100
6.3.2.1	Parameter Representation	100
6.3.2.2	Flow Chart of the Proposed Approach using DE and CSA	101
6.4	Simulation results and discussion	102
6.4.1	Results of Single Objective Optimization	103
6.4.2	Results of Multi-Objective Optimization	104
6.8	Summary	111
7	Conclusions and Future Scope	112
7.1	Conclusions	112
7.2	Future Scope.....	113
	Bibliography	114
	Appendix	123
	Dissemination	152
	Vitae	156

List of Figures

1.1	A schematic layout of a sample two bus unbalanced distribution system....	2
1.2	Classification of planning problem.....	7
1.3	Classification of solution strategies	7
2.1	A three-phase line section model.....	19
2.2	Encoding strategy for a chromosome in DE.....	23
2.3	Flow chart of the planning approach using DE	24
2.4	Flow chart of the planning approach using CSA.....	25
2.5	Flow chart of the planning approach using PSO algorithm.....	27
2.6	Flow chart of the planning approach using GA.....	28
2.7	A section of radial distribution system	30
2.8	An 8-bus unbalanced radial distribution system.....	30
2.9	Pseudocodes for formation of matrix A	31
2.10	Pseudocodes for formation of matrix C	33
2.11	Pseudocodes for deletion of extra load current.....	33
2.12	Complex power unbalance for: (a) 19-bus and (b) 25-bus system.....	40
2.13	Complex power unbalance for: (a) Indian 19-bus and (b) 34-bus system....	41
3.1	Connection diagram of capacitors in a sample unbalanced distribution	47
3.2	Flow chart of the proposed planning approach using DE	49
3.3	Flow chart of the proposed planning approach using CSA	50
3.4	AVD vs. bus number for different planning cases obtained with the DE for the 19- bus system	58
3.5	AVD vs. bus number for different planning cases obtained with the DE for the 25- bus system	58
3.6	AVD vs. bus number for different planning cases obtained with the DE for the Indian 19- bus system	59
3.7	AVD vs. bus number for different planning cases obtained with the DE for the 34- bus system	59
4.1	A three phase three wire line section model including a DSTATCOM Model placed at bus j	62
4.2	Phasor diagram of DSTATCOM currents with respect to voltages at phase a, b, and c respectively.....	64
4.3	Flow chart for the determination of reactive power injection by DSTATCOM for random location, and angle values.....	67
4.4	Flow chart of the planning approach using DE	69
4.5	Flow chart of the planning strategy using CSA.....	70

4.6	Voltage magnitude for phase a for different planning cases obtained with DE for Indian 19-bus system	74
4.7	Voltage magnitude for phase b for different planning cases obtained with DE for Indian 19-bus system	74
4.8	Voltage magnitude for phase c for different planning cases obtained with DE for Indian 19-bus system	75
4.9	Voltage magnitude for phase a for different planning cases obtained with DE for 25-bus system	75
4.10	Voltage magnitude for phase b for different planning cases obtained with DE for 25-bus system	76
4.11	Voltage magnitude for phase c for different planning cases obtained with DE for 25-bus system	76
4.12	Voltage magnitude for phase a for different planning cases obtained with DE for 34-bus system	77
4.13	Voltage magnitude for phase b for different planning cases obtained with DE for 34-bus system	77
4.14	Voltage magnitude for phase c for different planning cases obtained with DE for 34-bus system	78
5.1	Connection diagram of DGs in a sample unbalanced distribution system ...	84
5.2	Encoding strategy for a chromosome or nest in DE and CSA	85
5.3	Flow chart of the proposed planning approach using DE	86
5.4	Flow chart of the proposed planning approach using CSA	87
5.5	Voltage profiles for the 19-bus system as obtained with different planning cases.....	92
5.6	Power loss vs. branch number for phase a for different planning cases obtained with DE for Indian 19-bus system	93
5.7	Power loss vs. branch number for phase b for different planning cases obtained with DE for Indian 19-bus system	93
5.8	Power loss vs. branch number for phase c for different planning cases obtained with DE for Indian 19-bus system	94
5.9	Power loss vs. branch number for phase a for different planning cases obtained with DE for 34-bus system	94
5.10	Power loss vs. branch number for phase b for different planning cases obtained with DE for 34-bus system	95
5.11	Power loss vs. branch number for phase c for different planning cases obtained with DE for 34-bus system	95
6.1	Connection diagram of DGs and DSTATCOM in a sample unbalanced distribution system.....	99

6.2	Flow chart of the proposed planning approach using DE	101
6.3	Flow chart of the proposed planning approach using CSA	102
6.4	Negative sequence unbalance (NSU) vs. bus number for different planning cases obtained with the DE for the 19-bus system	107
6.5	Zero sequence unbalance (ZSU) vs. bus number for different planning cases obtained with the DE for the 19-bus system.....	107
6.6	NSU vs. bus number for different planning cases obtained with the DE for the 25-bus system	108
6.7	ZSU vs. bus number for different planning cases obtained with the DE for the 25-bus system.....	108
6.8	NSU vs. bus number for different planning cases obtained with the DE for the Indian 19-bus system	109
6.9	ZSU vs. bus number for different planning cases obtained with the DE for the Indian 19-bus system	109
6.10	NSU vs. bus number for different planning cases obtained with the DE for the 34-bus system	110
6.11	ZSU vs. bus number for different planning cases obtained with the DE for the 34-bus system	110

List of Tables

2.1	Phase identification data.....	29
2.2	Base case values for the 19-, 25, Indian 19, and 34-bus systems.....	35
2.3	Optimal parameters used in DE, PSO, CSA, and GA	36
2.4	Comparison of method proposed by J.H.Teng and proposed method.....	36
2.5	Comparison of results of 50 runs as obtained with DE, GA, PSO, and CSA For <i>Case A</i> planning for 19-bus systems	36
2.6	Comparison of results of 50 runs as obtained with DE, GA, PSO, and CSA For <i>Case A</i> planning for 25-bus systems	37
2.7	Comparison of the solutions obtained with planning <i>Cases A</i> and <i>B</i> using DE for 19-bus and 25-bus systems	37
2.8	Comparison of results of planning <i>Case B</i> of 50 runs as obtained with DE, and CSA, for 19- and 25-bus systems	37
2.9	Comparison of results of 50 runs as obtained with DE, GA, PSO, and CSA for <i>Case A</i> planning for the Indian 19-bus systems.....	38
2.10	Comparison of results of 50 runs as obtained with DE, GA, PSO, and CSA for <i>Case A</i> planning for 34-bus systems.....	38
2.11	Comparison of the solutions obtained with planning <i>Cases A</i> and <i>B</i> using DE for the Indian 19-bus and 34-bus systems	38
2.12	Comparison of results of planning <i>Case B</i> of 50 runs as obtained with DE, and CSA, for Indian 19- and 34- bus systems.....	39
2.13	Comparison of results of multi-objective optimization (<i>Case A</i>) of 50 runs as obtained with DE, CSA, PSO, and GA for 19-bus systems.....	41
2.14	Comparison of results of multi-objective optimization (<i>Case A</i>) of 50 runs as obtained with DE, CSA, PSO, and GA for 25-bus systems.....	41
2.15	Results of the multi-objective optimization of 50 runs obtained with DE	42
2.16	Comparison of the results as obtained with Case B planning using DE and CSA	42
2.17	Comparison of results of multi-objective optimization (<i>Case A</i>) of 50 runs as obtained with DE, CSA, PSO, and GA for the Indian 19-bus systems.....	42
2.18	Comparison of results of multi-objective optimization (<i>Case A</i>) of 50 runs as obtained with DE, CSA, PSO, and GA for the 34- bus systems.....	43
2.19	Results of the multi-objective optimization of 50 runs obtained with DE	43

2.20	Comparison of the results as obtained with Case B planning using DE and CSA	43
3.1	Comparison of the solutions obtained with planning for <i>Cases A</i> using DE for the 19-bus and 25-bus systems	51
3.2	Comparison of the solutions obtained with planning <i>Cases B</i> and <i>C</i> using DE for 19-bus and 25-bus systems	51
3.3	Comparison of the results as obtained with Case C planning using DE and CSA for 19-bus and 25-bus systems.....	52
3.4	Comparison of the solutions obtained with planning <i>Cases A</i> using DE for the Indian 19-bus and 34-bus systems	52
3.5	Comparison of the solutions obtained with planning <i>Cases B</i> and <i>C</i> using DE for the Indian 19-bus and 34-bus systems.....	53
3.6	Comparison of the results as obtained with Case C planning using DE and CSA for Indian 19-bus and 34-bus systems	53
3.7	Results of the multi-objective optimization of 50 runs obtained with DE for the 19- bus and 25- bus system.....	55
3.8	Results of the multi-objective optimization of 50 runs obtained with DE for the 19- bus and 25- bus system.....	55
3.9	Comparison of the multi-objective optimization results as obtained with Case C planning using DE and CSA for 19-bus and 25-bus systems	56
3.10	Results of the multi-objective optimization of 50 runs obtained with DE for the Indian 19- bus and 34- bus system	56
3.11	Results of the multi-objective optimization of 50 runs obtained with DE for the Indian 19- bus and 34- bus system	57
3.12	Comparison of the multi-objective optimization results as obtained with Case C planning using DE and CSA for Indian 19- bus and 34- bus systems .	57
4.1	Comparison of the solutions obtained with planning <i>Cases B</i> and <i>C</i> using DE for 19-bus and 25-bus systems	71
4.2	Comparison of the results as obtained with Case C planning using DE and CSA for 19-bus and 25-bus systems.....	71
4.3	Comparison of the solutions obtained with planning <i>Cases B</i> and <i>C</i> using DE for the Indian 19-bus and 34-bus systems.....	72
4.4	Comparison of the results as obtained with Case C planning using DE and CSA for Indian 19-bus and 34-bus systems	72
4.5	Results of the multi-objective optimization of 50 runs obtained with DE	78
4.6	Comparison of the multi-objective optimization results as obtained with Case C planning using DE and CSA for 19-bus and 25-bus systems	79
4.7	Results of the multi-objective optimization of 50 runs obtained with DE	79
4.8	Comparison of the results as obtained with Case C planning using DE and CSA for Indian 19-bus and 34-bus systems	79

4.9	The optimal location, angle, and KVA rating as obtained with DE for different bus systems	80
5.1	Comparison of results of planning <i>Case C</i> of 50 runs as obtained with DE, and CSA, for 19- and 25-bus systems	89
5.2	Comparison of results of planning <i>Case C</i> of 50 runs as obtained with DE, and CSA, for Indian 19- and 34-bus systems	89
5.3	Comparison of the results as obtained with Case C (multi-objective) planning using DE and CSA for 19- and 25- bus system	90
5.4	Comparison of the results as obtained with Case C (multi-objective) planning using DE and CSA for Indian 19- and 34- bus system.....	91
5.5	The optimal location and rating of DGs for the 19- bus, 25- bus, Indian 19- bus, and 34- bus system as obtained with DE.....	91
5.6	Comparison of the minimum bus voltage of the solutions obtained with different planning cases	91
6.1	Comparison of results of planning <i>Case C</i> of 50 runs as obtained with DE, and CSA, for 19- and 25-bus systems	103
6.2	Comparison of results of planning <i>Case C</i> of 50 runs as obtained with DE, and CSA, for Indian 19- and 34-bus systems	104
6.3	Comparison of the results as obtained with Case C (multi-objective) planning using DE and CSA for 19- bus and 25- bus system	105
6.4	Comparison of the results as obtained with Case C (multi-objective) planning using DE and CSA for Indian 19- and 34- bus system.....	105
6.5	The optimal location and rating of DGs and DSTATCOM for the 19- bus, 25- bus, Indian 19- bus, and 34- bus system as obtained with DE	106
6.6	The optimal DSTATCOM angle as obtained with DE for the 19- bus, 25- bus, Indian 19- bus, and 34- bus system	106

List of Abbreviations

AI	Artificial Intelligence
BL	Branch Length
BN	Branch Number
CSA	Cuckoo Search Algorithm
DE	Differential Evolution
DG	Distributed Generations
DSTATCOM	Distribution Static Compensators
FT	Fitness Function
GA	Genetic Algorithm
KCL	Kirchhoff's Current Law
KVL	Kirchhoff's Voltage Law
LC	Line Code
MATLAB	Matrix Laboratory
PSO	Particle Swarm Optimization
RB	Receiving End Bus
SB	Sending End Bus
SD	Standard Deviation
URDS	Unbalanced Radial Distribution System

List of Notations

ctz	Vector of different conductor types
I_j^{\max}	Maximum current at branch j
$\vec{I}_{sn_\alpha}^p$	Phasor sum of total branch/line current entering at the sending end bus for phase p for line/branch α
\overline{IL}_2^x	load current vector (in phasor form) for Phase x
\overline{IN}_2	Neutral current vector at bus 2
I_{12}^a	Current vector flowing in phase a
L	Positive integer value
ND	Number of DSTATCOM
NG	Number of members in a particle
NP	Number of particles in a group
NBR	Number of branches
P_2^a	Active load demand for phase a, at bus 2
P_i^{\min}	Minimum power generated by DG
P_i^{\max}	Maximum power generated by DG
PL_α^p	Real power loss for line α for phase p
$P_{D_{ip}}^{DG}$	Active and reactive power demand for p^{th} phase of i^{th} bus of the base-case network
Q_2^a	Reactive load demand for phase a, at bus 2
Q_j^x	Reactive power demand at bus j for phase x
$QC1$	First Capacitor rating placed at bus j
$Qdstat_{\max}$	Maximum value of DSTATCOM rating

\dot{s}_j^a	Individual phase loading (the dot above s represents complex value) for phase a
S_{i_a}	Complex power demand for bus i for phases a
$v_i(t)$	The i^{th} trial vector in iteration t
V_{rated}	Represents the rated phase voltage
VP_{ij}^r	Velocity of the j^{th} member of i^{th} particle at r^{th} iteration
V_s^{min}	Minimum bus voltage
V_s^{max}	Maximum bus voltage
$\vec{V}_{sn_\alpha}^p$	Receiving end bus voltage (in phasor form) for line/branch section α and phase p
$x_i(t)$	The i^{th} population member in iteration t
z_{12}^{aa}	Self-impedance of phase a
z_{12}^{ab}	Mutual impedance between phases
$[Zp]_{12}$	Phase impedance matrix for branch connected between bus 1 and 2
ϕ	Vector of capacitor locations

Chapter 1

Introduction and Literature Survey

1.1 Introduction

The main attributes of power systems are generating system, transmission system, and distribution system. Among these systems, the distribution system plays a pivotal role in power system as it provides energy to the consumers safely, reliably, and economically. However, due to high R/X ratio, and low operating voltages, most of the losses occur in the distribution system. Moreover, distribution systems are generally unbalanced due to unequal single phase loads at the three phases of the system, and also additional unbalancing is introduced due to nonequilateral conductor spacing. This, initiates voltage and current unbalance in the system and increases the total neutral current of the system causing unnecessary tripping of the relay. So, service quality and reliability of the distribution system reduces. Therefore, a suitable phase balancing strategy is required to mitigate the phase unbalancing in the unbalanced distribution systems. Also, apart from reducing the phase unbalancing in the unbalanced distribution systems, a suitable strategy is required to minimize the system power loss. In this regard, it is imperative for the distribution engineers to plan the unbalanced distribution systems in order to reduce the losses, voltage unbalances, and neutral current of the system for safe and reliable operation.

This chapter is organized as follows: An Overview of Unbalanced Distribution Networks Planning is presented in section 1.2. In Section 1.3, the approaches for the Unbalanced Distribution Networks Planning is discussed. In Section 1.4, the literature Survey is explained, Whereas Section 1.5 bring out the motivation points of the present

work. The dissertation objectives are presented in section 1.6. Finally, dissertation outline is presented in Section 1.8.

1.2 An Overview of Unbalanced Distribution Networks Planning

The distribution system is defined as the part of the power system, which distributes power to consumers [1]. In the present scenario alternating current (a.c.) distribution systems are widely used for power distribution due to it's simplicity and cost effectiveness in comparison to direct current (d.c.) distribution system. Further, the a.c. distribution are classified in view of load sharing as 1) Balanced distribution system, 2) Unbalanced distribution system. A schematic layout of a sample two bus unbalanced distribution system is shown in Fig. 1.1.

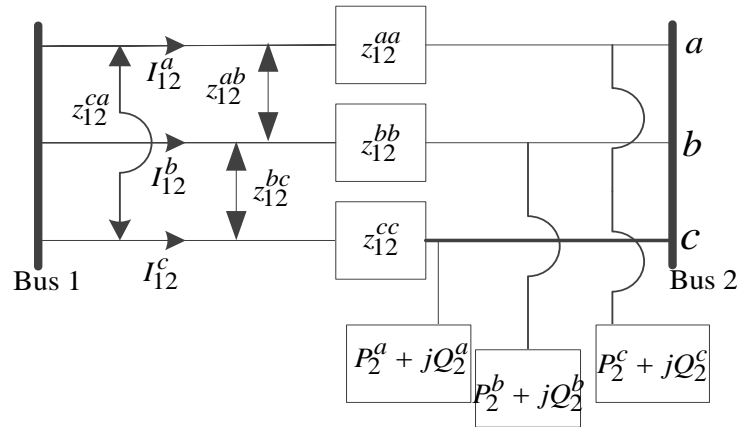


Fig. 1.1. A schematic layout of a sample two bus unbalanced distribution system

Where, z_{12}^{aa} , z_{12}^{bb} , and z_{12}^{cc} denotes self-impedance [2] of phase a, phase b, and phase c respectively; z_{12}^{ab} , z_{12}^{bc} , and z_{12}^{ca} denotes mutual impedance [carson] between phases; I_{12}^a , I_{12}^b , and I_{12}^c represents current vector flowing in phase a, phase b, and phase c in between bus 1 and 2 respectively; P_2^a , and Q_2^a denotes active load demand and reactive load

demand for phase a, at bus 2. For the two bus distribution network, the unbalanced condition can be derived from Fig. 1.1 as follows:

$$P_2^a \neq P_2^b \neq P_2^c \quad (1.1)$$

$$Q_2^a \neq Q_2^b \neq Q_2^c \quad (1.2)$$

However, for the conventional balanced distribution system; the necessary conditions are as follows:

$$P_2^a = P_2^b = P_2^c \quad (1.3)$$

$$Q_2^a = Q_2^b = Q_2^c \quad (1.4)$$

$$z_{12}^{ab} = z_{12}^{bc} = z_{12}^{ca} = 0 \quad (1.5)$$

$$z_{12}^{aa} = z_{12}^{bb} = z_{12}^{cc} \quad (1.6)$$

So, the balanced distribution system doesn't encounter the voltage, and current unbalance problem due to equal load sharing, and zero mutual impedance values.

Now, the load current vector (in phasor form; where $x \in a, b, c$) at phase a, b, and c can be computed for Fig. 1.1 as follows:

$$\overline{IL}_2^a = \frac{P_2^a - jQ_2^a}{\left(\overline{V}_2^a\right)^*} \quad (1.7)$$

$$\overline{IL}_2^b = \frac{P_2^b - jQ_2^b}{\left(\overline{V}_2^b\right)^*} \quad (1.8)$$

$$\overline{IL}_2^c = \frac{P_2^c - jQ_2^c}{\left(\overline{V}_2^c\right)^*} \quad (1.9)$$

Next, applying Kirchhoff's current law at bus 2 for Fig. 1.1, the branch currents are obtained as:

$$\overline{I}_{12}^a = \overline{IL}_2^a \quad (1.10)$$

$$\overline{I}_{12}^b = \overline{IL}_2^b \quad (1.11)$$

$$\overline{I}_{12}^c = \overline{IL}_2^c \quad (1.12)$$

Replacing the conditions of Eqs. (1.1)-(1.2) in Eqs. (1.7)-(1.9), it is clear that the load current vector is different for each of the phases. Thus, the neutral current vector (not shown in Fig. 1.1) is computed as:

$$\overline{IN}_2 = \overline{I}_{12}^a + \overline{I}_{12}^b + \overline{I}_{12}^c \quad (1.13)$$

From Eq. (1.13) it can be concluded the neutral current is high due to unequal branch currents. Further, the bus 2 voltage is calculated using Kirchhoff's voltage law as follows:

$$\begin{bmatrix} \overline{V}_2^a \\ \overline{V}_2^b \\ \overline{V}_2^c \end{bmatrix} = \begin{bmatrix} \overline{V}_1^a \\ \overline{V}_1^b \\ \overline{V}_1^c \end{bmatrix} - [Zp]_{12} \begin{bmatrix} \overline{I}_{12}^a \\ \overline{I}_{12}^b \\ \overline{I}_{12}^c \end{bmatrix} \quad (1.14)$$

Where, $[Zp]_{12}$ is the phase impedance matrix for branch connected between bus 1 and 2 for Fig. 1.1. and is given as:

$$[Zp]_{12} = \begin{bmatrix} z_{12}^{aa} & z_{12}^{ab} & z_{12}^{ac} \\ z_{12}^{ba} & z_{12}^{bb} & z_{12}^{bc} \\ z_{12}^{ca} & z_{12}^{cb} & z_{12}^{cc} \end{bmatrix} \quad (1.15)$$

It is noted from Eq. (1.11) as:

$$z_{12}^{ba} = z_{12}^{ab} \quad (1.16)$$

$$z_{12}^{bc} = z_{12}^{cb} \quad (1.17)$$

$$z_{12}^{ca} = z_{12}^{ac} \quad (1.18)$$

The detail formulation of the phase impedance matrix can be obtained from [2]. From Eq. (1.14), it is evident that the voltage also becomes unbalance due to unequal branch currents in phases. Moreover, the power loss and complex power unbalance increases due to unbalances in the voltage and the current; as power depends upon voltage and current. Thus, these issues in unbalanced distribution systems have enforced the planner to develop an appropriate planning strategy.

The distribution system planning is defined as the process that ensures safe and reliable operation of distribution systems; while satisfying various constraints [3]. The planning proposes a new distribution network/system with a different set of conductors and phase loading.

As discussed, the key technical issues for the unbalanced distribution systems planning are the high power loss, the voltage unbalance, the neutral current, and the power unbalance. Thus, there is need and scope to plan unbalanced distribution systems or propose a new/alternative distribution systems with low power loss, voltage, current, and power unbalance for safe and reliable operation.

1.3 Unbalanced Distribution Networks planning problem

The unbalanced distribution networks planning problem can be formulated as shown in Fig. 1.2.

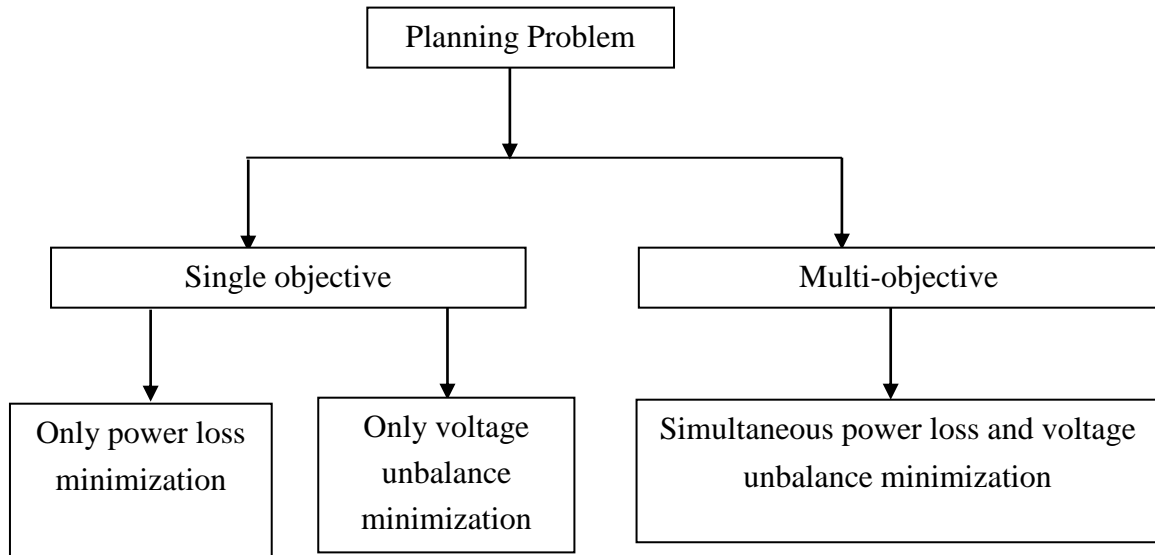


Fig. 1.2. Classification of planning problem

The unbalanced distribution networks planning problem can be categorized into two types; 1) Single objective, 2) Multi-objective.

In single objective problem, the goal is to either minimize or maximize a single (only one) objective function. Whereas, in multi-objective problem multiple objectives (more than one) objective functions are simultaneously minimized or maximized. The objectives are aggregated with some weighting coefficients into a single objective value. However, the weight assignment can be done depending upon the preference set by the operator.

1.3 Approaches for the Unbalanced Distribution Networks Planning

The planning approaches/solution strategies [4] of distribution system can be broadly classified as shown in Fig. 1.3.

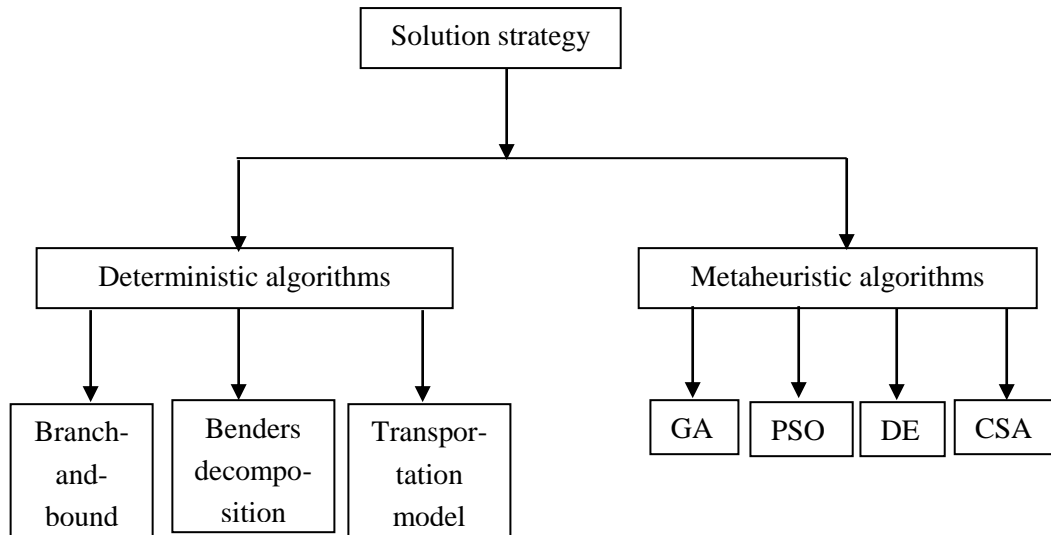


Fig. 1.3. Classification of solution strategies

The solution methodologies can be categorized into two types; 1) deterministic algorithms based, 2) metaheuristic algorithm based.

The salient features of the deterministic algorithms are:

- Suffer from the curse of dimensionality
- Difficulty in handling nonlinearity and nonconvexity
- Mostly, derivative based

The salient features of metaheuristic algorithms are:

- Multi-point search ability
- Efficient in handling nonlinearity and nonconvexity
- Derivative-free based

In recent times, the metaheuristic algorithms such as the DE, the CSA, the PSO, the GA, etc. are gaining popularity for solving complex real world problem in engineering, industry, power sector, etc. due to simplicity and easy calculation procedures.

1.5 Review of Literature

In this section, a literature survey corresponding to unbalanced distribution systems planning is presented. In the field of unbalanced distribution system planning, the three phase unbalanced load flow algorithm acts as a subroutine for the computation of the power loss, and the voltage magnitude of buses and its importance is discussed in [5-12]. The unbalanced load flow algorithm can be classified into two approaches; the Newton-Raphson based [5, 6] and the forward-backward based (FBS) approaches [6-12]. The NR-based approaches require the formation of the Jacobian matrix and the power flow mismatch calculation for obtaining load flow solutions. The FBS approach consists of two steps. In the first step, the current in each line/branch is calculated by Kirchhoff's current law (KCL). Then, the voltage at each bus is computed using the Kirchhoff's voltage law (KVL). Over the years the FBS based algorithm has gained popularity, due to its simple, easy, and efficient calculation procedure.

The phase balancing plays an important role in unbalanced distribution system planning, as it reduces the phase unbalancing among the three phases of the system. The numerous phase balancing strategy have been discussed in [13-25]. The solution strategies used in the literature are mostly based on metaheuristic algorithms. This includes single-point search based metaheuristic algorithms, such as the tabu search [13] and the simulated annealing [14] and population-based, i.e., multi-point search based metaheuristic algorithms, such as the genetic algorithm (GA) [15-17], artificial immune algorithm [18], differential evolution [19], and modified particle swarm optimization [20]. The authors in [21] have used the expert system for phase balancing. In [22], a mixed integer programming has been utilized in order to obtain optimal loading among the phases. The authors in [23] have developed a phase balancer for minimization of phase unbalancing. A current based index [24] has been used for the phase balancing. The

authors in [25] have utilized a mixed integer linear programming in order to obtain optimal phase balancing. Most of the researchers have used metaheuristic based algorithms as they provide a feasible solution in less time compared to the conventional algorithm such as mixed integer programming.

The selection of the proper conductor sizes is regarded as one of the key aspects in distribution system planning, as it improves the power loss and voltage profile of the system. Several works have been reported in the area of conductor size optimization [26-39]. The authors in [26] have proposed a two-step approach for minimizing the total cost, In [27], a heuristic approach was developed in order to minimize the system power loss and maximize the total saving, a mixed-integer linear programming method [28] was used to minimize the network power loss and investment cost. The PSO was used in [29] for the real power loss minimization, The authors in [30], have utilized evolutionary strategies for minimization of sum of the capital and the energy loss cost, In [31], a harmony search algorithm with differential operator was implemented for loss minimization and voltage profile improvement, a load flow method was employed in [32, 33] for the minimization of capital investment and real power loss cost. The authors in [34] have developed a fast algorithm for the determination of optimal conductor sizes. In [35], an evolutionary algorithm has been proposed in order to minimize the sum of capital investment and capitalized energy loss cost. The authors in [36] have obtained the optimal distribution planning through conductor grading. A simple method for conductor size selection has been developed in [37]. Khalil and Gorpinich [38] have used selective PSO for the optimal conductor sizing. The author in [39] has employed harmony search algorithm for the determination of optimal conductor sizing so as to minimize the system power loss. From the literature it can be observed that the metaheuristic algorithms work efficiently than other conventional approaches.

The integration of the reactive power compensating devices such as capacitor can reduce the power loss, improve the voltage profile, and the voltage unbalance of the distribution systems. Several works on the capacitor allocation and sizing have been discussed in [40-57]. The solution methodologies used for the capacitor allocation problem can be categorized into two types such as the heuristic based [40, 41] and the

artificial intelligence-based (AI) [42-57]. The AI-based techniques are genetic algorithm [42], the bat algorithm and the cuckoo search [43], the particle swarm optimization (PSO) [44], the multi-objective PSO [45], the non-dominated genetic algorithm version – II [46], the honeybee mating optimization [47], the modified cultural algorithm [48], the penalty free GA [49], the improved harmony search algorithm [50], the whale optimization algorithm [51], cuckoo search algorithm [52], the biography based optimization algorithm [53], the GA and sensitivity based analysis [54], the mine blast algorithm [55], limaçon inspired spider monkey algorithm [56], and PSO [57]. The authors in [57] have explained the benefits of the AI-based techniques over heuristic-based techniques.

Another compensating device, such as the distribution static compensator (DSTATCOM) has gained importance for the planning problem as they can reduce power loss, voltage profile, and voltage unbalance of the unbalanced distribution systems. Further, this device can inject continuous variable reactive power into the system. The literature survey in this regard is discussed in [58-82]. In [58] the authors have implemented a neural network based controller for reducing the rating of DSTATCOM. The authors in [59] have proposed a controller for reducing the current harmonics. Fujita and Akagi [60] have utilized the DSTATCOM as an active shunt filter for improving voltage stability of the distribution systems. In [61] a multi-level DSTATCOM is employed for reducing the voltage sag and swell. A control algorithm for the unbalanced load compensation is derived in [62]. A controller based on DSTATCOM for mitigation of voltage dips in low and medium voltage system is devised in [63]. The authors in [64] have implemented the DSTATCOM for the phase current balancing and load compensation. The power factor improvement in a power distribution system is explained in [65]. In [66] a new control algorithm for the reactive power compensation in unbalanced loading conditions is developed. The authors in [67] have proposed different control algorithms for minimizing the total harmonic distortions and improving the load balancing. A current control strategy is implemented in [68] for the current and the harmonic compensation. The main drawback of these works [58-68] is that the modelling of DSTATCOM has been carried out considering a source and a single sensitive load and without considering multiple sensitive loads. The particle swarm based optimization was employed in order to obtain the optimal location and the size of distributed generations

and DSTATCOM for minimizing the system power loss [69]. Jazebi *et. al.* [70] implemented differential evolution algorithm considering network reconfiguration so as to minimize the power loss distribution networks. The authors in [71] utilized bacterial foraging algorithm in order to reduce the power loss, the total operational cost, and the voltage profile index of distribution systems. Salman *et. al* [72] have proposed a binary gravitation search algorithm in order to minimize the voltage sag in a distribution system. In [73], an analytic method was applied in minimizing the total system power loss and minimum voltage magnitude. Farhoodnea *et. al* [74] have employed firefly algorithm for optimizing the average voltage total harmonic distortion, average voltage deviation, and total investment cost. Tolabi *et. al* [75] have proposed fuzzy ant colony optimization for minimizing the system loss, increasing load balancing index, and the voltage profile of a system by simultaneous reconfiguration, optimal allocation of DSTATCOM and a photovoltaic array. The impact of the distributed generator on the allocation and size of DSTATCOM was investigated in [76]. Here, the total cost of DSTATCOM was considered the objective function to be minimized. Jain *et. al.* [77] have applied the voltage stability index method in order to obtain the optimal location of the DSTATCOM. The minimization of real power loss was chosen as the objective function. In [78], a fuzzy shuffled frog-leaping algorithm was developed so as to reduce the total power loss, the equal load balancing index, and voltage deviation by reconfiguring the network in the presence of capacitors, and DSTATCOM. Taher and Afsari have implemented [79] an optimization algorithm called the immune algorithm in order to minimize the power loss and the size of the DSTATCOM. Xiaoguang *et. al.* [80] have used a genetic algorithm in order to obtain the optimal network configuration for minimizing the total cost of the system with the help of DSTATCOM and dynamic voltage restorer. In [81], a meta-heuristic algorithm called the bat algorithm was applied to minimize the system power loss. It is an established fact that [80], the metaheuristic algorithms give better results than other conventional algorithms.

In recent times, the distributed generations (DG) sources such as the solar (PV) and the wind turbines are gaining popularity due to clean and green energy. Further, it helps in reducing the network power loss, and the voltage profile improvement of the system. The contributions of the DGs have been presented in [82-101]. Classifying the solution

strategies for the DG allocation and sizing problem as: genetic algorithm [82,83], the location of the DG was determined by using multi-objective voltage index analysis and size of DG was obtained using fast approach [84], Load Flow Analysis [85], Firefly algorithm [86], global harmony search algorithm, improved particle swarm optimization (improved PSO), and loss sensitivity factors simulated annealing [87], accelerated PSO, principal component analysis method [88], PSO [89], real power flow sensitivity and real power loss sensitivity [90], modified artificial bee colony algorithm [91], Hybrid big-bang big crunch algorithm [92], supervised big-bang big crunch algorithm [93], GA based tabu search [94], modified artificial bee-colony algorithm [95], analytical method [96], voltage index analysis [97-98], an efficient analytical method [99], a combined genetic and analytical approach [100], and gravitational search based optimization algorithm [101].

From the above literature, it has been observed that the evolutionary algorithms such as the DE, the CSA, the PSO, the GA, etc. are found to be efficient in comparison to analytical approaches for unbalanced distribution system planning. Further, the system power loss, the voltage unbalance, and other parameters are reduced by separately optimizing the individual phase loading, conductor sizing, the capacitor, the DSTATCOM, and the DG location, and rating respectively. Moreover, a three phase unbalanced modelling of DSTATCOM for unbalanced distribution networks is developed. Apart from this, the research reveals that the metaheuristic algorithms tend to entrap in local optima. Also, due to the probabilistic nature of metaheuristic algorithms, it is not possible to obtain the optimal results in a single run. Thus, all these factors motivated to plan the unbalanced distribution networks integrating the reactive power compensating devices such as the capacitor, the DSTATCOM, and the renewable energy sources such as the solar, the wind turbine. The verification of the performance of some popular optimization algorithms such as DE, CSA, PSO, and GA, has been carried out both quantitatively and qualitatively for multiple computer simulations runs.

1.6 Motivation

The distribution systems are traditionally unbalanced due to unequal single phase loads at the buses of the unbalanced distribution systems. Additional unbalancing is introduced due to the asymmetrical orientation of conductors. Thus, the load current at each phase such as phase a, b, and c become unequal. This causes unequal voltages among the phases of the system, causing disruptions in the consumer equipment. Hence, service quality is reduced. Also, due to the high resistance of the conductors and the low operational voltage maximum losses occur in the distribution system. It has been observed from the literature that individual optimization of various decision variables like, phase balancing, conductor sizing, reactive power compensation devices such as capacitors, DSTATCOM and renewable devices such as solar and wind turbine can provide or plan a network with reduced objective functions such as; the power loss, complex power unbalance, voltage unbalance, and neutral current. However, no work has been carried out in the literature to investigate the impact of;

- 1) Simultaneous optimization of phase balancing, conductor sizing, capacitor location, and sizing,
- 2) Simultaneous optimization of phase balancing, conductor sizing, DG location, and sizing,
- 3) Simultaneous optimization of phase balancing, conductor sizing, DSTATCOM location, and rating,
- 4) Simultaneous optimization of phase balancing, conductor sizing, DG location and sizing, DSTATCOM location, and rating for the planning of unbalanced distribution systems. Therefore, there is a scope to plan the unbalanced distribution networks so as to overcome the high unbalance, the power loss, and other system problems considering the simultaneous optimization of these decision variables.

The traditional planning method for the unbalanced distribution system is linear/nonlinear mixed integer programming algorithms. However, the main drawback of this algorithm is the inefficient handling of nonlinearity in planning problem [4]. Thus, an efficient algorithm/solution strategy is required for this planning problem. The recent trend in distribution system planning indicates that the population-based metaheuristic

algorithms are increasingly used, as they overcome most of the deficiencies of the traditional algorithms. However, as metaheuristic algorithms are random in nature, so convergence is not guaranteed in a single simulation run. Hence, it is necessary to perform a statistical comparison among them in order to understand their relative merits and demerits for multiple simulation runs.

From, the above discussions it is clear that for unbalanced distribution system planning, there is a need and scope to perform a statistical performance comparison among some of the metaheuristic algorithms in order to identify the best algorithm. Thus, the statistical performance of the metaheuristic algorithms for the planning of unbalanced distribution systems including the capacitor, the DSTATCOM, and the DG is the main source of motivation for the planning of unbalanced distribution system.

1.7 Research Objectives and Scope

From the discussion above, the dissertation objectives are as follows:

- To develop and implement a forward-backward based three-phase unbalanced load flow algorithm for unbalanced distribution systems.
- To implement metaheuristic algorithms for the planning of unbalanced distribution systems without capacitors, DG, and DSTATCOM.
- To implement metaheuristic algorithms for the planning of unbalanced distribution systems with capacitors.
- To model a three-phase unbalanced DSTATCOM and integrate it in unbalanced distribution systems for the planning using metaheuristic algorithms.
- To implement metaheuristic algorithms for the planning of unbalanced distribution systems with DG and DSTATCOM.

The scope of the present work is limited to the planning of the unbalanced distribution system using metaheuristic algorithms with the aim of minimizing several objective functions. The planning considers peak load and DG power generation condition.

1.8 Dissertation Outline

The remaining chapters of this thesis are organized as follows:

The Chapter 2 presents the development of a three phase unbalanced load flow algorithm for the unbalanced distribution systems, which is used as a subroutine for the planning. In this chapter, six objective functions are formulated. In the first approach they are optimized separately according to single objective optimization. Then, they are aggregated with weights similar to a multi-objective approach. Four metaheuristic algorithm such as the DE, the CSA, the PSO, and the GA are used as the solution strategy for determination of the optimal loading and the conductor sizes of the four unbalanced test systems. Further, the results obtained with these algorithms are compared among themselves.

The chapter 3 presents the development and incorporation of the single phase capacitor model for the unbalanced distribution systems for its planning. The six objective functions as discussed in chapter 2 are considered. Firstly, these objective functions are optimized separately as per the single objective optimization approach. Next, they are aggregated with weights as per the multi-objective approach for simultaneous phase balancing, conductor sizing, and capacitor allocation and rating. The same optimization algorithms as mentioned in chapter 2 are implemented and compared with each other for the planning of unbalanced distribution systems integrating the capacitor.

The chapter 4 presents planning approaches to determine the optimal phase balancing, conductor sizes, and DSTATCOM location, and rating for the unbalanced distribution systems by optimizing the six objective as discussed in Chapter 2. A three phase forward backward sweep load flow algorithm including the DSTATCOM model is developed in order to evaluate the objective functions. The optimization results of the different evolutionary algorithms such as DE, CSA, PSO, and GA are compared with each other.

The chapter 5 presents the development and incorporation of the three single phase DG model for unbalanced distribution systems for its planning. Here, both the single and the multi-objective optimization approach are carried out for simultaneous phase balancing, conductor sizing, and DG allocation and rating. The metaheuristic optimization algorithms as mentioned in chapter 2 are implemented and compared with each other including the DG with the four test systems.

The chapter 6 presents the development and incorporation of the single phase DG and a three phase DSTATCOM model for unbalanced distribution systems for its planning. The optimal phase balancing, conductor sizing, DG allocation and rating, and DSTATCOM allocation and rating are determined by minimizing several objective functions as discussed in chapter 2. The optimization results of the DE, CSA, PSO, and GA algorithms are compared with each other for both the DG and the DSTATCOM integration in the test systems.

Finally, the chapter 7 presents the conclusions and future scope of this work. In this chapter, the entire work has been summarized and concluded in a lucid manner. This chapter explains the efficacy of the proposed methodologies for the unbalanced distribution system planning. Further, the possible future directions of this planning work have been pointed out.

Chapter 2

Planning of Unbalanced Radial Distribution Systems Using Evolutionary Computing Algorithms in the Absence of DG, Capacitor, and DSTATCOM

2.1 Introduction

In chapter 1, the planning of unbalanced radial distribution systems has been presented. It discusses about the importance of the planning of unbalanced distribution systems (URDS). It also focuses on different approaches for the planning of URDS. Further, a detailed literature review is discussed.

As discussed in chapter 1, no work has been reported in the literature for the simultaneous optimization of the phase balancing and the conductor size for URDS. Although different types of metaheuristic algorithm are used as the solution strategy for this planning problem, there is no qualitative and/or quantitative performance comparison among them or some of them on the results of this planning problem. Thus, a qualitative performance on the comparison of the results of these algorithms can be an interesting study. This is discussed in this Chapter. Since the convergence is not guaranteed in metaheuristic algorithms, multiple simulation runs are taken. The results of multiple simulation runs indicate the ability of the metaheuristic algorithms in replicating the

results. The mean and standard deviation of the results obtained with 50 independent simulation runs are used in the quantitative comparison.

The objective functions formulated in the proposed approach are total power loss, average voltage drop, total complex power unbalance, total neutral current, and voltage unbalance factor [15]. The Differential evolution (DE) [102, 103], Particle swarm optimization (PSO), Cuckoo search algorithm (CSA), and Genetic algorithm (GA) is used as the solution strategy for minimizing these objective functions in order to obtain optimal loading among the phases and conductor sizes. DE, PSO, CSA, and GA are population based metaheuristic algorithm. For the evaluation of each objective, a forward-backward sweep load flow algorithm is developed. The proposed approach is demonstrated on the 19-bus, the 25-bus, the Indian 19-bus, and the 34-bus unbalanced radial distribution systems. A quantitative performance comparison of DE with three popular metaheuristic algorithms, such as cuckoo search algorithm (CSA) [104], particle swarm optimization (PSO) [105], and GA [16] is provided and discussed. The performance of DE is found to be better among them.

This chapter is organized as follows: Problem Formulation is presented in section 2.2. In Section 2.3, the proposed planning approach using DE, PSO, CSA, and GA is described. The proposed three phase forward-backward sweep algorithm is provided in section 2.4. The simulation results are presented in section 2.5 and discussed. Section 2.6 concludes the paper.

2.2 Problem Formulation

The objective of this planning problem is the minimization of the various objective functions subject to some technical constraints. These objective functions are described below.

1) *Total Complex Power Unbalance*: The complex power unbalance can be evaluated as follows.

$$s_j^u = \sqrt{\frac{1}{3} \sum_{p=a}^c \left| \dot{s}_j^p - \dot{s}_j^0 \right|^2} \quad (2.1)$$

In which, the \dot{s}_j^0 stands for an ideal per phase loading, and

$$\dot{s}_j^0 = \frac{(\dot{s}_j^a + \dot{s}_j^b + \dot{s}_j^c)}{3} \quad (2.2)$$

The $s_j^u=0$ means the complex power of j^{th} feeder segment is perfectly balanced.

\dot{s}_j^a , \dot{s}_j^b and \dot{s}_j^c are individual phase loading. The dot above the labels s denotes the variables having a complex value, the superscripts a , b and c stand for the corresponding phases and j denotes the specified number of the feeder segment. The total complex power unbalance of a feeder is evaluated as:

$$TS_u = \sum_{j=1}^{NBR} s_j^u \quad (2.3)$$

In which, the NBR is the total number of feeder segments.

2) *Total Power Loss*: Power loss reduction can improve system voltage profile and operational efficiency of a distribution system. A three phase line/branch section model is shown in Fig. 2.1.

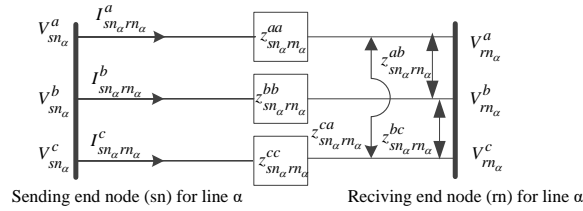


Fig. 2.1. A three-phase line section model

Where, $z_{sn_α rn_α}^{aa}$, $z_{sn_α rn_α}^{bb}$, and $z_{sn_α rn_α}^{cc}$ denote self-impedances for phases a , b , and c , respectively in Kron's reduction form; $z_{sn_α rn_α}^{ab}$, $z_{sn_α rn_α}^{bc}$, and $z_{sn_α rn_α}^{ca}$ denote mutual impedance between phases in Kron's reduction form.

From Fig. 1, the real power loss of the three phase line section is obtained by computing the difference between the sending and the receiving end bus power as given below.

$$PL_{\alpha}^p = \text{Re} \left\{ \sum_{p \in \{a,b,c\}} \left[\vec{V}_{sn_{\alpha}}^p \left(\vec{I}_{sn_{\alpha}}^p \right)^* - \vec{V}_{rn_{\alpha}}^p \left(\vec{I}_{rn_{\alpha}}^p \right)^* \right] \right\} \quad (2.4)$$

Where, $\vec{V}_{sn_{\alpha}}^p$ and $\vec{V}_{rn_{\alpha}}^p$ represent the sending end bus and receiving end bus voltage (in phasor form) for line/branch section α and phase p , respectively; $\vec{I}_{sn_{\alpha}}^p$ represents phasor

sum of total branch/line current entering at the sending end bus and $\vec{I}_{rn_\alpha}^p$ represents the branch current leaving at the receiving end bus for phase p for line/branch α . These two current are related according to the Eq. (2.5).

$$\vec{I}_{sn_\alpha}^p = \vec{I}_{rn_\alpha}^p + \vec{I}_{L_{sn}}^p \quad (2.5)$$

Where, $\vec{I}_{L_{sn}}^p$ represents load current for the sending end bus for phase p for line/branch section α . The total real power loss for a system having NBR number of line/branch sections can be obtained as:

$$PL = \sum_{\alpha=1}^{NBR} \sum_{p \in \{a,b,c\}} PL_\alpha^p \quad (2.6)$$

3) *Average Voltage Drop*: Better load balance can reduce the voltage drop formulated according to Eqs. (2.7)-(2.8).

$$AV_d = \frac{1}{NB} \sum_{k=1}^{NB} VD_k \quad (2.7)$$

$$VD_k = \frac{1}{3} \sum_{p \in \{a,b,c\}} \left| \frac{V_{rated} - V_k^p}{V_{rated}} \right| \times 100\% \quad (2.8)$$

In theses equations V_{rated} represents the rated phase voltage, V_k^p denotes the magnitude of the phase voltage of phase p at load point k . VD_k denotes the average of three phase voltage drops at load point k and NB is total number of buses.

4) *Total Voltage Unbalance Factors*: The total zero-sequence voltage unbalance factor (ZSUF), and total negative-sequence voltage unbalance factor (NSUF) are defined as below.

$$ZSUF = \sqrt{\frac{1}{NB} \sum_{k=1}^{NB} (d_{0,k})^2} \quad \{ \text{Where, } d_{0,k} = \frac{V_k^{(0)}}{V_k^{(1)}} \} \quad (2.9)$$

$$NSUF = \sqrt{\frac{1}{NB} \sum_{k=1}^{NB} (d_{2,k})^2} \quad \{ \text{Where, } d_{2,k} = \frac{V_k^{(2)}}{V_k^{(1)}} \} \quad (2.10)$$

Where $V_k^{(0)}$, $V_k^{(1)}$ and $V_k^{(2)}$ denote the zero, positive and negative-sequence voltages at load point k , respectively and $d_{0,k}$ and $d_{2,k}$ denote the zero and negative-sequence voltage unbalance factors at load point k , respectively.

5) *Total Neutral Current*: The neutral current is the summation of three phase currents of all branches.

$$I_N = \sum_{j=1}^{NBR} \sum_{p \in a,b,c} I_j^p \quad (2.11)$$

Where, the I_j^p represents the current in phase p of the branch of a given system, I_N is the total neutral current.

Two approaches are used to optimize these objectives. In the first approach, these objectives are separately optimized as follows:

$$\text{Maximize} \quad FTS = 1 / fs \quad (2.12)$$

Where FTS is the single objective fitness function, and fs is the objective function from Eq. (2.3), Eqs. (2.6-2.7), Eqs. (2.9-2.11). Out of these objective functions, each objective function is optimized only one at a time.

In the second approach, they are aggregated with weights as a multi-objective optimization problem as given below.

$$f = \left(w_1 \frac{TS_u - TS_u^{\min}}{TS_u^{\max} - TS_u^{\min}} + w_2 \frac{PL - PL^{\min}}{PL^{\max} - PL^{\min}} + w_3 \frac{AV_d - AV_d^{\min}}{AV_d^{\max} - AV_d^{\min}} + w_4 \frac{ZSUF - ZSUF^{\min}}{ZSUF^{\max} - ZSUF^{\min}} + w_5 \frac{NSUF - NSUF^{\min}}{NSUF^{\max} - NSUF^{\min}} + w_6 \frac{I_N - I_N^{\min}}{I_N^{\max} - I_N^{\min}} \right) \quad (2.13)$$

$$\text{Where,} \quad w_1 + w_2 + w_3 + w_4 + w_5 + w_6 = 1.0 \quad (2.14)$$

In multi-objective optimization approach, the fitness function (FT) for DE is assigned as follows:

$$\text{Maximize} \quad FT = 1 / f \quad (2.15)$$

These objective functions are minimized under the following constraints:

i. Voltage Constraint

Voltage at each bus must remain within the permissible range.

$$V_s^{\min} \leq V_s^{abc} \leq V_s^{\max} \quad (2.16)$$

ii. Thermal Constraint

The current flowing through each branch must be within the maximum current carrying capacity of the conductor.

$$I_j^{abc} \leq I_j^{\max} \quad (2.17)$$

2.3 Proposed Approach

DE is used as the solution methodology for planning problem of unbalanced radial distribution systems. A brief overview on DE is provided in the following subsection.

2.3.1 Differential Evolution (DE) Algorithm: An Overview

DE is a population-based multi-point search algorithm [102]. There are several variants of DE algorithm, and a state-of-art review can be obtained in [103]. The different variants of DE are classified using the notation: $DE/\alpha/\beta/\delta$; where α indicates the method for selecting the parent chromosome, β indicates the number of difference vectors used to perturb the base chromosome, and δ indicates the crossover mechanism used to create the offspring population. In this work, $DE/rand/1/bin$ variant is used. The acronym *bin* indicates crossover operation is controlled by a series of binomial experiments. The search starts with a randomly chosen initial population of n -dimensional chromosomes which are iteratively evolved using three operations, i.e., mutation, crossover, and selection. The i^{th} population member in iteration t is given by:

$$x_i(t) = (x_{i1}(t), x_{i2}(t), \dots, x_{in}(t)) \quad (2.18)$$

In each iteration, also called generation, a mutation vector is created, which is a vector difference of two randomly selected chromosomes. Then, crossover and selection operations are performed to generate trial vectors. The better chromosomes are selected by using selection operation. These processes are briefly discussed below.

2.3.1.1 Mutation

For each target individual $x_i(t)$, a mutant vector $h_i(t)$ is generated according to

$$h_i(t+1) = x_{r1}(t) + F(x_{r2}(t) - x_{r3}(t)) \quad r1 \neq r2 \neq r3 \neq i \quad (2.19)$$

Where, indices $r1, r2, r3 \in [1, \eta_{pop}]$ are generated randomly, $F \in [0, 2]$ is a scale factor which controls the mutation size.

2.3.1.2 Crossover

The trial vector is generated as follows:

$$v_i(t) = (v_{i1}(t), v_{i2}(t), \dots, v_{in}(t)) \quad (2.20)$$

$$v_{ij}(t+1) = \begin{cases} h_{ij}(t+1) & \text{rand}_{ij}[0,1] \leq CR \text{ or } j = j_{rand} \\ x_{ij}(t) & \text{rand}_{ij}[0,1] > CR \text{ or } j \neq j_{rand} \end{cases} \quad (2.21)$$

Where, CR is a crossover constant in the range [0, 1] specified by user, and j_{rand} is a randomly chosen integer in the range [1, η_{pop}] to ensure that the trial vector v_i gets at least one element from the mutation vector, rand_{ij} [0, 1] is a uniformly distributed random number for each j^{th} component of the i^{th} parameter vector.

2.3.1.3 Selection

The selection operation generates better offspring (vectors) from the target (parent) individual and the trial (child) vector:

$$x_i(t+1) = \begin{cases} v_i(t+1) & FT(v_i(t+1)) > FT(x_i(t)) \\ x_i(t) & FT(v_i(t+1)) < FT(x_i(t)) \end{cases} \quad (2.22)$$

Where, $FT(.)$ is the fitness function to be maximized.

2.3.1.4 Encoding Strategy

A chromosome for DE representing a candidate solution in this planning problem consists of two segments as shown in Fig. 2.2 They are:

- (i) The first segment represents complex power demand for each phase for each bus except the substation bus. $S_{i_a}, S_{i_b}, S_{i_c}$ represent complex power demand for bus i for phases a, b , and c , respectively and NB is the number of buses.
- (ii) The second segment represents types of conductor used in each branch, where NBR is the total number of branches.

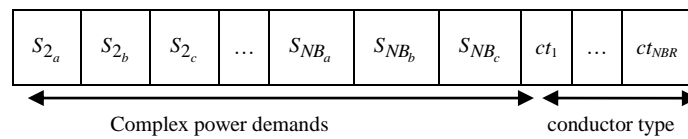


Fig. 2.2: Encoding strategy for a chromosome in DE

2.3.1.5 Flow Chart of the Proposed Approach using DE

The flowchart for the planning approach using DE is shown in Fig. 2.3. The proposed three phase forward-backward sweep load flow algorithm, one of the important subroutines used in the planning, is described in the following section.

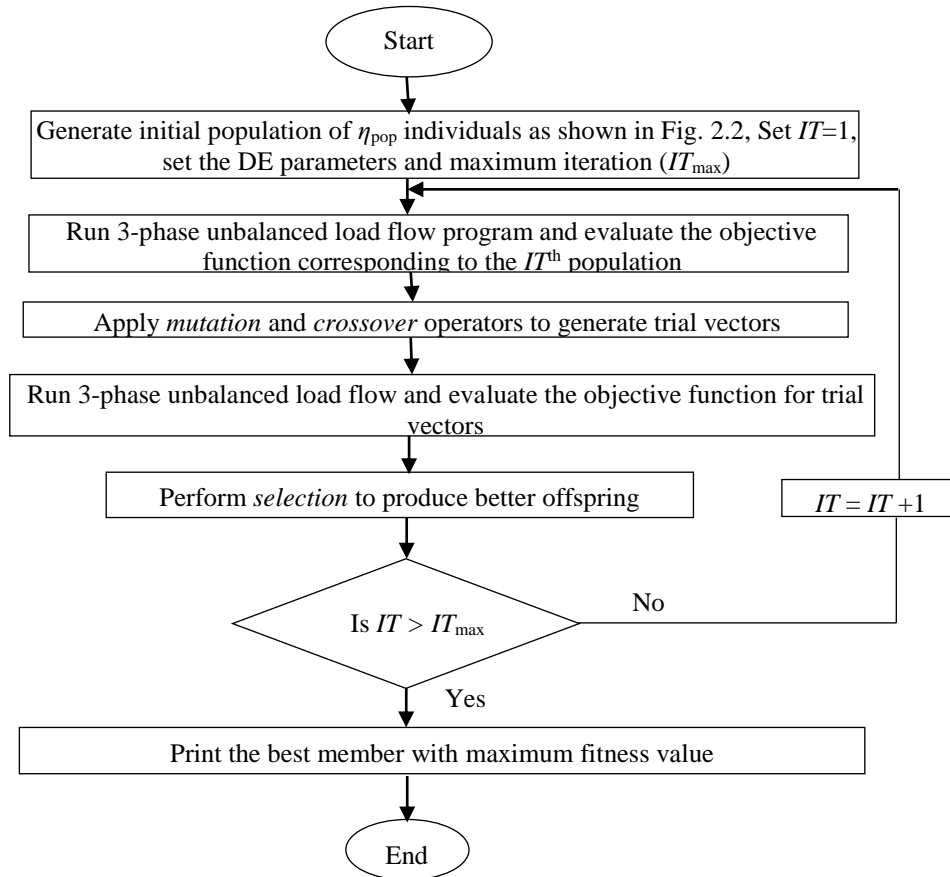


Fig. 2.3: Flow chart of the planning approach using DE

2.3.2 Overview of cuckoo search algorithm

Cuckoo search algorithm (CSA) was developed by Xin-She Yang and Suash Deb by observing the intelligent egg laying strategy of cuckoos. They lay their eggs in a randomly chosen host nest for their survival. If the host nest identifies cuckoo eggs, it will either throw away their eggs or build a new nest somewhere else. The nest in the CSA algorithm is same as the population, which is used in particle swarm optimization. Each egg in the nest represents the possible solution or decision variable for the optimization problem. The CSA follows three rules [104] as:

- Each cuckoo lays one egg at a time, and abandons in a random nest;
- The better quality eggs (good solutions) moves to next generations;
- A host bird can discover an alien egg with a probability, $p_a = [0, 1]$ and builds a new nest at a new location or completely abandons its own nest or throw away the eggs.

CSA generates random host nest using levy flight for new solution x_i^{t+1} as:

$$x_i^{t+1} = x_i^t + \alpha \times \text{Levy}(\lambda) \quad (2.23)$$

Where $\alpha > 0$, denotes the step size

$$\text{Levy}(\lambda) = \left| \frac{\Gamma(1 + \lambda) \times \sin(\frac{\pi \times \lambda}{2})}{\Gamma(\frac{1 + \lambda}{2}) \times \lambda \times 2^{\frac{\lambda-1}{2}}} \right|^{\frac{1}{\lambda}} \quad (2.24)$$

2.3.2.1 Flow chart of the planning approach using the cuckoo search algorithm

The flowchart of the planning approach using CSA is shown in Fig. 2.4.

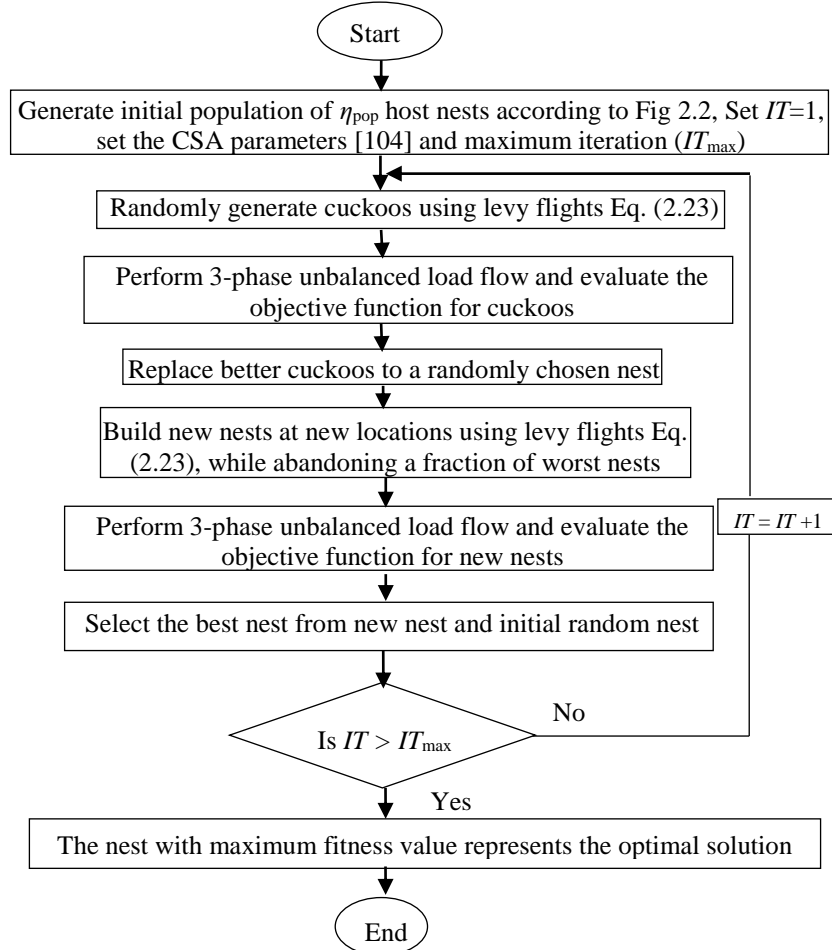


Fig. 2.4. Flow chart of the planning approach using CSA

2.3.3 Overview of particle swarm optimization algorithm

Eberhart and Kennedy developed particle swarm optimization (PSO) by observing the movement of birds and fishes [105]. It is basically a population based metaheuristic algorithm. In this algorithm, each particle is initialized with a random velocity. The particle changes its position and velocity by own observation and other particles movement. The initial position and velocity of the particle is computed as follows:

$$VP_{ij}^r = wVP_{ij}^r + C_1R_1(Pb_{ij} - P_{ij}^r) + C_2R_2(G_j^r - P_{ij}^r) \quad (i=1,2,\dots,NP;j=1,2,\dots,NG) \quad (2.25)$$

$$P_{ij}^{r+1} = P_{ij}^r + VP_{ij}^{r+1} \quad (i=1,2,\dots,NP;j=1,2,\dots,NG) \quad (2.26)$$

Where,

VP_{ij}^r is the velocity of the j^{th} member of i^{th} particle at r^{th} iteration;

$$V_{ij}^{\min} \leq V_{ij}^r \leq V_j^{\max}$$

P_{ij}^r is the current position of the j^{th} member of i^{th} particle at r^{th} iteration;

w is the weighing function or inertia weight factor

C_1 and C_2 are the acceleration constants

R_1 and R_2 is a random number between 0 and 1

NP is the number of particles in a group

NG is the number of members in a particle

The particles then change their movements using the following equations:

$$VP_{ij}^{new} = wVP_{ij} + C_1R_1(P_{ij}^{best} - P_{ij}^r) + C_2R_2(G_j^{best} - P_{ij}^r) \quad (i=1,2,\dots,NP;j=1,2,\dots,NG) \quad (2.27)$$

$$P_{ij}^{new} = P_{ij} + VP_{ij}^{new} \quad (i=1,2,\dots,NP;j=1,2,\dots,NG) \quad (2.28)$$

The inertia weight w is calculated as:

$$w = w^{\max} - \frac{w^{\max} - w^{\min}}{ITER^{\max}} * ITER \quad (2.29)$$

Where

$ITER^{\max}$ is the maximum number of iterations(generation) and

$ITER$ is the current number of iterations.

The maximum and minimum velocity limit in the j^{th} dimension is computed as:

$$V_j^{\max} = \frac{P_j^{\max} - P_j^{\min}}{\alpha} \quad \text{and} \quad V_j^{\min} = -\frac{P_j^{\max} - P_j^{\min}}{\alpha} \quad (2.30)$$

Where α is the chosen number of intervals in j^{th} dimension [105].

2.3.3.1 Flow chart of the planning approach using the PSO algorithm

The flowchart of the planning approach using PSO algorithm is shown in Fig. 2.5.

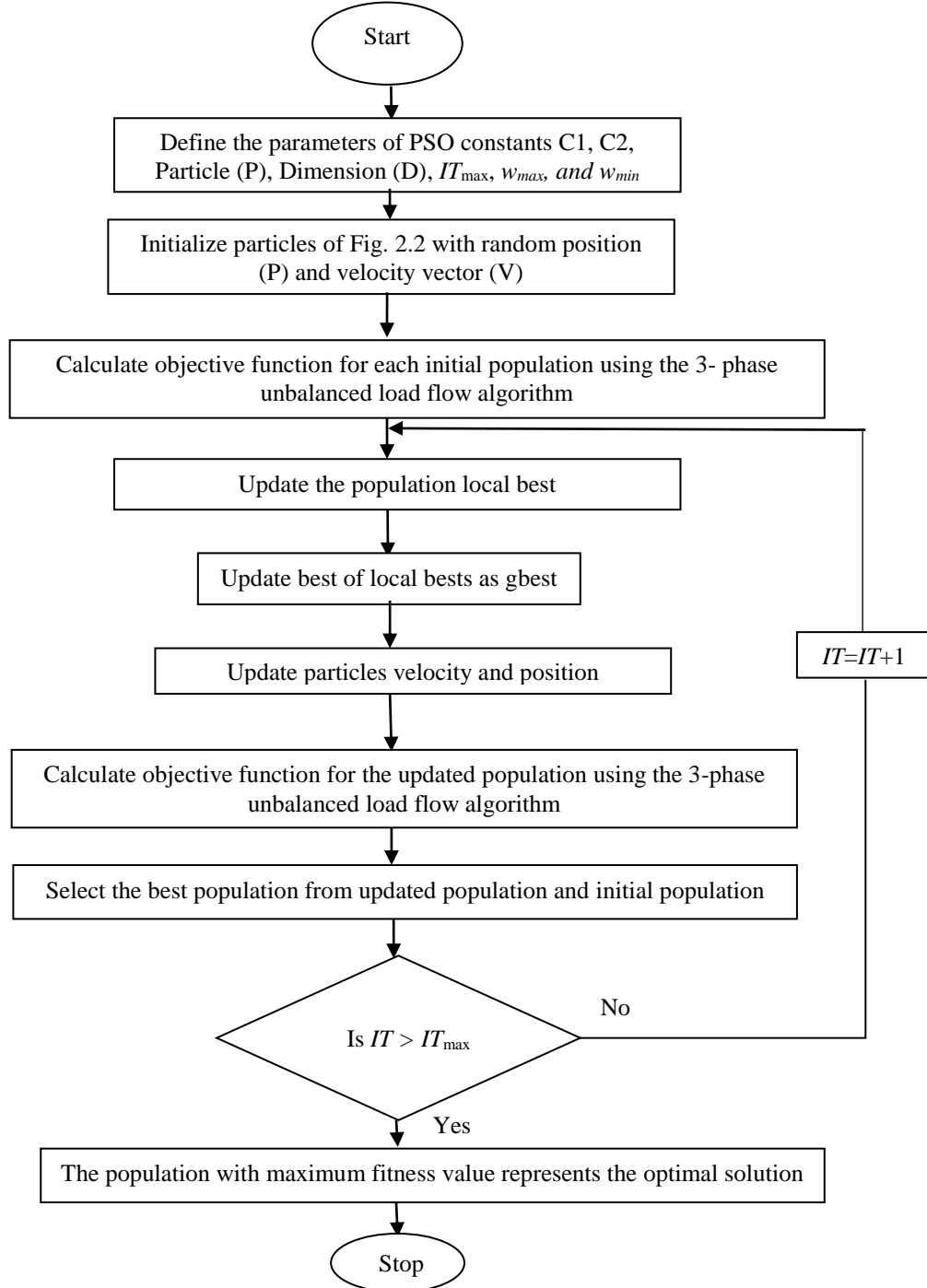


Fig. 2.5. Flow chart of the planning approach using PSO algorithm

2.3.4 Overview of genetic algorithm

Genetic algorithm (GA) [106] is a popular evolutionary computing algorithm that operates on the Darwinian survival of the fittest principle. In this algorithm, the best solution or chromosome is obtained iteratively using selection, crossover, and mutation operation for either minimization or maximization of the fitness function.

2.3.4.1 The flowchart for the planning approach using GA

The flow chart of the planning approach using GA is provided in Fig. 2.6.

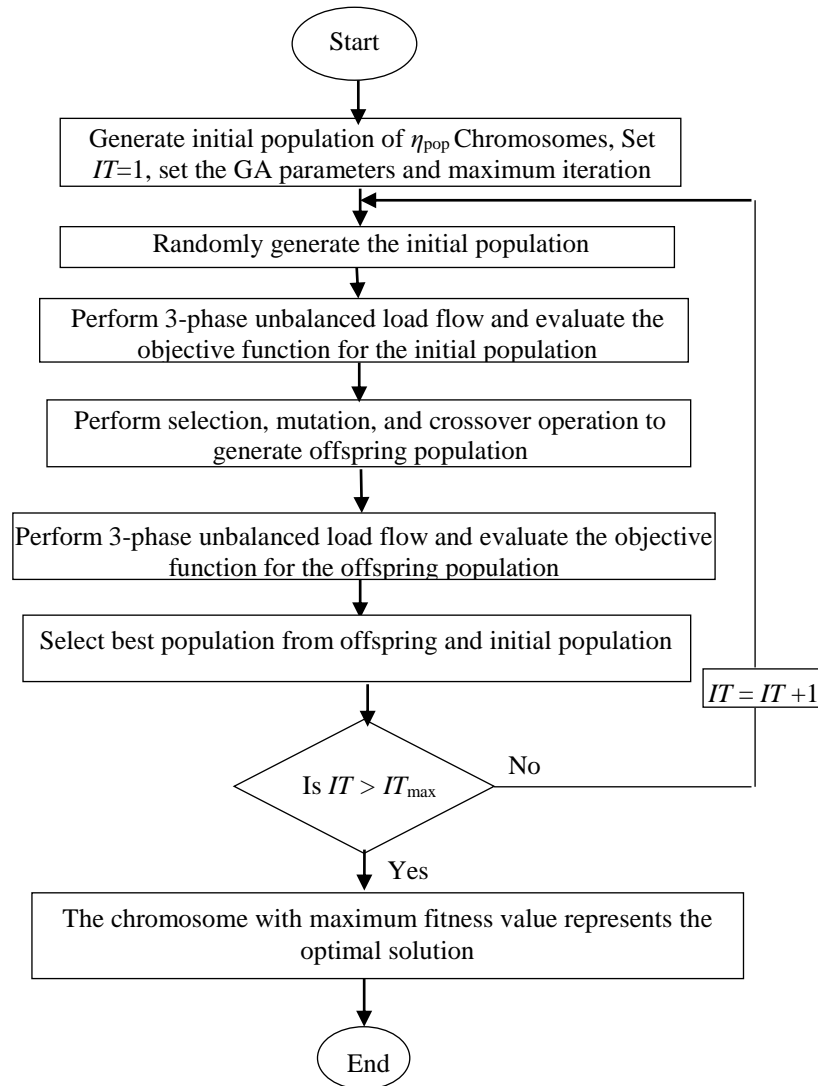


Fig. 2.6. Flow chart of the planning approach using GA

2.4 Three Phase Forward-Backward Sweep Load Flow Algorithm

In this algorithm, three matrices A , B , and C are developed to obtain load flow solutions. Here, the load flow solutions are obtained by utilizing these matrices. Matrix A is formed to know the downstream buses connected to a particular bus. Matrix B is formed to identify the end buses. Matrix C is formed to obtain the branch currents. In a multiphase system to know the type of branch such as 3-phase (ABCN, BACN, or CABN), 2-phase (ABN, BCN, or CAN) or 1-phase (AN, BN or CN) a phase identification data table is formulated in this algorithm. It contains the branch number, the conductor code $\{CC(k)\}$, and phase type. The phase identification data table for an 8-bus system shown in Fig. 2.7 is given below:

Table 2.1: Phase identification data

Branch number	Conductor code $\{CC(k)\}$	Phase type
1	1	<i>abcn</i>
2	2	<i>bcn</i>
3	3	<i>bn</i>
4	4	<i>cn</i>
5	4	<i>cn</i>
6	5	<i>an</i>
7	4	<i>cn</i>

In the above table each branch is assigned a specific phase type with the help of $\{CC(k)\}$. If $\{CC(k)\}$ is 1, then branch 1 is treated as three-phase with phase sequence ABCN. Similarly the phasing of other branches can be defined. The Table 1 is basically needed for calculating branch and load currents in the three phase load flow algorithm.

For any radial distribution system, the relation between number of branches (NBR) and number of buses (NB) is given by

$$NBR = NB - 1 \quad (2.31)$$

The relation between branch current and load current at a bus is explained using a segment of radial distribution system shown in Fig. 2.7.

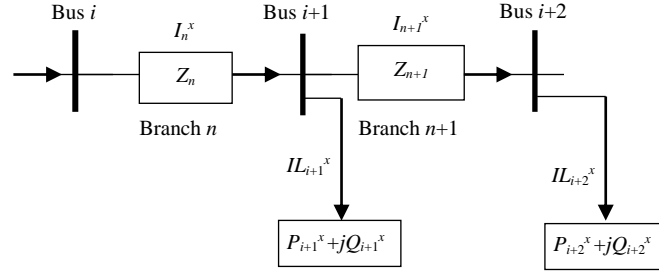


Fig.2.7: A section of radial distribution system

If bus $i+2$ is an end bus, then the relation between branch current and load current is given by

$$I_{n+1}^x = IL_{i+2}^x \quad (2.32)$$

For intermediate bus $i+1$, the relation between branch current and load current is given by

$$I_n^x = I_{n+1}^x + IL_{i+1}^x \quad (2.33)$$

Where I_n^x , I_{n+1}^x , IL_{i+1}^x , IL_{i+2}^x , P_{i+1}^x , Q_{i+1}^x , P_{i+2}^x , Q_{i+2}^x , Z_n , Z_{n+1} are current in branch n , load current at bus $i+1$, real load at bus $i+1$, reactive load at bus $i+1$ for phase x (x may be a or b or c) and impedance of branch n .

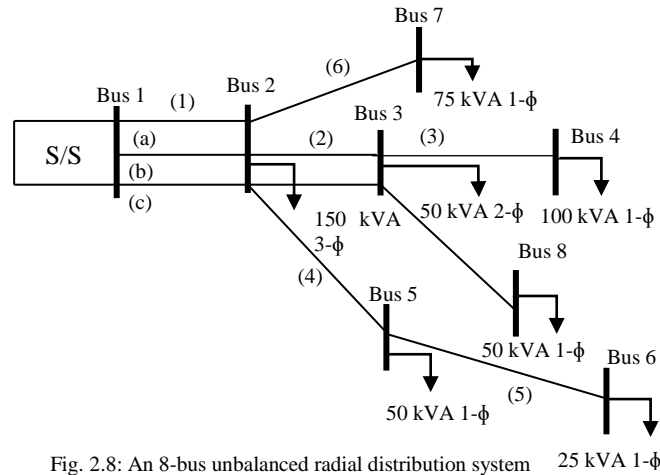


Fig. 2.8: An 8-bus unbalanced radial distribution system

For an 8-bus system, shown in Fig. 2.8, the algorithmic steps for power flow solutions using these matrices are explained below:

Step 1: Read input data

Step 2: Set the voltage at all buses to be 1, $-0.5-j0.866$, $0.5+j0.866$ in p.u. for phase-a, phase-b and phase-c respectively.

Step 3: Form matrix A

The pseudocode is given in Fig. 2.9

```

Begin
// N = Number of buses
// SN = Sending end bus
// RN = Receiving end bus
Initialize A=Ø
For i=1,..., N
    For j= 1,..., N-1
        If i = SN(j);
            A(i, RN(j))=1;
        End If
    End For
End For
End

```

Fig. 2.9: Pseudocodes for formation of matrix A

Step 4: Form matrix B from matrix A to know the end buses; for the given 8-bus system, it is found as:

$$B = [1 \ 3 \ 2 \ 0 \ 1 \ 0 \ 0 \ 0] \quad (2.34)$$

$B(4) = 0$ means bus 4 is an end bus. If $B(i) = 0$, branch current is equal to the load current.

For $i = 8$, $B(8) = 0$

$$I_7^b = IL_8^b \quad (2.35)$$

Step 5: Set iteration count $IT=1$;

Step 6: Calculate load current at all buses starting from bus $k=2$ to $k=NB$.

Step 7: Perform backward sweep to calculate branch current from bus $k=NB$ to $k=2$; this is done as follows:

- Check for end bus using B matrix, if end bus, use Eq. (2.32) to calculate branch current.
- Else use Eq. (2.33) to calculate branch currents.

For example, for bus 3 in the given 8-bus system, the current in branch 2 is calculated by an iterative process. The immediate downstream bus is to be searched iteratively, and it is found to be bus 4. The currents in branch 2 for phases b and c are:

$$I_2^b = IL_3^b + IL_8^b \quad (2.36)$$

$$I_2^c = IL_3^c + IL_4^c + IL_5^c + IL_6^c \quad (2.37)$$

Next downstream bus connected to bus 3 is found to be bus 8, the current in branch 2 for phase b and c becomes

$$I_2^b = 2IL_3^b + IL_8^b \quad (2.38)$$

$$I_2^c = 2IL_3^c + IL_4^c + IL_5^c + IL_6^c \quad (2.39)$$

So extra load current (IL_3^b, IL_3^c) is added for calculating current in branch 2

- Phase checking is to be done with the help of conductor code $\{CC(k)\}$ while executing step 1, 2 for calculation of respective phases. Depending upon the conductor code, each branch (feeder segment) is assigned to a particular phase. $CC(1) = 3$ means branch 1 is assigned as three phase (ABCN) conductors and $CC(6) = 1$ means branch 6 is assigned as single phase conductor.

The branch currents at the end of this step are

$$I_1^a = 3IL_2^a + IL_7^a \quad (2.40)$$

$$I_1^b = 3IL_2^b + 2IL_3^b + IL_8^b \quad (2.41)$$

$$I_1^c = 3IL_2^c + 2IL_3^c + IL_4^c + IL_5^c + IL_6^c \quad (2.42)$$

$$I_2^b = 2IL_3^b + IL_8^b \quad (2.43)$$

$$I_2^c = 2IL_3^c + IL_4^c + IL_5^c + IL_6^c \quad (2.44)$$

$$I_3^b = IL_4^b \quad (2.45)$$

$$I_4^c = IL_5^c + IL_6^c \quad (2.46)$$

$$I_5^c = IL_6^c \quad (2.47)$$

$$I_6^a = IL_7^a \quad (2.48)$$

$$I_7^b = IL_8^b \quad (2.49)$$

Step 8: Form matrix C from matrix A^T

Matrix C is formed to remove the extra load current added in branch 1 due to downstream bus loads in step 7. The pseudo code is given below:

```

Begin
  Initialize  $C=\emptyset$ 
  For  $i=1,\dots,N$ 
    For  $j=1,\dots,N-1$ 
      If  $A^T(i,j)=1$ 
         $C(i,:)=C(j,:);$ 
         $C(i,j)=1;$ 
      End If
    End For
  End For
End

```

Fig. 2.10: Pseudocodes for formation of matrix C

This computation of branch currents in all branches using matrix C is obtained using pseudocodes shown in Fig. 2.10.

```

Begin
  //  $I_n$  =Branch current
  //  $IL$  = Load current
  For  $t=2:N$ 
    If  $B(t)>1$ 
       $I_n(:,t-1)=I_n(:,t-1)-(B(t)-1)IL(:,t);$ 
       $tz=(B(t)-1)IL(:,t);$ 
      For  $j=N-1:-1:2$ 
        If  $(C(t,j)=1)$ 
           $I_n(:,j-1)=I_n(:,j-1)-tz;$ 
        End If
      End For
    End If
  End For
End

```

Fig. 2.11: Pseudocodes for deletion of extra load current

Now extra load current added ($2IL_2^a$, $2IL_2^b$, $2IL_2^c$, IL_3^b , IL_3^c) is to be deleted using the pseudocodes given in Fig. 2.11.

When $t=2$, $B(2)=3$,

Now

$$I_n(:,1)=I_n(:,1)-\{B(2)-1\}IL(:,2) \quad (2.50)$$

$$I_n(:,1)=I_n(:,1)-2IL(:,2) \quad (2.51)$$

Where $I_n(:,1)=I_1^a, I_1^b, I_1^c$, $IL(:,2)=IL_2^a, IL_2^b, IL_2^c$

$$I_1^a = IL_2^a + IL_7^a \quad (2.52)$$

$$I_1^b = IL_2^b + 2IL_3^b + IL_8^b \quad (2.53)$$

$$I_1^c = IL_2^c + 2IL_3^c + IL_4^c + IL_5^c + IL_6^c \quad (2.54)$$

$$tz = \{B(2)-1\}IL(:,2) \quad (2.55)$$

$$tz = 2IL(:,2) \quad (2.56)$$

Now inner loop (j) continues from N-1 to 2, that means 7, 6, ..., 2 to check whether $C(2, j) = 1$

$C(2, 7), C(2,6), C(2,5), C(2,4), C(2,3), C(2,2)$ is not equal to 1

So $I_n(:, 1) = [I_1^a, I_1^b, I_1^c]$ doesn't change.

When $t=3, B(3)=2$, now

$$I_n(:,2) = I_n(:,2) - \{B(3)-1\}IL(:,3) \quad (2.57)$$

$$I_n(:,2) = I_n(:,2) - 2IL(:,3) \quad (2.58)$$

Now branch 2 currents becomes

$$I_2^b = IL_3^b + IL_8^b \quad (2.59)$$

$$I_2^c = IL_3^c + IL_4^c + IL_5^c + IL_6^c \quad (2.60)$$

$$tz = IL(:,3) \quad (2.61)$$

Now inner loop (j) continues from N-1 to 2, that means 7, 6, ..., 2 to check whether $C(3, j) = 1$

Inside inner loop $C(3, 2) = 1$ for $j=2$

Equation $I_n(:, j-1) = I_n(:, j-1) - tz$ becomes

$$I_n(:,1) = I_n(:,1) - tz \quad (2.62)$$

$$I_n(:,1) = I_n(:,1) - IL(:,3) \quad (2.63)$$

$I_n(:,1)$ becomes

$$I_1^a = IL_2^a + IL_7^a \quad (2.64)$$

$$I_1^b = IL_2^b + IL_3^b + IL_8^b \quad (2.65)$$

$$I_1^c = IL_2^c + IL_3^c + IL_4^c + IL_5^c + IL_6^c \quad (2.66)$$

Where $IL(:, 3) = IL_3^b, IL_3^c$

For end buses, the pseudocodes need not to be executed.

Step 9: Perform forward sweep to update bus voltage and magnitudes for corresponding phases using $CC(k)$.

Step 10: If $\max(V_k^{m+1} - V_k^m) \leq 0.0001$ then execute step 12; otherwise step 11 is executed.

Step 11: $IT = IT + 1$, go to Step 6;

Step 12: Print the complex voltage at all buses.

2.5 Simulation results and discussions

The proposed algorithm is implemented using MATLAB 2012b [108]. In order to validate the effectiveness of the proposed algorithm, four test systems consisting of 19-bus, 25-bus, Indian 19-bus, and 34-bus unbalanced radial distribution systems are used. The base values for the 19-bus and Indian 19-bus system are taken as 11 kV and 1 MVA. For the 25-bus system, they are considered to be 4.16 kV and 30 MVA. For, the 34-bus system the base kV and MVA are taken as 24.9 kV, and 2.5 MVA. The base case load and line data are given in the appendix. The power loss, complex power unbalance, neutral current, ZSUF, and NSUF for the base case network of the 19- and 25-bus and Indian 19- and 34-bus systems are given in Table 2.2. The DE parameters are optimized with repetitive runs, and the optimal parameters are shown in Table 2.3. Table 2.4 shows that the proposed three-phase load flow algorithm is found to converge in fewer iterations as compared to [9]. Two different planning optimization cases are used. They are:

- *Case A:* planning for optimal phase balancing
- *Case B:* simultaneous planning for optimal phase balancing and conductor sizes

Firstly, different objective functions formulated are separately optimized as per single objective optimization approach, and the simulation results for all the four test systems are discussed in section 2.5.1. Then, they are aggregated according to Eq. (2.13) similar to a multi-objective optimization approach and results are discussed in section 2.5.2.

Table 2.2: Base case values for the 19-, 25-, Indian 19-, and 34-bus systems

Objective	19-bus system	25-bus system	Indian 19-bus system	34-bus system
PL (kW)	13.283	149.81	50.1072	578.3774
TS_u (MVA)	0.0218	0.0927	0.0727	0.0773
AV_d (%)	3.3083	4.7866	3.9784	7.0538
ZSUF (%)	0.0715	0.1835	0.0743	0.3344
NSUF (%)	0.0298	0.4059	0.0316	0.3898
I_N (p.u.)	2.3840	0.6370	7.9849	53.3436

Table 2.3: Optimal parameters used in DE, PSO, CSA, and GA

Parameters	DE	CSA [104]	PSO [105]	GA [106]
η_{pop}	150	150	150	150
IT_{max}	150	150	150	150
Individual parameters	CR=0.8	λ (constant)=1	$C_1=2.0$, $C_2=2.0$	CR=0.8
	F=1.5	---	$w_{max}=0.9$, $w_{min}=0.4$	Mutation probability=0.005

Table 2.4: Comparison of method proposed by J.H.Teng and proposed method

Methods	Number of iterations to get convergence	
	19-bus system	25-bus system
J.H.Teng [9]	3	4
Proposed Method	2	3

Table 2.5: Comparison of results of 50 runs as obtained with DE, GA, PSO, and CSA for *Case A* planning for 19-bus systems

Objective	19-bus system							
	DE		CSA		PSO		GA	
	Mean	SD	Mean	SD	Mean	SD	Mean	SD
PL (kW)	12.536	0	12.651	0.0002	12.7630	0.0003	12.7950	0.005
TS _u (MVA)	0.0003	0.0002	0.0124	0.0006	0.0136	0.0007	0.0164	0.0010
AV _d (%)	1.9385	0.0004	1.9556	0.0005	1.9603	0.005	1.9627	0.007
ZSUF (%)	0.0020	0.0014	0.0114	0.014	0.0214	0.017	0.0323	0.020
NSUF (%)	0.0014	0.0012	0.0057	0.0081	0.0078	0.0088	0.0145	0.007
I _N (p.u.)	2.2906	0	2.2907	0	2.2907	0	2.2907	0

Table 2.6: Comparison of results of 50 runs as obtained with DE, GA, PSO, and CSA for *Case A* planning for 25-bus systems

Objective	25-bus system							
	DE		CSA		PSO		GA	
	Mean	SD	Mean	SD	Mean	SD	Mean	SD
PL (kW)	135.92	0	136.215	0.167	136.73	0.234	137.025	0.773
TS _u (MVA)	0.0857	0.007	0.0895	0.008	0.0902	0.012	0.0905	0.013
AV _d (%)	4.4538	0.003	4.5185	0.007	4.5206	0.009	4.5253	0.009
ZSUF (%)	0.0714	0.010	0.0750	0.018	0.0816	0.026	0.0917	0.038
NSUF (%)	0.1586	0.007	0.1683	0.010	0.1720	0.016	0.1805	0.023
I _N (p.u.)	0.6031	0	0.6032	0	0.6032	0	0.6060	0.001

Table 2.7: Comparison of the solutions obtained with planning *Cases A and B* using DE for 19-bus and 25-bus systems

Objective	19-bus system				25-bus system			
	<i>Case A</i>		<i>Case B</i>		<i>Case A</i>		<i>Case B</i>	
	Mean	SD	Mean	SD	Mean	SD	Mean	SD
PL (kW)	12.536	0	1.7801	0.0214	135.92	0	109.312	0.006
TS _u (MVA)	0.0003	0.0002	0.0003	0.0023	0.0857	0.007	0.0857	0.014
AV _d (%)	1.9385	0.0004	0.7418	0.0039	4.4538	0.003	3.7645	0.038
ZSUF (%)	0.0020	0.0014	0.0027	0.0006	0.0714	0.010	0.0947	0.045
NSUF (%)	0.0014	0.0012	0.0011	0.0005	0.1586	0.007	0.1148	0.070
I _N (p.u.)	2.2906	0	2.2906	0	0.6031	0	0.6031	0

Table 2.8: Comparison of results of planning *Case B* of 50 runs as obtained with DE, and CSA, for 19- and 25-bus systems

Objective	19-bus system				25-bus system			
	DE		CSA		DE		CSA	
	Mean	SD	Mean	SD	Mean	SD	Mean	SD
PL (kW)	1.7801	0.0214	1.8942	0.0214	109.312	0.006	110.452	0.007
TS _u (MVA)	0.0003	0.0023	0.0004	0.0028	0.0857	0.014	0.0858	0.019
AV _d (%)	0.7418	0.0039	0.8562	0.0041	3.7645	0.038	3.8152	0.045
ZSUF (%)	0.0027	0.0006	0.0031	0.0007	0.0947	0.045	0.0949	0.060
NSUF (%)	0.0011	0.0005	0.0018	0.0007	0.1148	0.070	0.1161	0.081
I _N (p.u.)	2.2906	0	2.2907	0	0.6031	0	0.6032	0

Table 2.9: Comparison of results of 50 runs as obtained with DE, GA, PSO, and CSA for *Case A* planning for the Indian 19-bus systems

Objective	Indian 19-bus system							
	DE		CSA		PSO		GA	
	Mean	SD	Mean	SD	Mean	SD	Mean	SD
PL (kW)	45.6142	0	45.8238	0.0003	45.9142	0.0004	45.9845	0.0006
TS _u (MVA)	0.0091	0.0050	0.0095	0.0110	0.0113	0.0145	0.0215	0.158
AV _d (%)	3.3967	0.0248	3.4156	0.0310	3.5217	0.0325	3.6421	0.0341
ZSUF (%)	0.0120	0.0039	0.0215	0.0045	0.0267	0.0051	0.0280	0.0065
NSUF (%)	0.0048	0.0016	0.0055	0.0018	0.0068	0.0021	0.0075	0.0025
I _N (p.u.)	7.6206	0	7.6206	0	7.6206	0	7.6206	0

Table 2.10: Comparison of results of 50 runs as obtained with DE, GA, PSO, and CSA for *Case A* planning for 34-bus systems

Objective	34-bus system							
	DE		CSA		PSO		GA	
	Mean	SD	Mean	SD	Mean	SD	Mean	SD
PL (kW)	577.3367	0.0001	577.5142	0.0002	577.6141	0.0003	577.7613	0.0004
TS _u (MVA)	0.0183	0.0063	0.0195	0.0071	0.0213	0.0090	0.0243	0.0105
AV _d (%)	6.9142	0.0040	6.9243	0.0052	6.9351	0.0070	6.9415	0.0085
ZSUF (%)	0.1082	0.0064	0.1257	0.0085	0.1321	0.0095	0.1357	0.0112
NSUF (%)	0.0366	0.0075	0.0412	0.0090	0.0451	0.0103	0.0498	0.0121
I _N (p.u.)	53.3187	0.0002	53.3245	0.0003	53.3316	0.0004	53.3367	0.0005

Table 2.11: Comparison of the solutions obtained with planning *Cases A* and *B* using DE for the Indian 19-bus and 34-bus systems

Objective	Indian 19-bus system				34-bus system			
	<i>Case A</i>		<i>Case B</i>		<i>Case A</i>		<i>Case B</i>	
	Mean	SD	Mean	SD	Mean	SD	Mean	SD
PL (kW)	45.6142	0	18.9127	0.0214	577.3367	0.0001	565.4610	0.0081
TS _u (MVA)	0.0091	0.0050	0.0092	0.0064	0.0183	0.0063	0.0184	0.0071
AV _d (%)	3.3967	0.0248	1.8470	0.1939	6.9142	0.0040	6.9013	0.0158
ZSUF (%)	0.0120	0.0039	0.0130	0.0043	0.1082	0.0064	0.1095	0.1091
NSUF (%)	0.0048	0.0016	0.0053	0.0018	0.0366	0.0075	0.0378	0.0041
I _N (p.u.)	7.6206	0	7.6206	0	53.3187	0.0002	53.3187	0.0002

Table 2.12: Comparison of results of planning *Case B* of 50 runs as obtained with DE, and CSA, for Indian 19- and 34- bus systems

Objective	Indian19-bus system				34-bus system			
	DE		CSA		DE		CSA	
	Mean	SD	Mean	SD	Mean	SD	Mean	SD
PL (kW)	18.9127	0.0214	19.0132	0.0315	565.4610	0.0081	566.3212	0.0091
TS _u (MVA)	0.0092	0.0064	0.0095	0.0075	0.0184	0.0071	0.0192	0.0081
AV _d (%)	1.8470	0.1939	1.9132	0.2342	6.9013	0.0158	6.9234	0.0169
ZSUF (%)	0.0130	0.0043	0.0141	0.0055	0.1095	0.1091	0.1121	0.201
NSUF (%)	0.0053	0.0018	0.0062	0.0029	0.0378	0.0041	0.0384	0.0045
I _N (p.u.)	7.6206	0	7.6206	0.0001	53.3187	0.0002	53.3188	0.0003

2.5.1 Results of Single Objective Optimization

The results of single objective optimization considering each objective separately for planning *Case A* are given in Table 2.5 and 2.6, and Table 2.9 and 2.10 respectively for the 19-, and 25-bus and Indian 19- and 34-bus system. The results of 50 runs as obtained with DE are compared with those of GA, PSO, and CSA. The results clearly indicate that the performance of DE is better and consistent according to the mean objective function and standard deviation (SD), respectively as compared to the other three algorithms. A performance comparison between planning *Cases A* and *B* using DE is provided in Table 2.7 and 2.11 for 19- and 25-bus system and Indian 19- and 34-bus system respectively. Table 2.8 shows the Comparison of results of planning *Case B* of 50 runs as obtained with DE, and CSA, for 19- bus, and 25 bus. Table 2.12 shows the Comparison of results of planning *Case B* of 50 runs as obtained with DE, and CSA, for Indian 19- and 34- bus systems. It is observed that the solutions are significantly improved in view of power loss and average voltage drop in planning *Case B*. It is expected because the optimization of conductor sizes improves these two objectives. However, the conductor size optimization does not have any positive impact on the optimization of other objectives. Thus, the solutions obtained with the optimization of the other objectives either remain same or slightly differ than *Case A*.

2.5.2 Results of Multi-Objective Optimization

In this subsection, all the objective functions are aggregated with equal weights to give equal priority to each of them to optimize. However, unequal weights can be assigned if one objective is to be given more priority over the other. The results of 50 runs for *Case A*

planning as obtained with DE, are provided and compared with those obtained with GA, PSO, and CSA in Table 2.13, 2.14, 2.17, 2.18, for 19- 25-, Indian 19-, 34- bus systems respectively. The results again indicate the superiority of DE to the other three algorithms. The solutions obtained with the multi-objective optimization are found to have a slightly higher power loss, average voltage drop, and complex power unbalance as compared to the solutions obtained with the results of the respective single objective optimization. The reason may be the simultaneous optimization of many objectives may lead to a slightly inferior solution as compared to the solutions obtained with the respective single objective optimization. The improvements in power loss, power unbalance, and voltage magnitude as obtained with the DE-based planning optimization for the 19-bus, and Indian 19- bus system are found to be much higher as compared to the 25- bus, and 34- bus system. The reason may be the base case network of the 25-bus, and 34- bus system are relatively balanced. To have a pictorial view, the complex power unbalance of all the systems before and after optimization is plotted in Fig. 2.12 and 2.13. It is observed that the complex power unbalance is improved with this planning optimization in both systems. The performance comparison between planning *Cases A* and *B*, for 19-, and 25-bus and Indian 19- and 34-bus systems are given in Table 2.15 and 2.19 respectively, shows that the solutions are significantly improved in view of power loss and average voltage drop in planning *Case B*. Comparison of the results as obtained with Case B planning using DE and CSA for 19 -bus and 25- bus system are given in Table 2.16. Table 2.20 shows the Comparison of the results as obtained with Case B planning using DE and CSA for Indian 19- bus and 34- bus system. The complex power demand and conductor sizes as obtained with *Case B* planning in a sample run for all the systems are shown in Appendix (Table E.1- E.4).

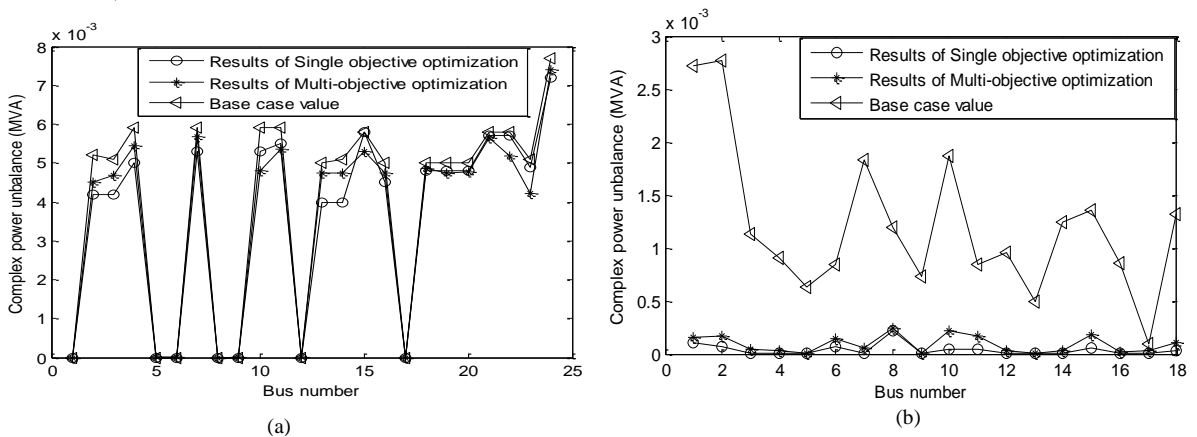


Fig. 2.12: Complex power unbalance for: (a) 19-bus and (b) 25-bus system

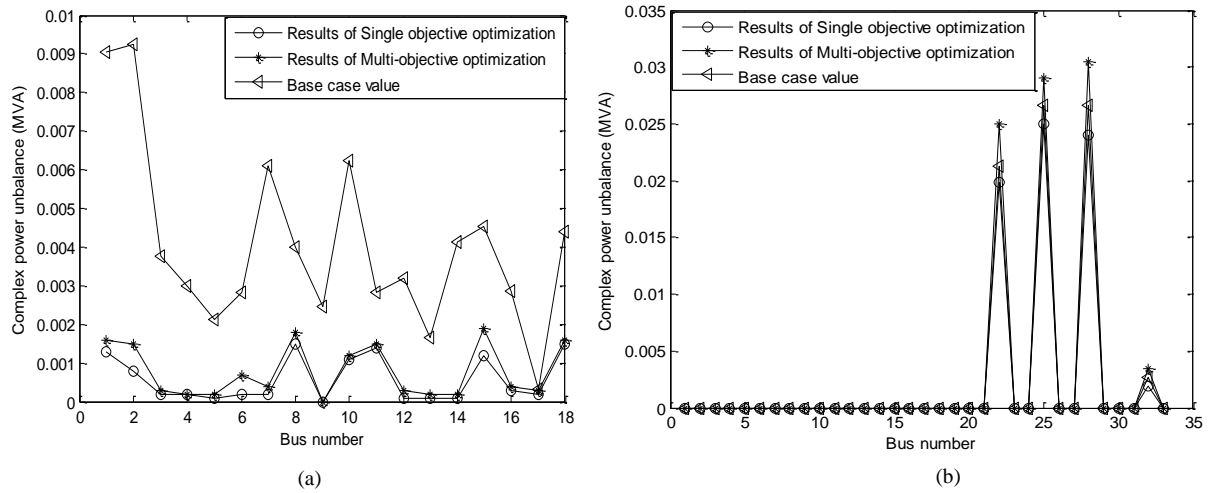


Fig. 2.13: Complex power unbalance for: (a) Indian 19-bus and (b) 34-bus system

Table 2.13: Comparison of results of multi-objective optimization (*Case A*) of 50 runs as obtained with DE, CSA, PSO, and GA for 19-bus systems

Objective	19-bus system							
	DE		CSA		PSO		GA	
	Mean	SD	Mean	SD	Mean	SD	Mean	SD
PL (kW)	12.561	0.0002	12.693	0.0007	12.788	0.0058	12.817	0.0072
TS _u (MVA)	0.0008	0.0011	0.0131	0.0016	0.0141	0.0019	0.0178	0.0022
AV _d (%)	1.9717	0.0003	1.9888	0.0003	1.9936	0.0006	2.0156	0.0017
ZSUF (%)	0.0025	0.0009	0.0113	0.0015	0.0130	0.0018	0.0180	0.0196
NSUF (%)	0.0055	0.0019	0.0077	0.0030	0.0109	0.0065	0.0188	0.0073
I _N (p.u.)	2.2906	0	2.2909	0.0002	2.3064	0.0016	2.3086	0.0019

Table 2.14: Comparison of results of multi-objective optimization (*Case A*) of 50 runs as obtained with DE, CSA, PSO, and GA for 25-bus systems

Objective	25-bus system							
	DE		CSA		PSO		GA	
	Mean	SD	Mean	SD	Mean	SD	Mean	SD
PL (kW)	136.25	0.0560	137.34	0.1442	140.93	0.7932	142.95	0.8435
TS _u (MVA)	0.0869	0.0023	0.0904	0.0031	0.0908	0.0048	0.0913	0.0056
AV _d (%)	4.4631	0.0013	4.5188	0.0124	4.5213	0.0136	4.5261	0.0123
ZSUF (%)	0.0726	0.0019	0.0772	0.0021	0.0848	0.0024	0.0947	0.0027
NSUF (%)	0.2135	0.0041	0.2415	0.0049	0.2746	0.0055	0.2878	0.0069
I _N (p.u.)	0.6031	0	0.6032	0.0003	0.6052	0.0004	0.6054	0.0010

Table 2.15: Results of the multi-objective optimization of 50 runs obtained with DE

Objective	19-bus system				25-bus system			
	Case A		Case B		Case A		Case B	
	Mean	SD	Mean	SD	Mean	SD	Mean	SD
PL (kW)	12.561	0.0002	2.2358	0.0593	136.25	0.0560	110.16	0.1745
TS _u (MVA)	0.0008	0.0011	0.0008	0.0008	0.0869	0.0023	0.0869	0.0145
AV _d (%)	1.9717	0.0003	1.4196	0.0220	4.4631	0.0013	4.0230	0.0945
ZSUF (%)	0.0025	0.0009	0.0054	0.0013	0.0726	0.0019	0.1754	0.0177
NSUF (%)	0.0055	0.0019	0.0204	0.0064	0.2135	0.0041	0.3881	0.0165
I _N (p.u.)	2.2906	0	2.2906	0	0.6031	0	0.6031	0

Table 2.16: Comparison of the results as obtained with Case B planning using DE and CSA

Objective	19-bus system				25-bus system			
	DE		CSA		DE		CSA	
	Mean	SD	Mean	SD	Mean	SD	Mean	SD
PL (kW)	2.2358	0.0593	2.3456	0.0645	110.16	0.1745	111.04	0.1943
TS _u (MVA)	0.0008	0.0008	0.0009	0.0011	0.0869	0.0145	0.0872	0.0152
AV _d (%)	1.4196	0.0220	1.5764	0.0345	4.0230	0.0945	4.3124	0.1231
ZSUF (%)	0.0054	0.0013	0.0061	0.0025	0.1754	0.0177	0.1832	0.0195
NSUF (%)	0.0204	0.0064	0.0215	0.0074	0.3881	0.0165	0.3942	0.0171
I _N (p.u.)	2.2906	0	2.2907	0.002	0.6031	0	0.6032	0.0001

Table 2.17: Comparison of results of multi-objective optimization (*Case A*) of 50 runs as obtained with DE, CSA, PSO, and GA for the Indian 19-bus systems

Objective	19-bus system							
	DE		CSA		PSO		GA	
	Mean	SD	Mean	SD	Mean	SD	Mean	SD
PL (kW)	46.2827	0.0158	46.3415	0.0169	46.4178	0.0178	46.6245	0.0192
TS _u (MVA)	0.0095	0.0055	0.0108	0.0131	0.0121	0.0145	0.0198	0.0176
AV _d (%)	3.7945	0.0598	3.8010	0.0617	3.8142	0.0734	3.9008	0.0845
ZSUF (%)	0.0245	0.0098	0.0278	0.0105	0.0295	0.0212	0.0310	0.0315
NSUF (%)	0.0125	0.0064	0.0148	0.0086	0.0175	0.0198	0.0202	0.0267
I _N (p.u.)	7.6206	0	7.6206	0.0001	7.6206	0.0003	7.6206	0.0005

Table 2.18: Comparison of results of multi-objective optimization (*Case A*) of 50 runs as obtained with DE, CSA, PSO, and GA for 34-bus systems

Objective	34-bus system							
	DE		CSA		PSO		GA	
	Mean	SD	Mean	SD	Mean	SD	Mean	SD
PL (kW)	577.6140	0.0002	577.7482	0.0005	577.8296	0.0005	577.9135	0.0006
TS _u (MVA)	0.0191	0.0068	0.0208	0.0081	0.0254	0.0095	0.0298	0.0110
AV _d (%)	6.9567	0.0052	6.9612	0.0092	6.9732	0.0104	6.9843	0.0123
ZSUF (%)	0.1561	0.0078	0.1612	0.0087	0.1675	0.0094	0.1705	0.0115
NSUF (%)	0.0415	0.0083	0.0497	0.0095	0.0512	0.0102	0.0561	0.0143
I _N (p.u.)	53.3189	0.0002	53.3261	0.0003	53.3354	0.0004	53.3378	0.0005

Table 2.19: Results of the multi-objective optimization of 50 runs obtained with DE

Objective	Indian 19-bus system				34-bus system			
	<i>Case A</i>		<i>Case B</i>		<i>Case A</i>		<i>Case B</i>	
	Mean	SD	Mean	SD	Mean	SD	Mean	SD
PL (kW)	46.2827	0.0158	20.2161	0.0266	577.6140	0.0002	566.0124	0.0093
TS _u (MVA)	0.0095	0.0055	0.0110	0.0014	0.0191	0.0068	0.0190	0.0082
AV _d (%)	3.5945	0.0598	1.8795	0.1939	6.9567	0.0052	6.9145	0.0172
ZSUF (%)	0.0245	0.0098	0.0281	0.0292	0.1561	0.0078	0.1143	0.1123
NSUF (%)	0.0125	0.0064	0.0169	0.0078	0.0412	0.0083	0.0385	0.0065
I _N (p.u.)	7.6206	0	7.6206	0	53.3189	0.0002	53.3189	0.0003

Table 2.20: Comparison of the results as obtained with Case B planning using DE and CSA

Objective	Indian 19-bus system				34-bus system			
	DE		CSA		DE		CSA	
	Mean	SD	Mean	SD	Mean	SD	Mean	SD
PL (kW)	20.2161	0.0266	21.3245	0.0325	566.0124	0.0093	567.321	0.0122
TS _u (MVA)	0.0110	0.0014	0.0143	0.0024	0.0190	0.0082	0.0232	0.0091
AV _d (%)	1.8795	0.1939	1.9432	0.2134	6.9145	0.0172	6.9856	0.0214
ZSUF (%)	0.0281	0.0292	0.0295	0.0333	0.1143	0.1123	0.1598	0.1456
NSUF (%)	0.0169	0.0078	0.0172	0.0090	0.0385	0.0065	0.0497	0.0071
I _N (p.u.)	7.6206	0	7.6207	0.002	53.3189	0.0003	53.3190	0.0005

2.6 Summary

In this chapter, a planning approach has been developed to determine the optimal phase balancing and the conductor sizes of four unbalanced radial distribution systems by optimizing the power loss, the complex power unbalance, the average voltage drop, the positive and the zero sequence unbalance factors, and the neutral current. A three phase forward-backward sweep load flow algorithm is developed and used in the planning approach. The DE and CSA are used as the solution strategy. The simultaneous optimization for the phase balancing and conductor size provides a network with better power loss and voltage profile. The performance of the DE is found to be better and consistent as compared to GA, PSO, and CSA.

However, the reduction in the power loss, the average voltage drop, and the neutral current are found to be less in comparison to their base case values by simultaneously optimizing the phase balancing and the conductor sizes for the 34- bus system. From Chapter 1, it is found that capacitors can reduce the system power loss in URDS by compensating reactive power. Thus, the next chapter focuses on the impact of the capacitors allocation on the power loss, the neutral current, and other objectives in the planning of URDS.

Chapter 3

Planning of Unbalanced Radial Distribution Systems with Capacitor Using Evolutionary Computing Algorithms

3.1 Introduction

In chapter 2, the planning of the URDS has been presented using differential evolution algorithms (DE) and CSA in the absence of capacitors. Several objective functions such as the total power loss, average voltage drop, total neutral current and total voltage unbalance have been minimized using these algorithms. However, the reduction in the power loss, the average voltage drop, and the neutral current are found to be less in comparison to their base case values by simultaneously optimizing the phase balancing and the conductor sizes for the 34- bus system.

From chapter 1, it is observed that capacitor can reduce power loss and improve voltage profile of distribution systems. Thus, in this chapter the planning of four URDS has been carried by integrating capacitors with the system. The objective functions considered are the total power loss, the average voltage drop, total neutral current and total voltage unbalance. The DE and CSA are employed as the solution strategy for minimizing these objective functions to obtain optimal capacitor location, rating, conductor sizing and

phase balancing. For the evaluation of each objective, a forward-backward load flow algorithm is developed. The proposed approach is demonstrated on the 19-bus, 25-bus, Indian 19-bus and 34-bus URDS.

This chapter is organized as follows: the Problem Formulation is presented in Section 3.2. In Section 3.3, the implementation of proposed planning approach using the DE is described. The simulation results are presented in Section 3.4. Section 3.5 concludes the chapter.

3.2 Problem Formulation

The aim of this planning problem is the minimization of the numerous objective functions subject to some technical constraints. The objective functions are discussed in Chapter 2. The technical constraints are as follows:

i. Voltage constraint: The voltage at each bus must lie between the lower and upper bound limit to avoid under voltage and over voltage problem.

$$V_s^{\min} \leq V_s^{abc} \leq V_s^{\max} \quad (3.1)$$

ii. Thermal constraint: The current flowing through each branch shouldn't exceed the maximum current-carrying capacity of the conductor for all the phases.

$$I_j^{abc} \leq I_j^{\max} \quad (3.2)$$

iii. Capacitor size constraint

The capacitor size should be an integral multiple of the smallest capacitor size available

$$QC_t \leq L \times QC_0 \quad L=1, 2, \dots, N \quad (3.3)$$

Where QC_0 denotes, the smallest capacitor size available, the maximum value of N is taken as 27 [107].

3.3 Implementation of DE and CSA for the planning problem

The proposed planning approach with DE and CSA utilizes a three-phase load flow algorithm as a supplementary program in order to obtain the bus voltage magnitudes and

power loss of a system. The load flow algorithm including the capacitors is explained in Section 3.3.1 and application of the DE and CSA are described in Section 3.3.2.

3.3.1 Three phase forward-backward sweep load flow algorithm incorporating capacitor

The proposed algorithm utilizes three matrices A , B , and C in order to obtain power flow solutions. The downstream buses connected to a particular bus are determined using matrix A . The end buses are identified with the help of matrix B and matrix C is developed in order to obtain the branch currents. The load flow algorithm consists of two steps. In the first step, the backward sweep is executed in order to find out the branch currents as follows:

$$\bar{I}_j^{x \in a,b,c} = \left(\frac{P_j^x - iQ_j^x}{\bar{V}_j^{x*}} \right) \quad (3.4)$$

Where, $\bar{I}_j^{x \in a,b,c}$, \bar{V}_j^{x*} , P_j^x , and Q_j^x are the load current and the voltage conjugate (in phasor form), active and reactive power demand at bus j for phase x

Then, the forward sweep is executed to obtain the bus voltages. More details of the algorithm have been discussed in Chapter 2.

3.3.1.1 Incorporation of Capacitor model in the distribution load flow

This subsection describes the incorporation of the capacitors in the unbalanced distribution systems. Fig. 3.1 shows the connection diagram for three shunt capacitors having rating QC1, QC2, and QC3 kVAR placed at bus j , in a sample line section of the unbalanced distribution system.

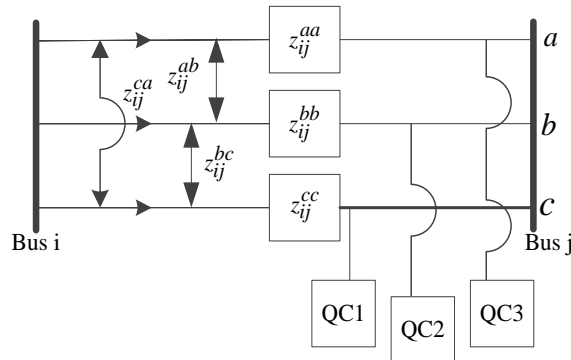


Fig. 3.1. Connection diagram of capacitors in a sample distribution system

Where, z_{ij}^{aa} , z_{ij}^{bb} , and z_{ij}^{cc} denotes the self-impedance of phase a, phase b, and phase c respectively; z_{ij}^{ab} , z_{ij}^{bc} , and z_{ij}^{ca} denotes the mutual impedance between phases. The capacitor ratings are considered to be discrete in value. The smallest and maximum size of the capacitor is taken as 150 and 4050 kVAR [107] respectively.

In order to incorporate the capacitor model, the reactive power demand at the bus at which a Capacitor unit is placed, say, at bus i , the Eqs. (3.4) is modified by:

$$Q_{D_{jp}}^C = Q_{D_{jp}}^{base} - Q_{jp}^C \quad (3.5)$$

Where, $Q_{D_{jp}}^C$ are the reactive power demand for p^{th} phase of j^{th} bus with a Capacitor unit and $Q_{D_{jp}}^{base}$ is the reactive power demand for p^{th} phase of j^{th} bus of the base-case network; Q_{jp}^C is the reactive power generated by the capacitor unit placed at p^{th} phase of j^{th} bus.

3.3.2 Proposed Planning Approach Using DE and CSA

In this chapter, DE and CSA are employed as the solution strategy for the planning problem of the unbalanced radial distribution networks. The detail description of this algorithm has been discussed in chapter 2.

3.3.2.1 Decision variable representation

The parameters (decision variables) for the DE and CSA in this planning problem consists of five decision variables and are represented as a vector D as follows:

$$D = [NC, QC, \phi, APD, ctz] \quad (3.6)$$

$$\phi = [\phi_1, \phi_2, \dots, \phi_N] \quad (3.7)$$

$$APD = [APD_{a,b,c}, APD_{a,b,c}, \dots, APD_N] \quad (3.8)$$

$$ctz = [ct_1, ct_2, \dots, ct_{NBR}] \quad (3.9)$$

Where ϕ denotes the vector of capacitor locations; QC denotes capacitor rating, APD vector represents the active and reactive power load in the phases a, b, and c for the bus N , NC represents the number of capacitors, and ctz represents a vector of different conductor types for NBR number of branches.

3.3.3 Flow chart of the planning approaches using DE and CSA

The flow chart of the solution strategies for the planning problem are provided in Fig. 3.2. and Fig. 3.3. respectively.

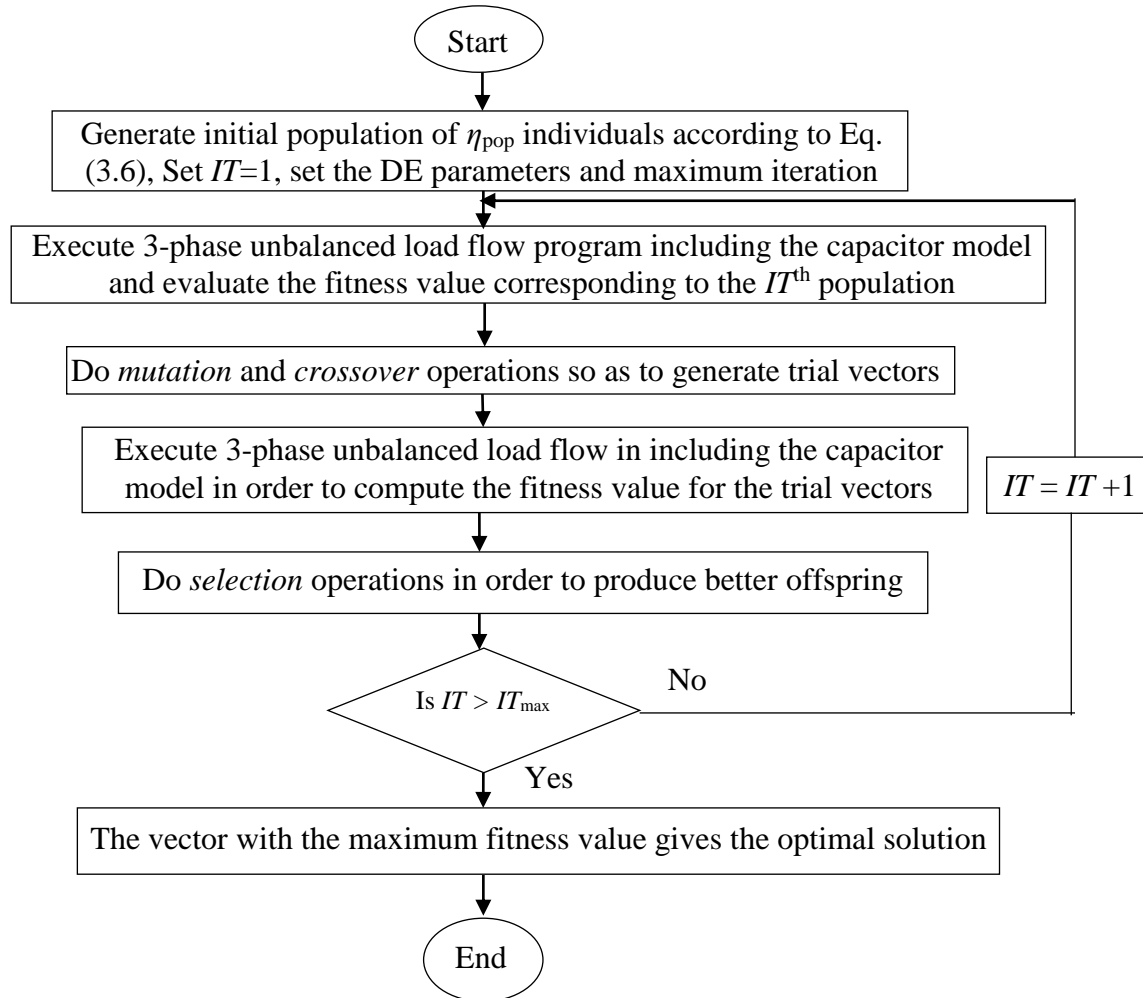


Fig. 3.2. Flow chart of the proposed planning approach using DE

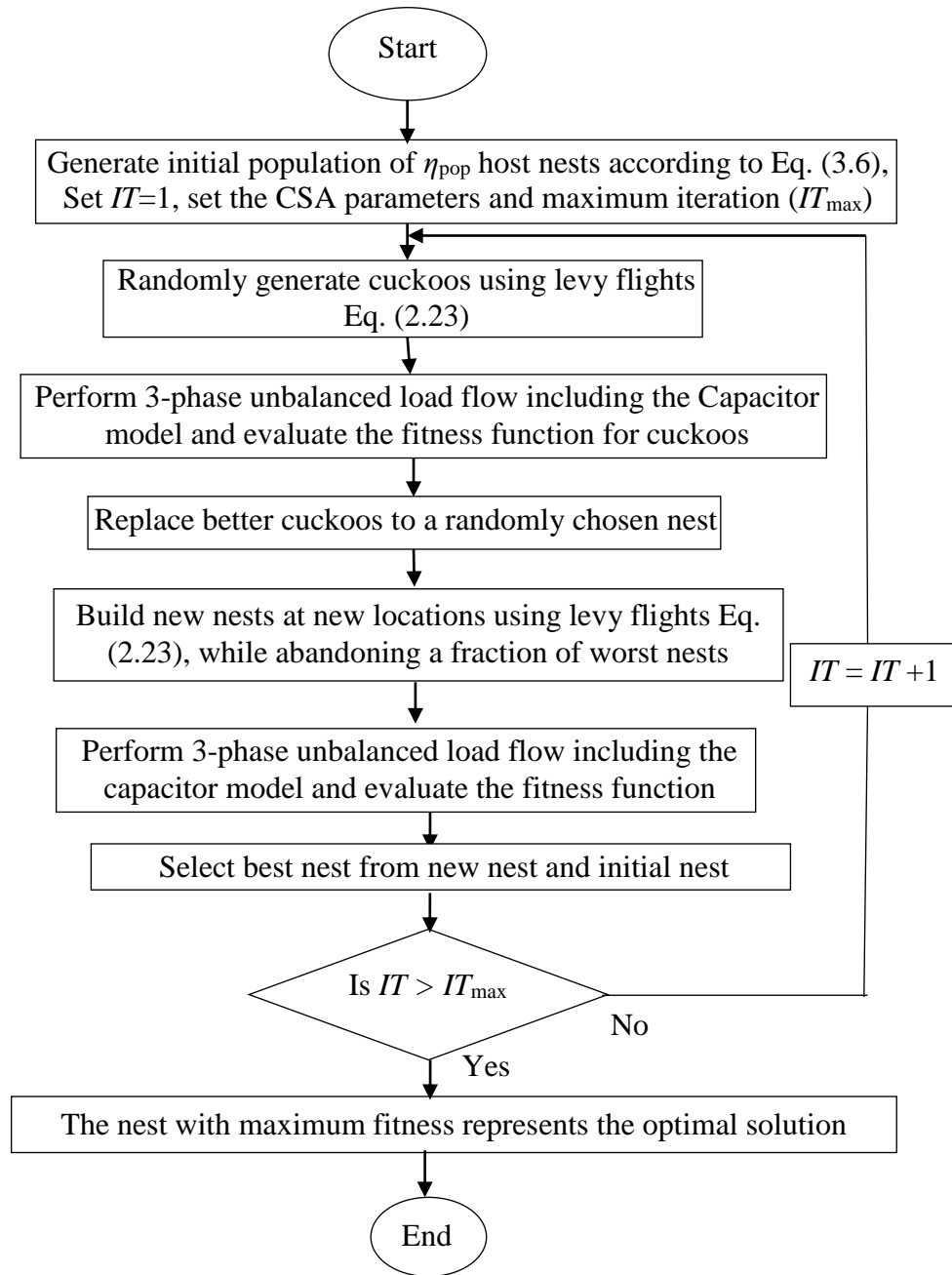


Fig. 3.3. Flow chart of the proposed planning approach using CSA

3.4 Simulation Results and discussions

The simulations are carried out with MATLAB R2012b software. The effectiveness of the proposed algorithm is verified on four unbalanced radial distribution networks, i.e. 19-bus, 25-bus, Indian 19-bus and 34-bus system. The base case results of these systems are provided in Table 2.2 of Chapter 2. The parameters of the DE are taken from Table 2.3 of Chapter 2. In this, Chapter, three different planning cases have been studied such as:

- *Case A*: planning for optimal phase balancing
- *Case B*: Simultaneous planning for optimal phase balancing and conductor sizing.
- *Case C*: Simultaneous planning for optimal phase balancing, conductor sizing, and capacitor allocation and sizing

Table 3.1: Comparison of the solutions obtained with planning for *Cases A* using DE for the 19-bus and 25-bus systems

Objective	19-bus system		25-bus system	
	<i>Case A</i>		<i>Case A</i>	
	Mean	SD	Mean	SD
PL (kW)	12.536	0	135.92	0
TS _u (MVA)	0.0003	0.0002	0.0857	0.007
AV _d (%)	1.9385	0.0004	4.4538	0.003
ZSUF (%)	0.0020	0.0014	0.0714	0.010
NSUF (%)	0.0014	0.0012	0.1586	0.007
I _N (p.u.)	2.2906	0	0.6031	0

Table 3.2: Comparison of the solutions obtained with planning *Cases B* and *C* using DE for 19-bus and 25-bus systems

Objective	19-bus system				25-bus system			
	<i>Case B</i>		<i>Case C</i>		<i>Case B</i>		<i>Case C</i>	
	Mean	SD	Mean	SD	Mean	SD	Mean	SD
PL (kW)	1.7801	0.0214	2.5431	0.0321	109.312	0.006	108.861	0.005
TS _u (MVA)	0.0003	0.0023	0.0023	0.0043	0.0857	0.014	0.0856	0.012
AV _d (%)	0.7418	0.0039	0.8453	0.0056	3.7645	0.038	3.5432	0.036
ZSUF (%)	0.0027	0.0006	0.0058	0.0022	0.0947	0.045	0.0957	0.034
NSUF (%)	0.0011	0.0005	0.0045	0.0018	0.1148	0.070	0.1151	0.067
I _N (p.u.)	2.2906	0	2.3061	0.0026	0.6031	0	0.5987	0

Table 3.3: Comparison of the results as obtained with Case C planning using DE and CSA for 19-bus and 25-bus systems

Objective	19-bus system				25-bus system			
	DE		CSA		DE		CSA	
	Mean	SD	Mean	SD	Mean	SD	Mean	SD
PL (kW)	2.5431	0.0321	2.5631	0.0435	108.861	0.005	109.512	0.006
TS _u (MVA)	0.0023	0.0043	0.0031	0.0056	0.0856	0.012	0.0860	0.021
AV _d (%)	0.8453	0.0056	0.9134	0.0061	3.5432	0.036	3.6721	0.045
ZSUF (%)	0.0058	0.0022	0.0061	0.0031	0.0957	0.034	0.0961	0.042
NSUF (%)	0.0045	0.0018	0.0054	0.0021	0.1151	0.067	0.1267	0.075
I _N (p.u.)	2.3061	0.0026	2.3062	0.0030	0.5987	0	0.5989	0.002

Table 3.4: Comparison of the solutions obtained with planning Cases A using DE for the Indian 19-bus and 34-bus systems

Objective	Indian 19-bus system		34-bus system	
	Case A		Case A	
	Mean	SD	Mean	SD
PL (kW)	45.6142	0	577.3367	0.0001
TS _u (MVA)	0.0091	0.0050	0.0183	0.0063
AV _d (%)	3.3967	0.0248	6.9142	0.0040
ZSUF (%)	0.0120	0.0039	0.1082	0.0064
NSUF (%)	0.0048	0.0016	0.0366	0.0075
I _N (p.u.)	7.6206	0	53.3187	0.0002

Table 3.5: Comparison of the solutions obtained with planning Cases B and C using DE for the Indian 19-bus and 34-bus systems

Objective	Indian19-bus system				34-bus system			
	Case B		Case C		Case B		Case C	
	Mean	SD	Mean	SD	Mean	SD	Mean	SD
PL (kW)	18.9127	0.0214	17.3845	0.0203	565.4610	0.0081	564.2358	0.0072
TS _u (MVA)	0.0092	0.0064	0.0091	0.0062	0.0184	0.0071	0.0183	0.0063
AV _d (%)	1.8470	0.1939	1.5432	0.2145	6.9013	0.0158	6.8021	0.0149
ZSUF (%)	0.0130	0.0043	0.0131	0.0048	0.1095	0.1091	0.1103	0.1023
NSUF (%)	0.0053	0.0018	0.0056	0.0017	0.0378	0.0041	0.0385	0.0039
I _N (p.u.)	7.6206	0	7.5125	0	53.3187	0.0002	52.7165	0.0001

Table 3.6: Comparison of the results as obtained with Case C planning using DE and CSA for Indian 19-bus and 34-bus systems

Objective	Indian19-bus system				34-bus system			
	DE		CSA		DE		CSA	
	Mean	SD	Mean	SD	Mean	SD	Mean	SD
PL (kW)	17.3845	0.0203	18.0123	0.0312	564.2358	0.0072	565.5432	0.0075
TS _u (MVA)	0.0091	0.0062	0.0094	0.0071	0.0183	0.0063	0.0191	0.0071
AV _d (%)	1.5432	0.2145	1.6132	0.2241	6.8021	0.0149	6.9132	0.0155
ZSUF (%)	0.0131	0.0048	0.0161	0.0051	0.1103	0.1023	0.1243	0.1121
NSUF (%)	0.0056	0.0017	0.0061	0.0018	0.0385	0.0039	0.0401	0.0045
I _N (p.u.)	7.5125	0	7.5126	0.002	52.7165	0.0001	52.7165	0.0003

3.4.1 Results of Single Objective Optimization

The single objective optimization is carried out as discussed in Chapter 2. The results of single objective optimization considering each objective separately for planning Case A are given in Table 3.1 and 3.4 respectively for the 19-, and 25-bus and Indian 19- and 34-bus system. Comparison of the results as obtained with Case C planning using DE and CSA for 19-bus and 25-bus systems is given in Table 3.3. From chapter 2, it is observed that the performance of DE is better and consistent according to the mean objective

function and the standard deviation (SD), respectively as compared to the other three algorithms. A performance comparison between planning *Cases B* and *C* using DE is provided in Table 3.2 and 3.5 for 19- and 25-bus system and Indian 19- and 34-bus system respectively. Table 3.6 shows the comparison of the results as obtained with Case C planning using DE and CSA for Indian 19-bus and 34-bus systems. It shows that the solutions are improved in view of the power loss the average voltage drop, and the neutral current in planning *Case C* for the Indian 19-bus, the 25- bus, and the 34-bus system. It is expected because the optimization of the conductor sizes and the capacitor placement and sizing improve these three objectives. However, the capacitor size and the conductor size optimization does not have any positive impact on the optimization of other objectives. Thus, the solutions obtained with the optimization of the other objectives either remain same or slightly different than *Case B*.

3.4.2 Results of Multi-Objective Optimization

The multi-objective optimization is carried out as discussed in Chapter 2. In this subsection, all the objective functions are aggregated with equal weights so as to get simultaneous optimization of all of them. The results of 50 runs for *Case A* planning as obtained with DE, are provided in Table 3.7 for 19- and 25-bus systems and in Table 3.10 for the Indian 19- bus and the 34- bus system. Comparison of the multi-objective optimization results as obtained with Case C planning using DE and CSA for 19-bus and 25-bus systems, and Indian 19- bus and 34- bus system are shown in Table 3.9 and 3.12 respectively. From Chapter 2, it can be seen that the DE provides a better solution in comparison to other metaheuristic algorithms such as the CSA, the PSO, and the GA. Hence, a performance comparison between planning *Cases B* and *C* using DE, for the 19-, and 25-bus and Indian 19- and 34-bus systems are given in Table 3.8 and 3.11 respectively. It shows that the solutions are improved in view of the power loss and the average voltage drop, and the neutral current in planning *Case C*. This can be due to simultaneous phase balancing, conductor sizing, and capacitor allocation and sizing optimization. The optimal location and sizing of capacitors are found to be 9, 11, and 12, and 150, 600, and 1350 kVAR at phase a, b, and c for the Indian 19, 25, and 34- bus system respectively. However, the inferior solutions are obtained in the 19- bus system with capacitors having rating 150 kVAR allocated at bus 9 for phase a, b, and c

respectively. This can be due to reactive power compensation of the capacitor. The average voltage drop (AVD) in % vs. bus number for different planning cases obtained with the DE for the 19-, 25-, Indian 19-, and 34- bus systems are shown in Figs. (3.4- 3.7). The complex power demand and the conductor sizes as obtained with Case C planning in a sample run for all the systems are shown in Appendix (Table F.1-F.4).

Table 3.7: Results of the multi-objective optimization of 50 runs obtained with DE for the 19- bus and 25- bus system

Objective	19-bus system		25-bus system	
	Case A		Case A	
	Mean	SD	Mean	SD
PL (kW)	12.561	0.0002	136.25	0.0560
TS _u (MVA)	0.0008	0.0011	0.0869	0.0023
AV _d (%)	1.9717	0.0003	4.4631	0.0013
ZSUF (%)	0.0025	0.0009	0.0726	0.0019
NSUF (%)	0.0055	0.0019	0.2135	0.0041
I _N (p.u.)	2.2906	0	0.6031	0

Table 3.8: Results of the multi-objective optimization of 50 runs obtained with DE for the 19- bus and 25- bus system

Objective	19-bus system				25-bus system			
	Case B		Case C		Case B		Case C	
	Mean	SD	Mean	SD	Mean	SD	Mean	SD
PL (kW)	2.2358	0.0593	2.5641	0.0324	110.16	0.1745	109.756	0.006
TS _u (MVA)	0.0008	0.0008	0.0025	0.0047	0.0869	0.0145	0.0870	0.014
AV _d (%)	0.7469	0.0220	1.8476	0.0059	4.0230	0.0945	3.5442	0.038
ZSUF (%)	0.0054	0.0013	0.0060	0.0024	0.1754	0.0177	0.1755	0.036
NSUF (%)	0.0204	0.0064	0.0205	0.0020	0.3881	0.0165	0.3892	0.077
I _N (p.u.)	2.2906	0	2.3062	0.0028	0.6031	0	0.5990	0

Table 3.9: Comparison of the multi-objective optimization results as obtained with Case C planning using DE and CSA for 19-bus and 25-bus systems

Objective	19-bus system				25-bus system			
	DE		CSA		DE		CSA	
	Mean	SD	Mean	SD	Mean	SD	Mean	SD
PL (kW)	2.5641	0.0324	2.5732	0.0412	109.756	0.006	110.121	0.009
TS _u (MVA)	0.0025	0.0047	0.0035	0.0051	0.0870	0.014	0.0875	0.021
AV _d (%)	1.8476	0.0059	1.9231	0.0061	3.5442	0.038	3.6932	0.054
ZSUF (%)	0.0060	0.0024	0.0071	0.0031	0.1756	0.036	0.1768	0.043
NSUF (%)	0.0205	0.0020	0.0261	0.0031	0.3892	0.077	0.3897	0.087
I _N (p.u.)	2.3062	0.0028	2.3063	0.0031	0.5990	0	0.5991	0.001

Table 3.10: Results of the multi-objective optimization of 50 runs obtained with DE for the Indian 19- bus and 34- bus system

Objective	Indian 19-bus system		34-bus system	
	Case A		Case A	
	Mean	SD	Mean	SD
PL (kW)	46.2827	0.0158	577.6140	0.0002
TS _u (MVA)	0.0095	0.0055	0.0191	0.0068
AV _d (%)	3.7945	0.0598	6.9567	0.0052
ZSUF (%)	0.0245	0.0098	0.1561	0.0078
NSUF (%)	0.0125	0.0064	0.0412	0.0083
I _N (p.u.)	7.6206	0	53.3189	0.0002

Table 3.11: Results of the multi-objective optimization of 50 runs obtained with DE for the Indian 19- bus and 34- bus system

Objective	Indian 19-bus system				34-bus system			
	Case B		Case C		Case B		Case C	
	Mean	SD	Mean	SD	Mean	SD	Mean	SD
PL (kW)	20.2161	0.0266	17.3912	0.0243	566.0124	0.0093	564.3961	0.0074
TS _u (MVA)	0.0110	0.0014	0.0109	0.0015	0.0190	0.0082	0.0189	0.0066
AV _d (%)	1.8795	0.1939	1.5450	0.1663	6.9145	0.0172	6.8045	0.0152
ZSUF (%)	0.0281	0.0292	0.0280	0.0250	0.1143	0.1123	0.1198	0.1025
NSUF (%)	0.0169	0.0078	0.0170	0.0057	0.0385	0.0065	0.0397	0.0041
I _N (p.u.)	7.6206	0	7.5134	0	53.3189	0.0003	52.8945	0.0003

Table 3.12: Comparison of the multi-objective optimization results as obtained with Case C planning using DE and CSA for Indian 19- bus and 34- bus systems

Objective	Indian 19-bus system				34-bus system			
	DE		CSA		DE		CSA	
	Mean	SD	Mean	SD	Mean	SD	Mean	SD
PL (kW)	17.3912	0.0243	18.4531	0.0345	564.3961	0.0074	565.9132	0.0085
TS _u (MVA)	0.0109	0.0015	0.0160	0.0032	0.0189	0.0066	0.0195	0.0075
AV _d (%)	1.5450	0.1663	1.6321	0.1861	6.8045	0.0152	6.9542	0.0161
ZSUF (%)	0.0280	0.0250	0.0301	0.0331	0.1198	0.1025	0.1289	0.1125
NSUF (%)	0.0170	0.0057	0.0264	0.0075	0.0397	0.0041	0.0425	0.0051
I _N (p.u.)	7.5134	0	7.5140	0.002	52.8945	0.0003	52.9121	0.0005

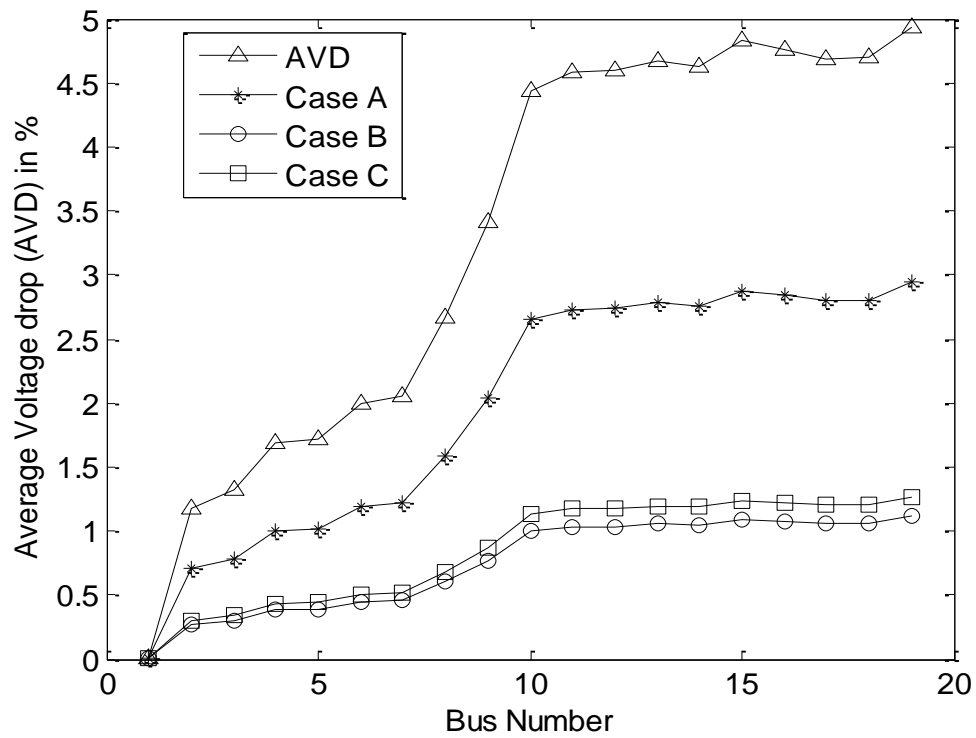


Fig. 3.4. AVD vs. bus number for different planning cases obtained with the DE for the 19- bus system

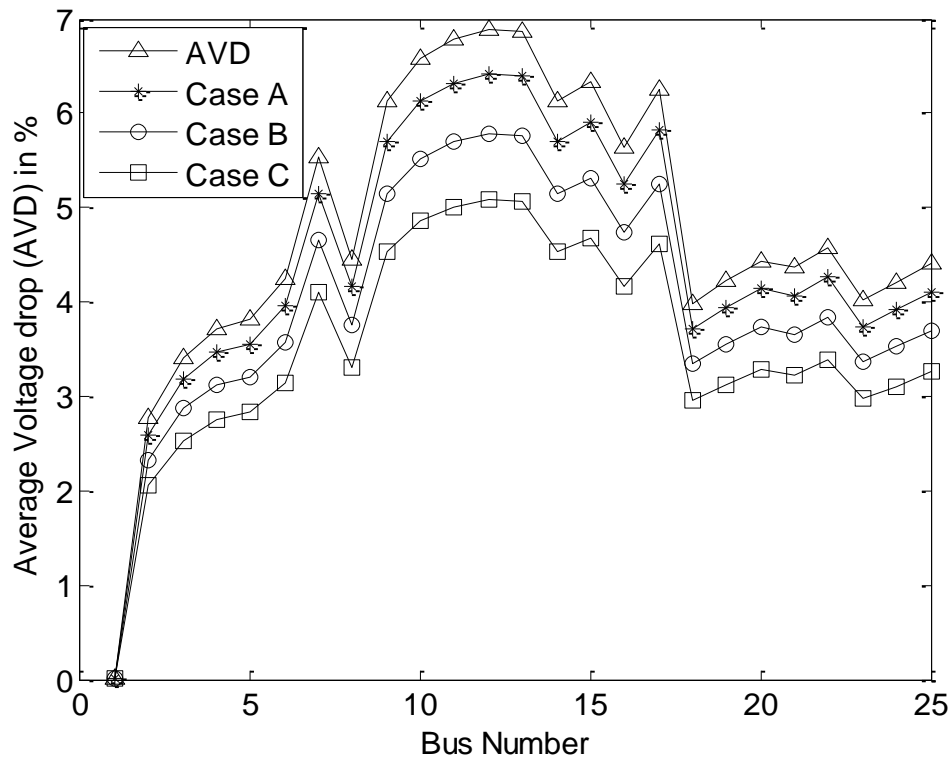


Fig. 3.5. AVD vs. bus number for different planning cases obtained with the DE for the 25- bus system

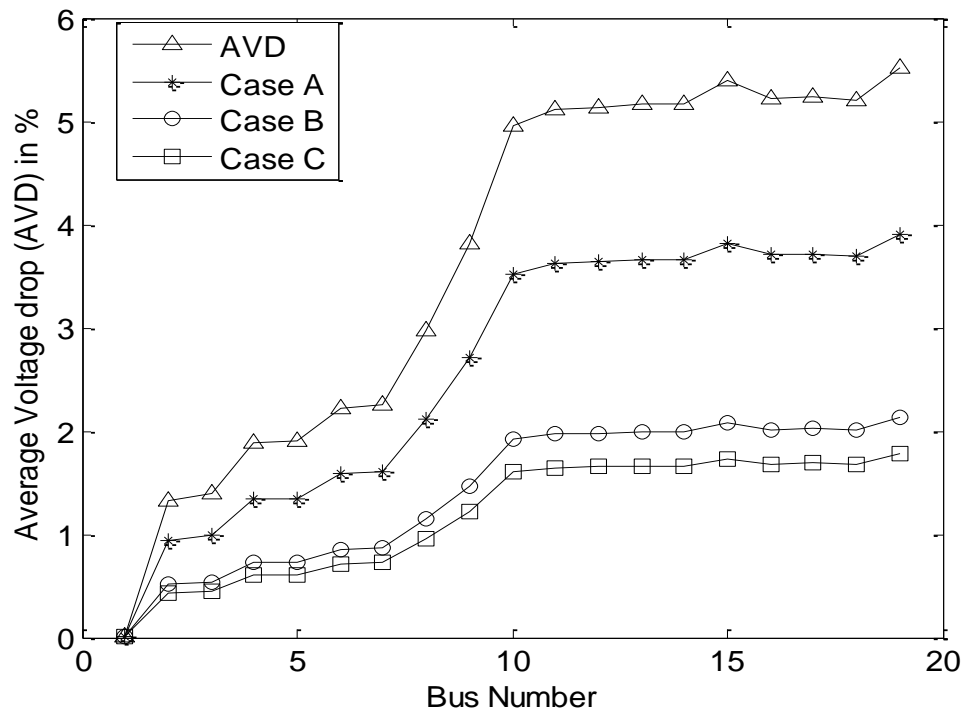


Fig. 3.6. AVD vs. bus number for different planning cases obtained with the DE for the Indian 19- bus system

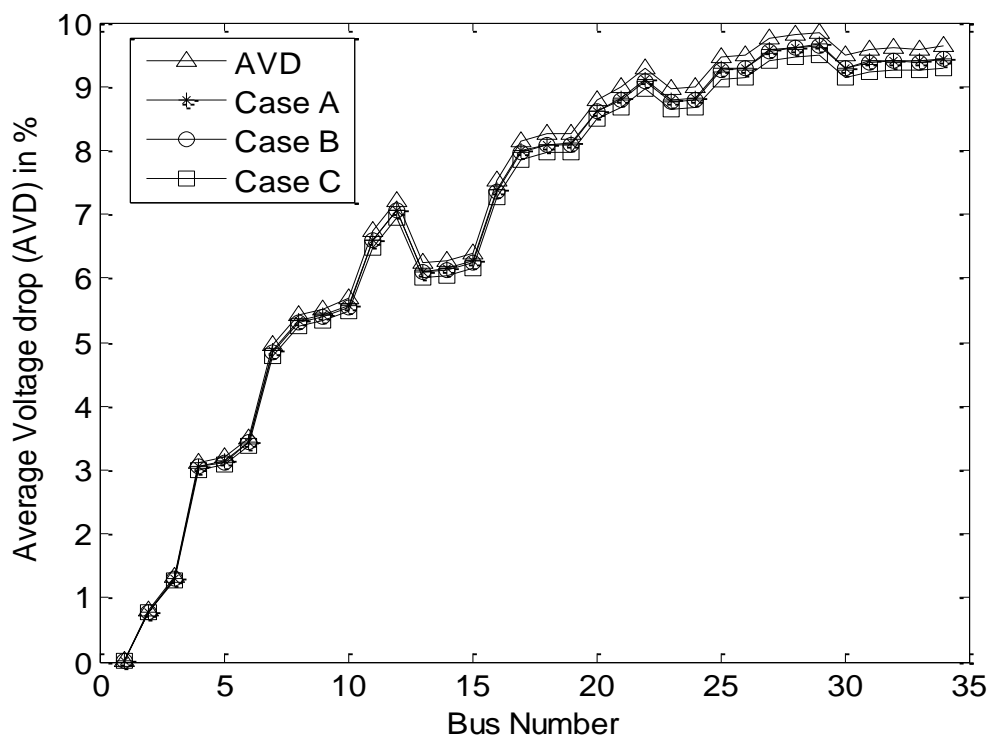


Fig. 3.7. AVD vs. bus number for different planning cases obtained with the DE for the 34- bus system

3.5 Summary

In this chapter, a planning approach has been developed in order to determine the optimal phase balancing the conductor sizes, and the capacitor location and the sizing of unbalanced radial distribution systems by optimizing the power loss, the complex power unbalance, the average voltage drop, the positive and zero sequence unbalance factors and the neutral current integrating capacitors. A three phase forward-backward sweep load flow algorithm is developed and used in the planning approach. The DE and CSA are employed as the solution methodology.

The simultaneous optimization for the phase balancing, the conductor sizing, the capacitor location and the sizing provides a network with lower power loss, average voltage drop, and neutral current for the Indian 19- bus, the 25- bus, and the 34- bus system. However, the simultaneous optimization for the phase balancing, the conductor sizing, the capacitor location and the sizing gives inferior solutions as obtained with DE in case of the 19- bus system for both single and multi-objective optimization. This can be due to the high discrete rating of the capacitor. From Chapter 1, it is found that the distribution static compensators can provide continuously variable reactive power into the system. Thus, the next chapter focuses on the planning of URDS considering the integration of distribution static compensators (DSTATCOM).

Chapter 4

Planning of Unbalanced Radial Distribution Systems with DSTATCOM Using Evolutionary Computing Algorithms

4.1 Introduction

In chapter 3, the planning of URDS has been presented using differential evolution algorithm (DE) and CSA in the presence of the capacitors. Several objective functions such as the total power loss, the average voltage drop, the total neutral current and the total voltage unbalance have been minimized using these algorithms. However, the simultaneous optimization for phase balancing, conductor sizing, capacitor location, and sizing gives inferior solutions in case of the 19- bus system.

From chapter 1, it is observed that distribution static compensators (DSTATCOM) can reduce power loss and improve voltage profile of distribution systems. Thus, in this chapter planning of four URDS has been carried integrating DSTATCOM with the system. A three-phase unbalanced modelling of DSTATCOM has been devised. The objective functions considered are the total power loss, the average voltage drop, the total neutral current and total voltage unbalance. The DE and CSA are employed as the solution strategy for minimizing these objective functions in order to obtain optimal DSTATCOM location, rating, conductor sizing and phase balancing. For the evaluation of each objective, a forward-backward sweep load flow algorithm including the DSTATCOM model is developed. The proposed approaches are demonstrated on the 19-bus, 25-bus, Indian 19-bus and 34-bus URDS.

This chapter is organized as follows: A three-phase unbalanced modelling of DSTATCOM is presented in Section 4.2. Problem Formulation is presented in Section 4.3. In Section 4.4, the implementation of the proposed planning approach using the DE and CSA are described. The simulation results are presented in Section 4.5. Section 4.6 concludes the chapter.

4.2 A three-phase unbalanced modelling of DSTATCOM

This section provides a brief description about the DSTATCOM modelling. Figure 4.1. depicts a three phase three wire line section model including a DSTATCOM between bus i and bus j .

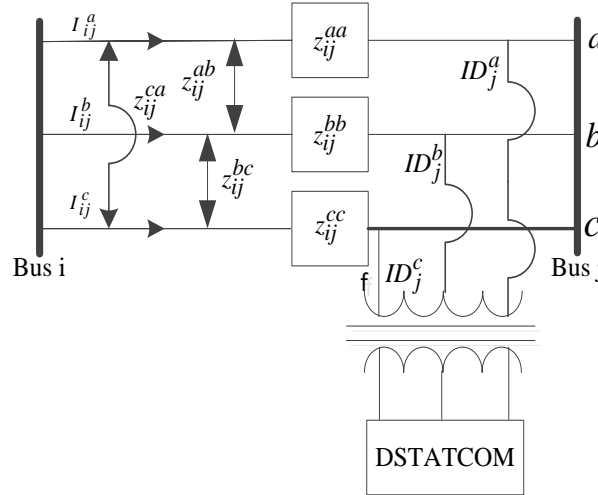


Fig. 4.1. DSTATCOM installation in bus j in a three-phase three wire line section model

Where, z_{ij}^{aa} , z_{ij}^{bb} , and z_{ij}^{cc} denotes self impedance of phase a, phase b, and phase c respectively; z_{ij}^{ab} , z_{ij}^{bc} , and z_{ij}^{ca} denotes mutual impedance between phases.

Applying Kirchhoff's voltage law (KVL) equation in between bus i and bus j when DSTATCOM is connected at bus j in Fig.4.1. We obtain the equation as follows:

$$\begin{bmatrix} V_j^a \angle(\alpha_1) \\ V_j^b \angle(-120^\circ + \alpha_2) \\ V_j^c \angle(120^\circ + \alpha_3) \end{bmatrix} = \begin{bmatrix} V_i^a \angle \delta_1 \\ V_i^b \angle \delta_2 \\ V_i^c \angle \delta_3 \end{bmatrix} - \begin{bmatrix} Z_{ij}^{aa} & Z_{ij}^{ab} & Z_{ij}^{ac} \\ Z_{ij}^{ba} & Z_{ij}^{bb} & Z_{ij}^{bc} \\ Z_{ij}^{ca} & Z_{ij}^{cb} & Z_{ij}^{cc} \end{bmatrix} \begin{bmatrix} I_{ij}^a \angle \theta_a \\ I_{ij}^b \angle \theta_b \\ I_{ij}^c \angle \theta_c \end{bmatrix} - \begin{bmatrix} Z_{ij}^{aa} & Z_{ij}^{ab} & Z_{ij}^{ac} \\ Z_{ij}^{ba} & Z_{ij}^{bb} & Z_{ij}^{bc} \\ Z_{ij}^{ca} & Z_{ij}^{cb} & Z_{ij}^{cc} \end{bmatrix} \begin{bmatrix} ID_j^a \angle(\alpha_1 + \pi/2) \\ ID_j^b \angle(\alpha_2 + \pi/2 - 120^\circ) \\ ID_j^c \angle(\alpha_3 + \pi/2 + 120^\circ) \end{bmatrix} \quad (4.1)$$

Where, ID_j^a , ID_j^b , and ID_j^c are the current injected by DSTATCOM at phase a, b, and c respectively.

Simplifying the equation (4.1) as follows:

$$\begin{bmatrix} V_j^a \angle(\alpha_1) \\ V_j^b \angle(-120^0 + \alpha_2) \\ V_j^c \angle(120^0 + \alpha_3) \end{bmatrix} = \begin{bmatrix} V_i^a \angle \delta_1 \\ V_i^b \angle \delta_2 \\ V_i^c \angle \delta_3 \end{bmatrix} - \begin{bmatrix} Z_{ij}^{aa} IL_j^a \angle \theta_a + Z_{ij}^{ab} IL_j^b \angle \theta_b + Z_{ij}^{ac} IL_j^c \angle \theta_c \\ Z_{ij}^{ba} IL_j^a \angle \theta_a + Z_{ij}^{bb} IL_j^b \angle \theta_b + Z_{ij}^{bc} IL_j^c \angle \theta_c \\ Z_{ij}^{ca} IL_j^a \angle \theta_a + Z_{ij}^{cb} IL_j^b \angle \theta_b + Z_{ij}^{cc} IL_j^c \angle \theta_c \end{bmatrix} - \begin{bmatrix} Z_{ij}^{aa} ID_j^a \angle(\alpha_1 + \pi/2) + Z_{ij}^{ab} ID_j^b \angle(\alpha_2 + \pi/2 - 120^0) + Z_{ij}^{ac} ID_j^c \angle(\alpha_3 + \pi/2 + 120^0) \\ Z_{ij}^{ba} ID_j^a \angle(\alpha_1 + \pi/2) + Z_{ij}^{bb} ID_j^b \angle(\alpha_2 + \pi/2 - 120^0) + Z_{ij}^{bc} ID_j^c \angle(\alpha_3 + \pi/2 + 120^0) \\ Z_{ij}^{ca} ID_j^a \angle(\alpha_1 + \pi/2) + Z_{ij}^{cb} ID_j^b \angle(\alpha_2 + \pi/2 - 120^0) + Z_{ij}^{cc} ID_j^c \angle(\alpha_3 + \pi/2 + 120^0) \end{bmatrix} \quad (4.2)$$

Simplifying eq. (4.2) for phase a, we obtain:

$$V_j^a \cos \alpha_1 = \text{Real}(V_i^a \angle \delta_1) - \text{Real}(Z_{ij}^{aa} IL_j^a \angle \theta_a + Z_{ij}^{ab} IL_j^b \angle \theta_b + Z_{ij}^{ac} IL_j^c \angle \theta_c) - \text{Real}(Z_{ij}^{aa} ID_j^a \angle(\alpha_1 + \pi/2) + Z_{ij}^{ab} ID_j^b \angle(\alpha_2 + \pi/2 - 120^0) + Z_{ij}^{ac} ID_j^c \angle(\alpha_3 + \pi/2 + 120^0)) \quad (4.3)$$

$$V_j^a \sin \alpha_1 = \text{Imag}(V_i^a \angle \delta_1) - \text{Imag}(Z_{ij}^{aa} IL_j^a \angle \theta_a + Z_{ij}^{ab} IL_j^b \angle \theta_b + Z_{ij}^{ac} IL_j^c \angle \theta_c) - \text{Imag}(Z_{ij}^{aa} ID_j^a \angle(\alpha_1 + \pi/2) + Z_{ij}^{ab} ID_j^b \angle(\alpha_2 + \pi/2 - 120^0) + Z_{ij}^{ac} ID_j^c \angle(\alpha_3 + \pi/2 + 120^0)) \quad (4.4)$$

Let, $a1 = \text{Real}(V_i^a \angle \delta_1) - \text{Real}(Z_{ij}^{aa} IL_j^a \angle \theta_a + Z_{ij}^{ab} IL_j^b \angle \theta_b + Z_{ij}^{ac} IL_j^c \angle \theta_c)$
 $a2 = \text{Imag}(V_i^a \angle \delta_1) - \text{Imag}(Z_{ij}^{aa} IL_j^a \angle \theta_a + Z_{ij}^{ab} IL_j^b \angle \theta_b + Z_{ij}^{ac} IL_j^c \angle \theta_c)$

Let, $b = V_j^a$, $b1 = V_j^b$, and $b2 = V_j^c$

$$b \cos \alpha_1 = a1 + ID_j^a (k1 \cos \alpha_1 + k2 \sin \alpha_1) + ID_j^b (k5 \cos(-120^0 + \alpha_2) + k6 \sin(-120^0 + \alpha_2)) + ID_j^c (k7 \cos(120^0 + \alpha_3) + k8 \sin(120^0 + \alpha_3)) \quad (4.5)$$

$$b \sin \alpha_1 = a2 + ID_j^a (k3 \cos \alpha_1 - k4 \sin \alpha_1) + ID_j^b (k9 \cos(-120^0 + \alpha_2) - k10 \sin(-120^0 + \alpha_2)) + ID_j^c (k11 \cos(120^0 + \alpha_3) - k12 \sin(120^0 + \alpha_3)) \quad (4.6)$$

Adding equation (4.5) and (4.6)

$$b \cos \alpha_1 + b \sin \alpha_1 = a1 + a2 + ID_j^a (k1 \cos \alpha_1 + k2 \sin \alpha_1) + ID_j^b (k5 \cos(-120^0 + \alpha_2) + k6 \sin(-120^0 + \alpha_2)) + ID_j^c (k7 \cos(120^0 + \alpha_3) + k8 \sin(120^0 + \alpha_3)) + ID_j^a (k3 \cos \alpha_1 - k4 \sin \alpha_1) + ID_j^b (k9 \cos(-120^0 + \alpha_2) - k10 \sin(-120^0 + \alpha_2)) + ID_j^c (k11 \cos(120^0 + \alpha_3) - k12 \sin(120^0 + \alpha_3)) \quad (4.7)$$

Simplifying equation (4.7)

$$b(\cos \alpha_1 + \sin \alpha_1) = a1 + a2 + [ID_j^a (\cos \alpha_1 (k1 + k3) + \sin \alpha_1 (k2 - k4)) + ID_j^b (\cos(-120^0 + \alpha_2) * (k5 + k9) + \sin(-120^0 + \alpha_2) * (k6 - k10)) + ID_j^c (\cos(120^0 + \alpha_3) * (k7 + k11) + \sin(120^0 + \alpha_3) * (k8 - k12))] \quad (4.8)$$

Again simplifying Eq. (4.8)

$$b(\cos \alpha_1 + \sin \alpha_1) = a1 + a2 + [ID_j^a (\cos \alpha_1 (ka) + \sin \alpha_1 (kb)) + ID_j^b (\cos(-120^0 + \alpha_2) * (kc) + \sin(-120^0 + \alpha_2) * (kd)) + ID_j^c (\cos(120^0 + \alpha_3) * (ke) + \sin(120^0 + \alpha_3) * (kf))] \quad (4.9)$$

Similarly for phase b

$$b1(\cos(-120^0 + \alpha_2) + \sin(-120^0 + \alpha_2)) = a3 + a4 + [ID_j^a (\cos \alpha_1 (kg) + \sin \alpha_1 (ki)) + ID_j^b (\cos(-120^0 + \alpha_2) * (kj) + \sin(-120^0 + \alpha_2) * (km)) + ID_j^c (\cos(120^0 + \alpha_3) * (kn) + \sin(120^0 + \alpha_3) * (ko))] \quad (4.10)$$

Similarly for phase c

$$b2(\cos(120^0 + \alpha_3) + \sin(120^0 + \alpha_3)) = a3 + a4 + [ID_j^a (\cos \alpha_1 (kp) + \sin \alpha_1 (kr)) + ID_j^b (\cos(-120^0 + \alpha_2) * (ks) + \sin(-120^0 + \alpha_2) * (kt)) + ID_j^c (\cos(120^0 + \alpha_3) * (ku) + \sin(120^0 + \alpha_3) * (kv))] \quad (4.11)$$

Solving Eq. (4.9)-eq. (4.11) simultaneously for different values of $\alpha_1, \alpha_2, \alpha_3$ we can obtain the values of DSTATCOM current magnitudes ID_j^a, ID_j^b , and ID_j^c respectively.

The range of $\alpha_1, \alpha_2, \alpha_3$ are taken as:

$$-1 < \alpha_1 < 1 \quad (4.12)$$

$$-1 < \alpha_2 < 1 \quad (4.13)$$

$$-1 < \alpha_3 < 1 \quad (4.14)$$

The reactive power that must be injected by the DSTATCOM at phase a, b, and c is expressed below:

$$jQ_{DSTAT}^a = (V_j^a \angle \alpha_1) \cdot (ID_j^a \angle (\alpha_1 + \pi/2))^* \quad (4.15)$$

$$jQ_{DSTAT}^b = (V_j^b \angle \alpha_2) \cdot (ID_j^b \angle (\alpha_2 + \pi/2))^* \quad (4.16)$$

$$jQ_{DSTAT}^c = (V_j^c \angle \alpha_3) \cdot (ID_j^c \angle (\alpha_3 + \pi/2))^* \quad (4.17)$$

It can be observed that DSTATCOM injects current in quadrature with the bus voltage where it is connected so as to compensate the reactive power only. This is explained in a phasor diagram as shown in Fig. 4.2.

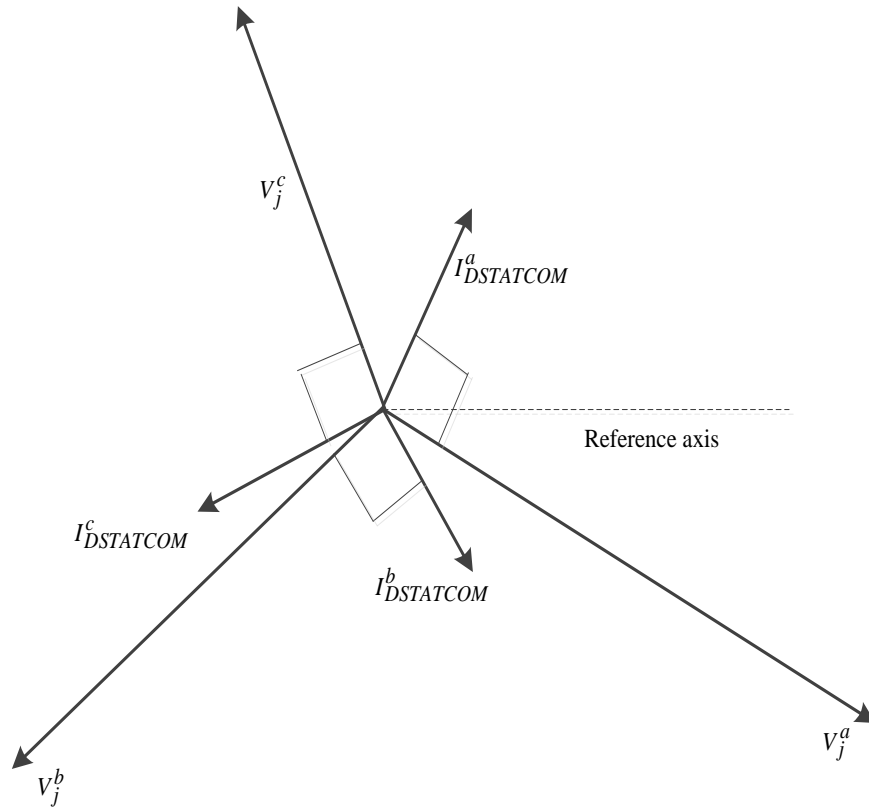


Fig. 4.2. Phasor diagram of dstatcom currents with respect to voltages at phase a, b, and c, respectively

4.3 Problem Formulation

The aim of this planning problem is the minimization of the numerous objective functions as discussed in Chapter 2; subject to some technical constraints as follows:

i. Voltage constraint: The voltage at each bus must lie between the lower and upper bound limit in order to avoid under voltage and over voltage problem.

$$V_s^{\min} \leq V_s^{abc} \leq V_s^{\max} \quad (4.18)$$

ii. Thermal constraint: The current flowing through each branch shouldn't exceed the maximum current-carrying capacity of the conductor for all the phases.

$$I_j^{abc} \leq I_j^{\max} \quad (4.19)$$

iii. DSTATCOM rating constraint

The DSTATCOM rating should be less than or equal to the maximum value of the DSTATCOM rating.

$$Qdsat_a \leq Qdstat_{\max} \quad (4.20)$$

Where $Qdsat_a$ denotes, the allowable DSTATCOM size, the maximum value of DSTATCOM rating is represented as $Qdstat_{\max}$.

4.4 Implementation of DE and CSA for the planning problem

The proposed planning approach with DE and CSA utilizes a three-phase load flow algorithm as an auxiliary program in order to obtain bus voltage magnitudes and power loss of a system. The load flow algorithm including the DSTATCOM is explained in Section 4.4.1 and application of the DE is described in Section 4.4.2.

4.4.1 Three phase forward-backward sweep load flow algorithm incorporating DSTATCOM

To compute the power flow solutions in URDS, the three-phase unbalanced DSTATCOM model is incorporated in the three-phase load flow algorithm. In this algorithm, two simple

steps called backward sweep step, and forward sweep step are utilized for the evaluation of power flow solutions. The load currents in unbalanced radial distribution systems are calculated using the backward sweep as follows:

$$\overline{IL}_j^a = \left(\frac{P_j^a - iQ_j^a}{\overline{V}_j^{a*}} \right) \quad (4.21)$$

$$\overline{IL}_j^b = \left(\frac{P_j^b - iQ_j^b}{\overline{V}_j^{b*}} \right) \quad (4.22)$$

$$\overline{IL}_j^c = \left(\frac{P_j^c - iQ_j^c}{\overline{V}_j^{c*}} \right) \quad (4.23)$$

Where, \overline{IL}_j^a , \overline{V}_j^{a*} , P_j^a , Q_j^a are the load current and voltage conjugate (in phasor form), active and reactive power demand at bus j for phase a

When, DSTATCOM is placed at bus, j , the modified reactive power demand is given by:

$$Q_j'^a = Q_j^a - Q_{DSTAT_j}^a \quad (4.24)$$

$$Q_j'^b = Q_j^b - Q_{DSTAT_j}^b \quad (4.25)$$

$$Q_j'^c = Q_j^c - Q_{DSTAT_j}^c \quad (4.26)$$

The modified load current, when DSTATCOM is placed at bus j , is computed using the modified reactive power demand as obtained from Eq. (4.24)-(4.26) and is expressed as:

$$\overline{IL}_j^a = \left(\frac{P_j^a - iQ_j'^a}{\overline{V}_j^{a*}} \right) \quad (4.27)$$

$$\overline{IL}_j^b = \left(\frac{P_j^b - iQ_j'^b}{\overline{V}_j^{b*}} \right) \quad (4.28)$$

$$\overline{IL}_j^c = \left(\frac{P_j^c - iQ_j'^c}{\overline{V}_j^{c*}} \right) \quad (4.29)$$

Then the branch currents are computed as follows:

$$\overline{I}^a(jk) = \overline{I}^a(k) + \sum_{j \in T} \overline{IL}_j^a \quad (4.30)$$

$$\overline{I}^b(jk) = \overline{I}^b(k) + \sum_{j \in T} \overline{IL}_j^b \quad (4.31)$$

$$\bar{I}^c(jk) = \bar{I}^c(k) + \sum_{j \in T} \bar{I}_j^c \quad (4.32)$$

Where $\bar{I}^a(jk)$ denotes the current flowing (in phasor form) in branch jk for phase- a and the set T consists of all buses connected to jk^{th} branch.

Then, the forward sweep is executed in order to obtain the bus voltages. This step is performed in order to obtain the voltage at each bus of an unbalanced distribution system as follows:

$$\begin{bmatrix} \bar{V}_k^a \\ \bar{V}_k^b \\ \bar{V}_k^c \end{bmatrix} = \begin{bmatrix} \bar{V}_j^a \\ \bar{V}_j^b \\ \bar{V}_j^c \end{bmatrix} - \begin{bmatrix} Z_{jk}^{aa} & Z_{jk}^{ab} & Z_{jk}^{ac} \\ Z_{jk}^{ba} & Z_{jk}^{bb} & Z_{jk}^{bc} \\ Z_{jk}^{ca} & Z_{jk}^{cb} & Z_{jk}^{cc} \end{bmatrix} \begin{bmatrix} \bar{I}_{jk}^a \\ \bar{I}_{jk}^b \\ \bar{I}_{jk}^c \end{bmatrix} \quad (4.33)$$

Where, bus j and k denote the sending end bus and the receiving end bus, respectively for branch jk .

The modelling of the three-phase DSTATCOM for the unbalanced distribution systems have three unknown parameters namely α_1 , α_2 , and α_3 . Where, α_1 is defined as the angular displacement of the voltage at phase a at the location where a DSTATCOM is connected. Similarly, α_2 and α_3 can be defined. Fig. 4.3. shows the flow chart of the load flow algorithm for the determination of reactive power injection by DSTATCOM for random location, and angle values

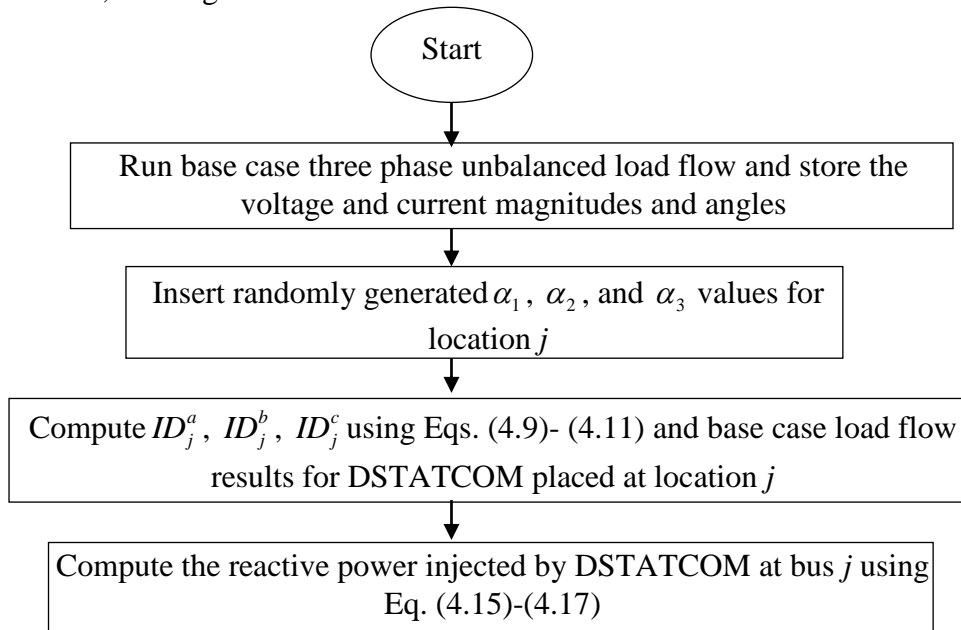


Fig. 4.3. Flow chart for the determination of reactive power injection by DSTATCOM for random location, and angle values

4.4.2 Proposed Planning Approach Using DE and CSA

In this chapter, DE and CSA are employed as the solution strategy for the planning problem of unbalanced radial distribution networks. The detail description of this algorithm can be found in chapter 2.

4.4.2.1 Decision variable representation

The parameters (decision variables) for the DE and CSA in this planning problem consists of three decision variables and are represented as a vector D as follows:

$$D = [\text{ANG}, \phi, \text{DR}, \text{APD}, \text{ctz}] \quad (4.34)$$

$$\text{ANG} = [\alpha_1, \alpha_2, \alpha_3, \dots, \alpha_{1_{\text{nop}}}, \alpha_{2_{\text{nop}}}, \alpha_{3_{\text{nop}}}] \quad (4.35)$$

$$\phi = [\phi_1, \phi_2, \dots, \phi_N] \quad (4.36)$$

$$\text{APD} = [\text{APD}_{a,b,c}, \text{APD}_{a,b,c}, \dots, \text{APD}_N] \quad (4.37)$$

$$\text{ctz} = [\text{ct}_1, \text{ct}_2, \dots, \text{ct}_{\text{NBR}}] \quad (4.38)$$

Where ANG represents vector of DSTATCOM angles ($\alpha_{1_{\text{nop}}}, \alpha_{2_{\text{nop}}}, \alpha_{3_{\text{nop}}}$) and are generated within the lower and the upper bound for number of population (nop), ϕ denotes the vector of DSTATCOM locations; APD vector represents the active and reactive power load for the phases a, b, and c for bus N , DR represents the rating of the DSTATCOM, and ctz represents a vector of different conductor types for the NBR number of branches. The flowchart of the proposed methods using DE and CSA are provided in Fig. 4.4 and Fig. 4.5 respectively.

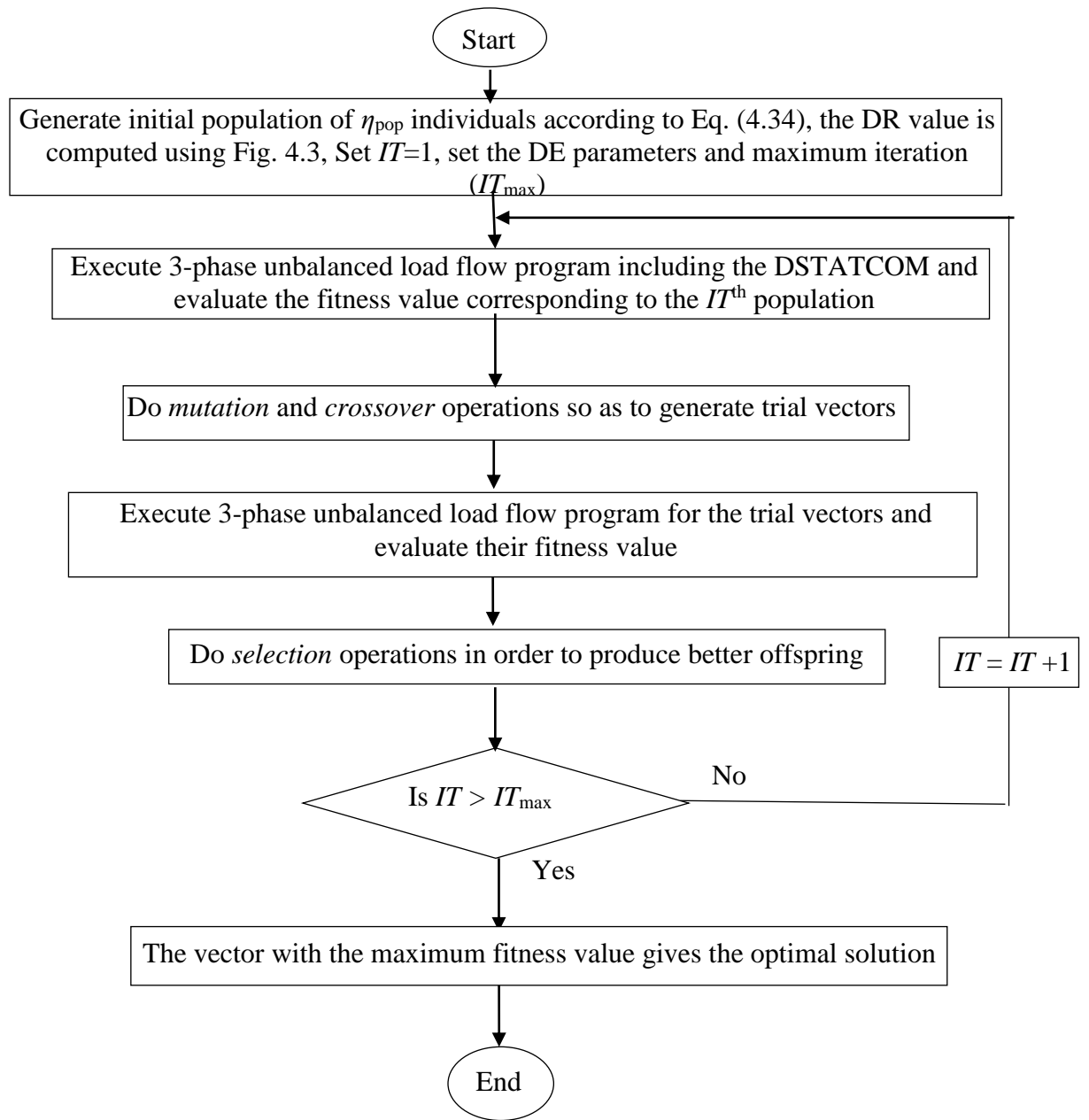


Fig. 4.4. Flow chart of the proposed planning approach using DE

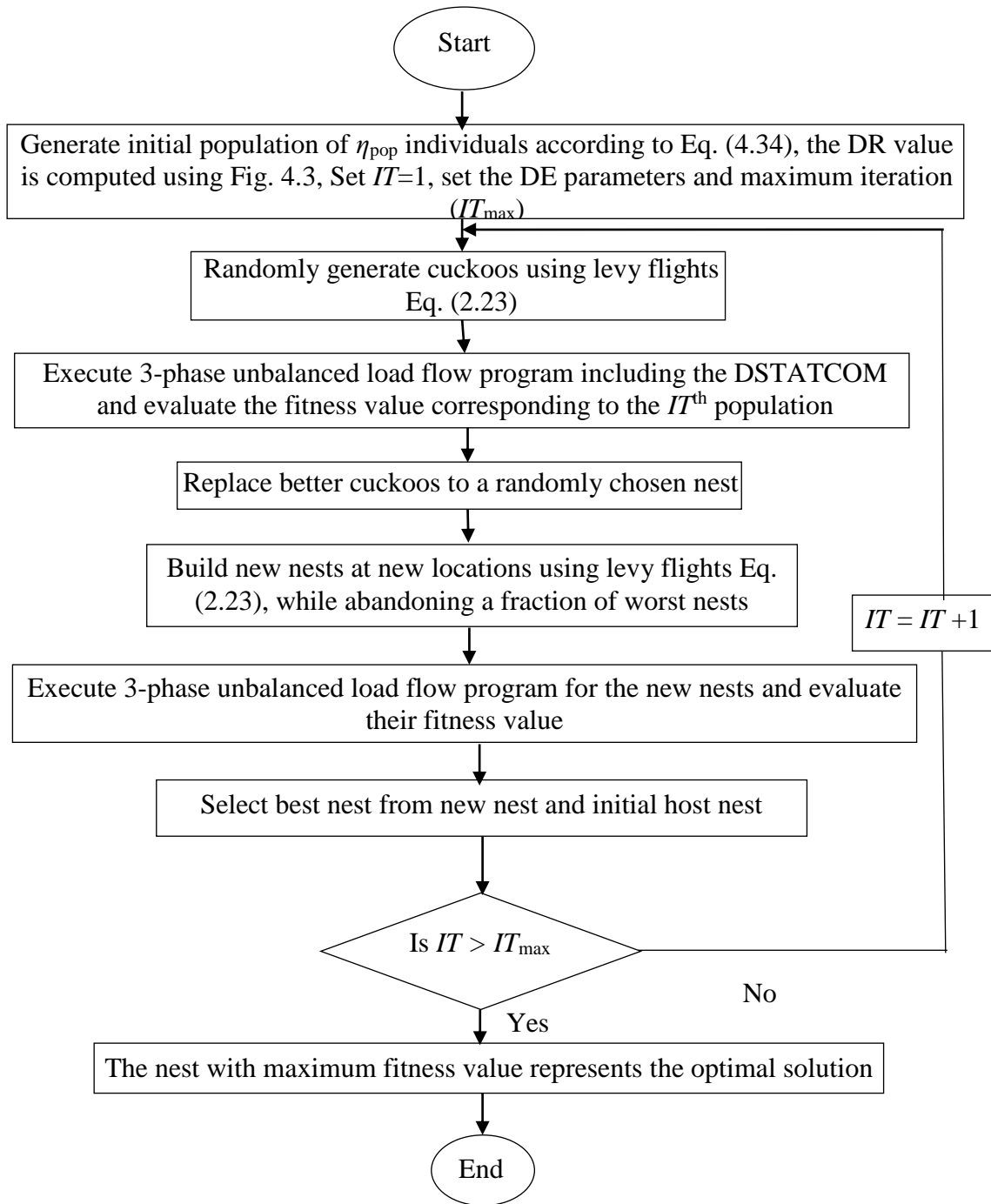


Fig. 4.5. Flow chart of the proposed planning approach using CSA

4.5 Simulation Results and discussions

The simulations are carried out with MATLAB R2012b software. The effectiveness of the proposed algorithm is verified on four unbalanced radial distribution networks, i.e. the 19-bus, 25-bus, Indian 19-bus and 34-bus system. The base case results of these systems are provided in Table 2.2 of Chapter 2. The maximum value of DSTATCOM rating is

considered as 10,000 kVAR [79]. The parameters of the DE are taken from Table 2.3 of Chapter 2. In this, chapter, three different planning cases are studied such as:

- *Case A*: planning for optimal phase balancing
- *Case B*: Simultaneous planning for the optimal phase balancing and the conductor sizing.
- *Case C*: Simultaneous planning for the optimal phase balancing, the conductor sizing, and the DSTATCOM allocation and sizing

Table 4.1: Comparison of the solutions obtained with planning *Cases B* and *C* using DE for 19-bus and 25-bus systems

Objective	19-bus system				25-bus system			
	<i>Case B</i>		<i>Case C</i>		<i>Case B</i>		<i>Case C</i>	
	Mean	SD	Mean	SD	Mean	SD	Mean	SD
PL (kW)	1.7801	0.0214	2.3212	0.0381	109.312	0.006	85.642	0.004
TS _u (MVA)	0.0003	0.0023	0.0050	0.0041	0.0857	0.014	0.0860	0.013
AV _d (%)	0.7418	0.0039	2.8623	0.0057	3.7645	0.038	3.4142	0.028
ZSUF (%)	0.0027	0.0006	0.0556	0.0023	0.0947	0.045	0.0951	0.029
NSUF (%)	0.0011	0.0005	0.0188	0.0019	0.1148	0.070	0.1152	0.058
I _N (p.u.)	2.2906	0	2.3134	0.0029	0.6031	0	0.5785	0

Table 4.2: Comparison of the results as obtained with Case C planning using DE and CSA for 19-bus and 25-bus systems

Objective	19-bus system				25-bus system			
	DE		CSA		DE		CSA	
	Mean	SD	Mean	SD	Mean	SD	Mean	SD
PL (kW)	2.3212	0.0381	2.5143	0.0412	85.642	0.004	86.345	0.009
TS _u (MVA)	0.0050	0.0041	0.0060	0.0051	0.0860	0.013	0.0875	0.021
AV _d (%)	2.8623	0.0057	2.9569	0.0061	3.4142	0.028	3.7645	0.031
ZSUF (%)	0.0556	0.0023	0.0632	0.0031	0.0951	0.029	0.0991	0.035
NSUF (%)	0.0188	0.0019	0.0192	0.0023	0.1152	0.058	0.1230	0.065
I _N (p.u.)	2.3134	0.0029	2.3142	0.0031	0.5785	0	0.5787	0.002

Table 4.3: Comparison of the solutions obtained with planning Cases B and C using DE for the Indian 19-bus and 34-bus systems

Objective	Indian19-bus system				34-bus system			
	Case B		Case C		Case B		Case C	
	Mean	SD	Mean	SD	Mean	SD	Mean	SD
PL (kW)	18.9127	0.0214	16.312	0.0200	565.4610	0.0081	436.2706	0.0072
TS _u (MVA)	0.0092	0.0064	0.0093	0.0011	0.0184	0.0071	0.0183	0.0063
AV _d (%)	1.8470	0.1939	1.4421	0.1135	6.9013	0.0158	4.1705	0.0149
ZSUF (%)	0.0130	0.0043	0.0131	0.0014	0.1095	0.1091	0.1103	0.1023
NSUF (%)	0.0053	0.0018	0.0054	0.0006	0.0378	0.0041	0.0385	0.0039
I _N (p.u.)	7.6206	0	7.4123	0	53.3187	0.0002	47.2024	0.0001

Table 4.4: Comparison of the results as obtained with Case C planning using DE and CSA for Indian 19-bus and 34-bus systems

Objective	Indian19-bus system				34-bus system			
	DE		CSA		DE		CSA	
	Mean	SD	Mean	SD	Mean	SD	Mean	SD
PL (kW)	16.312	0.0200	17.412	0.0312	436.2706	0.0072	437.5142	0.0081
TS _u (MVA)	0.0093	0.0011	0.0097	0.0021	0.0183	0.0063	0.0195	0.0073
AV _d (%)	1.4421	0.1135	1.5132	0.1581	4.1705	0.0149	4.5143	0.0161
ZSUF (%)	0.0131	0.0014	0.0161	0.0151	0.1103	0.1023	0.1823	0.1134
NSUF (%)	0.0054	0.0006	0.0071	0.0069	0.0385	0.0039	0.0412	0.0045
I _N (p.u.)	7.4123	0	7.5462	0.002	47.2024	0.0001	47.3145	0.0003

4.5.1 Results of Single Objective Optimization

The single objective optimization is performed as described in Chapter 2. The results of the single objective optimization considering each objective separately for planning Case A are given in Table 3.1 and 3.3 respectively for the 19-, and the 25-bus and Indian 19- and 34-bus system in chapter 3. From chapter 2, it is observed that the performance of DE is better and consistent according to the mean objective function and the standard deviation (SD), respectively as compared to the other three algorithms. A performance

comparison between the planning *Cases B* and *C* using the DE is provided in Table 4.1 and 4.3 for the 19- and the 25-bus system and the Indian 19- and 34-bus system respectively. Comparison of the results as obtained with Case C planning using DE and CSA for 19- bus and 25- bus are shown in Table 4.2. Table 4.4 shows these results for Indian 19-bus and 34-bus systems. It is observed that the solutions are improved in view of the power loss and the average voltage drop, and the neutral current in planning *Case C* for Indian 19-bus, 25- bus, and 34-bus system. It is expected because the optimization of the conductor sizes and the DSTATCOM placement and the sizing improves these three objectives. However, the DSTATCOM size and conductor size optimization does not have any positive impact on the optimization of other objectives. Thus, the solutions obtained with the optimization of the other objectives either remain same or slightly different than the *Case B*.

4.5.2 Results of Multi-Objective Optimization

The multi-objective optimization is executed as discussed in Chapter 2. In this subsection, all the objective functions are aggregated with equal weights so as to get simultaneous optimization of all of them. The results of 50 runs for the *Case A* planning as obtained with DE, are provided in Table 3.5 for 19- and 25-bus systems and in Table 3.7 for Indian 19- bus and the 34- bus system. From chapter 2, it can be seen that DE provides a better solution in comparison to other metaheuristic algorithms such as the CSA, the PSO, and the GA. Hence, a performance comparison between planning *Cases B* and *C* using DE, for 19-, and 25-bus and Indian 19- and 34-bus systems are given in Table 4.5 and 4.7 respectively. Comparison of the multi-objective optimization results as obtained with Case C planning using DE and CSA for 19-bus and 25-bus systems is shown in Table 4.6. Table 4.8 depicts these results for Indian 19- bus and 34- bus system. It shows that the solutions are improved in view of the power loss and the average voltage drop, and the neutral current in planning *Case C*. This can be due to simultaneous phase balancing, conductor sizing, and the DSTATCOM allocation and the sizing optimization. Optimal location, angle, and KVA rating as obtained with DE for different test systems are shown in Table 4.9. However, the inferior solutions are obtained in the 19- bus system with DSTATCOM having rating (30.8753, 32.0323, 34.5321) kVAR allocated at bus 9 for the phase a, b, and c respectively. This can be due to reactive power compensation by the

DSTATCOM. The voltage profile of the Indian 19, 25, 34- bus system at phase a, b, and c for the Case A, B, C, and base voltage are shown in Figs. (4.6)-(4.14) respectively. From these figures, it can be clearly seen that voltage magnitude at all buses has improved significantly in comparison to the base case voltage magnitude for the Case C optimization planning. The complex power demand and the conductor sizes as obtained with Case C planning in a sample run for the systems are shown in Appendix (Table G.1-G.4).

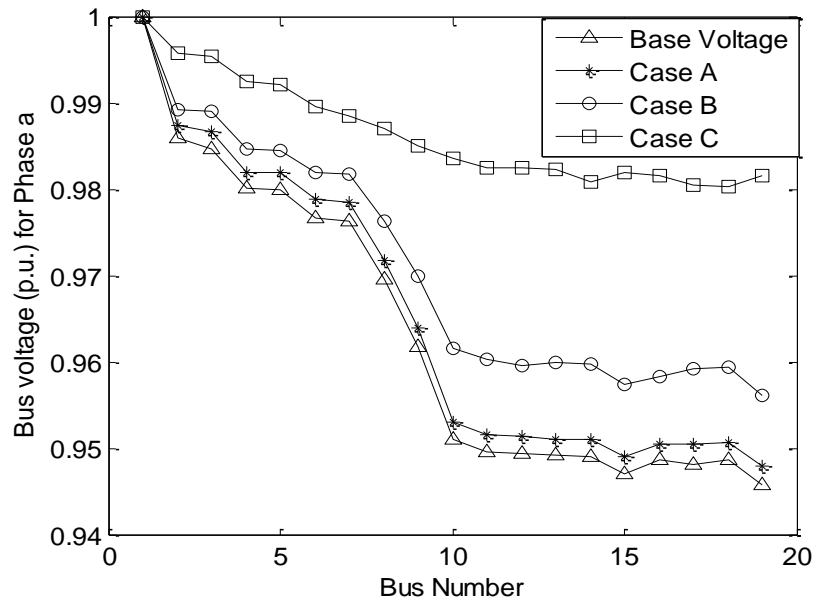


Fig. 4.6. Voltage magnitude for phase a for different planning cases obtained with DE for Indian 19-bus system

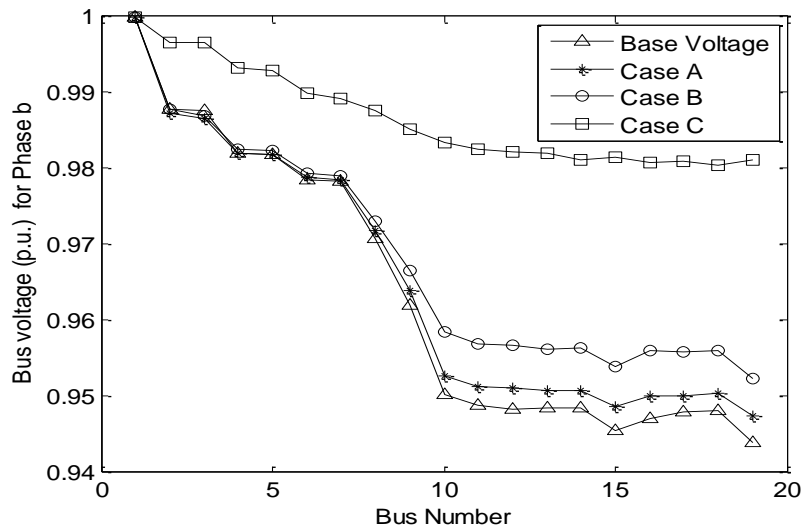


Fig. 4.7 Voltage magnitude for phase b for different planning cases obtained with DE for Indian 19-bus system

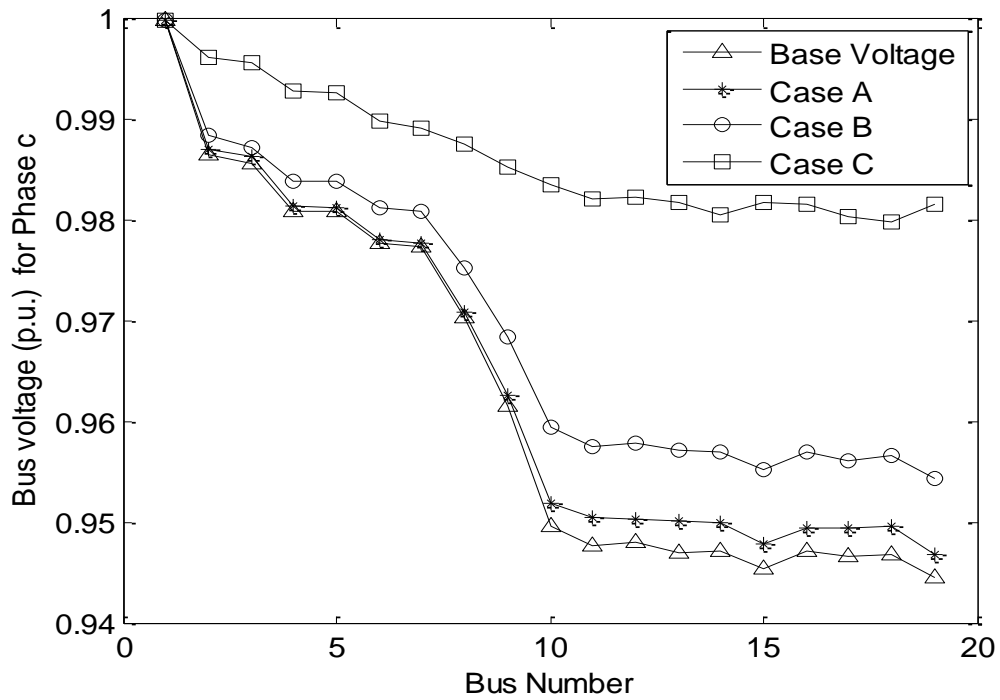


Fig. 4.8. Voltage magnitude for phase c for different planning cases obtained with DE for Indian 19-bus system

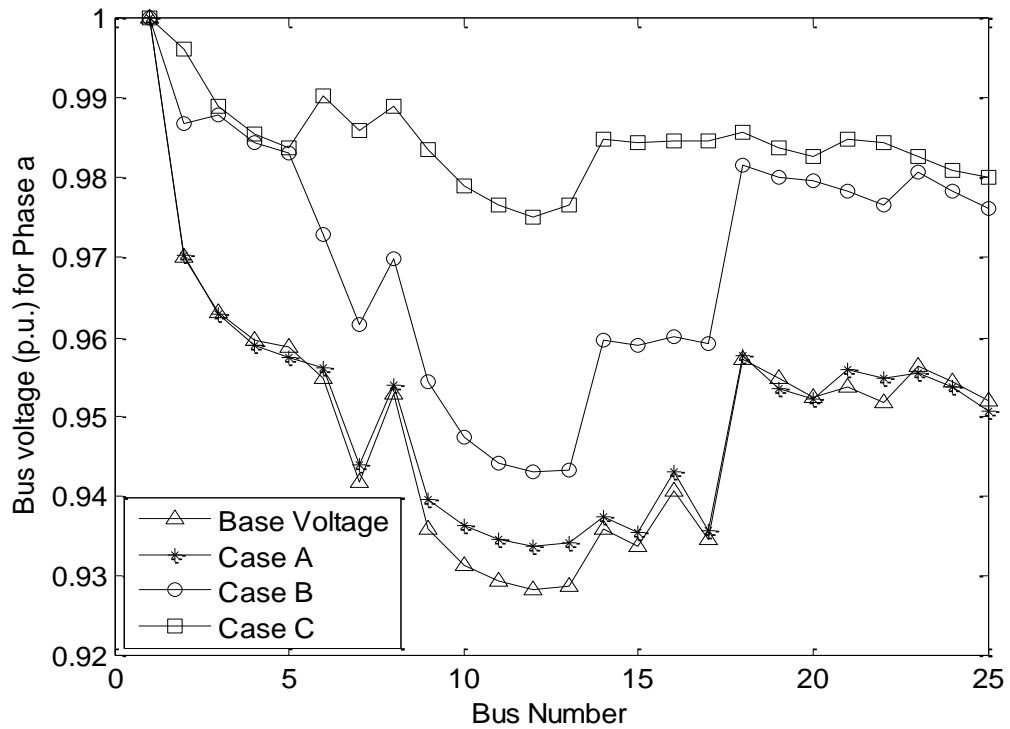


Fig. 4.9. Voltage magnitude for phase a for different planning cases obtained with DE for 25-bus system

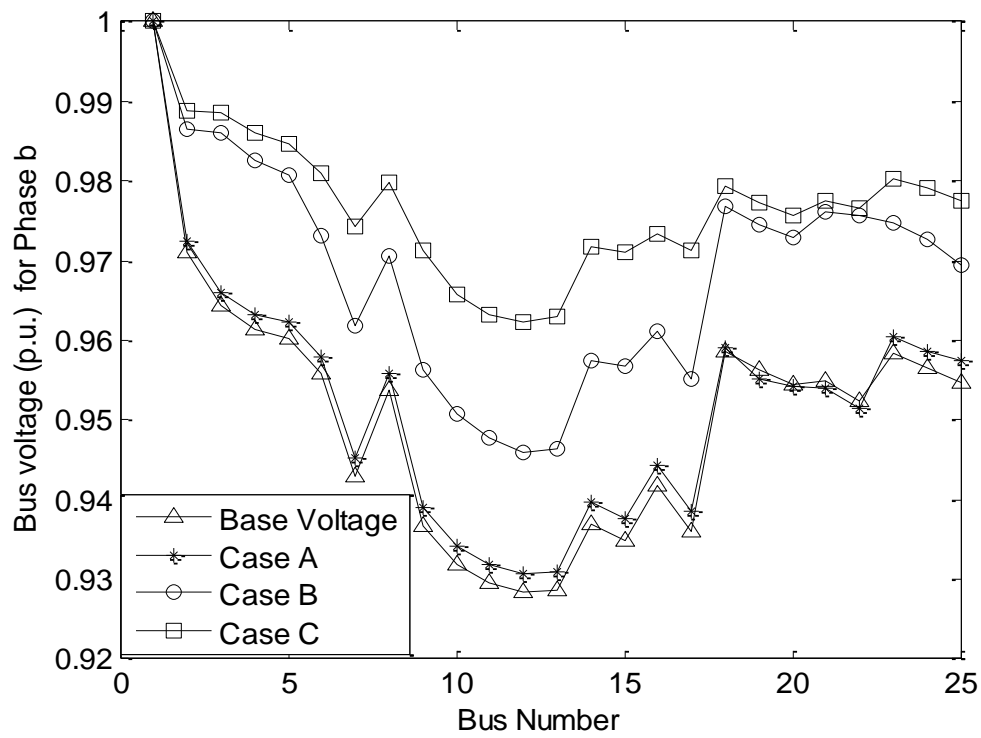


Fig.4.10. Voltage magnitude for phase b for different planning cases obtained with DE for 25-bus system

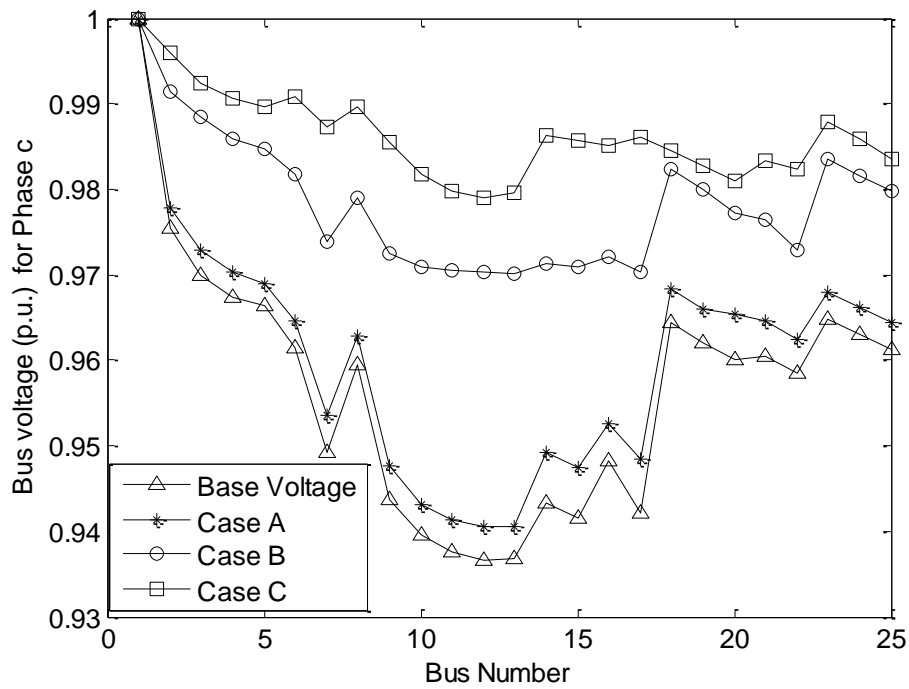


Fig. 4.11. Voltage magnitude for phase c for different planning cases obtained with DE for 25-bus system

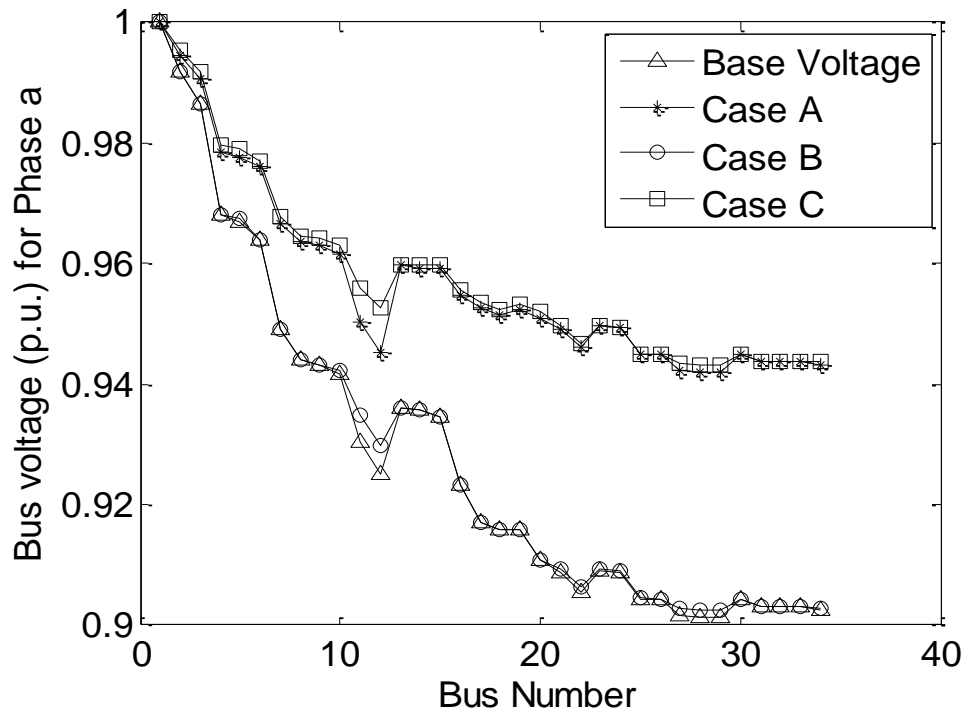


Fig. 4.12. Voltage magnitude for phase a for different planning cases obtained with DE for 34-bus system

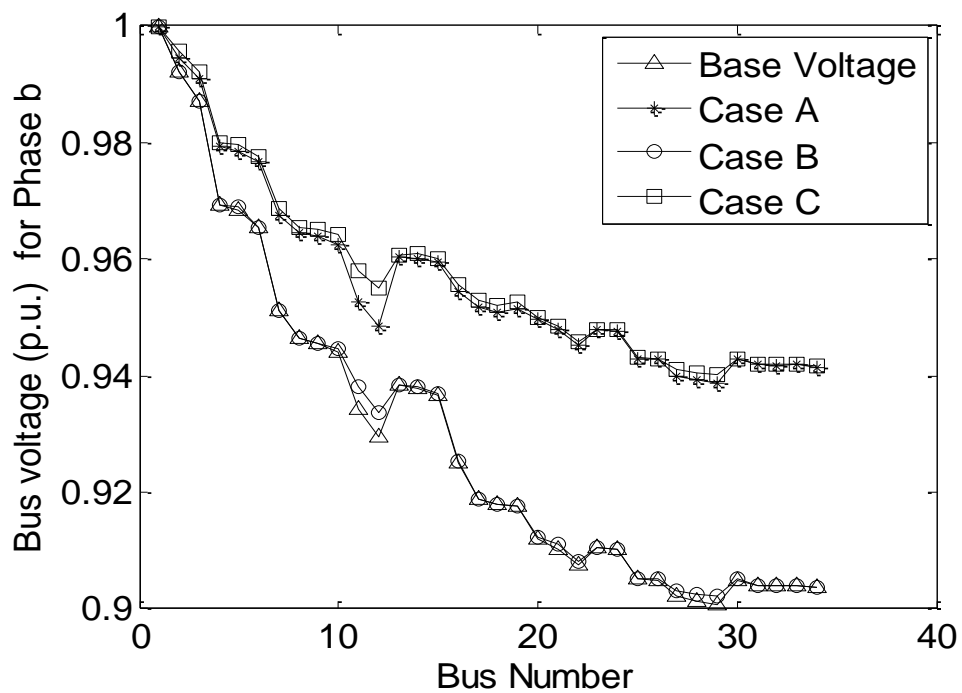


Fig. 4.13. Voltage magnitude for phase b for different planning cases obtained with DE for 34-bus system

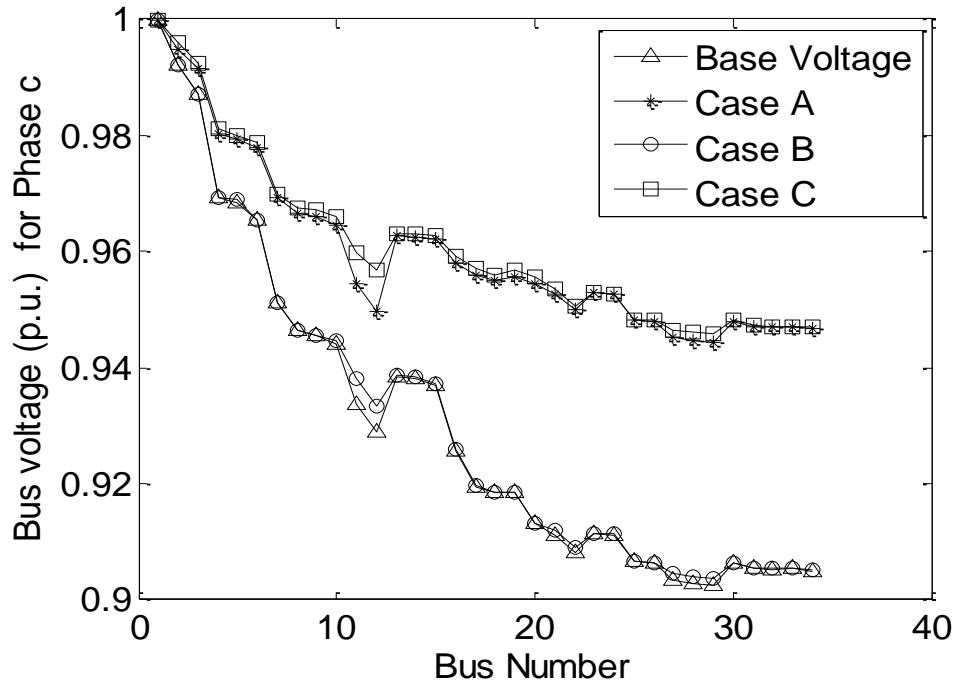


Fig. 4.14. Voltage magnitude for phase c for different planning cases obtained with DE for 34-bus system

Table 4.5: Results of the multi-objective optimization of 50 runs obtained with DE

Objective	19-bus system				25-bus system			
	Case B		Case C		Case B		Case C	
	Mean	SD	Mean	SD	Mean	SD	Mean	SD
PL (kW)	2.2358	0.0593	2.3245	0.0397	110.16	0.1745	85.648	0.005
TS _u (MVA)	0.0008	0.0008	0.0054	0.0045	0.0869	0.0145	0.0873	0.013
AV _d (%)	1.4196	0.0220	1.8714	0.0058	4.0230	0.0945	3.4401	0.029
ZSUF (%)	0.0054	0.0013	0.0056	0.0025	0.1754	0.0177	0.1752	0.032
NSUF (%)	0.0204	0.0064	0.0205	0.0021	0.3881	0.0165	0.3882	0.061
I _N (p.u.)	2.2906	0	2.3136	0.0032	0.6031	0	0.5688	0

Table 4.6: Comparison of the multi-objective optimization results as obtained with Case C planning using DE and CSA for 19-bus and 25-bus systems

Objective	19-bus system				25-bus system			
	DE		CSA		DE		CSA	
	Mean	SD	Mean	SD	Mean	SD	Mean	SD
PL (kW)	2.2358	0.0593	3.5289	0.0512	85.648	0.005	86.715	0.0643
TS _u (MVA)	0.0008	0.0008	0.0065	0.0061	0.0873	0.013	0.0885	0.023
AV _d (%)	1.4196	0.0220	2.9845	0.0071	3.4401	0.029	3.7821	0.035
ZSUF (%)	0.0054	0.0013	0.0075	0.0057	0.1752	0.032	0.1860	0.043
NSUF (%)	0.0204	0.0064	0.0232	0.0032	0.3882	0.061	0.3990	0.082
I _N (p.u.)	2.2906	0	2.3241	0.0042	0.5688	0	0.5791	0.005

Table 4.7: Results of the multi-objective optimization of 50 runs obtained with DE

Objective	Indian 19-bus system				34-bus system			
	Case B		Case C		Case B		Case C	
	Mean	SD	Mean	SD	Mean	SD	Mean	SD
PL (kW)	20.2161	0.0266	17.045	0.0208	566.0124	0.0093	437.2816	0.0074
TS _u (MVA)	0.0110	0.0014	0.0111	0.0012	0.0190	0.0082	0.0191	0.0065
AV _d (%)	1.8795	0.1939	1.4532	0.1154	6.9145	0.0172	4.1801	0.0151
ZSUF (%)	0.0281	0.0292	0.0279	0.0019	0.1143	0.1123	0.1150	0.1045
NSUF (%)	0.0169	0.0078	0.0171	0.0007	0.0385	0.0065	0.0395	0.0041
I _N (p.u.)	7.6206	0	7.4331	0	53.3189	0.0003	47.3256	0.0002

Table 4.8: Comparison of the multi-objective optimization results as obtained with Case C planning using DE and CSA for Indian 19- bus and 34- bus systems

Objective	Indian 19-bus system				34-bus system			
	DE		CSA		DE		CSA	
	Mean	SD	Mean	SD	Mean	SD	Mean	SD
PL (kW)	17.045	0.0208	18.1230	0.0343	437.2816	0.0074	438.0234	0.0095
TS _u (MVA)	0.0111	0.0012	0.0163	0.0025	0.0191	0.0065	0.0198	0.0081
AV _d (%)	1.4532	0.1154	1.5242	0.1302	4.1801	0.0151	4.6132	0.0172
ZSUF (%)	0.0279	0.0019	0.0301	0.0025	0.1150	0.1045	0.1932	0.1254
NSUF (%)	0.0171	0.0007	0.0205	0.0009	0.0395	0.0041	0.0452	0.0051
I _N (p.u.)	7.4331	0	7.5502	0.005	47.3256	0.0002	47.3321	0.0004

Table 4.9: The optimal location, angle, and KVA rating as obtained with DE for different bus systems

Bus system	Optimal Location	Optimal angle α (Degree)			Optimal KVA Rating		
		Phase a	Phase b	Phase c	Phase a	Phase b	Phase c
19- bus	9	0.5142	0.5321	0.5412	30.8753	32.0323	34.5321
25- bus	7	0.8145	0.8321	0.8124	569.326	571.510	569.721
Indian 19- bus	6	0.0712	0.0732	0.0743	62.5406	67.6044	69.4877
34- bus	22	-0.2124	-0.2143	-0.2156	599.432	601.435	602.414

4.6 Summary

In this chapter, a planning approach has been developed in order to determine the optimal phase balancing, conductor sizes, and the DSTATCOM location and the rating for the unbalanced radial distribution systems by optimizing various objective functions such as; the power loss, the complex power unbalance, the average voltage drop, the positive and zero sequence unbalance factors and the neutral current integrating DSTATCOM. A three phase forward-backward sweep load flow algorithm including the DSTATCOM model is developed and used in the planning approach. The DE and CSA are used as the solution strategy.

The simultaneous optimization for the phase balancing, the conductor sizing, the DSTATCOM location and the sizing provides a network with lower power loss, average voltage drop, neutral current, and better voltage profile for the Indian 19- bus, 25- bus, and 34- bus system. However, the simultaneous optimization for the phase balancing, the conductor sizing, the DSTATCOM location and the sizing gives inferior solutions in case of the 19- bus system. This can be due to reactive power compensation by DSTATCOM in the system. From Chapter 1, it is found that distributed generation (DG) can reduce the power loss and improve the voltage profile of a distribution system by injecting active power into it. However, it's impact on other objectives haven't been investigated yet. Thus, next chapter focuses on planning of URDS considering the integration of DGs.

Chapter 5

Planning of Unbalanced Radial Distribution Systems with DG Using Evolutionary Computing Algorithms

5.1 Introduction

In chapter 4, the planning of URDS has been presented using differential evolution algorithm (DE) and CSA in the presence of DSTATCOM. Several objective functions such as the total power loss, average voltage drop, total neutral current and total voltage unbalance have been minimized using this algorithm. However, the simultaneous optimization for phase balancing, conductor sizing, capacitor location and sizing gives inferior solutions in case of the 19- bus system.

From chapter 1, it is observed that distributed generations (DG) can reduce power loss and improve the voltage profile of distribution systems. Thus, in this chapter the planning of four URDS has been carried out by integrating DG with the system. The objective functions considered are the total power loss, the average voltage drop, the total neutral current and the total voltage unbalance. The DE and the Cuckoo search algorithm (CSA) are employed as the solution strategy for minimizing these objective functions in order to obtain optimal DG location, rating, the conductor sizing and the phase balancing. For the evaluation of each objective, a forward-backward load flow algorithm including the DG model is developed. The proposed approaches are demonstrated on the 19-bus, 25-bus, Indian 19-bus and 34-bus URDS.

This chapter is organized as follows: Problem Formulation is presented in section 5.2. In Section 5.3, the implementation of proposed planning approach using the DE and the CSA is described. The simulation results are presented in section 5.4. Section 5.5 concludes the chapter.

5.2 Problem Formulation

The objective of this planning problem is the minimization of various objective functions as discussed in chapter 2, subject to some technical constraints. These objective functions are described below.

This fitness function is maximized under the following constraints:

i. Voltage constraint: Voltage at each bus must remain within the permissible range.

$$V_s^{\min} \leq V_s^{abc} \leq V_s^{\max} \quad (5.1)$$

ii. Thermal constraint: The current flowing through each branch must be within the maximum current carrying capacity of the conductor.

$$I_j^{abc} \leq I_j^{\max} \quad (5.2)$$

iii. DG active generation limits: The DG output power should remain within their operational limits.

$$P_i^{\min} \leq P_i \leq P_i^{\max} \quad (5.3)$$

5.3 Implementation of DE and CSA for the planning problem

The proposed planning approach with DE and CSA utilizes a three-phase load flow algorithm as an auxiliary program in order to obtain bus voltage magnitudes and power loss of the URDS. The load flow algorithm including DGs is explained in Section 5.3.1 and application of DE and CSA is described in Section 5.3.2 and 5.3.3 respectively.

5.3.1 Three phase forward-backward sweep load flow algorithm incorporating DG

The load flow algorithm utilizes three matrices A , B , and C in order to obtain power flow solutions. The downstream buses connected to a particular bus are determined using matrix A . The end buses are identified with the help of matrix B and matrix C is developed in order to obtain the branch currents. This load flow algorithm consists of two steps. In the first step, the backward sweep is executed in order to find out the branch currents as follows:

$$\bar{I}_i^{p \in a,b,c} = \left(\frac{P_{D_{ip}}^{base} - iQ_{D_{ip}}^{base}}{\bar{V}_i^{P^*}} \right) \quad (5.4)$$

Where, $\bar{I}_i^{p \in a,b,c}$, $\bar{V}_i^{P^*}$ are the load current and voltage conjugate (in phasor form), and $P_{D_{ip}}^{base}$ are the active and reactive power demand for p^{th} phase of i^{th} bus of the base-case network and at bus i for phase p .

Then, the forward sweep is executed in order to obtain the bus voltages. More details of this algorithm are given in Chapter 2.

5.3.1.1 Incorporation of DG model in distribution load flow

This section describes the incorporation of the DGs in the unbalanced distribution systems. Fig. 5.1 shows the connection diagram for three DGs having rating DG1, DG2, and DG3 kW placed at bus j , in a sample line section of the unbalanced distribution system.

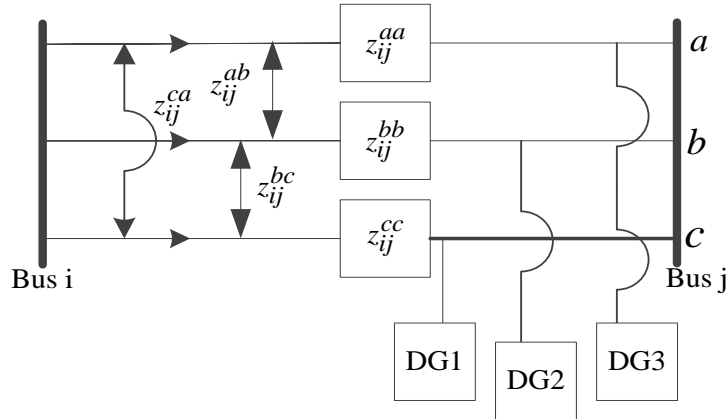


Fig. 5.1. Connection diagram of DGs in a sample unbalanced distribution system

Where, z_{ij}^{aa} , z_{ij}^{bb} , and z_{ij}^{cc} denotes self-impedance of phase a, phase b, and phase c respectively; z_{ij}^{ab} , z_{ij}^{bc} , and z_{ij}^{ca} denotes mutual impedance between phases. The DG ratings are considered to be continues in value. The minimum and maximum size of the DG is taken as 0 and 400 kW respectively.

In order to incorporate the DG model, the active power demand at the bus at which a DG unit is placed, say, at bus i , is modified by:

$$P_{D_{ip}}^{DG} = P_{D_{ip}}^{base} - P_{ip}^{DG} \quad (5.5)$$

Where, P_{Dip}^{DG} is the active and reactive power demand for p^{th} phase of i^{th} bus with a DG unit and P_{ip}^{DG} is the active power generated by the DG unit placed at p^{th} phase of i^{th} bus.

5.3.2 Proposed Planning Approach Using DE and CSA

In this chapter, the DE and the CSA are employed as the solution strategy for the planning problem of the unbalanced radial distribution networks. The detail description of these algorithm can be found in chapter 2.

5.3.2.1 Encoding Strategy

A chromosome for DE or nest for CSA representing a candidate solution in this planning problem consists of three segments as shown in Fig. 5.2. They are:

- (i) The first segment represents the complex power demand for each phase for each bus except the substation bus. Where, $S_{i_a}, S_{i_b}, S_{i_c}$ represent complex power demand for bus i for phases a, b , and c , respectively and NB is total number of buses.
- (ii) The second segment represents types of the conductor (ct) used in each branch, and NBR is total number of branches.
- (iii) The third segment represents DG power demand in each bus.

Where, $P_{ia}^{DG}, P_{ib}^{DG}, P_{ic}^{DG}$ are the power generation capacity for a DG unit located at i^{th} bus in phases a, b and c , respectively and NDG is the number of DGs. DGs are considered to be operating in constant PQ mode.

The chromosome string (CST) is given as:

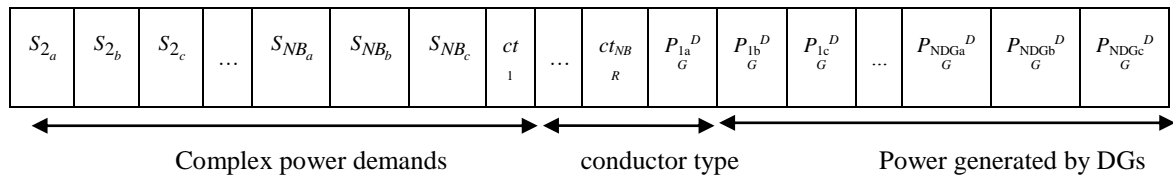


Fig. 5.2 Encoding strategy for a chromosome or nest in DE and CSA

The criteria for optimal location of DG is as follows:

$$P_{na}^{DG} > 0 \quad \text{If a DG can optimally be placed at } n^{\text{th}} \text{ bus.}$$

$$= 0 \quad \text{Otherwise}$$

5.3.2.2 Flow Chart of the Proposed Approach using DE and CSA

The flowchart for the overall planning approach using the DE and the CSA are shown in Fig. 5.3. and Fig. 5.4. respectively.

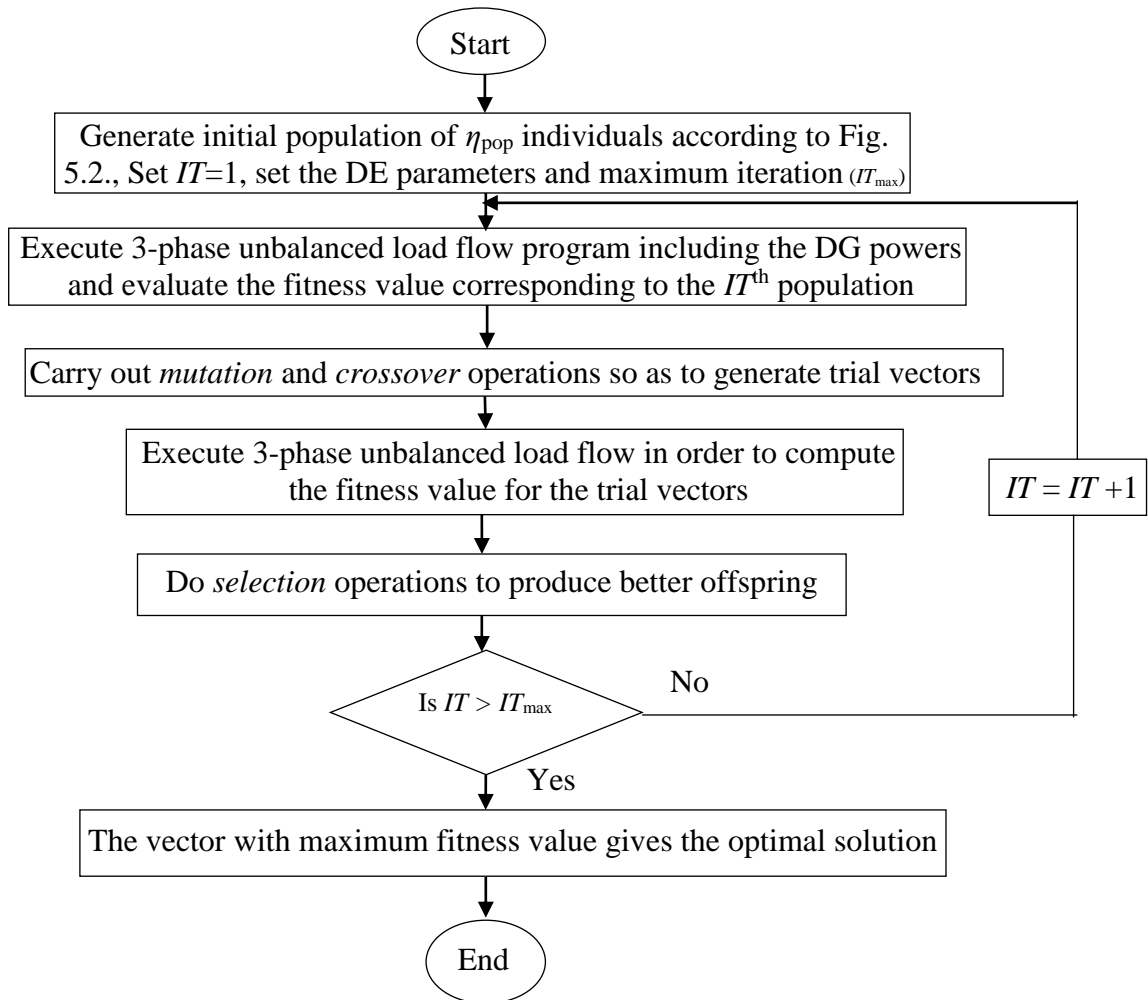


Fig. 5.3. Flow chart of the proposed planning approach using DE

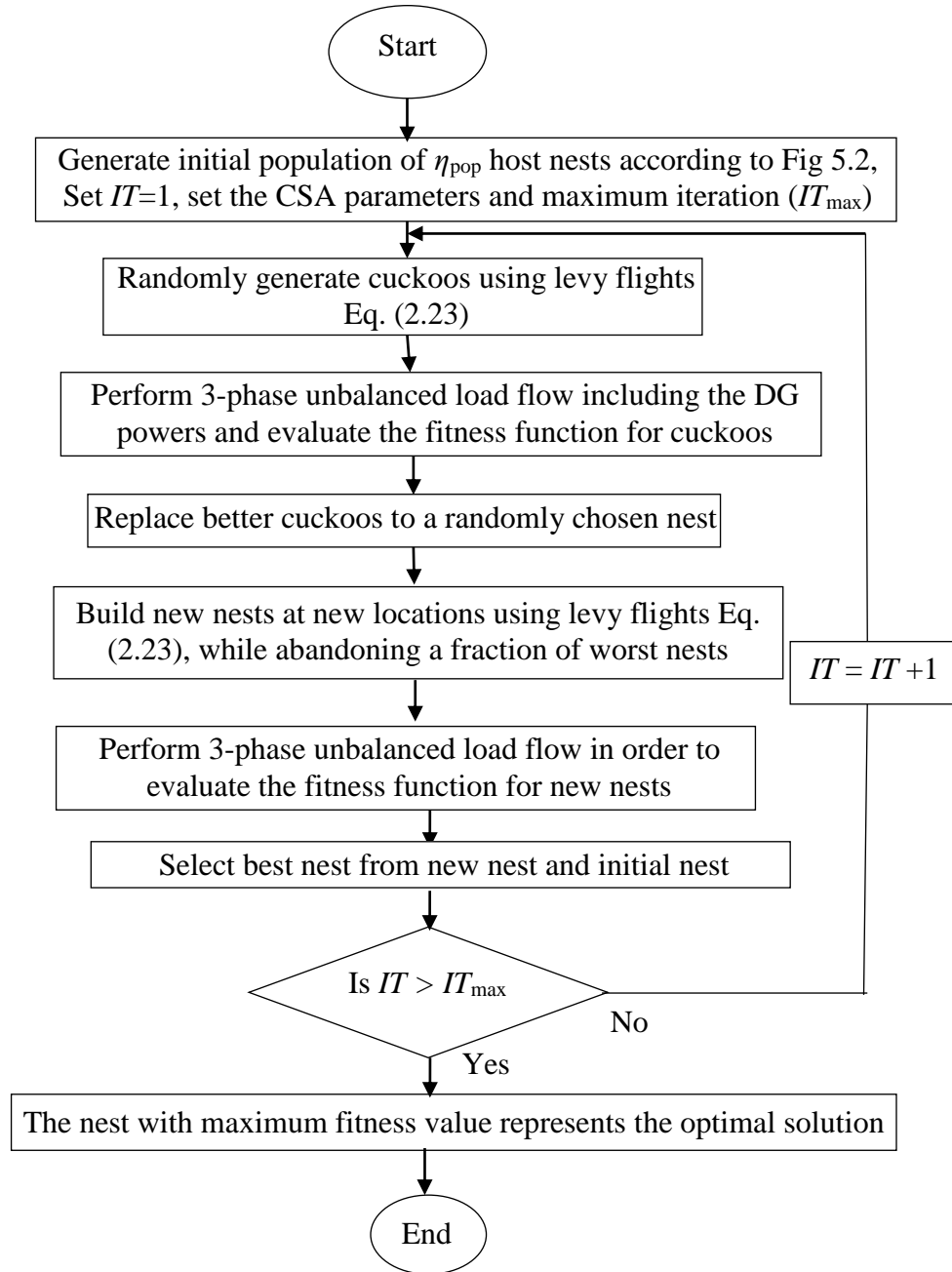


Fig. 5.4. Flow chart of the proposed planning approach using CSA

5.4 Simulation Results and discussions

The computer simulation study for the proposed planning approach is done in MATLAB 2012b environment using four test systems, i.e., 19-bus, 25-bus, Indian 19-bus, and 34-bus URDS. The total active and reactive power demand for the 19-bus system are 365.94 kW and 177.27 kVAR, respectively. For 25-bus system, these demands are 3240 kW and 2393 kVAR, respectively. For Indian 19-bus system, these demands are 1219.8 kW and 590.9 kVAR, respectively. For 34-bus system, these demands are 5850 kW and 4827.7 kVAR, respectively. The power loss, the complex power unbalance, the neutral current, the ZSUF, and the NSUF for the base case network of the 19-, 25-, Indian 19-, and 34-bus systems are given in Table 2.1. The DE parameters are optimized by taking repetitive simulation runs, and the optimal parameters are shown in Table 2.2. The DG penetration level i.e. the ratio of total DG active powers to total active power demand is considered to be 0.4 [92]. The DG units are assumed to be operated at unity power factor [92]. Three different planning optimization cases are used. They are:

- *Case A*: planning for optimal phase balancing
- *Case B*: simultaneous planning for the optimal phase balancing and conductor sizes
- *Case C*: simultaneous planning for optimal phase balancing, the conductor sizes and the DG power generation

All the objective functions are aggregated with equal weights so as to get simultaneous optimization of all of them.

5.4.1. Results of single objective optimization

The performance comparison between planning *Cases A* and *B* using DE are provided in Table 2.7 and 2.11 for 19- and 25-bus system and Indian 19- and 34-bus system respectively. The results of 50 runs for planning *Case C* (single objective) as obtained with DE and CSA are provided and compared with those obtained with CSA in Table 5.1 and Table 5.2 for the 19-bus, the 25-bus and the Indian 19-bus and 34-bus system. The results show that the performance of DE is better and consistent according to the mean objective function and the standard deviation (SD), respectively as compared to CSA.

Table 5.1 Comparison of results of planning *Case C* of 50 runs as obtained with DE, and CSA, for 19- and 25-bus systems

Objective	19-bus system				25-bus system			
	DE		CSA		DE		CSA	
	Mean	SD	Mean	SD	Mean	SD	Mean	SD
PL (kW)	1.4258	0.0612	1.5123	0.0635	71.543	0.1821	72.058	0.1951
TS _u (MVA)	0.0008	0.0006	0.0010	0.0009	0.0866	0.0149	0.0871	0.0166
AV _d (%)	0.6404	0.0004	0.7152	0.0005	3.2105	0.0983	3.3421	0.0991
ZSUF (%)	0.0048	0.0014	0.0058	0.0015	0.0932	0.0181	0.0945	0.0185
NSUF (%)	0.0102	0.0071	0.0110	0.0073	0.1041	0.0172	0.1154	0.0176
I _N (p.u.)	1.4744	0	1.4748	0.0015	0.5321	0	0.5328	0.0018

Table 5.2 Comparison of results of planning *Case C* of 50 runs as obtained with DE, and CSA, for Indian 19- and 34-bus systems

Objective	Indian 19-bus system				34-bus system			
	DE		CSA		DE		CSA	
	Mean	SD	Mean	SD	Mean	SD	Mean	SD
PL (kW)	14.412	0.0125	15.219	0.0128	310.3478	0.0058	312.1245	0.0061
TS _u (MVA)	0.0021	0.0009	0.0025	0.0011	0.0165	0.0055	0.0169	0.0058
AV _d (%)	1.3241	0.1135	1.3345	0.1235	3.1043	0.0145	3.1561	0.0151
ZSUF (%)	0.0045	0.0014	0.0050	0.0018	0.0983	0.1011	0.0992	0.1045
NSUF (%)	0.0018	0.0006	0.0021	0.0007	0.0295	0.0038	0.0305	0.0040
I _N (p.u.)	6.3245	0	6.3321	0.005	46.0145	0.0002	46.0247	0.0005

5.4.2. Results of Multi-Objective Optimization

The multi-objective performance comparison between planning *Cases A* and *B* using DE are provided in Table 2.15 and 2.19 for 19- and 25-bus system and Indian 19- and 34-bus system respectively. The comparative results among the solutions obtained with planning *Case C* (multi-objective) are given in Table 5.3 and Table 5.4 for the 19-bus, the 25-bus and the Indian 19-bus and the 34-bus system respectively. The reduction in power loss for the 19-bus and the 25-bus systems with *Case C* planning is found to be 87.76% and 51.6%, respectively compared to their respective base case values. Similarly, the reduction in power loss for the Indian 19-bus and the 34-bus systems with *Case C* planning is found to be 70.99% and 46.33%, respectively compared to their respective base case values. The minimum bus voltage magnitude (p.u.) is also found to be significantly improved with planning *Case C*. The voltage profile for the 19- bus networks as obtained with different planning cases are illustrated in Figs. 5.5. The optimal location and rating of DGs for the Indian 19- bus, and 34- bus system as obtained with DE are shown in Table 5.5. The minimum bus voltages for the solutions obtained with different planning cases are given in Table 5.6. The power loss vs. each branch number are shown in Fig. (5.6)-(5.11), for Indian 19-bus and 34-bus systems respectively. It can be seen that the power loss in each branch has reduced significantly with *Case C* planning for these four systems. The complex power demand and the conductor sizes as obtained with *Case C* planning in a sample run for all the systems are shown in Appendix (Table H.1-H.4).

Table 5.3 Comparison of the results as obtained with *Case C* (multi-objective) planning using DE and CSA for 19- and 25- bus system

Objective	19-bus system				25-bus system			
	DE		CSA		DE		CSA	
	Mean	SD	Mean	SD	Mean	SD	Mean	SD
PL (kW)	1.6258	0.0545	1.7242	0.0641	72.412	0.1823	73.012	0.1954
TS _u (MVA)	0.0009	0.0006	0.0011	0.0007	0.0867	0.0152	0.0875	0.0168
AV _d (%)	0.7404	0.0003	0.8404	0.0005	3.2201	0.0986	3.3425	0.0995
ZSUF (%)	0.0058	0.0012	0.0060	0.0013	0.1643	0.0186	0.1721	0.0195
NSUF (%)	0.0115	0.0067	0.0118	0.0070	0.3142	0.0175	0.3242	0.0181
I _N (p.u.)	1.4844	0	1.4856	0.0015	0.5327	0	0.5330	0.0020

Table 5.4 Comparison of the results as obtained with Case C (multi-objective) planning using DE and CSA for Indian 19- and 34- bus system

Objective	Indian 19-bus system				34-bus system			
	DE		CSA		DE		CSA	
	Mean	SD	Mean	SD	Mean	SD	Mean	SD
PL (kW)	14.534	0.0129	15.312	0.0132	310.3589	0.0059	312.1261	0.0063
TS _u (MVA)	0.0022	0.0011	0.0028	0.0015	0.0169	0.0058	0.0171	0.0060
AV _d (%)	1.3251	0.1141	1.3351	0.1238	3.1051	0.0148	3.1565	0.0154
ZSUF (%)	0.0046	0.0016	0.0052	0.0019	0.0988	0.1015	0.0995	0.1048
NSUF (%)	0.0020	0.0007	0.0023	0.0008	0.0299	0.0039	0.0308	0.0043
I _N (p.u.)	6.3261	0	6.3332	0.007	46.0152	0.0003	46.0251	0.0006

Table 5.5 The optimal location and rating of DGs for the 19- bus, 25- bus, Indian 19- bus, and 34- bus system as obtained with DE

Bus system	DG location(s)	Power generated by DG units (kW)		
		Phase a	Phase b	Phase c
19-bus	9	20.124	0	10.012
	10	16.240	100.321	0
Indian 19- bus	6	35.482	50.452	10.432
	17	100.321	291.233	0
25- bus	11	0	0	96
	12	400	400	400
34- bus	19	400	390.56	385.7
	22	380.865	388.039	394.836

Table 5.6 Comparison of the minimum bus voltage of the solutions obtained with different planning cases

Planning Case	Minimum bus voltage (p.u.)					
	19-bus system			25-bus system		
Base Case	0.9516	0.9498	0.9505	0.9284	0.9284	0.9366
Case A	0.9701	0.9695	0.9698	0.9285	0.9287	0.9367
Case B	0.9790	0.9788	0.9804	0.9472	0.9480	0.9555
Case C	0.9821	0.9819	0.9835	0.9648	0.9672	0.9708

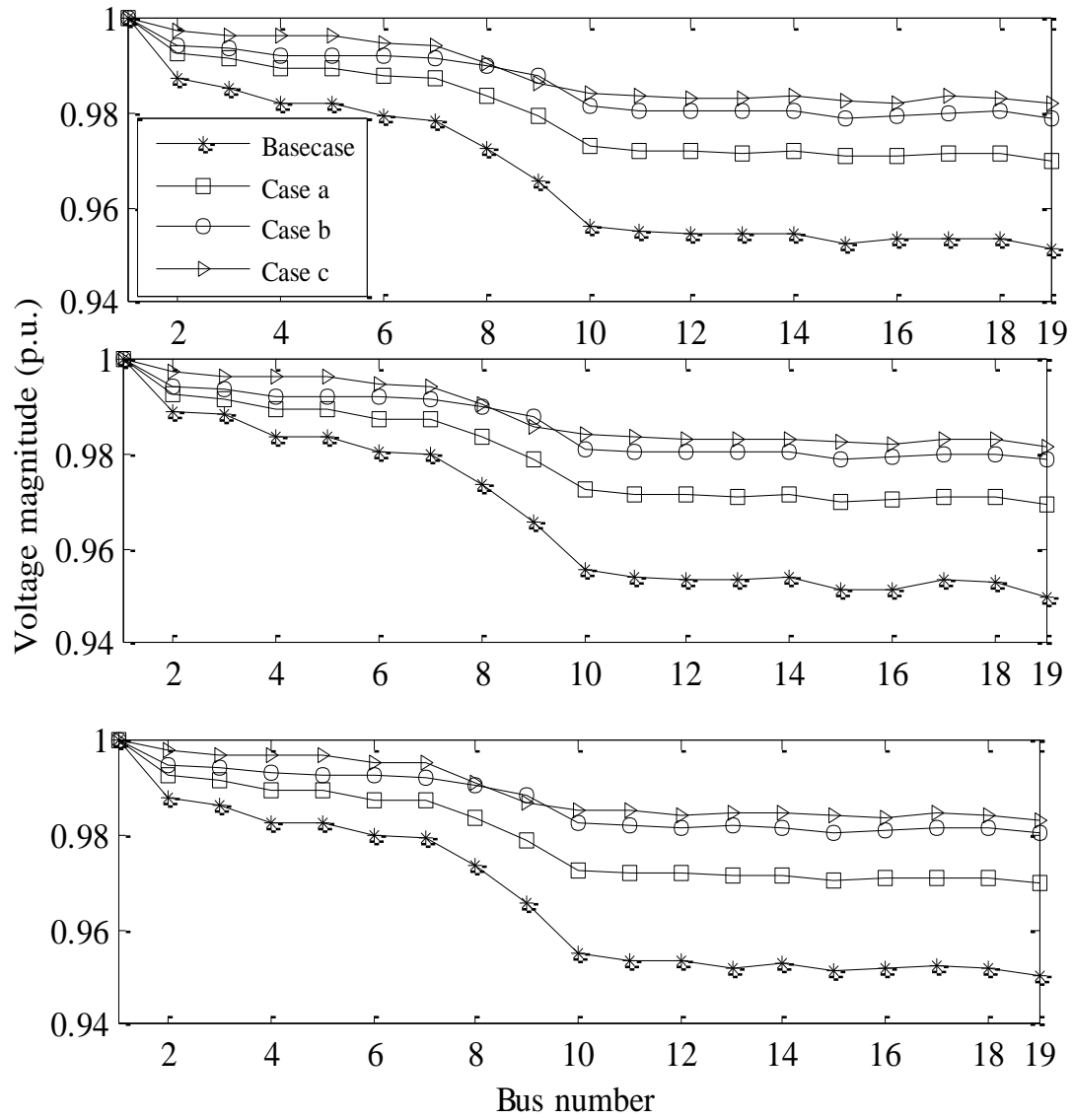


Fig. 5.5 Voltage profiles for the 19-bus system as obtained with different planning cases

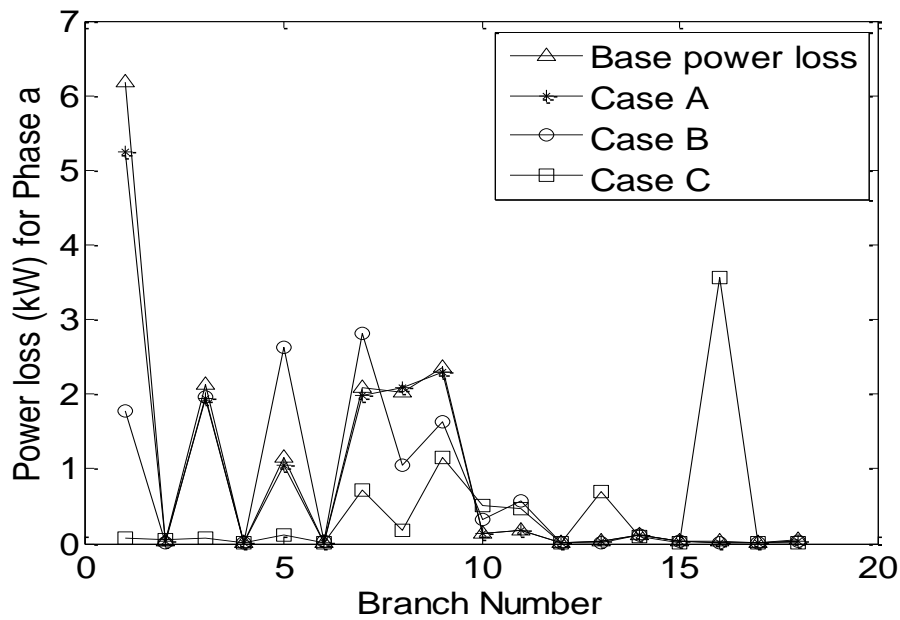


Fig. 5.6. Power loss vs. branch number for phase a for different planning cases obtained with DE for Indian 19-bus system

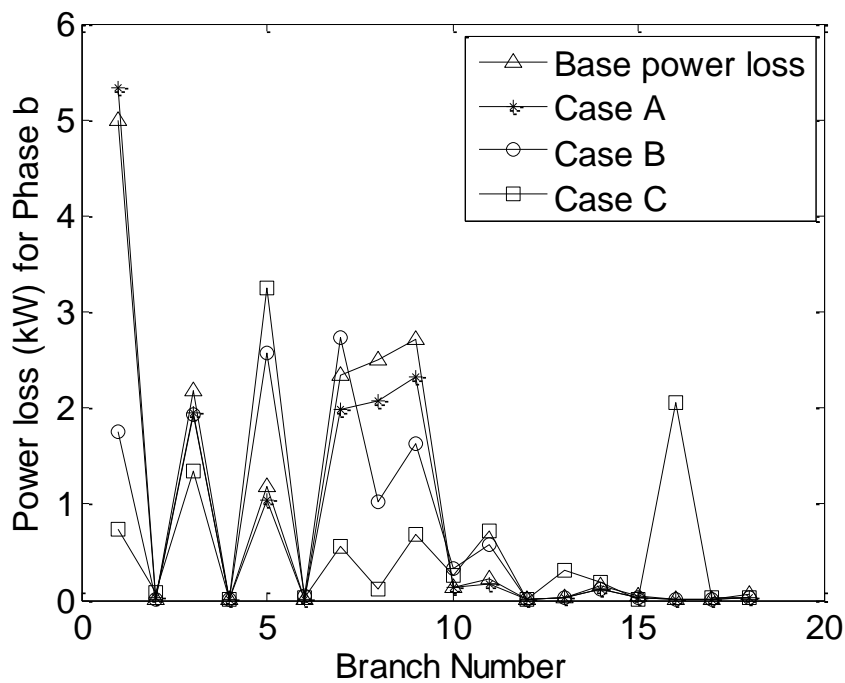


Fig. 5.7. Power loss vs. branch number for phase b for different planning cases obtained with DE for Indian 19-bus system

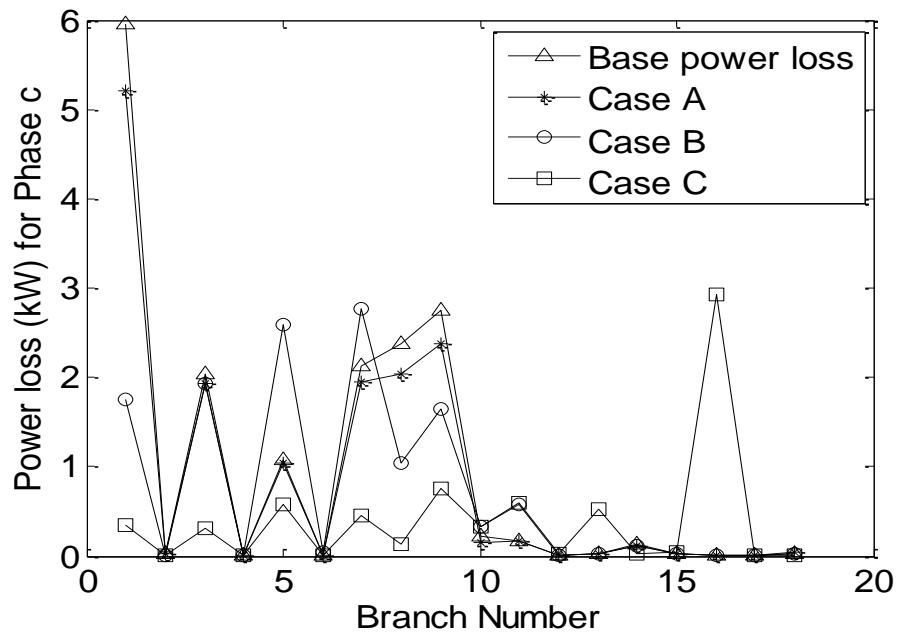


Fig. 5.8. Power loss vs. branch number for phase c for different planning cases obtained with DE for Indian 19-bus system

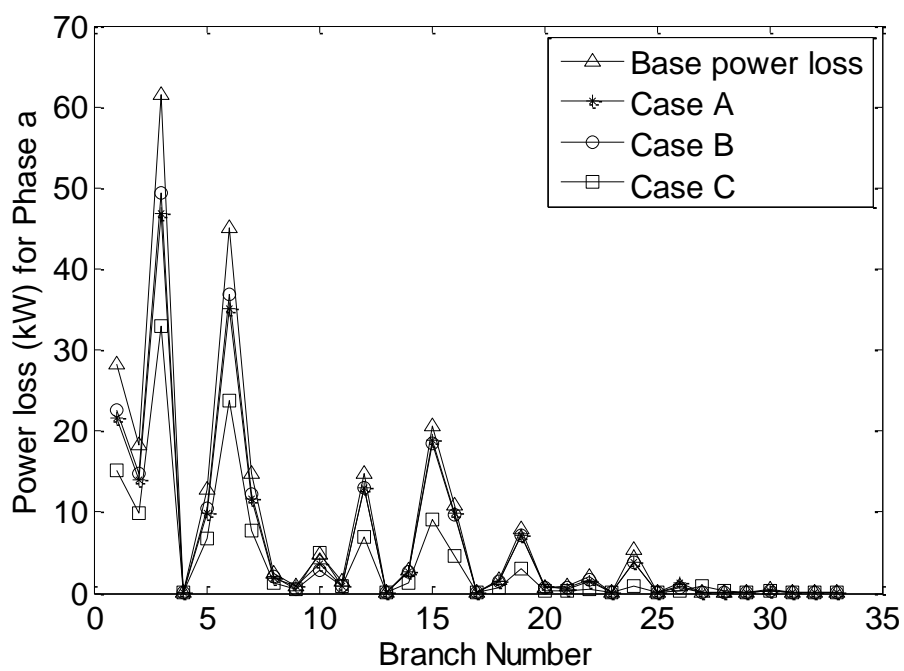


Fig. 5.9. Power loss vs. branch number for phase a for different planning cases obtained with DE for 34-bus system

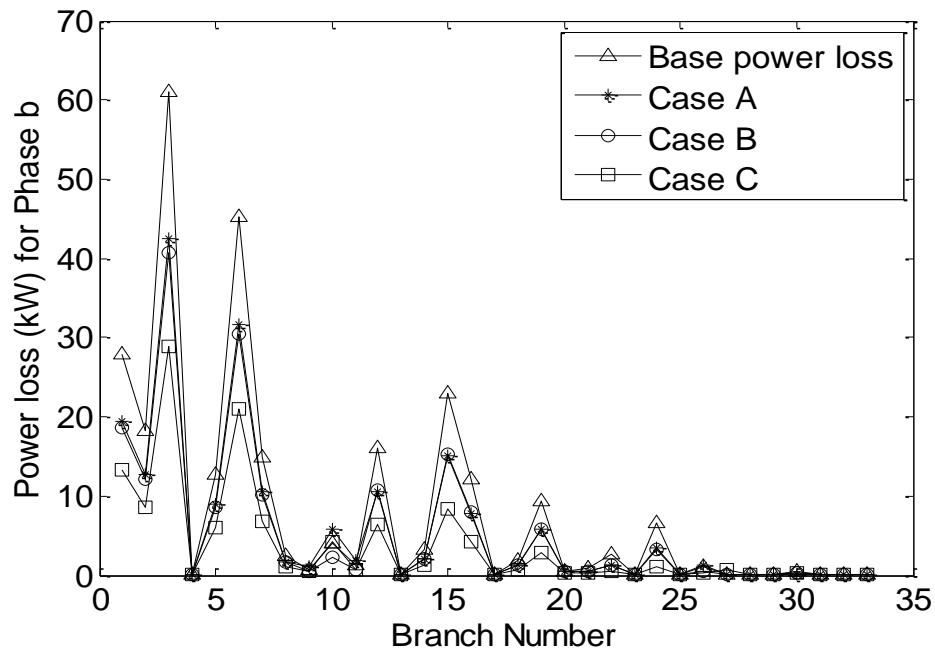


Fig. 5.10. Power loss vs. branch number for phase b for different planning cases obtained with DE for 34-bus system

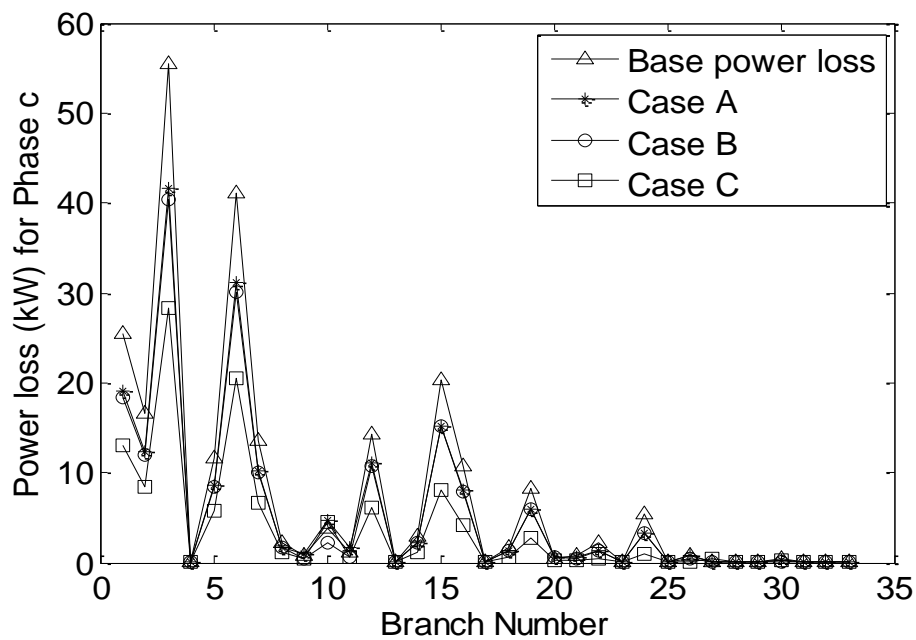


Fig. 5.11. Power loss vs. branch number for phase c for different planning cases obtained with DE for 34-bus system

5.5 Summary

In this chapter, a planning approach for determining the optimal phase balancing, conductor sizes, the DG power allocation and sizing of URDS has been presented by optimizing the power loss, the complex power unbalance, the average voltage drop, the positive and zero sequence unbalance factors, and the neutral current. A forward-backward load flow algorithm including the DG model has been developed and used in the planning approach. The DE and CSA are used as the solution methodology. The salient outcomes of this chapter are:

- A simultaneous optimization approach for the phase balancing, the conductor size, the DG allocation and sizing provides a network with reduced power loss, better voltage profile, and lower voltage unbalance factors.
- However, the simultaneous optimization for the phase balancing, the conductor sizing, the DG location and the sizing gives inferior results for the zero and negative sequence voltage unbalance for the 19- bus systems in comparison to the simultaneous optimization for the phase balancing, and the conductor sizing.
- The performance of DE is found to be better and consistent as compared to the CSA.

It can be observed from Chapter 4 that, the DSTATCOM can reduce the power loss and improve the voltage profile of the distribution systems and also DG can reduce the power loss, etc. However, the effect of simultaneous DG and DSTATCOM allocation on objectives such as the power loss, the average voltage drop, and etc. in URDS haven't been investigated yet. Thus, the concluding chapter focuses on planning of URDS considering the integration of DGs and DSTATCOMs.

Chapter 6

Planning of Unbalanced Radial Distribution Systems with DG and DSTATCOM Using Evolutionary Computing Algorithms

6.1 Introduction

In chapter 5, the planning of the URDS has been presented using the differential evolution algorithm (DE) and the cuckoo search algorithm (CSA) in the presence of DG. Several objective functions such as the total power loss, average voltage drop, total neutral current and total voltage unbalance have been minimized using this algorithm. However, the simultaneous optimization for the phase balancing, the conductor sizing, the DG location and the sizing gives inferior results for the zero and negative sequence voltage unbalance for the 19- bus system.

From chapter 1, chapter 4, and chapter 5 it is observed that distributed generations (DG) and the DSTATCOM can reduce the power loss and improve voltage profile of distribution systems. Thus, in this chapter planning of four URDS has been carried integrating DG and DSTATCOM with the system. A three-phase unbalanced modelling of the DG and the DSTATCOM has been devised. The objective functions considered are the total power loss, the average voltage drop, the total neutral current and the total voltage unbalance. The DE and the Cuckoo search algorithm (CSA) are employed as the solution strategy for minimizing these objective functions in order to obtain the optimal DG and the DSTATCOM location, rating, conductor sizing and phase balancing. For the evaluation of each objective, a forward-backward load flow algorithm including the DG

and DSTATCOM model is developed. The proposed approach is demonstrated on the 19-bus, 25-bus, Indian 19-bus and 34-bus URDS.

This chapter is organized as follows: The Problem Formulation is presented in Section 6.2. In Section 6.3, the implementation of proposed planning approach using the DE and the CSA are described. The simulation results are presented in section 6.4. Section 6.5 concludes the chapter.

6.2 Problem Formulation

The objective of this planning problem is the minimization of the various objective functions as discussed in Chapter 2, subject to some technical constraints.

This fitness function is maximized under the following constraints:

i. Voltage constraint: Voltage at each bus must remain within the permissible range.

$$V_s^{\min} \leq V_s^{abc} \leq V_s^{\max} \quad (6.1)$$

ii. Thermal constraint: The current flowing through each branch must be within the maximum current carrying capacity of the conductor.

$$I_j^{abc} \leq I_j^{\max} \quad (6.2)$$

iii. DG active generation limits: The DG output power should remain within their operational limits.

$$P_i^{\min} \leq P_i \leq P_i^{\max} \quad (6.3)$$

iv. DSTATCOM rating constraint

The DSTATCOM rating should be less than equal to the maximum value of DSTATCOM rating.

$$Q_{dsat}_a \leq Q_{dstat}_{\max} \quad (6.4)$$

Where Q_{dstat}_a denotes, the allowable DSTATCOM size, the maximum value of DSTATCOM rating is represented as Q_{dstat}_{\max} .

6.3 Implementation of DE and CSA for the planning problem

The proposed planning approach with the DE and the CSA utilizes a three-phase load flow algorithm as a supplementary tool to obtain the bus voltage magnitudes and power loss of the URDS. The load flow algorithm including the DGs and DSTATCOM is explained in

Section 6.3.1 and application of the DE and the CSA is described in Section 6.3.2 and 6.3.3 respectively.

6.3.1 Three phase forward-backward sweep load flow algorithm incorporating DG and DSTATCOM

As discussed in chapter 2, the load flow algorithm compute the power flow solutions with the help of three matrices A , B , and C . The downstream buses connected to a particular bus are determined using matrix A . The end buses are identified with the help of matrix B and matrix C is developed in order to obtain the branch currents. The load flow algorithm consists of two steps. In the first step, the backward sweep is executed in order to find out the branch currents as follows:

$$\bar{I}_j^{x \in a,b,c} = \left(\frac{P_j^x - iQ_j^x}{\bar{V}_j^{x*}} \right) \quad (6.5)$$

Where, $\bar{I}_j^{x \in a,b,c}$, \bar{V}_j^{x*} , P_j^x , and Q_j^x are the load current and voltage conjugate (in phasor form), active power and reactive power demand at bus j for phase x .

Then, the forward sweep is executed in order to obtain the bus voltages. More details of this algorithm have been discussed in Chapter 2.

6.3.1.1 Incorporation of DG and DSTATCOM model in the distribution load flow

This section describes the incorporation of the DGs and DSTATCOM in the unbalanced distribution systems. Fig. 6.1 shows the connection diagram for the three DGs having rating DG1, DG2, and DG3 kW placed at bus j , in a sample line section of the unbalanced distribution system.

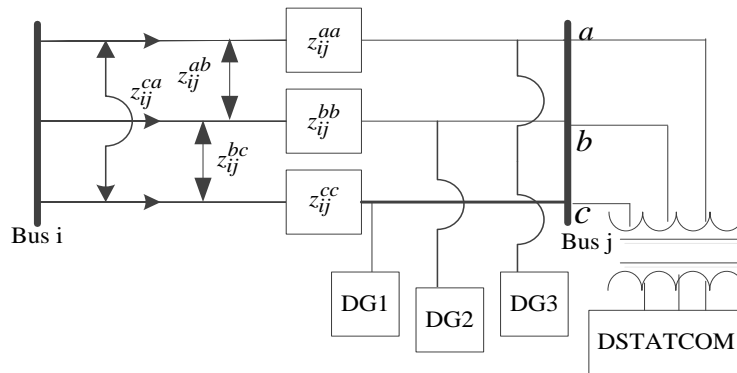


Fig. 6.1. Connection diagram of DGs and DSTATCOM in a sample distribution system

Where, z_{ij}^{aa} , z_{ij}^{bb} , and z_{ij}^{cc} denotes the self-impedance of phase a, phase b, and phase c respectively; z_{ij}^{ab} , z_{ij}^{bc} , and z_{ij}^{ca} denotes the mutual impedance between the phases. The DG and DSTATCOM ratings are considered to be continuous in value. The minimum and maximum size of the DG is taken as 0 and 400 kW respectively and the minimum and maximum size of DSTATCOM is chosen as 0 and 10,000 kVAR [79] respectively.

In order to incorporate the DG and DSTATCOM model, the active and reactive power demand at the bus at which a DG and DSTATCOM unit is placed, say, at bus i , is modified by:

$$\begin{aligned} P_{D_{ip}}^{DG} &= P_{D_{ip}}^{base} - P_{ip}^{DG} \\ Q_{D_{ip}}^{DSTAT} &= Q_{D_{ip}}^{base} - Q_{ip}^{DSTAT} \end{aligned} \quad (6.6)$$

Where, $P_{D_{ip}}^{DG}$ and $Q_{D_{ip}}^{DSTAT}$ are the active and reactive power demand for p^{th} phase of i^{th} bus with a DG and DSTATCOM unit and $P_{D_{ip}}^{base}$ and $Q_{D_{ip}}^{base}$ are the active and reactive power demand for p^{th} phase of i^{th} bus of the base-case network; P_{ip}^{DG} and Q_{ip}^{DSTAT} is the active and reactive power generated by the DG and DSTATCOM unit placed at p^{th} phase of i^{th} bus.

6.3.2 Proposed Planning Approach Using DE and CSA

In this chapter, the DE and the CSA are employed as the solution strategy for the planning problem of unbalanced radial distribution networks. The detail description of these algorithm are given in chapter 2.

6.3.2.1 Parameter Representation

The parameters (decision variables) for the DE and the CSA in this planning problem consists of three decision variables and is represented as a vector D as follows:

$$D = [\text{ANG}, \text{ND}, \phi, \text{NDG}, \text{APD}, \text{ctz}] \quad (6.7)$$

$$\text{ANG} = [\alpha_1, \alpha_2, \alpha_3, \dots, \alpha_{1_{\text{nop}}}, \alpha_{2_{\text{nop}}}, \alpha_{3_{\text{nop}}}] \quad (6.8)$$

$$\phi = [\phi_1, \phi_2, \dots, \phi_N] \quad (6.9)$$

$$\text{QD} = [\text{QD}_1, \text{QD}_2, \dots, \text{QD}_N] \quad (6.10)$$

$$\text{PDG} = [\text{PDG}_1, \text{PDG}_2, \dots, \text{PDG}_N] \quad (6.11)$$

$$\text{APD} = [\text{APD}_{a,b,c}, \text{APD}_{a,b,c}, \dots, \text{APD}_N] \quad (6.12)$$

$$\text{ctz} = [\text{ct}_1, \text{ct}_2, \dots, \text{ct}_{\text{NBR}}] \quad (6.13)$$

Where ANG represents vector of DSTATCOM angles ($\alpha_{1_{\text{nop}}}$, $\alpha_{2_{\text{nop}}}$, $\alpha_{3_{\text{nop}}}$) and are generated within the lower and the upper bound for number of population (nop), ϕ denotes the vector

of DSTATCOM and DG locations; QD, and PDG denotes the vector of DSTATCOM and DG rating, APD vector represents the active and reactive power load for the phases a, b, and c for bus N , ND represents the number of DSTATCOM, NDG represents number of DGs, and ctz represents a vector of different conductor types for the NBR number of branches.

6.3.2.2 Flow Chart of the Proposed Approach using DE and CSA

The flowchart for the overall planning approach using DE and CSA are shown in Fig. 6.2. and Fig. 6.3. respectively.

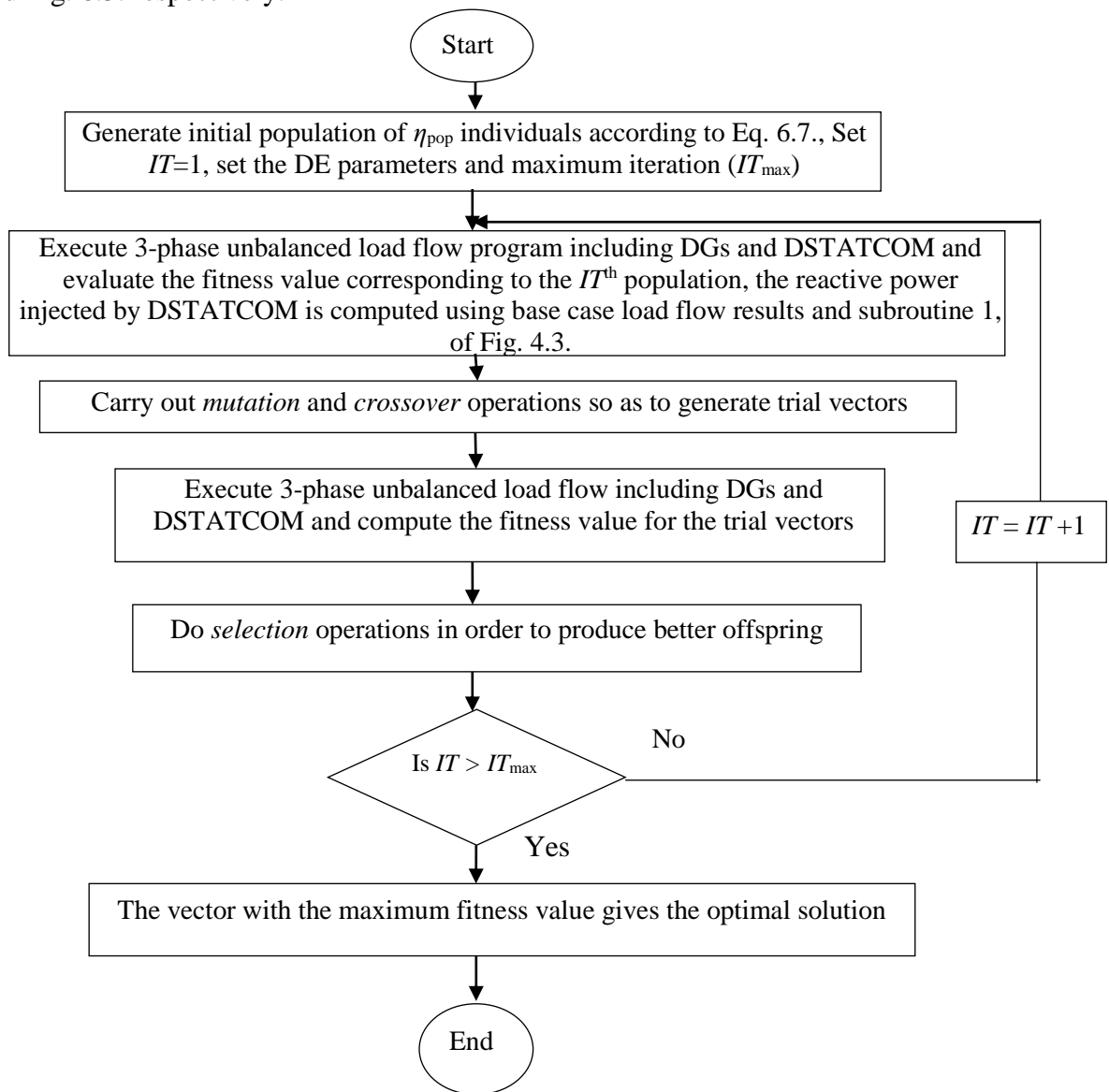


Fig. 6.2. Flow chart of the proposed planning approach using DE

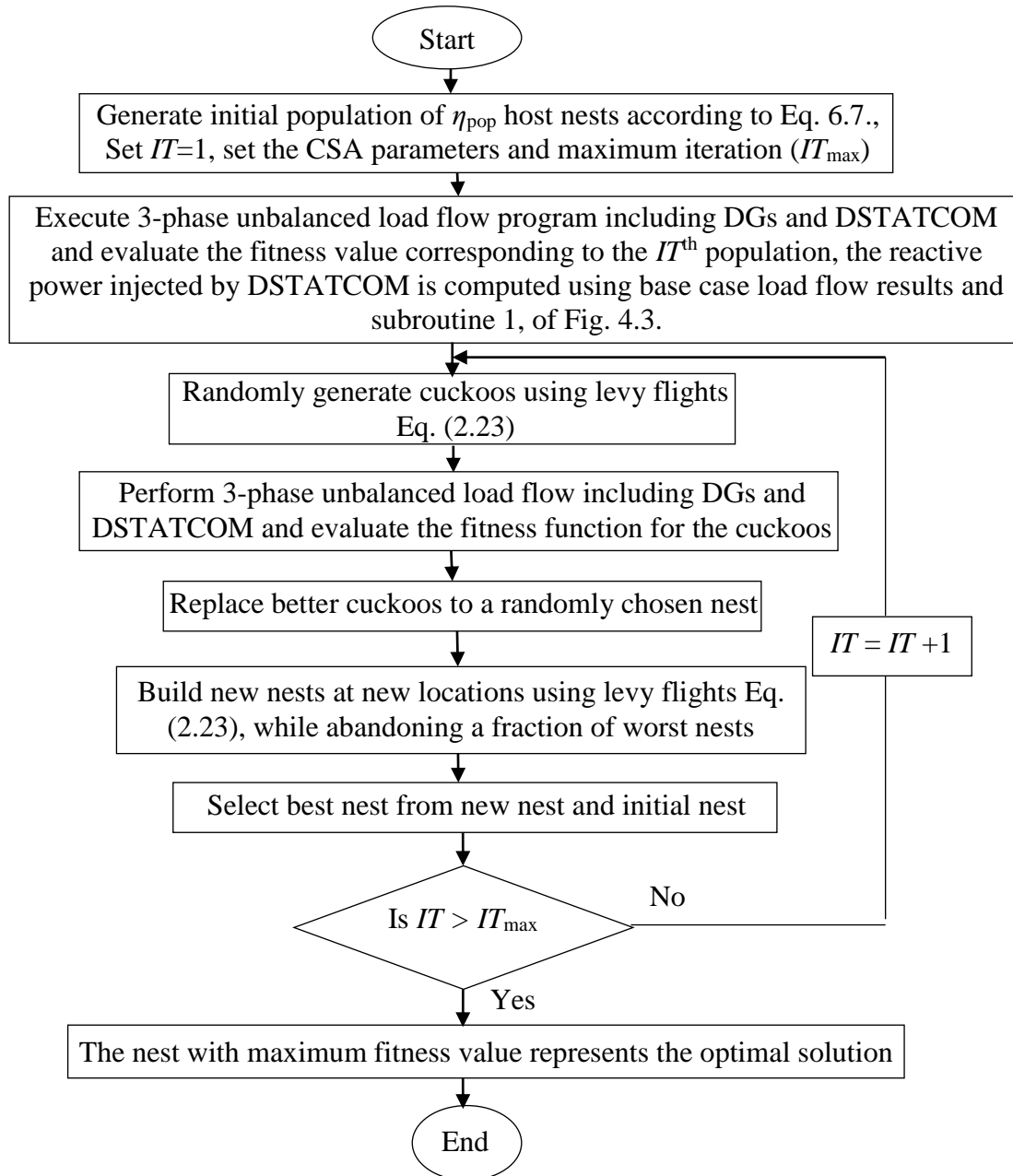


Fig. 6.3. Flow chart of the proposed planning approach using CSA

6.4 Simulation Results and discussions

The computer simulation for the proposed planning approach has been carried out in MATLAB 2012b environment using four test systems, i.e., the 19-bus, 25-bus, Indian 19-bus, and 34-bus URDS. The power loss, the complex power unbalance, the neutral current, the ZSUF, and the NSUF for the base case network of the 19-, 25-, Indian 19-, and 34-bus systems are given in Table 2.1. The DE parameters are optimized by taking repetitive simulation runs, and the optimal parameters are shown in Table 2.2. The DG penetration level i.e. the ratio of total DG active powers to total active power demand is considered to be 0.4 as taken in Chapter 5. The DG units are assumed to be operated at unity power

factor. The maximum rating of DSTATCOM is considered as 10,000 kVAR. Three different planning optimization cases are used. They are:

- *Case A*: planning for optimal phase balancing
- *Case B*: simultaneous planning for the optimal phase balancing and the conductor sizes
- *Case C*: simultaneous planning for the optimal phase balancing, the conductor sizes, the DG active power generation, and the DSTATCOM reactive power generation

All the objective functions are aggregated with equal weights so as to get simultaneous optimization of all of them.

6.4.1. Results of single objective optimization

The single objective performance comparison between planning *Cases A* and *B* using DE are provided in Table 2.7 and 2.11 for 19- and 25-bus system and Indian 19- and 34-bus system respectively. The results of 50 runs for the planning *Case C* (single objective) as obtained with the DE and the CSA are compared, and are shown in Table 6.1 and Table 6.2 for the 19-bus, the 25-bus and the Indian 19-bus and the 34-bus system. The results show that the performance of the DE is better and consistent according to the mean objective function and standard deviation (SD), respectively as compared to the CSA.

Table 6.1 Comparison of results of planning *Case C* of 50 runs as obtained with DE, and CSA, for 19- and 25-bus systems

Objective	19-bus system				25-bus system			
	DE		CSA		DE		CSA	
	Mean	SD	Mean	SD	Mean	SD	Mean	SD
PL (kW)	1.3266	0.0562	1.4102	0.0620	45.3224	0.1745	46.478	0.1846
TS _u (MVA)	0.0002	0.0007	0.0008	0.0009	0.0745	0.0135	0.0805	0.0154
AV _d (%)	0.3512	0.0002	0.4005	0.0006	1.0067	0.0812	1.2140	0.0912
ZSUF (%)	0.0019	0.0011	0.0054	0.0014	0.0034	0.0171	0.0098	0.0183
NSUF (%)	0.0013	0.0065	0.0254	0.0072	0.0040	0.0156	0.0087	0.0165
I _N (p.u.)	1.3218	0	1.3245	0.0014	0.4183	0	0.4195	0.0015

Table 6.2 Comparison of results of planning *Case C* of 50 runs as obtained with DE, and CSA, for Indian 19- and 34-bus systems

Objective	Indian 19-bus system				34-bus system			
	DE		CSA		DE		CSA	
	Mean	SD	Mean	SD	Mean	SD	Mean	SD
PL (kW)	12.213	0.0115	14.219	0.0120	267.3229	0.0051	280.452	0.0058
TS _u (MVA)	0.0018	0.0008	0.0021	0.0012	0.0145	0.0048	0.0154	0.0051
AV _d (%)	1.1024	0.1004	1.2056	0.1132	2.9106	0.0132	2.9854	0.0148
ZSUF (%)	0.0035	0.0012	0.0045	0.0016	0.0959	0.0954	0.0982	0.1021
NSUF (%)	0.0012	0.0005	0.0016	0.0006	0.0280	0.0031	0.0295	0.0041
I _N (p.u.)	5.4495	0	5.5067	0.003	36.8510	0.0003	36.9801	0.0006

6.4.2. Results of multi-objective optimization

The multi-objective performance comparison between planning *Cases A* and *B* using DE are provided in Table 2.15 and 2.19 for 19- and 25-bus system and Indian 19- and 34-bus system respectively. The comparative results of the solutions obtained with planning *Case C* (multi-objective) are given in Table 6.3 and Table 6.4 for the 19-bus, the 25-bus and the Indian 19-bus and the 34-bus system respectively. The power loss, the system unbalance, and the average voltage drop, for the 19- and the 25- bus system are found to be reduced by 90.01%, 96.78%, 88.542%, and 69.74%, 18.23%, 78.59%, respectively with respect to base case values. Similarly, for the Indian 19- and the 34- bus system these objectives are found to be reduced by 75.62%, 97.52%, 70.03%, and 53.78%, 80.07%, 57.67%, respectively with respect to base case values. The ZSUF and NSUF for the 19-, 25-, Indian -19, and 34- bus networks as obtained with different planning cases are illustrated in Figs. (6.4)- (6.11) respectively. It can be seen these values have been reduced significantly with Case C planning for the four test systems. The optimal location and rating of the DGs and the DSTATCOM obtained with DE are shown in Table 6.5. The optimal DSTATCOM angle as obtained with DE for the 19- bus, 25- bus, Indian 19- bus, and 34- bus system are shown in Table 6.6. The complex power demand and the conductor sizes as obtained with *Case C* planning in a sample run for all the systems are shown in Appendix (Table I.1-I.4).

Table 6.3 Comparison of the results as obtained with Case C (multi-objective) planning using DE and CSA

Objective	19-bus system				25-bus system			
	DE		CSA		DE		CSA	
	Mean	SD	Mean	SD	Mean	SD	Mean	SD
PL (kW)	1.3342	0.0585	1.4245	0.0631	46.4101	0.1840	47.513	0.1905
TS _u (MVA)	0.0007	0.0009	0.0009	0.0010	0.0758	0.0141	0.0895	0.0168
AV _d (%)	0.3831	0.0004	0.4241	0.0007	1.0245	0.0823	1.2430	0.0995
ZSUF (%)	0.0023	0.0015	0.0061	0.0018	0.0041	0.0181	0.0105	0.0221
NSUF (%)	0.0032	0.0065	0.0298	0.0074	0.0048	0.0168	0.0095	0.0175
I _N (p.u.)	1.3210	0	1.3261	0.0017	0.4240	0	0.4251	0.0021

Table 6.4 Comparison of the results as obtained with Case C (multi-objective) planning using DE and CSA

Objective	Indian 19-bus system				34-bus system			
	DE		CSA		DE		CSA	
	Mean	SD	Mean	SD	Mean	SD	Mean	SD
PL (kW)	13.015	0.0121	15.112	0.0131	268.5412	0.0058	281.114	0.0061
TS _u (MVA)	0.0019	0.0009	0.0025	0.0018	0.0151	0.0055	0.0162	0.0067
AV _d (%)	1.1145	0.1145	1.2145	0.1161	2.9541	0.0137	3.1042	0.0194
ZSUF (%)	0.0039	0.0015	0.0051	0.0018	0.0981	0.0961	0.0995	0.1324
NSUF (%)	0.0015	0.0007	0.0019	0.0010	0.0292	0.0035	0.0341	0.0054
I _N (p.u.)	5.4567	0	5.5142	0.006	36.8645	0.0004	36.9957	0.0007

Table 6.5 The optimal location and rating of DGs and DSTATCOM for the 19- bus, 25- bus, Indian 19- bus, and 34- bus system as obtained with DE

Bus system	DG location(s)	DSTATCOM location	Power generated by DG units (kW)			Reactive power injected by DSTATCOM unit (kVAR)		
			Phase a	Phase b	Phase c	Phase a	Phase b	Phase c
19- bus	12	6	24.3267	30	23.1483	34.6143	33.0143	31.3421
	19		10.5250	30	28.376			
25- bus	14	13	151.061	231.822	277.389	570.225	683.312	569.923
	22		185.273	294.619	155.836			
Indian 19- bus	7	12	75.123	80.432	77.812	68.4123	61.2132	63.5406
	10		82.432	79.421	92.743			
34- bus	22	5	392.413	383.412	389.912	598.451	599.725	600.231
	9		379.214	400.0	395.043			

Table 6.6: The optimal DSTATCOM angle as obtained with DE for the 19- bus, 25- bus, Indian 19- bus, and 34- bus system

Bus system	Optimal angle α (Degree)		
	Phase a	Phase b	Phase c
19- bus	0.5576	0.5178	0.5210
25- bus	0.8265	0.8165	0.8231
Indian 19- bus	0.0735	0.0704	0.0721
34- bus	-0.2019	-0.2113	-0.2203

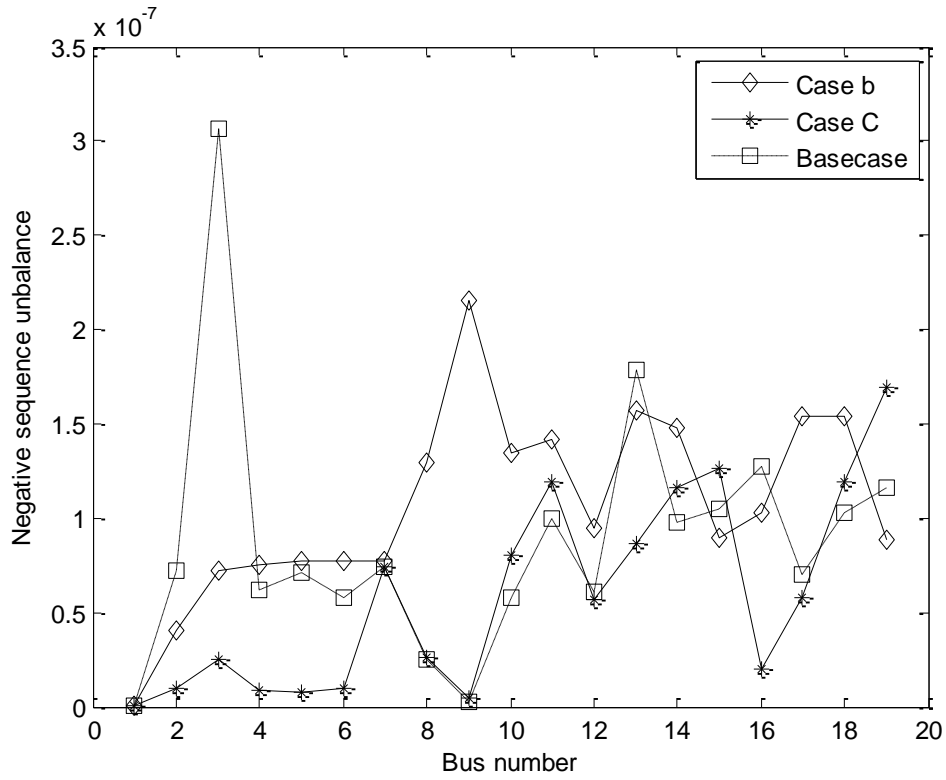


Fig. 6.4. Negative sequence unbalance (NSU) vs. bus number for different planning cases obtained with the DE for the 19-bus system

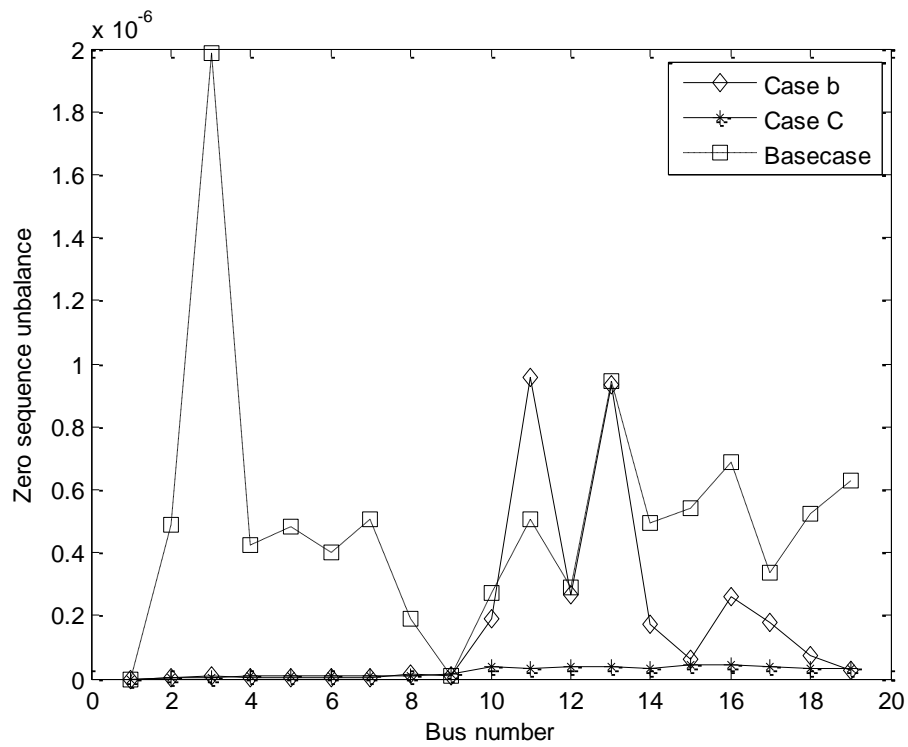


Fig. 6.5. Zero sequence unbalance (ZSU) vs. bus number for different planning cases obtained with the DE for the 19-bus system

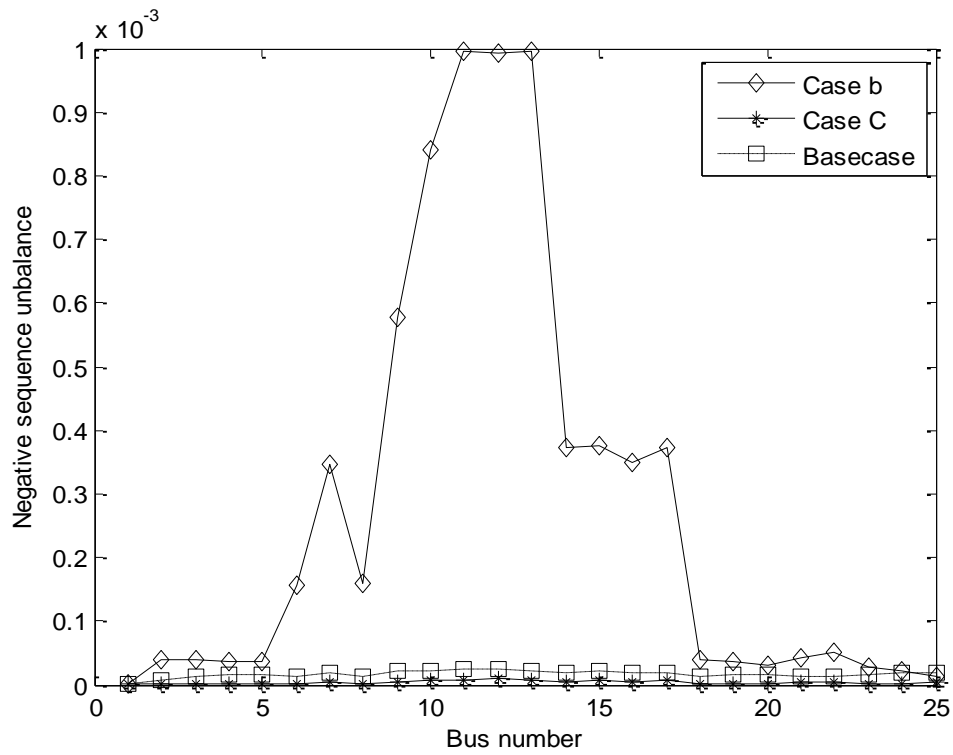


Fig. 6.6. NSU vs. bus number for different planning cases obtained with the DE for the 25-bus system

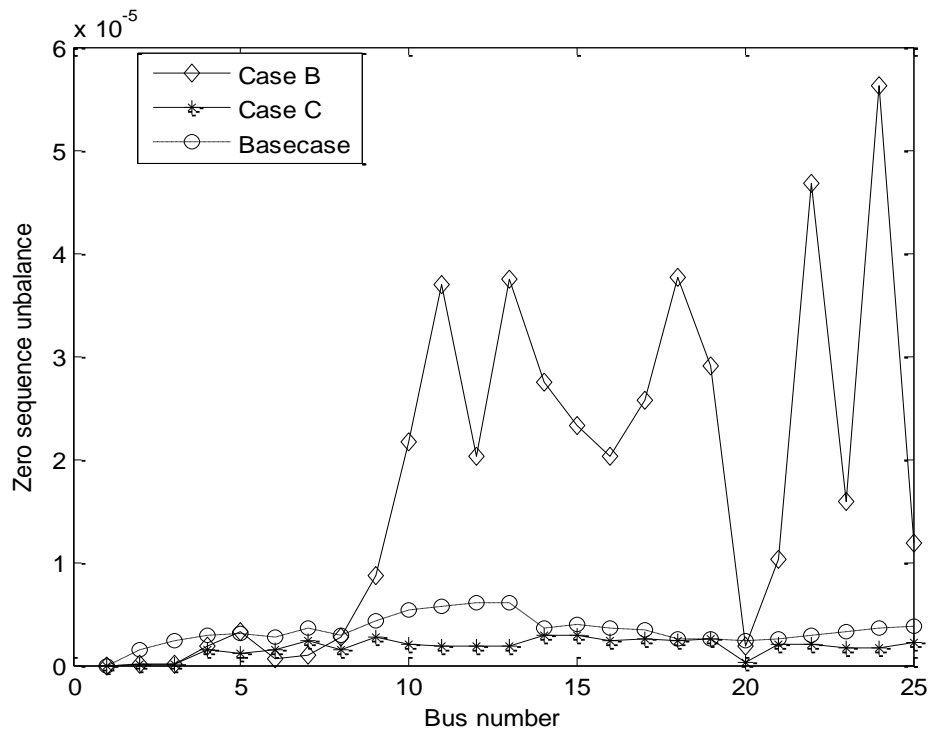


Fig. 6.7. ZSU vs. bus number for different planning cases obtained with the DE for the 25-bus system

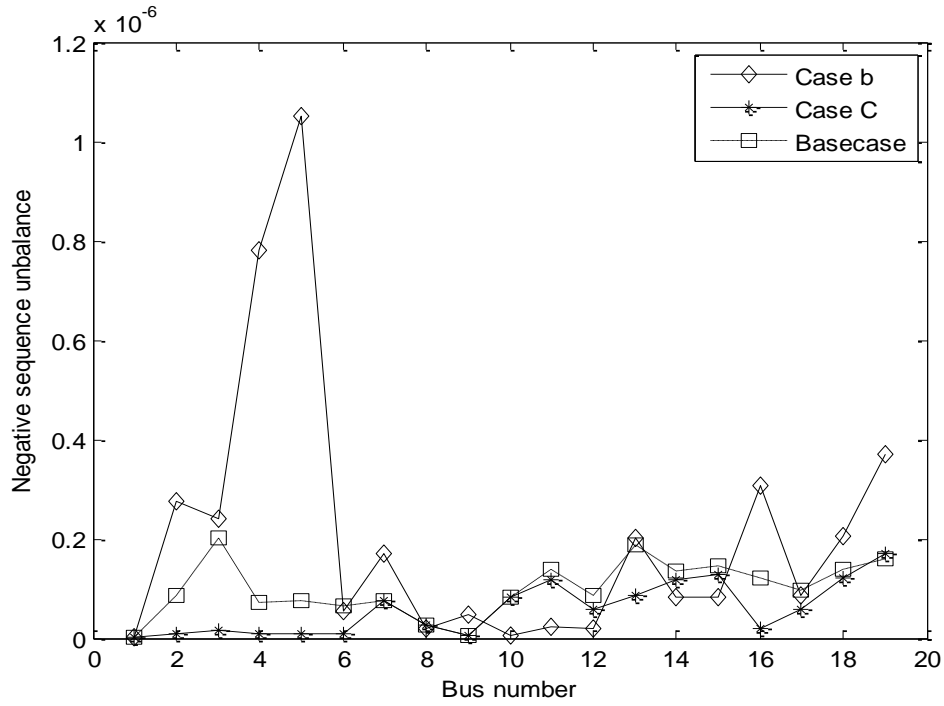


Fig. 6.8. NSU vs. bus number for different planning cases obtained with the DE for the Indian 19-bus system

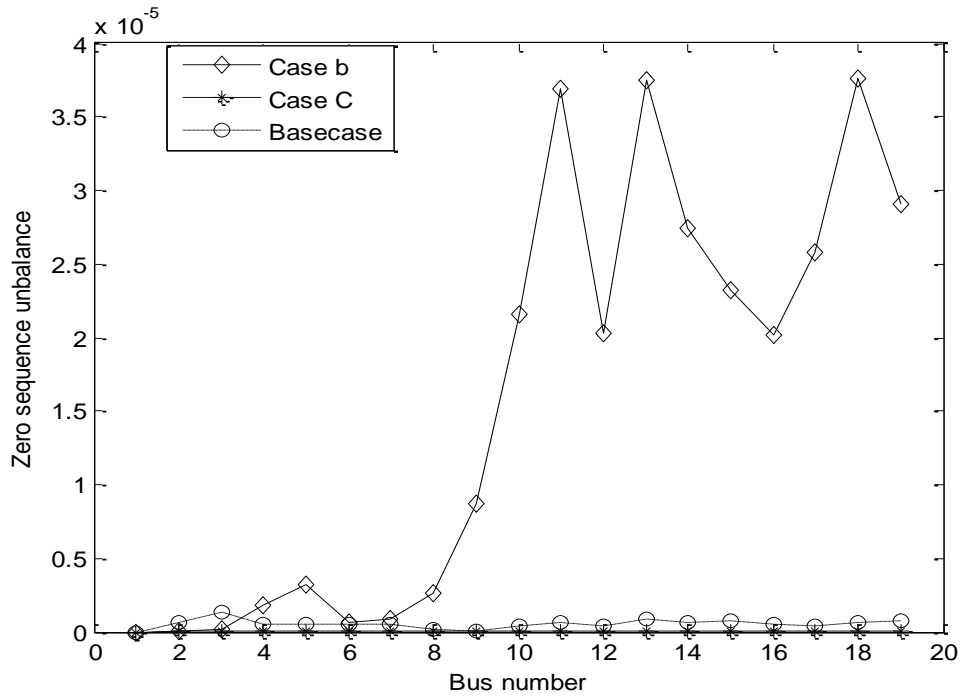


Fig. 6.9. ZSU vs. bus number for different planning cases obtained with the DE for the Indian 19-bus system

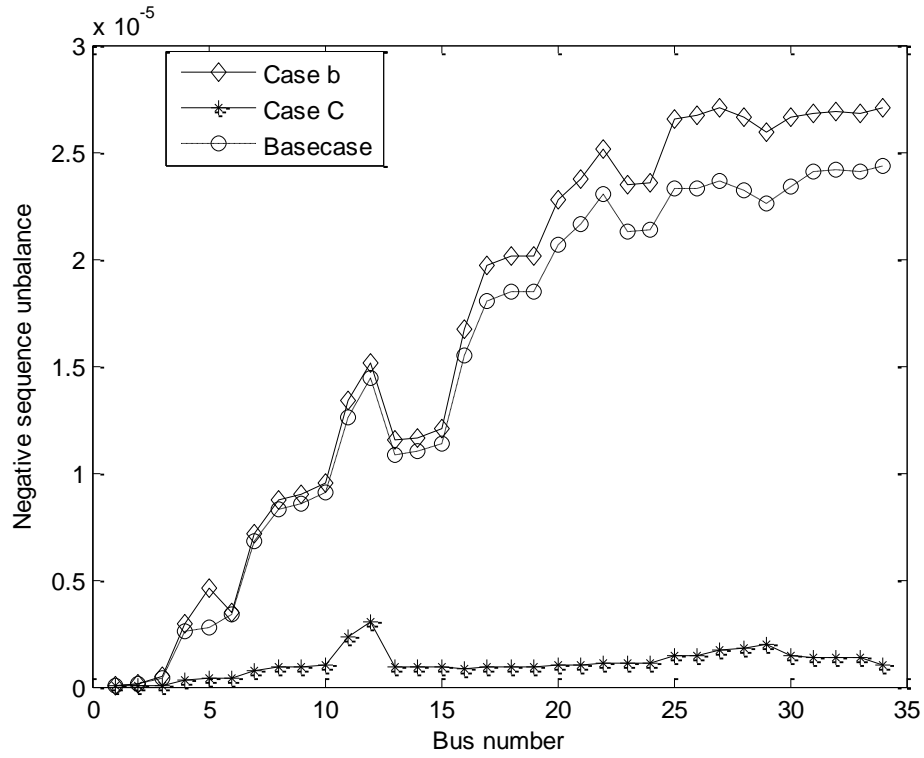


Fig. 6.10. NSU vs. bus number for different planning cases obtained with the DE for the 34-bus system

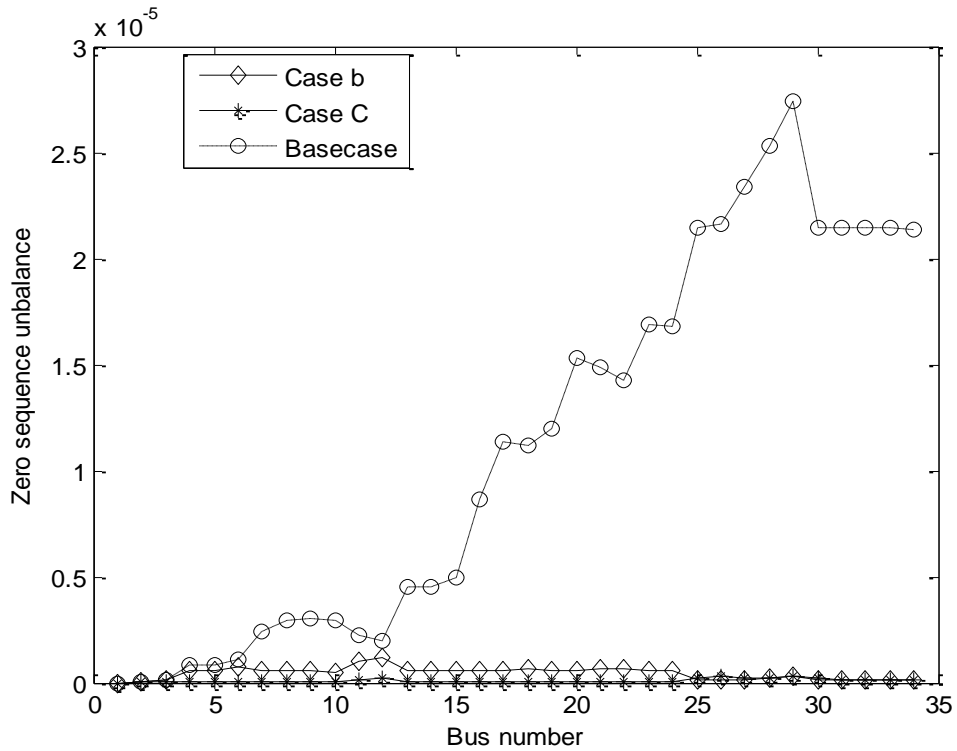


Fig. 6.11. ZSU vs. bus number for different planning cases obtained with the DE for the 34-bus system

6.5 Summary

In this chapter, a planning approach has been devised in order to determine the optimal phase balancing, the conductor sizes, the DG active power allocation and sizing, and the DSTATCOM reactive power allocation and sizing in URDS has been presented by optimizing the power loss, the complex power unbalance, the average voltage drop, the positive and the zero sequence unbalance factors and the neutral current. A forward-backward load flow algorithm including the DG and the DSTATCOM model has been developed and used in the planning approach. The DE and the CSA are utilized as the solution strategy. The important findings of this chapter are as follows:

- The simultaneous optimization approach for the phase balancing, the conductor size, the DG, the DSTATCOM allocation and sizing provides a network with reduced power loss, better voltage profile, lower average voltage drop, lower voltage unbalance factors, lower neutral current, and a lower system unbalance.
- However, the locations and ratings of the DGs and the DSTATCOM are found to be quite different for the four test systems. This may be due to different active and reactive power demand of the systems.
- The DE algorithm gives better solutions in comparison to the CSA for all objectives in terms of mean and standard deviation for both the single and the multi-objective optimization.

Chapter 7

Conclusions and Future Scope

7.1 Conclusions

The main objective of this research work is, the planning of unbalanced distribution systems integrating reactive power compensating devices such as the capacitors, the DSTATCOM, and the renewable devices such as solar and wind turbine. The thesis work commenced with the introduction to unbalanced distribution systems planning, and different planning approaches. A three-phase unbalanced load flow algorithm is developed and used for obtaining the power flow solutions. Six objective functions such as the total power loss, the average voltage drop, the total zero sequence unbalance, the negative sequence voltage unbalance, the total neutral current, and the total complex power unbalance are considered in this work. These objective functions are optimized both separately and combined into aggregated multiobjective approach so as to obtain a distribution network with lower power loss, voltage unbalance, total neutral current, etc. Four metaheuristic algorithms such as the DE, the CSA, the PSO, and the GA are employed as the optimization algorithm, and comparative analysis is carried out among them regarding Mean and standard deviation to evaluate the relative merits and demerits of each algorithm over other. The test systems for implementation of these algorithms considered are as 1) 19 –bus, 2) Practical Indian 19-bus 3) 25-bus, 4) 34-bus. From the simulation results, it is observed that simultaneous optimization of phase loading and conductor sizes lower power loss, and improves the voltage magnitude of each bus. However, no significant improvement of other objectives is observed with this optimization.

As discussed in the literature, the reactive power compensating devices such as the capacitors can also reduce the power loss, and the improve the voltage profile of the systems. Hence, a simultaneous optimization of capacitor location and rating, the phase

loading, and the conductor sizing is done to optimize the six objectives. The simulation results show that all these objectives are reduced for Indian 19-, 25-, and 34- bus system. But, inferior results are obtained for the 19- bus system. This, may be due to overcompensation of the system due to discrete size and high rating of capacitors. Therefore, another compensating device such as DSTATCOM is incorporated in the unbalanced distribution systems. A three phase unbalanced modelling of DSTATCOM is devised for generation of the variable reactive power, which was not done earlier. But, still, the simulation results show that simultaneous optimization phase loading, conductor sizing, DSTATCOM location, and rating gives poor results in comparison to simultaneous optimization of phase loading, conductor sizing for a smaller test system such as the 19-bus.

However, the simulation results depict that the integration of the DGs and the DSTATCOM into the unbalanced distribution system gives best results for all the six objective functions in comparison to simultaneous optimization of phase balancing and conductor sizing, and only phase balancing.

The DE algorithm gives better solutions in comparison to the CSA for all objectives in terms of mean and standard deviation for both the single and the multi-objective optimization for all planning studies.

Overall it can be summarized that the simulation results indicate the efficacy of metaheuristic algorithms for the planning of unbalanced distribution system with the integration of devices DG, and DSTATCOM for minimization of several objective functions.

7.2 Future Scope

This research has shown the positive impact of integration of DG and DSTATCOM in the unbalanced distribution system planning with the help of metaheuristic algorithms. Based on the observations from this work, the further investigations are required in the follow aspects:

- The planning of unbalanced distribution system can be carried out considering uncertainties with load and power generation.
- The planning approaches can be extended with the inclusion of reliability aspects, and other objectives.
- The investigation can be carried out with other metaheuristic approaches for the planning problem.

PLANNING OF UNBALANCED RADIAL DISTRIBUTION SYSTEMS WITH CAPACITOR USING DIFFERENTIAL EVOLUTION ALGORITHM

Padarbinda. SAMAL¹, Sanjeeb. MOHANTY², Sanjib. GANGULY³

^{1,2}Department of Electrical Engineering, National Institute of Technology, Rourkela, India-769008

³Department of Electronics and Electrical Engineering, Indian Institute of Technology Guwahati

¹Corresponding author's email: padarbindasamal87@gmail.com

Abstract: This work presents a planning approach for unbalanced radial distribution systems using differential evolution (DE) algorithm so as to determine the optimal capacitor location and phase balancing. Four objective functions are considered in the planning problem. They are the minimization of (i) total system real power loss, (ii) average voltage drop, (iii) total neutral current, and (iv) total negative-sequence voltage unbalance. These objectives are optimized under the constraints of minimum and maximum voltage limits for each bus voltage and thermal limit of each line. A modified three phase forward-backward sweep based load flow algorithm is employed as a supplementary tool for the evaluation of these objective functions. The simulation results obtained with the Indian 19-bus and 34-bus unbalanced radial distribution networks show that significant improvement in power loss, average voltage drop, and total neutral current can be achieved with simultaneous optimization for capacitor location, sizing and phase balancing.

Key words: Unbalanced radial distribution networks, three phase load flow, capacitor, differential evolution algorithm.

1. Introduction

The main aim of distribution system planning is to develop a distribution network that can sustain future demand reliably and efficiently. However, distribution systems are inherently unbalanced due to uneven single phase, three-phase loads. This results in an increase in power loss, neutral current and voltage unbalance and consequently the system performance reduces. Therefore, an appropriate phase balancing is required so as to reduce these effects.

Recent developments show significant phase balancing schemes [1-12]. In [1], the authors have used evolutionary algorithm for minimizing wire replacement cost, transformer positioning cost, load

balancing cost. A modified particle swarm optimization algorithm was used in [2] to minimize phase unbalance in a radial distribution system. In [3], a phase balancer device was developed for mitigation of neutral current, and phase unbalance. The authors in [4], utilised mixed integer programming for minimization of phase swapping cost. A population-based algorithm called immune algorithm was employed in [5], to minimize customer service interruption cost, labor cost, and neutral current. The authors in [6], proposed non-dominated sorting genetic algorithm II for minimization of energy loss, neutral current, and number of reconnections. In [7], the authors have reduced the phase unbalancing by changing the transformer winding connections. An expert system was devised in [8], to minimize the total loss cost. A self-adaptive differential evolution algorithm [9] was used for phase balancing of distribution networks. The authors in [10], utilized tabu search algorithm for minimization of total system cost. In [11], simulated annealing was used for minimizing phase swapping cost. The authors in [12], have utilized differential algorithm (DE) for minimization of complex power unbalance, power loss, voltage unbalance, and neutral current.

In recent years numerous works have done in the area of capacitor allocation in distribution networks [13-20]. In [13], the authors have used cuckoo search algorithm for minimizing total system power loss. A system approach was devised in [14] for profit maximization in distribution networks. Cultural algorithm [15] was employed for power loss minimization and voltage profile improvement in distribution networks. The authors in [16] utilized particle swarm optimization for power loss minimization. A bacteria foraging based algorithm was used in [17] for maximizing capacitor saving function, minimizing active power losses, and voltage profile improvement. In [18], genetic algorithm (GA) was employed for minimization of operating costs of

MODELLING AND ALLOCATION OF A DSTATCOM ON THE PERFORMANCE IMPROVEMENT OF UNBALANCED RADIAL DISTRIBUTION SYSTEMS

Padarbinda. SAMAL¹, Sanjeeb. MOHANTY², Sanjib. GANGULY³

^{1,2}Department of Electrical Engineering, National Institute of Technology, Rourkela, India-769008

³Department of Electronics and Electrical Engineering, Indian Institute of Technology Guwahati

¹Corresponding author's email: padarbindasamal87@gmail.com

Abstract: In this paper a three phase modelling of DSTATCOM has been carried out for unbalanced radial distribution systems. Further the modelled DSTATCOM has been incorporated in the load flow algorithm and placed at each bus of distribution systems one at a time except the source bus. The placement of the DSTATCOM clearly indicates that system power loss decreases and the voltage profile improvement takes place with respect to base case. A 25 bus system and a 19-bus unbalanced radial distribution systems are considered as the test systems.

Key words: Unbalanced radial distribution systems, three phase modelling, distribution static synchronous compensator, load flow.

1. Introduction

The distribution system is considered to be a lossy system due to high R/X ratio of the distribution lines, and the low operating voltage. Moreover, the distribution systems suffer various power quality issues such as overvoltage, undervoltage, harmonic distortion, etc. This in turn reduces the operational efficiency, the service quality, and the reliability of distribution systems. In recent times, the custom power devices such as distribution static synchronous compensator (DSTATCOM) [1] are considered as the best tool to alleviate all the power quality problems. In all of the works, the DSTATCOM is allocated in balanced radial distribution systems and its impact on the system performance is studied [2-14]. The particle swarm based optimization was employed to obtain the optimal location and size of distributed generations and DSTATCOM for minimizing the system power loss [2]. Jazebi *et. al.* [3] implemented differential evolution algorithm considering network

reconfiguration so as to minimize the power loss distribution networks. The authors in [4] utilized bacterial foraging algorithm in order to reduce the power loss, the total operational cost, and the voltage profile index of distribution systems. Salman *et. al* [5] proposed binary gravitation search algorithm to minimize the voltage sag in a distribution system. In [6], an analytic method was applied in minimizing the total system power loss and minimum voltage magnitude. Farhoodnea *et. al* [7] employed firefly algorithm for optimizing the average voltage total harmonic distortion, average voltage deviation, and total investment cost. Tolabi *et. al* [8] proposed fuzzy ant colony optimization for minimizing the system loss, increasing load balancing index, and voltage profile of a system by simultaneous reconfiguration, optimal allocation of DSTATCOM and photovoltaic array. The impact of distributed generator on the allocation and size of DSTATCOM was investigated in [9]. Here, the total cost of DSTATCOM was considered the objective function to be minimized. Jain *et. al.* [10] applied voltage stability index method in order to obtain the optimal location of DSTATCOM. The minimization of real power loss was chosen as the objective function. In [11], a fuzzy shuffled frog-leaping algorithm was developed so as to reduce the total power loss, equal load balancing index, and voltage deviation by reconfiguring the network in presence of capacitors, and DSTATCOM. Taher and Afsari implemented [12] an optimization algorithm called the immune algorithm in order to minimize the power loss and size of the DSTATCOM. Xiaoguang *et. al.* [13] have used genetic algorithm for obtaining the optimal network configuration for minimizing the total cost of the system with the help of DSTATCOM and dynamic voltage restorer. In [14], a meta-heuristic algorithm called bat algorithm was applied to minimize the system power loss. However, no works have been reported for the optimal placement and sizing of

Planning of unbalanced radial distribution systems using differential evolution algorithm

Padarbinda Samal¹ · Sanjib Ganguly² ·
Sanjeeb Mohanty¹

Received: 15 July 2015 / Accepted: 4 April 2016
© Springer-Verlag Berlin Heidelberg 2016

Abstract This paper presents a planning approach for unbalanced radial distribution systems using differential evolution algorithm (DE) so as to determine the optimal phase balancing and conductor sizes. The objective functions used in the planning are minimization of: (1) total complex power unbalance, (2) total power loss, (3) average voltage drop, (4) voltage unbalance factor, and (5) total neutral current. The optimization is done under the constraints of minimum and maximum voltage limits for each bus voltage and thermal limit of each line. A three phase forward–backward sweep load flow algorithm is developed and used for the determination of these objective functions. The effectiveness of the proposed planning algorithm is corroborated on 19-bus and IEEE 25-bus unbalanced radial distribution systems. The results show that significant improvements in power loss and voltage drop with simultaneous optimization for phase balancing and conductor sizes. The performance of DE is found to be better and consistent as compared to some other meta-heuristic algorithms studied here.

Keywords Unbalanced radial distribution systems · Three phase load flow · Differential evolution algorithm

Abbreviations

\bar{I}_n^a Branch current for n th branch, phase a (in phasor form).
 $I L_k^a$ Load current for k th bus, phase a (in phasor form).

✉ Sanjib Ganguly
sanjib191@gmail.com

¹ Department of Electrical Engineering, National Institute of Technology Rourkela, Rourkela, India

² Department of Electronics and Electrical Engineering, Indian Institute of Technology Guwahati, Guwahati, India

Appendix

Appendix A

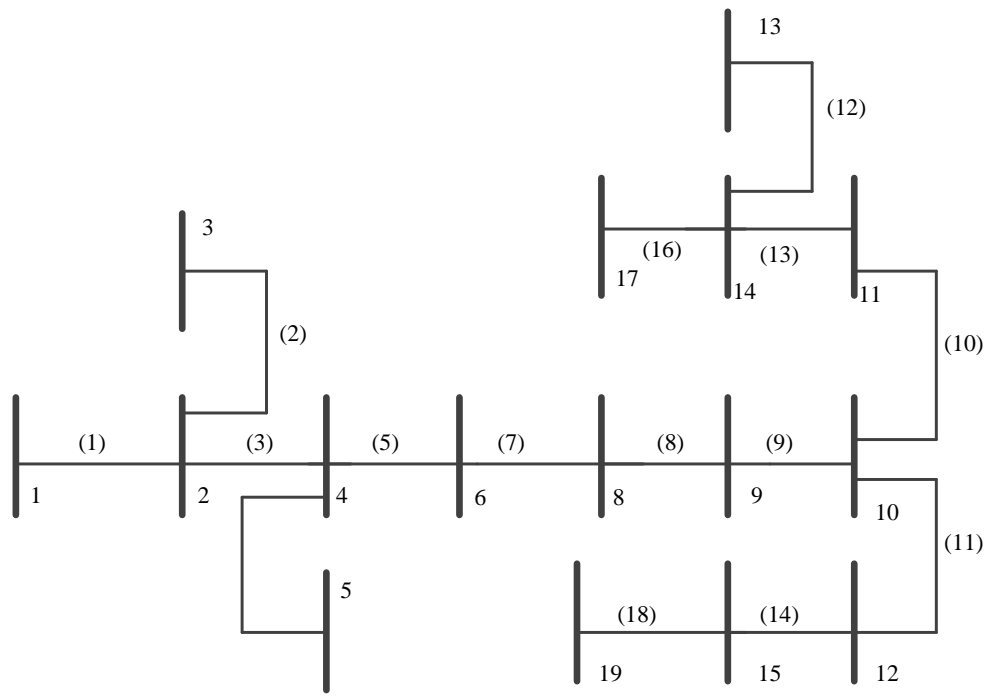


Fig. A.1 A 19-bus URDS schematic diagram, (a) 1,2,3...,19 denotes bus number (b) (1), (2),(3),...,(18) denotes branch numbers (c) All the branches are considered three phase lines

Table A.1. Different types of conductor used in the 19-bus [97] system

Conductor type	19 -bus system	
	Self-impedance (Ω/mile)	Mutual impedance (Ω/mile)
1 (3- ϕ)	$Z_{aa} = 1.5609 + j0.67155$ $Z_{bb} = 1.5609 + j0.67155$ $Z_{cc} = 1.5609 + j0.67155$	$Z_{ab} = 0.5203 + j0.22385$ $Z_{bc} = 0.5203 + j0.22385$ $Z_{ca} = 0.5203 + j0.22385$
2 (3- ϕ)	$Z_{aa} = 0.6074 + j0.5417$ $Z_{bb} = 0.6117 + j0.5377$ $Z_{cc} = 0.6096 + j0.5374$	$Z_{ab} = 0.0104 + j0.1054$ $Z_{bc} = 0.0116 + j0.1414$ $Z_{ca} = 0.0094 + j0.0785$
3 (3- ϕ)	$Z_{aa} = 0.6871 + j1.2773$ $Z_{bb} = 0.7003 + j1.2518$ $Z_{cc} = 0.6940 + j1.2642$	$Z_{ab} = 0.0315 + j0.2824$ $Z_{bc} = 0.0350 + j0.3862$ $Z_{ca} = 0.0289 + j0.2047$

Table A.2. Load data of 19-bus system (SB=Sending end bus, RB=Receiving end bus, BN=Branch number, LC=Line code, BL=Branch length)

SB	RB	BN	LC	BL (km)	Base case complex load demand		
					Phase A	Phase B	Phase C
1	2	1	1	3.0	10.38+j5.01	5.19+j2.52	10.38+j5.01
2	3	2	1	5.0	11.01+j5.34	5.19+j2.52	9.72+j4.71
3	4	3	1	1.5	4.05+j1.95	5.67+j2.76	6.48+j3.15
4	5	4	1	1.5	6.48 + j3.15	5.19+j2.52	4.53+j2.19
4	6	5	1	1.0	4.20 + j2.04	3.09 + j1.50	2.91 + j1.42
6	7	6	1	2.0	9.72 + j4.71	8.10 + j3.93	8.10 + j3.93
6	8	7	1	2.5	7.44 + j3.60	5.34 + j2.58	3.39 + j1.65
8	9	8	1	3.0	12.30 + j5.97	14.91 + j7.23	13.29 + j6.42
9	10	9	1	5.0	3.39 + j1.65	4.20 + j2.04	2.58 + j1.26
10	11	10	1	1.5	7.44 + j3.60	7.44 + j3.60	11.01 + j5.34
10	12	11	1	1.5	9.72 + j4.71	8.10 + j3.93	8.10 + j3.93
11	13	12	1	5.0	4.38 + j2.13	5.34 + j2.58	6.48 + j3.15
11	14	13	1	1.0	3.09 + j1.50	3.09 + j1.50	4.05 + j1.95
12	15	14	1	5.0	4.38 + j2.13	4.86 + j2.34	6.96 + j3.36
12	16	15	1	6.0	7.77 + j3.78	10.38 + j5.01	7.77 + j3.78
14	17	16	1	3.5	6.48 + j3.12	4.86 + j2.34	4.86 + j2.34
14	18	17	1	4.0	5.34 + j2.58	5.34 + j2.58	5.52 + j2.67
15	19	18	1	4.0	8.76 + j4.23	10.05+ j4.86	7.14 + j3.45

Appendix B

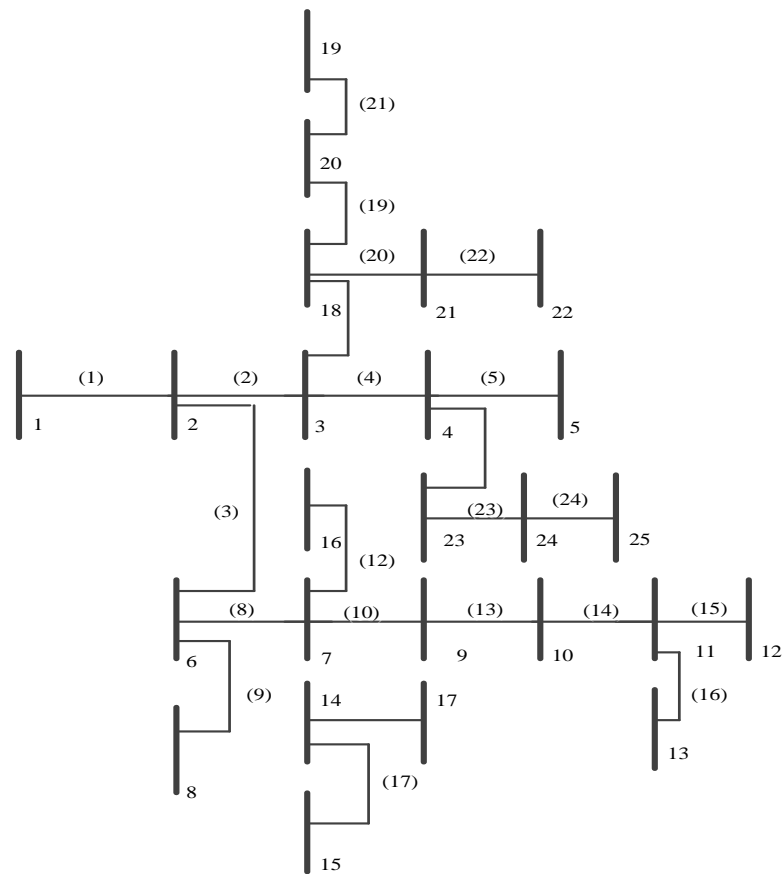


Fig. B.1 A 25-bus URDS schematic diagram

Table B.1. Different types of conductor used in the 25-bus [92] system

Conductor type	25-bus system	
	Self-impedance (Ω/mile)	Mutual impedance (Ω/mile)
1 (3- ϕ)	$Z_{aa} = 0.3686 + j0.6852$ $Z_{bb} = 0.3757 + j0.6715$ $Z_{cc} = 0.3723 + j0.6782$	$Z_{ab} = 0.0169 + j0.1515$ $Z_{bc} = 0.0188 + j0.2072$ $Z_{ca} = 0.0155 + j0.1098$
2 (3- ϕ)	$Z_{aa} = 0.9775 + j0.8717$ $Z_{bb} = 0.9844 + j0.8654$ $Z_{cc} = 0.9810 + j0.8648$	$Z_{ab} = 0.0167 + j0.1697$ $Z_{bc} = 0.0186 + j0.2275$ $Z_{ca} = 0.0152 + j0.1264$
3 (3- ϕ)	$Z_{aa} = 1.9280 + j1.4194$ $Z_{bb} = 1.9308 + j1.4215$ $Z_{cc} = 1.9337 + j1.4236$	$Z_{ab} = 0.0161 + j0.1183$ $Z_{bc} = 0.0161 + j0.1183$ $Z_{ca} = 0.0161 + j0.1183$

Table B.2. Load data of 25-bus system

SB	RB	BN	LC	BL (feet)	Base case complex load demand		
					Phase A	Phase B	Phase C
1	2	1	1	1000	0	0	0
2	3	2	1	500	$35 + j25$	$40 + j30$	$45 + j32$
2	6	3	2	500	$40 + j30$	$45 + j32$	$35 + j25$
3	4	4	1	500	$50 + j40$	$60 + j45$	$50 + j35$
3	18	5	2	500	$40 + j30$	$40 + j30$	$40 + j30$
4	5	6	2	500	$40 + j30$	$40 + j30$	$40 + j30$
4	23	7	2	400	$60 + j45$	$50 + j40$	$50 + j35$
6	7	8	2	500	0	0	0
6	8	9	2	1000	$40 + j30$	$40 + j30$	$40 + j30$
7	9	10	2	500	$60 + j45$	$50 + j40$	$50 + j35$
7	14	11	2	500	$50 + j35$	$60 + j45$	$50 + j40$
7	16	12	2	500	$40 + j30$	$40 + j30$	$40 + j30$
9	10	13	2	500	$35 + j25$	$40 + j30$	$45 + j32$
10	11	14	2	300	$45 + j32$	$35 + j25$	$40 + j30$
11	12	15	3	200	$50 + j35$	$60 + j45$	$50 + j40$
11	13	16	3	200	$35 + j25$	$45 + j32$	$40 + j30$
14	15	17	2	300	$133.3 + j100$	$133.3 + j100$	$133.3 + j100$
14	17	18	3	300	$40 + j30$	$35 + j32$	$45 + j32$
18	20	19	2	500	$35 + j25$	$40 + j30$	$45 + j32$
18	21	20	3	400	$40 + j30$	$35 + j25$	$45 + j32$
20	19	21	3	400	$60 + j45$	$50 + j35$	$50 + j40$
21	22	22	3	400	$50 + j35$	$60 + j45$	$50 + j35$
23	24	23	2	400	$35 + j25$	$45 + j32$	$40 + j30$
24	25	24	3	400	$60 + j45$	$50 + j30$	$50 + j35$

Appendix C

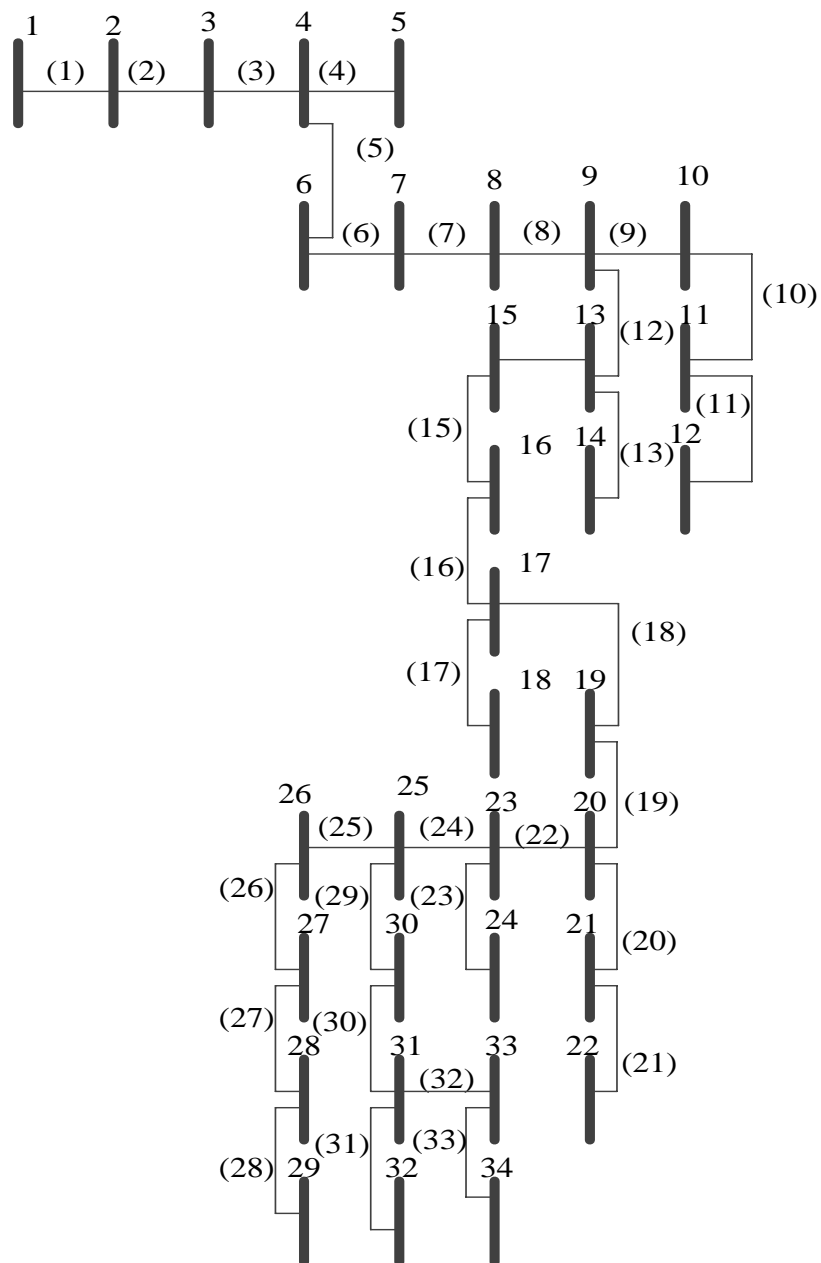


Fig. C.1 A 34-bus URDS schematic diagram

Table C.1. Load data of 34-bus [109] system

SB	RB	BN	LC	BL (mile)	Base case complex load demand		
					Phase A	Phase B	Phase C
1	2	1	1	0.4895	46.67 + j24.50	46.67+ j24.50	46.67+ j24.50
2	3	2	1	0.3277	46.67+ j24.50	46.67+ j24.50	46.67+ j24.50
3	4	3	1	1.1334	73.33+ j36.82	73.33+ j36.82	73.33+ j36.82
4	5	4	2	1.1063	100+ j52.67	100 +j52.67	100+ j52.67
4	6	5	1	0.2672	70+ j36.87	70 +j36.87	70 +j36.87
6	7	6	1	0.9955	50+ j26.33	50+ j26.33	50+ j26.33
7	8	7	1	0.3410	50 +j26.33	50+ j26.33	50 +j26.33
8	9	8	1	0.0587	100+ j52.67	100+ j52.67	100+ j52.67
9	10	9	2	0.3238	150+ j79.01	150+ j79.01	150+ j79.01
10	11	10	2	2.9062	150+ j79.01	150+ j79.01	150+ j79.01
11	12	11	2	1.9818	300+ j158.03	300+ j158.03	300+ j158.03
9	13	12	1	0.6911	50+ j26.33	50+ j26.33	50+ j26.33
13	14	13	2	0.5740	90+ j47.41	90+ j47.41	90+ j47.41
13	15	14	1	0.1591	86.67+ j45.65	86.67+ j45.65	86.67+ j45.65
15	16	15	1	1.2430	83.33+ j43.89	83.33+ j43.89	83.33+ j43.89
16	17	16	1	0.7200	83.33+ j43.89	83.33+ j43.89	83.33+ j43.89
17	18	17	2	1.3120	100+ j52.67	100+ j52.67	100+ j52.67
17	19	18	1	0.1430	50+ j26.33	50+ j26.33	50+ j26.33
19	20	19	1	0.7162	76.67+ j40.38	76.67+ j40.38	76.67+ j40.38
20	21	20	2	0.7347	140+ j73.74	140+ j73.74	140+ j73.74
21	22	21	2	2.0004	180+ j94.82	180+ j94.82	180+ j94.82
20	23	22	1	0.3067	40+ j 21.07	80+ j42.14	80+ j42.14
23	24	23	2	0.3069	100+ j52.67	100+ j52.67	100+ j52.67
23	25	24	1	1.1044	33.33+ j17.55	33.33+ j17.55	33.33+ j17.55
25	26	25	2	0.0530	40+ j21.07	40+ j47.41	90+ j47.41
26	27	26	2	0.8773	283.33+ j149.25	283.33+ j149.25	283.33+ j149.25
27	28	27	2	0.6896	43.33+ j22.82	43.33+ j22.82	43.33+ j22.82
28	29	28	2	0.7219	20+ j10.53	70+ j36.87	70+ j36.87
25	30	29	1	0.1030	53.33+ j28.09	53.33+ j28.09	53.33+ j28.09
30	31	30	1	0.6215	46.67	46.67	46.67
31	32	31	2	0.1629	130+ j68.48	130+ j68.48	130+ j68.48
31	33	32	2	0.0530	60+ j31.60	60+ j31.60	60+ j31.60
33	34	33	2	0.9206	60+ j31.60	60+ j31.60	60+ j31.60

Table C.2. Different types of conductor used in the 34-bus system

Conductor type	Self-impedance per mile (Ω)	Mutual impedance per mile (Ω)
1 (3- ϕ)	$Z_{aa} = 0.7443 + j 1.2106$	$Z_{ab} = 0.1594 + j 0.4822$
	$Z_{bb} = 0.7651 + j 1.1815$	$Z_{bc} = 0.1624 + j 0.4398$
	$Z_{cc} = 0.7482 + j 1.1970$	$Z_{ca} = 0.1546 + j 0.3878$
2 (3- ϕ)	$Z_{aa} = 1.3196 + j 1.3521$	$Z_{ab} = 0.1939 + j 0.5477$
	$Z_{bb} = 1.2760 + j 1.3306$	$Z_{bc} = 0.1973 + j 0.5070$
	$Z_{cc} = 1.3240 + j 1.3434$	$Z_{ca} = 0.2028 + j 0.4547$

Appendix D

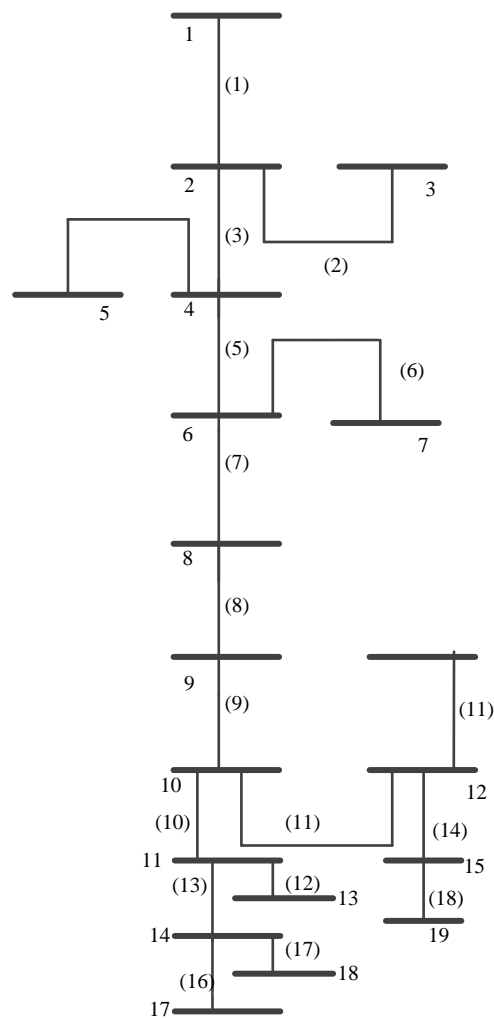


Fig. D.1 A Indian 19-bus URDS schematic diagram

Table D.1. Load data of the Indian 19-bus [110] system

SB	RB	BN	LC	BL (km)	Base case complex load demand		
					Phase A	Phase B	Phase C
1	2	1	1	3.0	34.6 +j16.7	17.3 +j8.40	34.6 +j16.7
2	3	2	2	4.0	36.7 +j17.8	17.3 +j8.4	32.4 +j15.7
2	4	3	3	1.5	13.5 +j6.5	18.9 +j9.2	21.6 +j10.5
4	5	4	4	1.5	21.6+ j10.5	17.3 +j8.4	15.1 +j7.3
4	6	5	5	1.0	14.0 +j6.8	10.3 +j5.0	9.7 +j4.7
6	7	6	5	2.0	32.4 +j15.7	27.0 +j13.1	27.0 +j13.1
6	8	7	2	2.5	24.8+ j12. 0	17.8 +j8.6	11.3+ j5.5
8	9	8	1	3.0	41.0+j19.9	49.7 +j24.1	44.3+j21.4
9	10	9	6	5.0	11.3 +j5.5	14.0 +j6.8	8.6 +j4.2
10	11	10	3	1.5	24.8 +j12.0	24.8 +j12.0	36.7 +j17.8
11	12	11	3	1.5	32.4+j15.7	27.0+j13.1	27.0+j13.1
11	13	12	2	5.0	14.6 +j7.1	17.8+ j8.6	21.6+j10.5
14	14	13	5	1.0	10.3 +j5.0	10.3 +j5.0	13.5+ j6.5
14	15	14	6	5.0	14.6 +j7.1	16.2 +j7.8	23.2 +j11.2
10	16	15	1	6.0	25.9 +j12.6	34.6+j16.7	25.9+j12.6
12	17	16	7	3.5	21.6 +j10.5	16.2 +j7.8	16.2 +j7.8
12	18	17	8	4.0	17.8 +j8.6	17.8 +j8.6	18.4+ j8.9
15	19	18	9	4.0	29.2+j14.1	33.5+j16.2	23.8 +j11.5

Table D.2. Different types of conductor used in the 34-bus system

Conductor typed	Self-impedance (p.u.)	Mutual impedance (p.u.)
1 (3- ϕ)	$Z_{aa} = 0.0387 + j 0.0167$	$Z_{ab} = 0.0129 + j 0.0056$
	$Z_{bb} = 0.0387 + j 0.0167$	$Z_{bc} = 0.0129 + j 0.0056$
	$Z_{cc} = 0.0387 + j 0.0167$	$Z_{ca} = 0.0129 + j 0.0056$
2 (3- ϕ)	$Z_{aa} = 0.0323 + j 0.0139$	$Z_{ab} = 0.0108 + j 0.0046$
	$Z_{bb} = 0.0323 + j 0.0139$	$Z_{bc} = 0.0108 + j 0.0046$
	$Z_{cc} = 0.0323 + j 0.0139$	$Z_{ca} = 0.0108 + j 0.0046$
3 (3- ϕ)	$Z_{aa} = 0.0193 + j 0.0083$	$Z_{ab} = 0.0064 + j 0.0028$
	$Z_{bb} = 0.0193 + j 0.0083$	$Z_{bc} = 0.0064 + j 0.0028$
	$Z_{cc} = 0.0193 + j 0.0083$	$Z_{ca} = 0.0064 + j 0.0028$
4 (3- ϕ)	$Z_{aa} = 0.0097 + j 0.0042$	$Z_{ab} = 0.0032 + j 0.0014$
	$Z_{bb} = 0.0097 + j 0.0042$	$Z_{bc} = 0.0032 + j 0.0014$
	$Z_{cc} = 0.0097 + j 0.0042$	$Z_{ca} = 0.0032 + j 0.0014$
5 (3- ϕ)	$Z_{aa} = 0.0129 + j 0.0055$	$Z_{ab} = 0.0043 + j 0.0018$
	$Z_{bb} = 0.0129 + j 0.0056$	$Z_{bc} = 0.0043 + j 0.0018$
	$Z_{cc} = 0.0129 + j 0.0056$	$Z_{ca} = 0.0043 + j 0.0018$
6(3- ϕ)	$Z_{aa} = 0.0645 + j 0.0278$	$Z_{ab} = 0.0215 + j 0.0093$
	$Z_{bb} = 0.0645 + j 0.0278$	$Z_{bc} = 0.0215 + j 0.0093$
	$Z_{cc} = 0.0645 + j 0.0278$	$Z_{ca} = 0.0215 + j 0.0093$
7 (3- ϕ)	$Z_{aa} = 0.0451 + j 0.0194$	$Z_{ab} = 0.015 + j 0.0065$
	$Z_{bb} = 0.0451 + j 0.0194$	$Z_{bc} = 0.015 + j 0.0065$
	$Z_{cc} = 0.0451 + j 0.0194$	$Z_{ca} = 0.015 + j 0.0065$
8 (3- ϕ)	$Z_{aa} = 0.0258 + j 0.0111$	$Z_{ab} = 0.0086 + j 0.0037$
	$Z_{bb} = 0.0258 + j 0.0111$	$Z_{bc} = 0.0086 + j 0.0037$
	$Z_{cc} = 0.0258 + j 0.0111$	$Z_{ca} = 0.0086 + j 0.0037$
9(3- ϕ)	$Z_{aa} = 0.0516 + j 0.0222$	$Z_{ab} = 0.0172 + j 0.0074$
	$Z_{bb} = 0.0516 + j 0.0222$	$Z_{bc} = 0.0172 + j 0.0074$
	$Z_{cc} = 0.0516 + j 0.0222$	$Z_{ca} = 0.0172 + j 0.0074$

Appendix E

Table E.1. Individual load demand of each bus obtained with Case *B* Multi-objective optimization
for 19-bus system

SB	RB	BN	LC	BL (km)	Complex load demand obtained with Case <i>B</i> multi-objective optimization			Optimal conductor type
					Phase A	Phase B	Phase C	
1	2	1	1	3.0	8.73+j4.21	8.68+j4.09	8.58+j4.24	3
2	3	2	1	5.0	8.66+j 3.48	8.65+j 4.34	8.61+j4.75	2
3	4	3	1	1.5	5.41+j 2.57	5.40+j2.67	5.39+ j2.61	3
4	5	4	1	1.5	5.40+j 2.42	5.40+j2.73	5.40+j2.71	3
4	6	5	1	1.0	3.40+j1.63	3.40+j1.64	3.40+j1.69	3
6	7	6	1	2.0	8.66+j4.27	8.64+j4.31	8.62+j3.99	1
6	8	7	1	2.5	5.39+j2.62	5.39+j2.77	5.39+j2.42	3
8	9	8	1	3.0	13.14+j4.81	14.04+j6.96	13.32+j7.79	3
9	10	9	1	5.0	3.40+j1.64	3.40+j1.63	3.40+j1.68	1
10	11	10	1	1.5	8.68+j4.35	8.53+j4.26	8.69+j3.94	2
10	12	11	1	1.5	8.65+j4.84	8.54+j4.11	8.71+j3.62	2
11	13	12	1	5.0	5.40+j2.96	5.40+j2.52	5.40+ j2.42	2
11	14	13	1	1.0	3.40+j1.71	3.40+j1.62	3.40+j1.62	2
12	15	14	1	5.0	5.41+j2.62	5.39+j2.50	5.40+j2.71	2
12	16	15	1	6.0	8.58+j4.04	8.74+j4.01	8.58+j4.52	1
14	17	16	1	3.5	5.39+j2.39	5.40+j2.51	5.41+j2.90	2
14	18	17	1	4.0	5.40+j2.52	5.40+j2.62	5.40+j2.63	1
15	19	18	1	4.0	8.67+j3.70	8.66+j3.58	8.62+j5.26	1

Table E.2. Individual load demand of each bus that obtained with Case B Multi-objective optimization for 25-bus system

S	B	R	B	N	L	BL (feet)	Complex load demand obtained with Case B multi-objective optimization			Optimal conductor type
							Phase A	Phase B	Phase C	
1	2	1	1			1000	0	0	0	1
2	3	2	1			500	39+ j29	40+ j29	41+ j31	1
2	6	3	2			500	40+ j28	41+ j30	39+ j29	1
3	4	4	1			500	52+ j40	55+ j41	53+ j39	1
3	18	5	2			500	40 + j30	40 + j30	40 + j30	2
4	5	6	2			500	40 + j30	40 + j30	40 + j30	1
4	23	7	2			400	54+ j41	53+ j40	53+ j39	1
6	7	8	2			500	0	0	0	2
6	8	9	2			1000	40 + j30	40 + j30	40 + j30	1
7	9	10	2			500	54+ j41	53+ j40	53+ j39	1
7	14	11	2			500	53+ j40	53+ j39	54+ j41	1
7	16	12	2			500	40 + j30	40 + j30	40 + j30	3
9	10	13	2			500	39+ j28	40+ j30	41+ j29	2
10	11	14	2			300	41+ j29	39+ j30	40+ j28	1
11	12	15	3			200	53+ j40	54+ j41	53+ j39	1
11	13	16	3			200	39+ j28	41+ j29	40+ j30	2
14	15	17	2			300	133.3 + j100	133.3 + j100	133.3 + j100	1
14	17	18	3			300	40 + j29	39+ j28	41+ j30	1
18	20	19	2			500	39+ j28	40+ j29	41+ j30	1
18	21	20	3			400	40+ j30	39+ j28	41+ j29	3
20	19	21	3			400	54+ j41	53+ j39	53+ j40	1
21	22	22	3			400	52+ j39	55 + j41	53+ j40	1
23	24	23	2			400	39+ j28	41 + j29	40+ j30	1
24	25	24	3			400	55+ j36	52+ j37	53+ j37	1

Table E.3. Individual load demand of each bus that obtained with Case B Multi-objective optimization for Indian 19-bus system

SB	RB	BN	LC	BL (km)	Complex load demand obtained with Case B multi-objective optimization			Optimal conductor type
					Phase A	Phase B	Phase C	
1	2	1	1	3.0	$27.87 + j14.28$	$28.25 + j13.19$	$30.37 + j14.32$	4
2	3	2	2	4.0	$29.68 + j14.92$	$28.54 + j14.29$	$28.16 + j12.68$	4
2	4	3	3	1.5	$18.05 + j9.40$	$18.13 + j8.48$	$17.81 + j8.31$	5
4	5	4	4	1.5	$17.98 + j8.90$	$18.09 + j8.36$	$17.91 + j8.93$	5
4	6	5	5	1.0	$11.32 + j5.52$	$11.34 + j5.46$	$11.33 + j5.51$	5
6	7	6	5	2.0	$28.73 + j14.30$	$29.26 + j15.01$	$28.40 + j12.57$	5
6	8	7	2	2.5	$18.05 + j8.39$	$17.76 + j8.44$	$18.08 + j9.26$	5
8	9	8	1	3.0	$47.41 + j17.44$	$44.39 + j26.70$	$43.19 + j21.25$	8
9	10	9	6	5.0	$11.28 + j5.41$	$11.28 + j5.52$	$11.33 + j5.56$	3
10	11	10	3	1.5	$29.90 + j15.25$	$28.82 + j12.69$	$27.57 + j13.84$	5
10	12	11	3	1.5	$27.80 + j12.62$	$29.02 + j14.21$	$29.56 + j15.06$	2
11	13	12	2	5.0	$17.90 + j8.76$	$18.12 + j8.89$	$17.96 + j8.53$	5
11	14	13	5	1.0	$11.35 + j5.48$	$11.36 + j5.47$	$11.37 + j5.53$	6
12	15	14	6	5.0	$18.10 + j8.36$	$17.80 + j9.08$	$18.08 + j8.65$	2
12	16	15	1	6.0	$28.70 + j15.85$	$29.03 + j12.85$	$28.66 + j13.19$	5
14	17	16	7	3.5	$18.17 + j8.35$	$17.97 + j8.47$	$17.85 + j9.27$	2
14	18	17	8	4.0	$17.98 + j9.10$	$17.99 + j8.45$	$18.02 + j8.54$	5
15	19	18	9	4.0	$28.57 + j14.60$	$29.59 + j12.92$	$28.32 + j14.26$	8

Table E.4. Individual load demand of each bus that obtained with *Case B* Multi-objective optimization for 34-bus system

SB	RB	BN	LC	BL (mile)	Complex load demand obtained with <i>Case B</i> multi-objective optimization			Optimal conductor type
					Phase A	Phase B	Phase C	
1	2	1	1	0.4895	$46.57 + j24.6$	$46.77 + j24.4$	$46.67 + j24.3$	1
2	3	2	1	0.3277	$46.67 + j24.40$	$46.57 + j24.60$	$46.67 + j24.50$	1
3	4	3	1	1.1334	$73.23 + j38.52$	$73.13 + j38.72$	$73.33 + j38.32$	1
4	5	4	2	1.1063	$100.1 + j52.57$	$100.0 + j52.47$	$100.0 + j52.87$	1
4	6	5	1	0.2672	$70.0 + j36.87$	$69.0 + j35.87$	$71.0 + j37.87$	2
6	7	6	1	0.9955	$50.0 + j26.23$	$51.0 + j26.43$	$49.0 + j26.33$	1
7	8	7	1	0.341	$50.0 + j26.33$	$50.0 + j25.33$	$50.0 + j27.33$	1
8	9	8	1	0.0587	$100.0 + j52.67$	$101.0 + j53.67$	$99.0 + j51.67$	1
9	10	9	2	0.3238	$150.0 + j79.01$	$150.0 + j79.01$	$150.0 + j79.01$	1
10	11	10	2	2.9062	$151.0 + j79.01$	$149.0 + j78.01$	$150.0 + j77.01$	1
11	12	11	2	1.9818	$301.0 + j158.03$	$299.0 + j157.03$	$300.0 + j159.03$	1
9	13	12	1	0.6911	$50.0 + j25.33$	$50.0 + j27.33$	$50.0 + j26.33$	1
13	14	13	2	0.5740	$91.0 + j47.31$	$90.0 + j47.51$	$89.0 + j47.41$	2
13	15	14	1	0.1591	$86.67 + j45.65$	$86.57 + j45.55$	$86.77 + j45.75$	1
15	16	15	1	1.2430	$83.32 + j43.89$	$82.34 + j43.89$	$84.33 + j43.89$	1
16	17	16	1	0.72	$83.33 + j43.89$	$83.32 + j43.89$	$83.34 + j43.89$	1
17	18	17	2	1.3120	$100.0 + j52.57$	$100.0 + j52.77$	$100.0 + j52.67$	2
17	19	18	1	0.143	$50.0 + j26.23$	$51.0 + j26.43$	$49.0 + j26.33$	1
19	20	19	1	0.7162	$76.67 + j40.38$	$76.57 + j40.38$	$76.77 + j40.38$	1
20	21	20	1	0.7257	$140.0 + j73.74$	$140.0 + j72.74$	$140.0 + j74.74$	2
21	22	21	2	2.0004	$180.0 + j94.82$	$181.0 + j94.82$	$179.0 + j94.82$	1
20	23	22	2	0.3067	$40.0 + j21.07$	$40.0 + j21.07$	$80.0 + j42.14$	1
23	24	23	1	0.3069	$100.0 + j52.67$	$100.0 + j52.77$	$100.0 + j52.57$	1
23	25	24	2	1.1044	$33.33 + j17.55$	$33.32 + j17.56$	$33.34 + j17.54$	1
25	26	25	1	0.053	$40.0 + j21.07$	$40.0 + j21.07$	$90.0 + j47.41$	1
26	27	26	2	0.8773	$283.3 + j149.25$	$284.3 + j149.26$	$282.3 + j149.24$	2
27	28	27	2	0.6896	$43.33 + j22.82$	$43.23 + j22.72$	$43.43 + j22.92$	1
28	29	28	2	0.7219	$20.0 + j10.53$	$20.0 + j10.63$	$20.0 + j10.43$	1
25	30	29	1	0.1030	$53.23 + j28.08$	$53.43 + j28.10$	$53.33 + j28.09$	1
30	31	30	1	0.6215	$46.67 + j24.4$	$46.68 + j24.6$	$46.65 + j24.5$	2
31	32	31	2	0.1629	$129.0 + j68.48$	$131.0 + j68.38$	$130.0 + j68.58$	2
31	33	32	2	0.053	$59.0 + j31.6$	$61.0 + j31.6$	$60.0 + j31.6$	1
33	34	33	2	0.9206	$61.0 + j31.5$	$60.0 + j31.4$	$59.0 + j31.6$	3

Appendix F

Table F.1. Individual load demand of each bus that obtained with *Case C* Multi-objective optimization for 19-bus system

SB	RB	BN	LC	BL (km)	Complex load demand obtained with <i>Case B</i> multi-objective optimization			Optimal conductor type
					Phase A	Phase B	Phase C	
1	2	1	1	3.0	8.72+j4.20	8.69+j4.09	8.58+j4.23	2
2	3	2	1	5.0	8.68+j 3.43	8.63+j 4.35	8.61+j4.78	2
3	4	3	1	1.5	5.42+j 2.57	5.39+j2.68	5.39+ j2.60	3
4	5	4	1	1.5	5.38+j 2.41	5.41+j2.73	5.41+j2.72	3
4	6	5	1	1.0	3.40+j1.63	3.40+j1.64	3.40+j1.69	3
6	7	6	1	2.0	8.65+j4.25	8.64+j4.33	8.63+j3.99	1
6	8	7	1	2.5	5.39+j2.60	5.39+j2.75	5.39+j2.42	3
8	9	8	1	3.0	13.10+j4.71	14.00+j6.96	13.32+j7.89	3
9	10	9	1	5.0	3.40+j1.66	3.40+j1.63	3.40+j1.66	1
10	11	10	1	1.5	8.66+j4.35	8.55+j4.26	8.69+j3.94	2
10	12	11	1	1.5	8.65+j4.74	8.57+j4.11	8.68+j3.72	3
11	13	12	1	5.0	5.40+j2.96	5.40+j2.52	5.40+ j2.42	2
11	14	13	1	1.0	3.40+j1.71	3.40+j1.62	3.40+j1.62	2
12	15	14	1	5.0	5.41+j2.62	5.39+j2.50	5.40+j2.71	2
12	16	15	1	6.0	8.58+j4.04	8.74+j4.01	8.58+j4.52	2
14	17	16	1	3.5	5.39+j2.39	5.40+j2.51	5.41+j2.90	2
14	18	17	1	4.0	5.40+j2.52	5.40+j2.62	5.40+j2.63	3
15	19	18	1	4.0	8.67+j3.70	8.66+j3.58	8.62+j5.26	1

Table F.2. Individual load demand of each bus that obtained with Case C Multi-objective optimization for 25-bus system

SB	RB	BN	LC	BL (feet)	Complex load demand obtained with Case B multi-objective optimization			Optimal conductor type
					Phase A	Phase B	Phase C	
1	2	1	1	1000	0	0	0	1
2	3	2	1	500	40+ j30	39+ j29	41+ j29	2
2	6	3	2	500	39+ j29	41+ j30	40+ j30	1
3	4	4	1	500	53+ j39	54+ j41	53+ j40	1
3	18	5	2	500	40 + j30	40 + j30	40 + j30	1
4	5	6	2	500	40 + j30	40 + j30	40 + j30	1
4	23	7	2	400	53+ j41	53+ j41	54+ j38	1
6	7	8	2	500	0	0	0	2
6	8	9	2	1000	40 + j30	40 + j30	40 + j30	1
7	9	10	2	500	54+ j40	53+ j41	53+ j39	1
7	14	11	2	500	53+ j41	54+ j39	53+ j40	1
7	16	12	2	500	40 + j30	40 + j30	40 + j30	2
9	10	13	2	500	39+ j29	41+ j30	40+ j30	1
10	11	14	2	300	41+ j29	39+ j30	40+ j28	1
11	12	15	3	200	53+ j40	54+ j40	53+ j40	3
11	13	16	3	200	39+ j29	40+ j30	41+ j30	1
14	15	17	2	300	133.3 + j100	133.3 + j100	133.3 + j100	1
14	17	18	3	300	40 + j29	39+ j28	41+ j30	1
18	20	19	2	500	39+ j28	40+ j29	41+ j30	1
18	21	20	3	400	40+ j30	39+ j28	41+ j29	3
20	19	21	3	400	54+ j41	53+ j39	53+ j40	1
21	22	22	3	400	52+ j39	55 + j41	53+ j40	1
23	24	23	2	400	39+ j29	40 + j30	41+ j30	1
24	25	24	3	400	55+ j36	52+ j37	53+ j37	1

Table F.3. Individual load demand of each bus that obtained with Case C Multi-objective optimization for Indian 19-bus system

S	B	R	B	N	L	C	BL (km)	Complex load demand obtained with Case B multi-objective optimization			Optimal conductor type
								Phase A	Phase B	Phase C	
1	2	1	1				3.0	27.85 +j14.26	28.27 +j13.20	30.37+j14.33	5
2	3	2	2				4.0	29.66 +j14.90	28.55+j14.30	28.17 +j12.69	4
2	4	3	3				1.5	18.07 + j9.42	18.12 + j8.47	17.80 + j8.30	4
4	5	4	4				1.5	17.95 + j8.90	18.11 + j8.36	17.92 + j8.93	4
4	6	5	5				1.0	11.33+ j5.53	11.35+ j5.45	11.31 + j5.51	3
6	7	6	5				2.0	28.73 + j14.30	29.26+ j15.01	28.40 + j12.57	8
6	8	7	2				2.5	18.07+ j8.39	17.75+ j8.44	18.07+ j9.26	2
8	9	8	1				3.0	47.40 + j17.42	44.39 + j26.72	43.20 + j21.25	6
9	10	9	6				5.0	11.28 + j5.40	11.28 + j5.52	11.33+ j5.55	5
10	11	10	3				1.5	29.90 + j15.25	28.82 + j12.69	27.57 + j13.84	5
10	12	11	3				1.5	27.80 + j12.62	29.02 + j14.21	29.56 + j15.06	1
11	13	12	2				5.0	17.90 +j 8.76	18.12 + j8.89	17.96 + j8.53	5
11	14	13	5				1.0	11.35 + j5.48	11.36+ j5.47	11.37 + j5.53	3
12	15	14	6				5.0	18.10 + j8.36	17.80 + j9.08	18.08 + j8.65	2
12	16	15	1				6.0	28.72 + j15.85	29.03 +j12.85	28.64 + j13.19	5
14	17	16	7				3.5	18.17 + j8.32	17.97 + j8.49	17.85 +j 9.28	5
14	18	17	8				4.0	17.98 + j9.07	17.99 + j8.48	18.02 + j8.54	4
15	19	18	9				4.0	28.57 + j14.60	29.57 + j12.92	28.34 + j14.26	2

Table F.4. Individual load demand of each bus that obtained with Case C Multi-objective optimization for 34-bus system

SB	RB	BN	LC	BL (mile)	Complex load demand obtained with Case B multi-objective optimization			Optimal conductor type
					Phase A	Phase B	Phase C	
1	2	1	1	0.4895	46.59 + j24.5	46.76 + j24.4	46.66 + j24.4	1
2	3	2	1	0.3277	46.69 + j24.40	46.56 + j24.60	46.66 + j24.50	1
3	4	3	1	1.1334	73.23+ j38.58	73.12+ j38.68	73.34+ j38.34	1
4	5	4	2	1.1063	100.1 + j52.67	100.0 + j52.67	100.0 + j52.67	1
4	6	5	1	0.2672	70.0+ j36.85	69.0+ j35.88	71.0+ j37.88	2
6	7	6	1	0.9955	50.0 + j26.33	51.0 + j26.33	49.0 + j26.33	1
7	8	7	1	0.341	50.0 + j27.33	50.0 + j25.33	50.0 + j25.33	1
8	9	8	1	0.0587	100.0 + j52.67	101.0 + j53.67	99.0 + j51.67	1
9	10	9	2	0.3238	150.0 + j79.01	150.0 + j79.01	150.0 + j79.01	1
10	11	10	2	2.9062	150.0 + j78.01	149.0 + j79.01	149.0 + j77.01	1
11	12	11	2	1.9818	301.0+ j158.03	299.0+ j157.03	300.0+ j159.03	1
9	13	12	1	0.6911	50.0 + j25.33	50.0 + j27.33	50.0 + j26.33	1
13	14	13	2	0.5740	91.0 + j47.31	90.0 + j47.51	89.0 + j47.41	2
13	15	14	1	0.1591	86.67 + j45.65	86.57 + j45.55	86.77 + j45.75	1
15	16	15	1	1.2430	83.32 + j43.89	82.34 + j43.89	84.33 + j43.89	1
16	17	16	1	0.72	83.33 + j43.89	83.32 + j43.89	83.34 + j43.89	1
17	18	17	2	1.3120	100.0 + j52.57	100.0 + j52.77	100.0 + j52.67	2
17	19	18	1	0.143	50.0 + j26.23	51.0 + j26.43	49.0 + j26.33	1
19	20	19	1	0.7162	76.67 + j40.38	76.57 + j40.38	76.77 + j40.38	1
20	21	20	1	0.7257	140.0+ j73.74	140.0+ j72.74	140.0+ j74.74	2
21	22	21	2	2.0004	180.0 + j94.82	181.0 + j94.82	179.0 + j94.82	1
20	23	22	2	0.3067	40.0 + j21.07	40.0 + j21.07	80.0 + j42.14	1
23	24	23	1	0.3069	100.0+ j52.67	100.0+ j52.77	100.0+ j52.57	1
23	25	24	2	1.1044	33.33 + j17.55	33.32 + j17.56	33.34 + j17.54	1
25	26	25	1	0.053	40.0+ j21.07	40.0+ j21.07	90.0 + j 47.41	1
26	27	26	2	0.8773	283.33 + j149.25	284.33 + j149.26	282.33 + j149.24	2
27	28	27	2	0.6896	43.33 + j22.82	43.23 + j22.72	43.43 + j22.92	1
28	29	28	2	0.7219	20.0 + j10.53	20.0 + j10.63	20.0 + j10.43	1
25	30	29	1	0.1030	53.23 + j28.08	53.43 + j28.10	53.33 + j28.09	1
30	31	30	1	0.6215	46.67 + j24.4	46.68 + 24.6	46.65 + j24.5	1
31	32	31	2	0.1629	129.0+ j68.48	131.0+ j68.38	130.0+ j68.58	2
31	33	32	2	0.053	59.0+ j31.6	61.0+ j31.6	60.0+ j31.6	1
33	34	33	2	0.9206	61.0 + j31.5	60.0 + j31.4	59.0 + j31.6	1

Appendix G

Table G.1. Individual load demand of each bus that obtained with Case C Multi-objective optimization for 19-bus system

S	B	R	B	N	L	C	BL (km)	Complex load demand obtained with <i>Case B</i> multi-objective optimization			Optimal conductor type
								Phase A	Phase B	Phase C	
1	2	1	1				3.0	8.68+j4.18	8.71+j4.11	8.60+j4.23	3
2	3	2	1				5.0	8.65+j 3.43	8.63+j 4.35	8.64+j4.78	2
3	4	3	1				1.5	5.41+j 2.59	5.40+j2.66	5.39+ j2.60	3
4	5	4	1				1.5	5.38+j 2.41	5.41+j2.73	5.41+j2.72	3
4	6	5	1				1.0	3.40+j1.65	3.40+j1.64	3.40+j1.67	3
6	7	6	1				2.0	8.63+j4.23	8.62+j4.33	8.62+j4.01	1
6	8	7	1				2.5	5.39+j2.60	5.39+j2.75	5.39+j2.42	3
8	9	8	1				3.0	13.10+j4.71	14.00+j6.96	13.32+j7.89	3
9	10	9	1				5.0	3.40+j1.66	3.40+j1.63	3.40+j1.66	1
10	11	10	1				1.5	8.66+j4.35	8.55+j4.26	8.69+j3.94	2
10	12	11	1				1.5	8.65+j4.74	8.57+j4.11	8.68+j3.72	3
11	13	12	1				5.0	5.40+j2.96	5.40+j2.52	5.40+ j2.42	2
11	14	13	1				1.0	3.40+j1.71	3.40+j1.62	3.40+j1.62	2
12	15	14	1				5.0	5.41+j2.62	5.39+j2.50	5.40+j2.71	2
12	16	15	1				6.0	8.58+j4.04	8.74+j4.01	8.58+j4.52	1
14	17	16	1				3.5	5.39+j2.39	5.40+j2.51	5.41+j2.90	2
14	18	17	1				4.0	5.40+j2.52	5.40+j2.62	5.40+j2.63	3
15	19	18	1				4.0	8.67+j3.70	8.66+j3.58	8.62+j5.26	2

Table G.2. Individual load demand of each bus that obtained with Case C Multi-objective optimization for 25-bus system

SB	RB	BN	LC	BL (feet)	Complex load demand obtained with <i>Case B</i> multi-objective optimization			Optimal conductor type
					Phase A	Phase B	Phase C	
1	2	1	1	1000	0	0	0	1
2	3	2	1	500	39+ j29	40+ j29	41+ j30	2
2	6	3	2	500	40+ j29	41+ j30	39+ j30	1
3	4	4	1	500	52+ j40	54+ j40	54+ j40	1
3	18	5	2	500	40 + j30	40 + j30	40 + j30	1
4	5	6	2	500	40 + j30	40 + j30	40 + j30	1
4	23	7	2	400	52+ j40	54+ j41	54+ j39	1
6	7	8	2	500	0	0	0	2
6	8	9	2	1000	40 + j30	40 + j30	40 + j30	1
7	9	10	2	500	54+ j40	53+ j41	53+ j39	1
7	14	11	2	500	53+ j41	54+ j39	53+ j40	1
7	16	12	2	500	40 + j30	40 + j30	40 + j30	2
9	10	13	2	500	39+ j29	41+ j30	40+ j30	1
10	11	14	2	300	41+ j29	39+ j30	40+ j28	1
11	12	15	3	200	53+ j40	54+ j40	53+ j40	3
11	13	16	3	200	39+ j29	40+ j30	41+ j30	1
14	15	17	2	300	133.3 + j100	133.3 + j100	133.3 + j100	1
14	17	18	3	300	40 + j29	39+ j28	41+ j30	1
18	20	19	2	500	39+ j28	40+ j29	41+ j30	1
18	21	20	3	400	40+ j30	39+ j28	41+ j29	3
20	19	21	3	400	54+ j41	53+ j39	53+ j40	1
21	22	22	3	400	52+ j39	55 + j41	53+ j40	1
23	24	23	2	400	39+ j29	40 + j30	41+ j30	1
24	25	24	3	400	55+ j36	52+ j37	53+ j37	1

Table G.3. Individual load demand of each bus that obtained with Case C Multi-objective optimization for Indian 19-bus system

SB	RB	BN	LC	BL (km)	Complex load demand obtained with Case B multi-objective optimization			Optimal conductor type
					Phase A	Phase B	Phase C	
1	2	1	1	3.0	27.82 +j14.36	28.30 +j13.20	30.37+j14.23	4
2	3	2	2	4.0	29.66 +j14.90	28.55+j14.30	28.17 +j12.69	4
2	4	3	3	1.5	18.08 + j9.42	18.11 + j8.47	17.80 + j8.30	3
4	5	4	4	1.5	17.95 + j8.90	18.11 + j8.36	17.92 + j8.93	4
4	6	5	5	1.0	11.35+ j5.53	11.33+ j5.45	11.31+ j5.5120	5
6	7	6	5	2.0	28.73 +j14.30	29.26+ j15.01	28.40 + j12.57	8
6	8	7	2	2.5	18.07+ j8.39	17.75+ j8.44	18.07+ j9.26	2
8	9	8	1	3.0	47.41 + j17.42	44.39 + j26.72	43.19 + j21.25	6
9	10	9	6	5.0	11.28 + j5.40	11.28 + j5.52	11.33+ j5.55	5
10	11	10	3	1.5	29.90 + j15.25	28.82 + j12.69	27.57 + j13.84	5
10	12	11	3	1.5	27.80 + j12.62	29.02 + j14.21	29.56 + j15.06	1
11	13	12	2	5.0	17.90 + j8.76	18.12 + j8.89	17.96 + j8.53	5
11	14	13	5	1.0	11.35 + j5.48	11.36+ j5.47	11.37 + j5.53	6
12	15	14	6	5.0	18.10 + j8.36	17.80 + j9.08	18.08 + j8.65	2
12	16	15	1	6.0	28.72 + j15.85	29.03 + j12.85	28.64 + j13.19	5
14	17	16	7	3.5	18.17 + j8.32	17.97 + j8.49	17.85 + j9.28	8
14	18	17	8	4.0	17.98 + j9.07	17.99 + j8.48	18.02 + j8.54	4
15	19	18	9	4.0	28.57 + j14.60	29.57 + j12.92	28.34 + j14.26	2

Table G.4. Individual load demand of each bus that obtained with Case C Multi-objective optimization for 34-bus system

S	B	R	B	N	L	BL (mile)	Complex load demand obtained with Case B multi-objective optimization			Optimal conductor type
							Phase A	Phase B	Phase C	
1	2	1	1			0.4895	46.69 + j24.4	46.76 + j24.4	46.56 + j24.5	2
2	3	2	1			0.3277	46.69 + j24.40	46.56 + j24.60	46.66 + j24.50	1
3	4	3	1			1.1334	73.23+ j38.58	73.12+ j38.68	73.34+ j38.34	1
4	5	4	2			1.1063	100.1 + j52.67	100.0 + j52.67	100.0 + j52.67	1
4	6	5	1			0.2672	70.0+ j36.85	69.0+ j35.88	71.0+ j37.88	1
6	7	6	1			0.9955	50.0 + j26.33	51.0 + j26.33	49.0 + j26.33	1
7	8	7	1			0.341	50.0 + j27.33	50.0 + j25.33	50.0 + j25.33	1
8	9	8	1			0.0587	100.0 + j52.67	101.0 + j53.67	99.0 + j51.67	1
9	10	9	2			0.3238	150.0 + j79.01	150.0 + j79.01	150.0 + j79.01	2
10	11	10	2			2.9062	150.0 + j78.01	149.0 + j79.01	149.0 + j77.01	1
11	12	11	2			1.9818	301.0+ j158.03	299.0+ j157.03	300.0+ j159.03	1
9	13	12	1			0.6911	50.0 + j25.33	50.0 + j27.33	50.0 + j26.33	1
13	14	13	2			0.5740	91.0 + j47.31	90.0 + j47.51	89.0 + j47.41	1
13	15	14	1			0.1591	86.67 + j45.65	86.57 + j45.55	86.77 + j45.75	1
15	16	15	1			1.2430	83.32 + j43.89	82.34 + j43.89	84.33 + j43.89	1
16	17	16	1			0.72	83.33 + j43.89	83.32 + j43.89	83.34 + j43.89	1
17	18	17	2			1.3120	100.0 + j52.57	100.0 + j52.77	100.0 + j52.67	2
17	19	18	1			0.143	50.0 + j26.23	51.0 + j26.43	49.0 + j26.33	1
19	20	19	1			0.7162	76.67 + j40.38	76.57 + j40.38	76.77 + j40.38	1
20	21	20	1			0.7257	140.0+ j73.74	140.0+ j72.74	140.0+ j74.74	2
21	22	21	2			2.0004	180.0 + j94.82	181.0 + j94.82	179.0 + j94.82	1
20	23	22	2			0.3067	40.0 + j21.07	40.0 + j21.07	80.0 + j42.14	1
23	24	23	1			0.3069	100.0+ j52.67	100.0+ j52.77	100.0+ j52.57	1
23	25	24	2			1.1044	33.33 + j17.55	33.32 + j17.56	33.34 + j17.54	1
25	26	25	1			0.053	40.0+ j21.07	40.0+ j21.07	90.0 + j47.41	1
26	27	26	2			0.8773	283.33 + j149.25	284.33 + j149.26	282.33 + j149.24	2
27	28	27	2			0.6896	43.33 + j22.82	43.23 + j22.72	43.43 + j22.92	1
28	29	28	2			0.7219	20.0 + j10.53	20.0 + j10.63	20.0 + j10.43	1
25	30	29	1			0.1030	53.23 + j28.08	53.43 + j28.10	53.33 + j28.09	1
30	31	30	1			0.6215	46.67 + j24.4	46.68 + j24.6	46.65 + j24.5	1
31	32	31	2			0.1629	129.0+ j68.48	131.0+ j68.38	130.0+ j68.58	2
31	33	32	2			0.053	60.0+ j31.6	60.0+ j31.6	60.0+ j31.6	1
33	34	33	2			0.9206	60.0 + j31.5	60.0 + j31.4	60.0 + j31.6	1

Appendix H

Table H.1. Individual load demand of each bus that obtained with Case C Multi-objective optimization for 19-bus system

S	B	R	B	N	L	C	BL (km)	Complex load demand obtained with Case C multi-objective optimization			Optimal conductor type
								Phase A	Phase B	Phase C	
1	2	1	1				3.0	8.67+j4.16	8.70+j4.13	8.59+j4.23	2
2	3	2	1				5.0	8.64+j 3.45	8.64+j 4.35	8.64+j4.76	2
3	4	3	1				1.5	5.40+j 2.61	5.40+j2.64	5.40+ j2.60	2
4	5	4	1				1.5	5.39+j 2.46	5.40+j2.68	5.41+j2.72	3
4	6	5	1				1.0	3.39+j1.66	3.40+j1.64	3.41+j1.66	1
6	7	6	1				2.0	8.63+j4.23	8.62+j4.33	8.62+j4.01	1
6	8	7	1				2.5	5.39+j2.65	5.39+j2.70	5.39+j2.42	3
8	9	8	1				3.0	13.10+j4.69	14.00+j6.98	13.32+j7.89	3
9	10	9	1				5.0	3.39+j1.66	3.40+j1.64	3.41+j1.65	3
10	11	10	1				1.5	8.64+j4.35	8.57+j4.26	8.69+j3.94	2
10	12	11	1				1.5	8.62+j4.74	8.60+j4.11	8.68+j3.72	3
11	13	12	1				5.0	5.40+j2.94	5.40+j2.52	5.40+ j2.44	2
11	14	13	1				1.0	3.40+j1.67	3.40+j1.64	3.40+j1.64	3
12	15	14	1				5.0	5.41+j2.62	5.39+j2.50	5.40+j2.71	3
12	16	15	1				6.0	8.58+j4.04	8.74+j4.01	8.58+j4.52	1
14	17	16	1				3.5	5.39+j2.39	5.40+j2.51	5.41+j2.90	2
14	18	17	1				4.0	5.40+j2.52	5.40+j2.62	5.40+j2.63	3
15	19	18	1				4.0	8.67+j3.70	8.66+j3.58	8.62+j5.26	2

Table H.2. Individual load demand of each bus that obtained with Case C Multi-objective optimization for 25-bus system

S	B	R	B	N	L	C	BL (feet)	Complex load demand obtained with Case C multi-objective optimization			Optimal conductor type
								Phase A	Phase B	Phase C	
1	2	1	1				1000	0	0	0	1
2	3	2	1				500	40+ j30	39+ j29	41+ j29	1
2	6	3	2				500	40+ j30	41+ j30	39+ j29	1
3	4	4	1				500	53+ j40	54+ j40	53+ j40	1
3	18	5	2				500	40 + j30	40 + j30	40 + j30	2
4	5	6	2				500	40 + j30	40 + j30	40 + j30	1
4	23	7	2				400	53+ j39	53+ j41	54+ j40	1
6	7	8	2				500	0	0	0	1
6	8	9	2				1000	40 + j30	40 + j30	40 + j30	1
7	9	10	2				500	54+ j40	53+ j40	53+ j40	1
7	14	11	2				500	53+ j41	54+ j40	53+ j39	3
7	16	12	2				500	40 + j30	40 + j30	40 + j30	2
9	10	13	2				500	40+ j29	41+ j30	39+ j30	1
10	11	14	2				300	41+ j29	39+ j30	40+ j28	1
11	12	15	3				200	53+ j40	54+ j40	53+ j40	2
11	13	16	3				200	39+ j29	40+ j30	41+ j30	1
14	15	17	2				300	133.3 + j100	133.3 + j100	133.3 + j100	1
14	17	18	3				300	40 + j29	39+ j28	41+ j30	2
18	20	19	2				500	39+ j28	40+ j28	41+ j31	1
18	21	20	3				400	40+ j29	39+ j29	41+ j29	1
20	19	21	3				400	53+ j41	54+ j39	53+ j40	1
21	22	22	3				400	52+ j40	55 + j41	53+ j39	1
23	24	23	2				400	39+ j29	39+ j30	40+ j30	1
24	25	24	3				400	54+ j36	53+ j37	53+ j37	3

Table H.3. Individual load demand of each bus that obtained with Case C Multi-objective optimization for Indian 19-bus system

SB	RB	BN	LC	BL (km)	Complex load demand obtained with Case C multi-objective optimization			Optimal conductor type
					Phase A	Phase B	Phase C	
1	2	1	1	3.0	$27.81 + j14.34$	$28.31 + j13.21$	$30.37 + j14.24$	3
2	3	2	2	4.0	$29.67 + j14.92$	$28.53 + j14.29$	$28.19 + j12.68$	4
2	4	3	3	1.5	$18.07 + j9.40$	$18.11 + j8.48$	$17.79 + j8.31$	3
4	5	4	4	1.5	$17.95 + j8.91$	$18.11 + j8.35$	$17.92 + j8.93$	4
4	6	5	5	1.0	$11.36 + j5.53$	$11.32 + j5.48$	$11.32 + j5.48$	4
6	7	6	5	2.0	$28.72 + j14.30$	$29.26 + j15.01$	$28.39 + j12.57$	4
6	8	7	2	2.5	$18.05 + j8.39$	$17.78 + j8.44$	$18.06 + j9.26$	8
8	9	8	1	3.0	$47.40 + j17.43$	$44.39 + j26.72$	$43.20 + j21.24$	6
9	10	9	6	5.0	$11.30 + j5.45$	$11.29 + j5.50$	$11.30 + j5.52$	5
10	11	10	3	1.5	$29.88 + j15.24$	$28.82 + j12.69$	$27.59 + j13.85$	2
10	12	11	3	1.5	$27.82 + j12.62$	$29.02 + j14.21$	$29.54 + j15.06$	5
11	13	12	2	5.0	$17.88 + j8.76$	$18.12 + j8.89$	$17.96 + j8.53$	5
11	14	13	5	1.0	$11.34 + j5.48$	$11.37 + j5.49$	$11.37 + j5.51$	6
12	15	14	6	5.0	$18.09 + j8.33$	$17.81 + j9.08$	$18.08 + j8.68$	1
12	16	15	1	6.0	$28.71 + j15.85$	$29.03 + j12.85$	$28.65 + j13.19$	5
14	17	16	7	3.5	$18.17 + j8.31$	$17.97 + j8.50$	$17.85 + j9.28$	5
14	18	17	8	4.0	$17.96 + j9.07$	$17.99 + j8.48$	$18.04 + j8.54$	3
15	19	18	9	4.0	$28.55 + j14.60$	$29.57 + j12.92$	$28.36 + j14.26$	2

Table H.4. Individual load demand of each bus that obtained with Case C Multi-objective optimization for 34-bus system

SB	RB	BN	LC	BL (mile)	Complex load demand obtained with Case C multi-objective optimization			Optimal conductor type
					Phase A	Phase B	Phase C	
1	2	1	1	0.4895	46.66 + j24.4	46.76 + j24.4	46.59 + j24.5	2
2	3	2	1	0.3277	46.65 + j24.40	46.60 + j24.60	46.66 + j24.50	1
3	4	3	1	1.1334	73.27+ j38.58	73.10+ j38.68	73.32+ j38.34	1
4	5	4	2	1.1063	100.1 + j52.67	100.0 + j52.67	100.0 + j52.67	1
4	6	5	1	0.2672	71.0+ j36.85	69.0+ j35.88	70.0+ j37.88	2
6	7	6	1	0.9955	51.0 + j26.32	50.0 + j26.34	49.0 + j26.33	1
7	8	7	1	0.341	49.0 + j27.33	51.0 + j25.33	50.0 + j25.33	1
8	9	8	1	0.0587	100.0 + j52.67	100.0 + j53.67	100.0 + j51.67	1
9	10	9	2	0.3238	151.0 + j79.01	149.0 + j79.01	150.0 + j79.01	2
10	11	10	2	2.9062	150.0 + j78.01	149.0 + j79.01	149.0 + j77.01	1
11	12	11	2	1.9818	301.0+ j158.03	299.0+ j157.03	300.0+ j159.03	1
9	13	12	1	0.6911	50.0 + j25.33	50.0 + j27.33	50.0 + j26.33	1
13	14	13	2	0.5740	90.0 + j47.31	90.0 + j47.51	90.0 + j47.41	1
13	15	14	1	0.1591	86.68 + j45.65	86.57 + j45.55	86.76 + j45.75	1
15	16	15	1	1.2430	83.33 + j43.89	82.33 + j43.89	84.33 + j43.89	1
16	17	16	1	0.72	83.33 + j43.89	83.32 + j43.89	83.34 + j43.89	1
17	18	17	2	1.3120	100.0 + j52.60	100.0 + j52.74	100.0 + j52.67	1
17	19	18	1	0.143	50.0 + j26.23	51.0 + j26.43	49.0 + j26.33	1
19	20	19	1	0.7162	76.64 + j40.38	76.60 + j40.38	76.77 + j40.38	1
20	21	20	1	0.7257	140.0+ j73.78	140.0+ j72.70	140.0+ j74.74	2
21	22	21	2	2.0004	180.0 + j94.82	180.0 + j94.82	180.0 + j94.82	1
20	23	22	2	0.3067	40.0 + j21.07	40.0 + j21.07	80.0 + j42.14	1
23	24	23	1	0.3069	100.0+ j52.67	100.0+ j52.77	100.0+ j52.57	2
23	25	24	2	1.1044	33.33 + j17.55	33.32 + j17.56	33.34 + j17.54	1
25	26	25	1	0.053	90.0+ j47.41	40.0+ j21.07	40.0 + j47.41	1
26	27	26	2	0.8773	283.33 + j149.25	284.33 + j149.26	282.33 + j149.24	1
27	28	27	2	0.6896	43.31 + j22.84	43.25 + j22.72	43.43 + j22.90	1
28	29	28	2	0.7219	21.0 + j10.53	19.0 + j10.63	20.0 + j10.43	1
25	30	29	1	0.1030	53.25 + j28.08	53.42 + j28.10	53.33 + j28.09	1
30	31	30	1	0.6215	46.69 + j24.4	46.67 + j24.6	46.64 + j24.5	1
31	32	31	2	0.1629	129.0+ j68.48	131.0+ j68.38	130.0+ j68.58	1
31	33	32	2	0.053	59.0+ j31.6	60.0+ j31.6	61.0+ j31.6	1
33	34	33	2	0.9206	60.0 + j31.5	60.0 + j31.4	60.0 + j31.6	1

Appendix I

Table I.1. Individual load demand of each bus that obtained with Case C Multi-objective optimization for 19-bus system

SB	RB	BN	LC	BL (km)	Complex load demand obtained with Case C multi-objective optimization			Optimal conductor type
					Phase A	Phase B	Phase C	
1	2	1	1	3.0	8.65+j4.15	8.71+j4.14	8.63+j4.23	3
2	3	2	1	5.0	8.64+j 3.43	8.65+j 4.38	8.64+j4.75	3
3	4	3	1	1.5	5.40+j 2.59	5.40+j2.64	5.40+ j2.62	3
4	5	4	1	1.5	5.38+j 2.41	5.41+j2.73	5.41+j2.72	2
4	6	5	1	1.0	3.40+j1.65	3.40+j1.66	3.40+j1.65	3
6	7	6	1	2.0	8.63+j4.25	8.62+j4.31	8.62+j4.01	1
6	8	7	1	2.5	5.39+j2.65	5.39+j2.70	5.39+j2.42	3
8	9	8	1	3.0	13.10+j4.71	14.00+j6.96	13.32+j7.89	2
9	10	9	1	5.0	3.40+j1.66	3.40+j1.63	3.40+j1.66	1
10	11	10	1	1.5	8.66+j4.35	8.55+j4.26	8.69+j3.94	3
10	12	11	1	1.5	8.65+j4.74	8.57+j4.11	8.68+j3.72	3
11	13	12	1	5.0	5.40+j2.96	5.40+j2.52	5.40+ j2.42	2
11	14	13	1	1.0	3.40+j1.71	3.40+j1.62	3.40+j1.62	2
12	15	14	1	5.0	5.41+j2.62	5.39+j2.50	5.40+j2.71	2
12	16	15	1	6.0	8.65+j4.04	8.70+j4.01	8.58+j4.52	1
14	17	16	1	3.5	5.39+j2.39	5.40+j2.51	5.41+j2.90	3
14	18	17	1	4.0	5.40+j2.52	5.40+j2.62	5.40+j2.63	3
15	19	18	1	4.0	8.65+j3.70	8.66+j3.58	8.64+j5.26	2

Table I.2. Individual load demand of each bus that obtained with Case C Multi-objective optimization for 25-bus system

SB	RB	BN	LC	BL (feet)	Complex load demand obtained with Case C multi-objective optimization			Optimal conductor type
					Phase A	Phase B	Phase C	
1	2	1	1	1000	0	0	0	2
2	3	2	1	500	40+ j30	40+ j29	40+ j29	1
2	6	3	2	500	41+ j29	40+ j30	39+ j30	1
3	4	4	1	500	53+ j40	54+ j40	53+ j40	1
3	18	5	2	500	40 + j30	40 + j30	40 + j30	2
4	5	6	2	500	40 + j30	40 + j30	40 + j30	1
4	23	7	2	400	53+ j40	54+ j40	53+ j40	2
6	7	8	2	500	0	0	0	1
6	8	9	2	1000	40 + j30	40 + j30	40 + j30	1
7	9	10	2	500	53+ j40	53+ j41	54+ j39	1
7	14	11	2	500	53+ j41	54+ j39	53+ j40	1
7	16	12	2	500	40 + j30	40 + j30	40 + j30	1
9	10	13	2	500	39+ j29	41+ j30	40+ j30	1
10	11	14	2	300	41+ j29	39+ j30	40+ j28	1
11	12	15	3	200	53+ j40	54+ j40	53+ j40	3
11	13	16	3	200	39+ j29	40+ j30	41+ j30	1
14	15	17	2	300	133.3 + j100	133.3 + j100	133.3 + j100	3
14	17	18	3	300	40 + j29	40+ j29	40+ j29	1
18	20	19	2	500	39+ j28	40+ j29	41+ j30	1
18	21	20	3	400	40+ j30	39+ j28	41+ j29	1
20	19	21	3	400	53+ j41	53+ j39	54+ j40	1
21	22	22	3	400	52+ j39	55 + j41	53+ j40	1
23	24	23	2	400	39+ j30	40 + j29	41+ j30	1
24	25	24	3	400	54+ j36	53+ j37	53+ j37	2

Table I.3. Individual load demand of each bus that obtained with Case C Multi-objective optimization for Indian 19-bus system

SB	RB	BN	LC	BL (km)	Complex load demand obtained with Case C multi-objective optimization			Optimal conductor type
					Phase A	Phase B	Phase C	
1	2	1	1	3.0	$27.81 + j14.32$	$28.31 + j13.24$	$30.37 + j14.23$	3
2	3	2	2	4.0	$29.61 + j14.84$	$28.55 + j14.35$	$28.22 + j12.70$	4
2	4	3	3	1.5	$18.08 + j9.42$	$18.11 + j8.47$	$17.80 + j8.30$	4
4	5	4	4	1.5	$17.95 + j8.90$	$18.11 + j8.36$	$17.92 + j8.93$	4
4	6	5	5	1.0	$11.34 + j5.53$	$11.33 + j5.45$	$11.33 + j5.51$	3
6	7	6	5	2.0	$28.72 + j14.30$	$29.26 + j15.01$	$28.39 + j12.57$	5
6	8	7	2	2.5	$18.04 + j8.39$	$17.78 + j8.44$	$18.07 + j9.26$	2
8	9	8	1	3.0	$47.41 + j17.42$	$44.39 + j26.72$	$43.19 + j21.25$	8
9	10	9	6	5.0	$11.30 + j5.40$	$11.28 + j5.52$	$11.35 + j5.55$	7
10	11	10	3	1.5	$29.88 + j15.25$	$28.84 + j12.69$	$27.57 + j13.84$	5
10	12	11	3	1.5	$27.80 + j12.62$	$29.02 + j14.21$	$29.56 + j15.06$	4
11	13	12	2	5.0	$17.89 + j8.76$	$18.11 + j8.89$	$17.96 + j8.53$	5
11	14	13	5	1.0	$11.35 + j5.48$	$11.36 + j5.47$	$11.37 + j5.53$	4
12	15	14	6	5.0	$18.10 + j8.36$	$17.80 + j9.08$	$18.08 + j8.65$	2
12	16	15	1	6.0	$28.72 + j15.85$	$29.03 + j12.85$	$28.64 + j13.19$	5
14	17	16	7	3.5	$18.17 + j8.32$	$17.97 + j8.49$	$17.85 + j9.28$	6
14	18	17	8	4.0	$17.98 + j9.07$	$17.99 + j8.48$	$18.02 + j8.54$	1
15	19	18	9	4.0	$28.54 + j14.63$	$29.57 + j12.92$	$28.37 + j14.23$	2

Table I.4. Individual load demand of each bus that obtained with Case C Multi-objective optimization for 34-bus system

SB	RB	BN	LC	BL (mile)	Complex load demand obtained with Case C multi-objective optimization			Optimal conductor type
					Phase A	Phase B	Phase C	
1	2	1	1	0.4895	46.67 + j24.41	46.76 + j24.42	46.58 + j24.49	1
2	3	2	1	0.3277	46.67 + j24.39	46.58 + j24.60	46.66 + j24.49	1
3	4	3	1	1.1334	73.23+ j38.58	73.12+ j38.68	73.34+ j38.34	1
4	5	4	2	1.1063	100.1 + j52.67	100.0 + j52.67	100.0 + j52.67	2
4	6	5	1	0.2672	69.0+ j36.85	70.0+ j35.88	71.0+ j37.88	1
6	7	6	1	0.9955	50.0 + j26.33	51.0 + j26.33	49.0 + j26.33	1
7	8	7	1	0.341	50.0 + j27.33	50.0 + j25.33	50.0 + j25.33	1
8	9	8	1	0.0587	99.0 + j52.67	101.0 + j53.67	100.0 + j51.67	1
9	10	9	2	0.3238	150.0 + j79.01	150.0 + j79.01	150.0 + j79.01	1
10	11	10	2	2.9062	150.0 + j78.01	149.0 + j79.01	149.0 + j77.01	1
11	12	11	2	1.9818	300.0+ j157.03	300.0+ j158.03	300.0+ j159.03	1
9	13	12	1	0.6911	50.0 + j25.33	50.0 + j27.33	50.0 + j26.33	2
13	14	13	2	0.5740	91.0 + j47.31	90.0 + j47.51	89.0 + j47.41	1
13	15	14	1	0.1591	86.67 + j45.65	86.57 + j45.55	86.77 + j45.75	1
15	16	15	1	1.2430	83.32 + j43.89	82.34 + j43.89	84.33 + j43.89	1
16	17	16	1	0.72	83.33 + j43.89	83.32 + j43.89	83.34 + j43.89	1
17	18	17	2	1.3120	100.0 + j52.57	100.0 + j52.77	100.0 + j52.67	2
17	19	18	1	0.143	50.0 + j26.23	51.0 + j26.43	49.0 + j26.33	1
19	20	19	1	0.7162	76.67 + j40.38	76.57 + j40.38	76.77 + j40.38	1
20	21	20	1	0.7257	140.0+ j73.74	140.0+ j72.74	140.0+ j74.74	1
21	22	21	2	2.0004	180.0 + j94.82	181.0 + j94.82	179.0 + j94.82	1
20	23	22	2	0.3067	40.0 + j21.07	40.0 + j21.07	80.0 + j42.14	2
23	24	23	1	0.3069	100.0+ j52.67	100.0+ j52.77	100.0+ j52.57	1
23	25	24	2	1.1044	33.33 + j17.55	33.32 + j17.56	33.34 + j17.54	1
25	26	25	1	0.053	40.0+ j21.07	40.0+ j21.07	90.0 + j47.41	1
26	27	26	2	0.8773	283.33 + j149.25	284.33 + j149.26	282.33 + j149.24	1
27	28	27	2	0.6896	43.33 + j22.82	43.23 + j22.72	43.43 + j22.92	2
28	29	28	2	0.7219	20.0 + j10.53	20.0 + j10.63	20.0 + j10.43	1
25	30	29	1	0.1030	53.23 + j28.08	53.43 + j28.10	53.33 + j28.09	1
30	31	30	1	0.6215	46.67 + j24.4	46.66 + j24.6	46.67 + j24.5	1
31	32	31	2	0.1629	129.0+ j68.48	131.0+ j68.38	130.0+ j68.58	1
31	33	32	2	0.053	60.0+ j31.6	60.0+ j31.6	60.0+ j31.6	1
33	34	33	2	0.9206	60.0 + j31.5	60.0 + j31.4	60.0 + j31.6	1

Bibliography

- [1] T. Gonen, *Electric Power Distribution System Engineering*. McGraw-Hill publication, New York, 1986.
- [2] W.H.Kersting, *Distribution System Modelling and Analysis*, CRC Press, 2000.
- [3] H. L. Willis, *Power Distribution Planning Reference Book, Second Edition*. CRC Press, 1997.
- [4] S. Ganguly, N. C. Sahoo, and D. Das, "Recent advances on power distribution system planning: A state-of-the-art survey," *Energy Systems*, vol. 4. pp. 165–193, 2013.
- [5] W.H. Kersting and D.L. Mendive, "An application of Ladder network theory to the solution of three phase radial load flow problem", *IEEE PES Winter meeting-1976*.
- [6] D. Shirmohammadi, H. W. Hong, A. Semlyen, and G. X. Luo, "A compensation-based power flow method for weakly meshed distribution and transmission networks," *IEEE Trans. Power Syst.*, vol. 3, pp. 753–762, May 1988.
- [7] C. S. Cheng and D. Shirmohammadi, "A three-phase power flow method for real-time distribution system analysis," *IEEE Trans. Power Syst.*, vol.10, pp. 671–679, May 1995.
- [8] D. Thukaram, H. M. Wijekoon Banda, and J. Jerome, "A robust three phase power flow algorithm for radial distribution systems," *Electric Power Syst. Res.*, vol. 50, no. 3, pp. 227–236, 1999.
- [9] J.H. Teng, "A direct approach for distribution system load flow solutions," *IEEE Trans. Power Delivery*, vol.18, no-3, pp. 882-887, July-2003.
- [10] W.C. Wu and B.M. Zhang, "A three-phase power flow algorithm for distribution system power flow based on loop-analysis method," *Electrical Power and Energy Systems*, vol. 30, no. 1, pp. 8-15, 2008.
- [11] M. F. AlHajri and M. E. El-Hawary, "Exploiting the radial distribution structure in developing a fast and flexible radial power flow for unbalanced three-phase networks," *IEEE Transactions on Power Delivery*, vol. 25, no. 1, pp. 378-389, 2010.
- [12] G. Chang, S.-Y. Chu, M.-F. Hsu, C.-S. Chuang, and H.-L. Wang, "An efficient power flow algorithm for weakly meshed distribution systems," *Elect. Power Syst. Res.*, vol. 84, no. 1, pp. 90–99, 2012.
- [13] A.M. Cossi, R. Romero, J. Roberto, S. Mantovani, "Planning and projects of secondary electric power distribution systems," *IEEE Trans Power Syst.*, vol. 24, no. 1, pp. 205–213, Aug. 2009.

-
- [14] J. Zhu, G. Bilbro, and M. Chow, "Phase balancing using simulated annealing", *IEEE Trans. Power Systems*, vol. 14, no. 4, pp. 1508–1513, Nov. 1999.
- [15] Tsai-Hsiang chen and Jeng-tyan Cherng, "Optimal phase arrangement of distribution transformers connected to a primary feeder for system unbalance improvement and loss reduction using genetic algorithm," *IEEE Trans. Power Syst.*, vol. 15, no. 3, pp.994-1000, August 2000.
- [16] Ignacio Pérez Abril, "NSGA-II phase balancing of primary distribution circuits by the reconnection of their circuit laterals and distribution transformers", *International Journal of Electrical Power & Energy Systems*, vol. 109, pp. 1-7, 2014.
- [17] A. M. Cossi, R. Romero, and J. R. S. Mantovani, "Planning of secondary distribution circuits through evolutionary algorithms," *IEEE Trans. Power Del.*, vol. 20, no. 3, pp. 1599–1608, Jan. 2005.
- [18] M. Huang, C. Chen, C. Lin, M. Kang, H. Chuang, and C. Huang, "Three-phase balancing of distribution feeders using immune algorithm," *IET Gen. Transm. Distrib.*, vol. 2, no. 3, pp. 383–392, 2008.
- [19] M. Sathiskumar, A. Nirmal kumar, L. Lakshminarasimman, and S. Thiruvankadam, "A self adaptive hybrid differential evolution algorithm for phase balancing of unbalanced distribution system," *International Journal of Electrical Power & Energy Systems*, vol. 42, no. 1, pp. 91–97, 2012.
- [20] Y. Tuppabung and W. Kurutach, "The Modified Particle Swarm Optimization for Phase Balancing," *TENCON 2006. 2006 IEEE Reg. 10 Conf.*, vol. 00, pp. 1–4, 2006.
- [21] C.H. Lin, C.S. Chen, H.J. Chuang, M.Y. Huang, and C.W. Huang, "An expert system for three-phase balancing of distribution feeders", *IEEE Trans. Power Systems*, vol. 23, no. 3, pp 1488-1496, August 2008.
- [22] J. Zhu, M. Y. Chow, and F. Zhang, "Phase balancing using mixed integer programming", *IEEE Trans. Power Systems*, vol. 13, no. 4, pp. 1487–1492, Nov. 1998.
- [23] N. Gupta, A. Swarnkar, K.R. Niazi, "A novel strategy for phase balancing in three phase four-wire distribution systems". *IEEE PES General Meeting 2011*, 24–29 July 2011: 1–7.
- [24] W.-M. Lin and H.-C. Chin, "A current index based load balance technique for distribution systems," in *Power System Technology, 1998. Proceedings. POWERCON '98. 1998 International Conference on*, 1998, vol. 1, pp. 223–227 vol.1.
- [25] H. M. Khodr, I. J. Zepa, P. M. De Oliveira-De Jesús, and M. A. Matos, "Optimal phase balancing in distribution system using mixed-integer linear programming," in *2006 IEEE PES Transmission and Distribution Conference and Exposition: Latin America, TDC'06*, 2006.

- [26] D. Kaur and J. Sharma, "Optimal conductor sizing in radial distribution systems planning," *Int. J. Electr. Power Energy Syst.*, vol. 30, no. 4, pp. 261–271, 2008.
- [27] Z. Wang, H. Liu, D. C. Yu, X. Wang, and H. Song, "A practical approach to the conductor size selection in planning radial distribution systems," *IEEE Trans. Power Deliv.*, vol. 15, no. 1, pp. 350–354, 2000.
- [28] J. F. Franco, M. J. Rider, M. Lavorato, and R. Romero, "Optimal conductor size selection and reconductoring in radial distribution systems using a mixed-integer LP approach," *IEEE Trans. Power Syst.*, vol. 28, no. 1, pp. 10–20, 2013.
- [29] L. Mohammadian, M. T. Hagh, E. Babaei, and S. Khani, "Using PSO for optimal planning, and reducing loss of distribution networks," in *Electrical Power Distribution Networks (EPDC), 2012 Proceedings of 17th Conference on*, 2012, pp. 1–6.
- [30] F. Mendoza, D. Requena, J. Bemal-agustin, and J. Dominguez-navarro, "Optimal Conductor Size Selection in Radial Power Distribution Systems Using Evolutionary Strategies," *2006 IEEE/PES Transm. Distrib. Conf. Expo. Lat. Am.*, vol. 00, no. 1, pp. 1–5, 2006.
- [31] R. S. Rao, K. Satish, and S. V. L. Narasimham, "Optimal Conductor Size Selection in Distribution Systems Using the Harmony Search Algorithm with a Differential Operator," *Electr. Power Components Syst.*, vol. 40, no. 1, pp. 41–56, 2012.
- [32] R. Ranjan, B. Venkatesh, and D. Das, "A new algorithm for power distribution system planning," *Electr. Power Syst. Res.*, vol. 62, no. 1, pp. 55–65, 2002.
- [33] S. Sivanagaraju, N. Sreenivasulu, M. Vijayakumar, and T. Ramana, "Optimal conductor selection for radial distribution systems," *Electr. Power Syst. Res.*, vol. 63, no. 2, pp. 95–103, 2002.
- [34] H. N. Tram and D. L. Wall, "Optimal conductor selection in planning radial distribution systems," *IEEE Trans. Power Syst.*, vol. 3, no. 1, pp. 200–206, Feb. 1988.
- [35] R. Ranjan, A. Chaturvedi, P. S. Solanki, and D. Das, "Optimal conductor selection of radial distribution feeders using evolutionary programming," in *TENCON 2003. Conference on Convergent Technologies for Asia-Pacific Region*, 2003, vol. 1, pp. 456–459 Vol.1.
- [36] M. Ponnaivaikko and K. s. P. Rao, "An Approach to Optimal Distribution System Planning Through Conductor Gradation," *IEEE Trans. Power Appar. Syst.*, vol. PAS-101, no. 6, pp. 1735–1742, Jun. 1982.
- [37] P. S. N. Rao, "An Extremely Simple Method of Determining Optimal Conductor Sections for Radial Distribution Feeders," *IEEE Trans. Power Appar. Syst.*, vol. PAS-104, no. 6, pp. 1439–1442, Jun. 1985.
- [38] T. M. Khalil and A. V Gorpinich, "Optimal conductor selection and capacitor placement for loss reduction of radial distribution systems by selective particle swarm optimization,"

- in *2012 Seventh International Conference on Computer Engineering Systems (ICCES)*, 2012, pp. 215–220.
- [39] M. Vahid, N. Manouchehr, A. Jamaledin, and S. D. Hossein, “Combination of optimal conductor selection and capacitor placement in radial distribution systems for maximum loss reduction,” in *2009 IEEE International Conference on Industrial Technology*, 2009, pp. 1–5.
- [40] V. V. S. N. Murty and A. Kumar, “Capacitor Allocation in Radial Distribution System with Time Varying ZIP Load Model and Energy Savings,” *Procedia Comput. Sci.*, vol. 70, pp. 377–383, 2015.
- [41] A. R. Abul’Wafa, “Optimal capacitor allocation in radial distribution systems for loss reduction: A two stage method,” *Electr. Power Syst. Res.*, vol. 95, pp. 168–174, 2013.
- [42] S. Azim and K. S. Swarup, “Optimal Capacitor Allocation in Radial Distribution Systems under APDRP,” in *2005 Annual IEEE India Conference - Indicon*, 2005, pp. 614–618.
- [43] S. K. Injeti, V. K. Thunuguntla, and M. Shareef, “Optimal allocation of capacitor banks in radial distribution systems for minimization of real power loss and maximization of network savings using bio-inspired optimization algorithms,” *Int. J. Electr. Power Energy Syst.*, vol. 69, pp. 441–455, 2015.
- [44] A. A. Ejajal and M. E. El-Hawary, “Optimal capacitor placement and sizing in unbalanced distribution systems with harmonics consideration using particle swarm optimization,” *IEEE Trans. Power Deliv.*, vol. 25, no. 3, pp. 1734–1741, 2010.
- [45] S. Ganguly, N. C. Sahoo, and D. Das, “Multi-objective planning of electrical distribution systems using particle swarm optimization,” *Electr. Power Energy Convers. Syst. 2009. EPECS ’09. Int. Conf.*, vol. 46, pp. 65–78, 2009.
- [46] M. Farsadi, T. S. Dizaji, and H. Hosseinejad, “Capacitor allocation in order to maximize the loss reduction benefit and improve the voltage profile based on NSGA-II,” *ELECO 2015 - 9th Int. Conf. Electr. Electron. Eng.*, pp. 515–520, 2016.
- [47] A. Kavousi-Fard and H. Samet, “Multi-objective Performance Management of the Capacitor Allocation Problem in Distributed System Based on Adaptive Modified Honey Bee Mating Optimization Evolutionary Algorithm,” *Electr. Power Components Syst.*, vol. 41, no. 13, pp. 1223–1247, 2013.
- [48] V. Halder and N. Chakraborty, “Power loss minimization by optimal capacitor placement in radial distribution system using modified cultural algorithm,” *Int. Trans. Electr. Energy Syst.*, vol. 25, no. 1, pp. 54–71, 2015.
- [49] J. Vuletić and M. Todorovski, “Optimal capacitor placement in distorted distribution networks with different load models using Penalty Free Genetic Algorithm,” *Int. J. Electr. Power Energy Syst.*, vol. 78, pp. 174–182, 2016.

-
- [50] E. S. Ali, S. M. Abd Elazim, and A. Y. Abdelaziz, "Improved Harmony Algorithm for optimal locations and sizing of capacitors in radial distribution systems," *Int. J. Electr. Power Energy Syst.*, vol. 79, pp. 275–284, 2016.
- [51] D. B. Prakash and C. Lakshminarayana, "Optimal siting of capacitors in radial distribution network using Whale Optimization Algorithm," *Alexandria Eng. J.*, 2016.
- [52] A. Askarzadeh, "Capacitor placement in distribution systems for power loss reduction and voltage improvement: a new methodology," *IET Gener. Transm. Distrib.*, vol. 10, no. 14, pp. 3631–3638, 2016.
- [53] H. Sadeghi and N. Ghaffarzadeh, "A Simultaneous Biogeography based Optimal Placement of DG Units and Capacitor Banks in Distribution Systems with Nonlinear Loads," *J. Electr. Eng.*, vol. 67, no. 5, pp. 351–357, 2016.
- [54] W. M. Da Rosa, P. Rossoni, J. C. Teixeira, E. A. Belati, and P. T. L. Asano, "Optimal allocation of capacitor banks using genetic algorithm and sensitivity analysis," *IEEE Lat. Am. Trans.*, vol. 14, no. 8, pp. 3702–3707, 2016.
- [55] S. M. Abd Elazim and E. S. Ali, "Optimal locations and sizing of capacitors in radial distribution systems using mine blast algorithm," *Electr. Eng.*, 2016.
- [56] A. Sharma, H. Sharma, A. Bhargava, N. Sharma, and J. C. Bansal, "Optimal placement and sizing of capacitor using Limaçon inspired spider monkey optimization algorithm," *Memetic Comput.*, 2016.
- [57] C.-S. Lee, H. V. H. Ayala, and L. dos Santos Coelho, "Capacitor placement of distribution systems using particle swarm optimization approaches," *Int. J. Electr. Power Energy Syst.*, vol. 64, pp. 839–851, 2015.
- [58] B. Singh, J. Solanki, and V. Verma, "Neural network based control of reduced rating DSTATCOM," *Proc. INDICON 2005 An Int. Conf. IEEE India Counc.*, vol. 2005, pp. 516–520, 2005.
- [59] G. Escobar, A. A. Valdez, R. E. Torres-Olguín, and M. F. Martínez-Montejano, "A repetitive-based controller in stationary reference frame for D-Statcom in unbalanced operation," in *IEEE International Symposium on Industrial Electronics*, 2006, vol. 2, pp. 1388–1393.
- [60] H. Fujita and H. Akagi, "Voltage-Regulation Performance of a Shunt Active Filter Intended for Installation on a Power Distribution System," *Power Electron. IEEE Trans.*, vol. 22, no. 3, pp. 1046–1053, May 2007.
- [61] C. Sharmeeela, G. Uma, M. R. Mohan, and K. Karthikeyan, "Multi-level distribution STATCOM for reducing the effect of voltage sag and swell," *Power Syst. Technol. 2004. PowerCon 2004. 2004 Int. Conf.*, vol. 1, pp. 306 – 310 Vol.1, 2004.

-
- [62] B. Blazic and I. Papic, "A new mathematical model and control of D-StatCom for operation under unbalanced conditions," *Electr. Power Syst. Res.*, vol. 72, no. 3, pp. 279–287, 2004.
- [63] R. Cai, M. Bongiorno, A. Sannino, and C. Rong, "Control of D-STATCOM for Voltage Dip Mitigation," *IEEE Futur. Power Syst. 2005 Int. Conf.*, p. 6 pp.–6, 2005.
- [64] X. Shukai, S. Qiang, Z. Yongqiang, and L. Wenhua, "Development of a D-STATCOM prototype based on cascade inverter with isolation transformer for unbalanced load compensation," *Proc. IEEE Int. Conf. Ind. Technol.*, vol. 2005, pp. 1051–1056, 2005.
- [65] K. Anuradha, B. P. Muni, and A. D. Rajkumar, "Simulation of cascaded H-bridge converter based DSTATCOM," *2006 1st IEEE Conf. Ind. Electron. Appl.*, 2006.
- [66] X. Fu, J. Wang, and Y. Ji, "A novel control method for D-STATCOM under unbalanced conditions," *2006 Int. Conf. Power Syst. Technol. POWERCON2006*, pp. 1–6, 2007.
- [67] M. Labeeb and B. S. Lathika, "Design and analysis of DSTATCOM using SRFT and ANN-fuzzy based control for power quality improvement," *2011 IEEE Recent Adv. Intell. Comput. Syst. RAICS 2011*, pp. 274–279, 2011.
- [68] Y. Wang, Q. Xu, Y. Hu, and G. Chen, "Fast-transient Repetitive Controller Based Current Control Strategy for a Cascaded DSTATCOM," *ECCE IEEE*, pp. 6704–6709, 2015.
- [69] S. Devi and M. Geethanjali, "Optimal location and sizing determination of Distributed Generation and DSTATCOM using Particle Swarm Optimization algorithm," *Int. J. Electr. Power Energy Syst.*, vol. 62, pp. 562–570, 2014.
- [70] S. Jazebi, S. H. Hosseini, and B. Vahidi, "DSTATCOM allocation in distribution networks considering reconfiguration using differential evolution algorithm," *Energy Convers. Manag.*, vol. 52, no. 7, pp. 2777–2783, 2011.
- [71] K. R. D. K. Ravi, "Optimal size and siting of multiple DG and DSTATCOM in radial distribution system using Bacterial Foraging Optimization Algorithm," *Ain Shams Eng. J.*, pp. 1–13, 2015.
- [72] S. Nesrullah, M. Azah, and S. Hussain, "Reliability Improvement in Distribution Systems by Optimal Placement of DSTATCOM Using Binary Gravitational Search Algorithm," *Przegląd Elektrotechniczny (Electrical Rev.)*, vol. 88, no. 2, pp. 295–299, 2012.
- [73] S. M. S. Hussain and M. Subbaramiah, "An analytical approach for optimal location of DSTATCOM in radial distribution system," in *2013 International Conference on Energy Efficient Technologies for Sustainability*, 2013, pp. 1365–1369.
- [74] M. Farhoodnea, A. Mohamed, H. Shareef, and H. Zayandehroodi, "Optimum D-STATCOM placement using firefly algorithm for power quality enhancement," in *Power Engineering and Optimization Conference (PEOCO), 2013 IEEE 7th International*, 2013, pp. 98–102.

-
- [75] H. B. Tolabi, M. H. Ali, S. Member, and M. Rizwan, "Simultaneous Reconfiguration, Optimal Placement of DSTATCOM, and Photovoltaic Array in a Distribution System Based on Fuzzy-ACO Approach," *IEEE Trans. Sustain. Energy*, vol. 6, no. 1, pp. 210–218, 2015.
- [76] M. A. Eldery, E. F. El-Saadany, and M. M. A. Salama, "Effect of distributed generator on the allocation D-STATCOM in distribution network," in *Power Engineering Society General Meeting, 2005. IEEE, 2005*, pp. 2360–2364 Vol. 3.
- [77] A. Jain, A. R. Gupta, and A. Kumar, "An efficient method for D-STATCOM placement in radial distribution system," in *Power Electronics (IICPE), 2014 IEEE 6th India International Conference on*, 2014, pp. 1–6.
- [78] H. D. Dehnavi and S. Esmaceli, "A new multiobjective fuzzy shuffled frog-leaping algorithm for optimal reconfiguration of radial distribution systems in the presence of reactive power compensators," *Turkish J. Electr. Eng. Comput. Sci.*, vol. 21, no. 3, 2013.
- [79] S. A. Taher and S. A. Afsari, "Optimal location and sizing of DSTATCOM in distribution systems by immune algorithm," *Int. J. Electr. Power Energy Syst.*, vol. 60, pp. 34–44, 2014.
- [80] Sheng Xiaoguang, Tongzhen Wei, and Qunhai Huo, "Optimal configuration of multi-DFACTS joint operation in distributed network," *2014 IEEE Conf. Expo Transp. Electrification Asia-Pacific (ITEC Asia-Pacific)*, pp. 1–5, 2014.
- [81] K. R. D. T. Yuvaraj, K. Ravi, "DSTATCOM allocation in distribution networks considering load variations using bat algorithm," *Ain Shams Eng. J.*, pp. 1–13, 2015.
- [82] S. A. Taher and M. H. Karimi, "Optimal reconfiguration and DG allocation in balanced and unbalanced distribution systems," *Ain Shams Eng. J.*, vol. 5, no. 3, pp. 735–749, 2014.
- [83] C. Yammani, S. Maheswarapu, and S. Matam, "Enhancement of voltage profile and loss minimization in Distribution Systems using optimal placement and sizing of power system modeled DGs," *J. Electr. Syst.*, vol. 7, no. 4, pp. 448–457, 2011.
- [84] M. N., A. T., and A. D. Kulkarni, "A Weighted Multi-objective Index Based Optimal Distributed Generation Planning in Distribution System," *Procedia Technol.*, vol. 21, pp. 279–286, 2015.
- [85] A. T. Davda and B. R. Parekh, "System impact analysis of Renewable Distributed Generation on an existing Radial Distribution Network," *2012 IEEE Electr. Power Energy Conf. EPEC 2012*, pp. 128–132, 2012.
- [86] K. Nadhir, D. Chabane, and B. Tarek, "Firefly algorithm for optimal allocation and sizing of Distributed Generation in radial distribution system for loss minimization," *2013 Int. Conf. Control. Decis. Inf. Technol. CoDIT 2013*, pp. 231–235, 2013.

- [87] I. S. Kumar and P. K. Navuri, "Optimal Access Point and Capacity of Distributed Generators in Radial Distribution Systems for Loss Minimization Including Load Models," *Distrib. Gener. Altern. Energy J.*, vol. 29, no. 2, pp. 24–51, 2014.
- [88] K. Mahesh, P. A. Nallagownden, and I. A. Elamvazuthi, "Optimal placement and sizing of DG in distribution system using accelerated PSO for power loss minimization," in *2015 IEEE Conference on Energy Conversion (CENCON)*, 2015, pp. 193–198.
- [89] M. T. A. Y. Mohammadi and M. Faramarzi, "PSO algorithm for sitting and sizing of distributed generation to improve voltage profile and decreasing power losses," in *Electrical Power Distribution Networks (EPDC), 2012 Proceedings of 17th Conference on*, 2012, pp. 1–5.
- [90] A. Kumar and W. Gao, "Voltage profile improvement and line loss reduction with distributed generation in deregulated electricity markets," in *TENCON 2008 - 2008 IEEE Region 10 Conference*, 2008, pp. 1–6.
- [91] I. Hussain and A. K. Roy, "Optimal distributed generation allocation in distribution systems employing modified artificial bee colony algorithm to reduce losses and improve voltage profile," in *Advances in Engineering, Science and Management (ICAESM), 2012 International Conference on*, 2012, pp. 565–570.
- [92] M. Sedighzadeh, M. Esmaili, and M. Esmacili, "Application of the hybrid Big Bang-Big Crunch algorithm to optimal reconfiguration and distributed generation power allocation in distribution systems," *Energy*, vol. 76, pp. 920–930, Nov. 2014.
- [93] M. M. Othman, W. El-Khattam, Y. G. Hegazy, and A. Y. Abdelaziz, "Optimal Placement and Sizing of Distributed Generators in Unbalanced Distribution Systems Using Supervised Big Bang-Big Crunch Method," *IEEE Trans. Power Syst.*, pp. 1–9, 2014.
- [94] M. Mohammadi and M. Nafar, "Optimal placement of multitypes {DG} as independent private sector under pool/hybrid power market using GA-based Tabu Search method," *Int. J. Electr. Power Energy Syst.*, vol. 51, pp. 43–53, 2013.
- [95] I. Hussain and A. K. Roy, "Optimal distributed generation allocation in distribution systems employing modified artificial bee colony algorithm to reduce losses and improve voltage profile," in *Advances in Engineering, Science and Management (ICAESM), 2012 International Conference on*, 2012, pp. 565–570.
- [96] D. Q. Hung, N. Mithulanathan, and R. C. Bansal, "Analytical strategies for renewable distributed generation integration considering energy loss minimization," *Appl. Energy*, vol. 105, pp. 75–85, 2013.
- [97] T. Ramana, V. Ganesh, and S. Sivanagaraju, "Distributed Generator Placement and Sizing in Unbalanced Radial Distribution System," *Cogeneration & Distributed Generation Journal*, vol. 25, pp. 52–71, 2010.

- [98] A. D. Kulkarni, "A Weighted Multi-objective Index Based Optimal Distributed Generation Planning in Distribution System," *Procedia Technol.*, vol. 21, pp. 279–286, 2015.
- [99] K. Mahmoud, N. Yorino, and A. Ahmed, "Optimal Distributed Generation Allocation in Distribution Systems for Loss Minimization," *IEEE Trans. Power Syst.*, vol. 31, no. 2, pp. 960–969, 2015.
- [100] D. Q. Hung and N. Mithulananthan, "Multiple distributed generator placement in primary distribution networks for loss reduction," *Ind. Electron. IEEE Trans.*, vol. 60, no. 4, pp. 1700–1708, 2013.
- [101] M. R. H. M. Rasdi, I. Musirin, Z. A. Hamid, H. C. M. Haris, and U. T. Mara, "Gravitational Search Algorithm Application in Optimal Allocation and Sizing of Multi Distributed Generation," no. March, pp. 364–368, 2014.
- [102] K. Price, R. Storn, and J. Lampinen, *Differential Evolution: A Practical Approach to Global Optimization*. Berlin, Germany: Springer-Verlag, 2005.
- [103] S. Das and P. N. Suganthan, "Differential evolution—A survey of the state-of-the-art," *IEEE Trans. Evol. Comput.*, vol. 15, no. 1, pp. 4–31, Feb. 2011.
- [104] X.-S. Yang, "Cuckoo search via levy flights," in *Nature & Biologically Inspired Computing, 2009. NaBIC 2009. World Congress on. IEEE*, 2009, pp. 210–214.
- [105] J. Kennedy and R. C. Eberhart, "Particle swarm optimization". *Proc. Of IEEE International Conference on Neural Networks*, Piscataway, NJ. pp. 1942-1948 (1995).
- [106] D.E. Goldberg, *Genetic Algorithms in Search, Optimization and Machine Learning*, Boston: Addison Wesley, 1989.
- [107] Y. Baghzouz and S. Ertem, "Shunt capacitor sizing for radial distribution feeders with distorted substation voltages," *IEEE Trans. Power Deliv.*, vol. 5, no. 2, pp. 650–657, 1990.
- [108] The Math Works Inc, MATLAB R2012b.
- [109] C. S. Chen, C. T. Hsu, and Y. H. Yan, "Optimal distribution feeder capacitor placement considering mutual coupling effect of conductors," *IEEE Trans. Power Deliv.*, vol. 10, no. 2, pp. 987–994, 1995.
- [110] K. Prakash and M. Sydulu, "Topological and primitive impedance based load flow method for radial and weakly meshed distribution systems," *Iran. J. Electr. Comput. Eng.*, vol. 10, no. 1, pp. 10–18, 2011.

Dissemination

International Journal Articles

- [1] P. Samal, S. Mohanty, and S. Ganguly, "Planning of Unbalanced Radial Distribution Systems With Capacitor Using Differential Evolution Algorithm," *Journal of Electrical Engineering*, vol. 17. no.1, pp. 523–530, 2017.
- [2] P. Samal, S. Mohanty, and S. Ganguly, "Modelling and Allocation of a DSTATCOM on the Performance Improvement of Unbalanced Radial Distribution Systems," *Journal of Electrical Engineering*, vol. 16. no.2, pp. 323–332, 2016.
- [3] P. Samal, S. Ganguly, and S. Mohanty, "Planning of unbalanced radial distribution systems using differential evolution algorithm," *Energy Syst.*, pp. 1–22, 2016. DOI.10.1007%2Fs12667-016-0202-z.
- [4] P. Samal, S. Mohanty, and S. Ganguly, "Modelling, optimal sizing and allocation of DSTATCOM in unbalanced radial distribution systems using differential evolution algorithm," *International Journal of Numerical Modelling: Electronic Networks, Devices and Fields*, (Communicated).
- [5] P. Samal, S. Mohanty, and S. Ganguly, "Distributed Generation Integrated Planning of Unbalanced Radial Distribution Systems Using Differential Evolution Algorithm, Iranian Journal of Science and Technology, Transactions of Electrical Engineering (Communicated).
- [6] P. Samal, S. Ganguly, and S. Mohanty "A Fuzzy Multi-Objective Approach for the Integration of Distributed Generation in Unbalanced Radial Distribution Networks Under Load and Generation Uncertainties," *International Journal of Fuzzy Systems*, Springer (Communicated).

Conference Presentations

- [1] P. Samal, S. Mohanty, and S. Ganguly, "Planning of Distributed Generation and Capacitor in an Unbalanced Radial Distribution System using Cuckoo Search Algorithm," in *ICEMS*, 2016 IEEE, pp. 1–4.
- [2] P. Samal, S. Mohanty, and S. Ganguly, "Simultaneous capacitor allocation and conductor sizing in unbalanced radial distribution systems using differential evolution algorithm," in *NPSC*, 2016 IEEE, pp. 1–4.
- [3] P. Samal, S. Mohanty, and S. Ganguly, "Effect of DSTATCOM allocation on the performance of an unbalanced radial distribution systems," in *ICETECH*, 2016 IEEE, pp. 1–5.
- [4] P. Samal and S. Ganguly, "A modified forward backward sweep load flow algorithm for unbalanced radial distribution systems," in *Power Energy Society General Meeting*, 2015 IEEE, pp. 1–5.

Vitae

Name : Padarbinda Samal

Date of Birth : 28th March 1987

Permanent Address : Qr. No-148/149,
C/O R.C. Samal, Co-operative housing
complex, , C.S. Pur,
Post KIIT, Bhubaneswar
Khurda (District),
Odisha- 751024, India.

E-mail : padarbindasamal87@gmail.com

Academic Qualifications:

- Pursuing Ph. D. in Electrical Engineering, National Institute of Technology, Rourkela.
- M. Tech. in Power systems engineering, V.S.S.U.T, Burla, Odisha.
- B. Tech. in Electrical and Electronics Engineering (EEE) from Silicon Institute of Technology, Bhubaneswar